NASA TECHNICAL MEMORANDUM NASA TM-76908

SCIENTIFIC TRANSACTIONS No. 11 OF THE INSTITUTE OF MECHANICS, MOSCOW STATE UNIVERSITY

A. L. Gonor, Editor

Translation of "Nauchnyye Trudy Nr. 11," Moscow State University, Institute of Mechanics, 1971, pp 1-137

NATIONAL AERONAUTICS AND SPACE ADMINISTRATION
WASHINGTON, D.C. 20546 APRIL 1982

STANDARD TITLE PAGE

1. Report No. NASA TM- 76908	2. Government Accession No. TT 78-58000	3. Recipient's Catalog No.
4. Title and Subtitle SCIENTIFIC TRANSACTIONS No. 11 OF THE INSTITUTE OF MECHANICS, MOSCOW STATE UNIVERSITY		5. Report Date APRIL 1982 6. Performing Organization Code
7. Author(s) A. L. Gonor, Editor		8. Performing Organization Report No. 10. Work Unit No.
9. Performing Organization Name and Address Franklin Book Programs, Inc. Cairo, Egypt		11. Contract or Grant No. NSF-C-724 13. Type of Report and Period Covered Translation
12. Sponsoring Agency Name and Address National Aeronautics & Space Administration and National Science Foundation, Washington, D.C. 20546		14. Sponsoring Agency Code

15. Supplementary Notes

Translation of "Nauchnyye Trudy Nr. 11," Moscow, Moscow State University, Institute of Mechanics, 1971, pp 1-137

16. Abstract

The present issue of the scientific transactions of the Institute of Mechanics consists of two parts. The results of flow around wings, the determination of the optimal form, and the interaction of the wake with the accompanying flow at supersonic and hypersonic speeds of the free-stream flow are given in the first part. The second part comprises methods of numerical and analytical calculation of one=dimensional unsteady and two-dimensional steady motions of fuel-gas mixtures with exothermic reactions.

17. Key Words (Selected by Author(s))	18. Distribution Statement Unlimited		
19. Security Classif. (of this report) Unclassified	20. Security Classif. (of this page)	21. No. of Pages	22. Price

NASA-HQ

CONTENTS

ANNOTATION

The present issue of the scientific works consists of two parts. The results of the flow around wings, the determination of the optimal forms, and the interaction of the wake with the cocurrent flow at supersonic and hypersonic speeds of the free-stream flow are given in the first part.

The second part comprises methods of numerical and analytical calculation of one-dimensional unsteady and two-dimensional steady motions of fuel-gas mixtures with exothermic reactions.

FOREWORD

The present collected papers are dedicated to the aerodynamics of the super- and hypersonic flows and theories of the supersonic motion of a gas with waves of detonation and combustion. In these trends, investigations are performed and seminares are made in the Institute of Mechanics during many years under the leadership of the associate member of the Academy of Sciences of the USSR, G.G. Chernov. During the last time, a number of new results were obtained, comprising the contents of the given issue of the scientific works. In the first part, problems of the flow around triangular and V-shaped wings with gas flow of high supersonic velocity are investigated (A.L. Gonor, N.A. Ostapenko and V.I. Lapygin). Further, in the paper of L.V. Gogish and G.Yu. Stepanov, an integral method of calculation of the interaction of turbulent wake with a flow in a canal or a jet is suggested. Problems of the optimum forms of a body at hypersonic velocities, in the frame of the approximation laws of resistance, are resolved in the works of A.L. Gonor and V.I. Lapygin. The results of an experimental investigation of supersonic flow around a right-angled wing, in a wide range of elongation and angles of attack, are given in the paper of M.P. Falunin. G.S. Ulyanov studied the effect of the penetrability of a plate on the power action of the supersonic flow.

The second part of the issue, comprising the methods of calculation of the motion of fuel mixtures, is started with the paper of S.A. Nedvedev. In this paper, the problem of the decay of the burst is resolved in non-self-similar arrangement, taking into account the ignition delay and the final reaction rate. V.P. Korobeinikov, V.A. Levin and V.V. Markov use similar models of fuel medium to solve the problem of point explosion with plane, cylindrical and spherical waves. In the paper of L.I. Zak and V.A. Levin, the gas motion, caused by a piston, is investigated assuming that the heat effect of the reaction is small and that a linearization, relative to the adiabatic flow in front of the piston, can be produced. The flow around a body by a stationary supersonic flow of fuel mixture is investigated in the last three works of the collection. In the first one of them, S.M. Gilinskii investigates the growth of the initial disturbances and the possible nonstationary conditions of combustion at the hupersonic flow around the bow of a blunt body. The second paper of S.M. Gilinskii and M.L. Khaikin is dedicated to the use of the boundary layer method for the composition of an analytical solution of the supersonic flow around a wedge and a cone by a fuel mixture. The third work of S.M. Gilinskii "Linearized supersonic nonequilibrium flow of a fuel mixture of gases near a wedge" comprises an analytical solution of flow around a wedge in the case of a small heat effect of reaction, obtained, as in the work of L.I. Zak and V.A. Levin, on the basis of using linearization relative to the corresponding adiabatic flow.

PART I

SUPER- AND HYPERSONIC GAS FLOW

CALCULATION OF THE ENTROPY LAYER ON THE SURFACE OF A TRIANGULAR WING

By

A.L. Gonor, N.A. Ostapenko

On solving the problem of hypersonic flow around a triangular wing [1], a singularity in the distribution of the surface speed is involved. For this reason the obtained solution must be corrected in the region of the location of these singularities, adjoining to the plane of symmetry. A similar situation already arised in the general theory of the supersonic conical flow, when such singularities appeared in the solution on the surface of the body and it was necessary to make a specific solution in a region, called the entropy layer [2, 3, 6-8]. The calculation of the entropy layer on a wing has many things in common with the mentioned investigations; however there are important differences as a result of taking the specific features of surface solution into account. The problem of the flow around a plane triangular wing is analyzed below in detail, although this method can be transposed also for the general case.

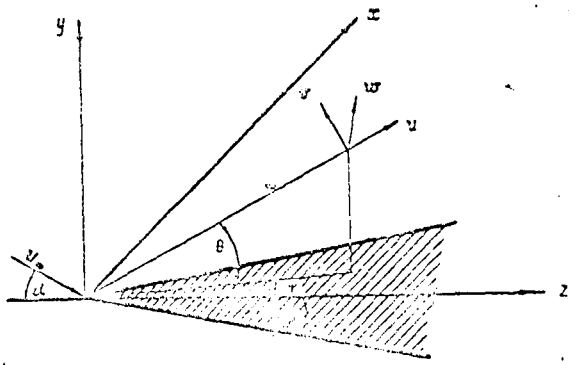

Fig. 1

1. The formulae of a conical flow in the coordinate system of τ, θ, φ (Fig. 1) after transition to the new variable $\psi = \psi(\theta, \varphi)$ satisfying the formula $v\varphi_\theta + w\sin\theta\,\psi_\varphi = 0$ according to reference [1] will have the following form:

$$\begin{aligned}
&\frac{W}{\cos\theta}\frac{\partial u}{\partial\varphi} - v^2 - w^2 = 0,\\
&\frac{W}{\cos\theta}\frac{\partial v}{\partial\varphi} + uv + w^2 tg\,\theta = -\frac{1}{\rho\theta_\psi}\frac{\partial P}{\partial\psi},\\
&\frac{\varkappa}{\varkappa-1}\frac{P}{\rho} + \frac{u^2+v^2+w^2}{2} = c,\\
&\frac{\partial}{\partial\varphi}\left[\frac{P}{\rho^\varkappa}\right] = 0,\\
&\frac{\partial}{\partial\varphi}\ln(\rho w\theta_\psi) + 2\frac{u}{w}\cos\theta = 0,\\
&w\theta_\varphi = v\cos\theta.
\end{aligned} \qquad (1.1)$$

$$\frac{W}{\cos\theta}\frac{\partial W}{\partial\varphi} + uw - vw\,tg\,\theta = -\frac{1}{\rho\cos\theta}\left[\frac{\partial P}{\partial\varphi} - \frac{\theta_\varphi}{\theta_\psi}\frac{\partial P}{\partial\psi}\right]. \qquad (1.2)$$

Here u, v, W — are the corresponding velocity projections on the axes τ, θ, φ relative to the velocity of the free-stream flow U_∞; P, ρ, γ are the pressure, density and ratio of specific heats. The density and pressure are relative to the quantities ρ_∞ and $\rho_\infty U_\infty^2$, respectively. The coordinate $\psi = $ const determines the stream surface. The projection of the Eulerian equation on the direction of the axis φ (1.2) is written for further direct use.

In the system (1.1) and in the boundary conditions on the shock wave $\theta^*(\varphi)$ after the substitution of $\theta^* = \varepsilon\bar\theta^*$, $\rho = \varepsilon^{-1}\bar\rho$, $V = \varepsilon\bar V$ the terms, having the order of $\varepsilon^{1+\ell}$ are neglected (ε is the characteristic ratio of the densities in front of the shock wave and behind it, $\ell > 0$). From the solution in reference [1], the formula for the pressure will have the following form:

$$P = \sin^2\alpha + \varepsilon P_1^*(\varphi) + \varepsilon P_2(\varepsilon, \varphi, \psi), \qquad (1.3)$$

where:

$$P_1^*(\varphi) = \sin 2\alpha\,(\theta^*\cos\varphi - \theta^*_\varphi\sin\varphi) - \sin^2\alpha.$$

Here the bar of θ^* is omited, α is the angle of attack. The value of P_2 and the other parameters of the flow are expressed as f_i by the solution of the integral-differential equation determining the form of the shock wave.

The surface of the wing in the solution of reference [1] is the stream surface $\varphi = \beta$ (β is the half-angle of the triangular wing at the top). However, in the small interval $0 \leqslant \varphi \leqslant \varphi_1$ the stream surfaces cross the surface of the wing (a weak flowing of $\sim \varepsilon^2$ takes place). Consequently, it is necessary to make a correction for the solution in certain surroundings of the origin of the coordinate.

Let us introduce the variables Δ and τ instead of u and w:

$$u = \Delta \cos\tau \ , \quad w = \Delta \sin\tau \ .$$

Formula (1.2) by using (1.1) with the new variables will have the form:

$$tg\tau\left(\frac{\partial\tau}{\cos\theta\,\partial\varphi} + 1 - \frac{V}{\Delta} tg\theta\cos\tau + \frac{V^2}{\Delta^2}\right) = -B \ ,$$

$$B = \frac{1}{\rho\Delta^2\cos\theta}\left[\frac{\partial p}{\partial\varphi} - \frac{\partial_\varphi}{\partial_\psi}\frac{\partial p}{\partial\psi}\right] \ . \qquad (1.4)$$

It is easy to ascertain that, according to (1.3) and (1.4), the pressure gradient will be taken into account only with terms of $\sim \varepsilon^2$. Therefore with an accuracy of values of $\sim \varepsilon^2$, we will have

$$tg\tau\left(\frac{\partial\tau}{\partial\varphi} + 1\right) = 0 \ . \qquad (1.5)$$

Accordingly the equality of the formula in the brackets to zero, by using the condition on the shock wave, gives the following solution which is coincident with [1]

$$\tau = -\varphi - \alpha_1(\varphi') \ , \qquad (1.6)$$

where $\alpha_1(\varphi')$ is determined from the condition on the shock wave at $\varphi' = \varphi$ (Fig. 2).

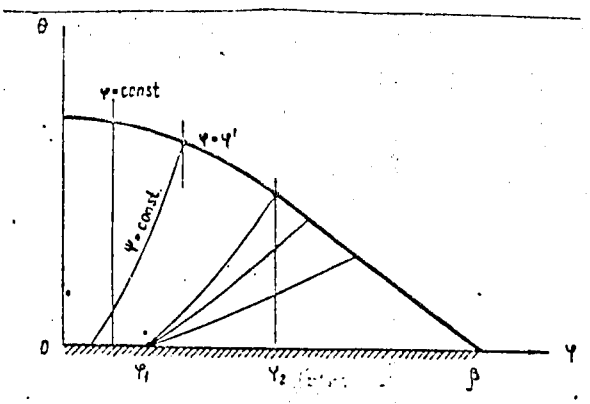

Fig. 2

In the surroundings of the shock wave, the second possible solution $\tau = v$ contradicts with the boundary condition. Therefore the surface solution can be only formula (1.6), at the same time the transverse component of the velocity W has a singularity on the surface of the wing. This shows that in the region of the flow where $\tau \approx 0$, , the small corrections, neglected in the derivation of formula (1.5), become comparable with the remaining terms. In particular, the pressure gradient appears essential along the wing span. Let us show this, introducing for convenience the following designation:

$$D = \left(\frac{V}{\Delta} tg\,\theta \cos\tau - \frac{V^2}{\Delta^2}\right) tg\,\tau \,. \qquad (1.7)$$

Then, putting $\tau = \tau^0 + \xi^2 \tau^{(2)} + \ldots$ [below, the upper index (k) will denote the coefficient, standing at ξ^k] , where τ^0 corresponds to (1.6), for $\tau^{(2)}$ we obtain the following relation:

$$tg\,\tau^0 \left(\frac{\partial \tau^{(2)}}{\partial \varphi} - \frac{\theta^{(1)2}}{2}\right) = D^{(2)} - B^{(2)} \,,$$

$$D^{(2)} = \left(\frac{V^{(1)}}{\Delta^{(0)}} \theta^{(1)} \cos\tau^0 - \frac{V^{(1)2}}{\Delta^{(0)2}}\right) tg\,\tau^0 \,,$$

$$B^{(2)} = \frac{1}{\rho^{(1)} \Delta^{(0)}} \left[\frac{\partial p^{(1)}}{\partial \varphi} - \frac{\theta_\varphi^{(1)}}{\theta_\psi^{(1)}} \frac{\partial p^{(1)}}{\partial \psi}\right] . \qquad (1.8)$$

From equation (1.8), it is shown that $\partial\tau^{(2)}/\partial\varphi$ has a singularity at the points where τ^0 becomes zero. Hereby, the essential term is determined by the pressure gradient $B^{(2)}$.

At $B^{(2)} \neq 0$, the singularity certainly exists; at $B^{(2)} = 0$ (plane of symmetry) it may be not existing and therefore a special investigation is needed here. Thus, in the solution of [1] (below we shall call it the surface solution), on approaching to a certain critical surface $\varphi = -\alpha_1(\varphi')$ a special term appears in the formula of τ, namely:

$$\tau^{(2)} \approx B^{(2)}_{\varphi=\alpha_1(\varphi')} \ln[\alpha_1(\varphi') + \varphi] .$$

This inequality in the solution indicates the presence of a certain term. Although this term is negligibly small in the surface flow and evenly small in all the region, a quantity of a "principal" order appears in the region, where nonuniform convergence exists. From the foregoing, it is shown that such term is a function of B.

2. The equation (1.5) has two solutions:

$$\frac{\partial\tau}{\partial\varphi} = 1 \quad \text{and} \quad \tau = 0 .$$

The first solution has a singularity near $\tau^0 = 0$. Therefore in the investigation of the nonuniform convergence of the solution, the analysis of the expansion, obtained from the second solution of [7], is completely reasonable.

Let us represent τ_i (where i- denotes the inside solution) by the form

$$\tau_i = \varepsilon^2 \tau_i^{(2)} + \ldots \qquad (2.1)$$

Substituting formula (2.1) in equation (1.4), we obtain after a simple calculation:

$$\tau_i^{(2)} = D_i^{(2)} - B_i^{(2)} . \qquad (2.2)$$

By means of (1.8), we find that $D_i \sim O(\varepsilon^2)$

$$B_i^{(2)} = \frac{1}{\rho_i^{(1)} \Delta_i^{(0)}} \left[\frac{\partial P_i^{(1)}}{\partial \varphi} - \frac{\theta_{i\psi}^{(1)}}{\theta_{i\varphi}^{(1)}} \frac{\partial P_i^{(1)}}{\partial \psi} \right] \qquad (2.3)$$

hence it is clear that, $\rho_i^{(1)}$, $\Delta_i^{(0)} P_i^{(1)}$ must be determined for the determination of $\tau^{(2)}$.

Let us assume that these quantities can be determined, and let us consider the question of coupling of the inside and surface solutions. To prove that the two solutions are coupled, it is necessary to ascertain that they have a common region and are asymptotically equivalent in their common region. On the basis of the second of these two conditions, it is possible to conclude that the inside and surface solutions are not coupled, because these solutions intersect and the slope of the curves has a discontinuity at the point of intersection. Thus, the first terms of the expansion can not be asymptotically equivalent in any common region.

This might have been expected for two reasons: the scale of the independent variable is the same in every region and the arbitrary constant (or, moreover, the arbitrary function of φ), by which the coupling of solutions might have been realized, is absent.

The problem of coupling can be investigated by several methods [4,7].

The method, used below, is closely related to the behavior of the surface solution. On analyzing the surface solution, it was clear that the term of second order of smallness has a logarithmic singularity at $\varphi \to -\alpha_1(\varphi')$. The terms of the next order have still more essential singularity. It is possible to show that the ratio of the successive terms is an indefinite quantity in the surroundings of the singular point. It is possible to eliminate this divergence of expansion by the modification method of expansion, as shown in the method of PLG [5], in which the dependent and independent variables are expressed by an additional variable and are decomposed in series of ε. This gives additional freedom, which can be used to a certain extent for the control of the behavior of expansion near the singularity.

If we consider equation (1.4) for small values of τ and introduce the following approximations:

$$tg\,\tau \sim \tau, \quad \tau = \varphi^0 + \varepsilon^2 \tau^{(2)}, \quad \text{where} \quad \varphi^0 = -\varphi - \alpha_1(\varphi')$$

$$\cos\theta = 1 - \varepsilon^2 \frac{\theta^{(1)2}}{2} + \cdots, \quad \text{then we obtain}$$

$$\left(\varphi^0 + \varepsilon^2 \tau^{(2)}\right) \frac{\partial \tau^{(2)}}{\partial \varphi^0} = B^{(2)} - D^{(2)} - \varphi^0 \frac{\theta^{(1)2}}{2}.$$

This equation indicates the possibility of using the method of PLG:

Let us rewrite the equation (1.4) in the form:

$$\frac{\partial \tau}{\partial \varphi} = -\frac{(tg\tau + C)\cos\theta}{tg\,\tau} \quad , \text{ where } \quad C = B - D \; .$$

Let us introduce the auxiliary function of $f(z)$ and the variable z and change the previous equations to the equivalent system of the equations:

$$f(z)\frac{\partial \tau}{\partial z} = -(tg\,\tau + C) \; ,$$

$$f(z)\frac{\partial \varphi}{\partial z} = \frac{tg\,\tau}{\cos\theta} \; .$$

The function of $f(z)$ is selected in such a manner that the expansion for τ and φ begins with the terms $\tau^0 = z - \alpha_1(\varphi')$ and z, respectively. Thus,

$$f(z) = tg\,\tau^0 \; .$$

The principal set of equations will take the following form :

$$tg\,\tau^0 \frac{\partial \tau}{\partial z} = -(tg\,\tau + C) \; ,$$

$$tg\,\tau^0 \frac{\partial \varphi}{\partial z} = \frac{tg\,\tau}{\cos\theta} \; . \qquad (2.4)$$

All the variables can be represented in the form of the following series:

$$C = \sum_{n=0}^{\infty} \varepsilon^n C^{(n)} \; ,$$

$$\tau = \tau^0 + \varepsilon^2 \tau^{(2)} + \dots \; ,$$

$$\varphi = z + \sum_{n=1}^{\infty} \varepsilon^n \varphi^{(n)}(z) \; .$$

The functions of $C^{(n)}$ and $\cos\theta$ will be expressed by Z:

$$C^{(n)}(\varphi) = C^{(n)}(z) + \varepsilon \frac{dC^{(n)}(z)}{dz}\varphi^{(1)} + \dots$$

$$\cos\theta = 1 - \varepsilon^2 \cdot \frac{\theta^{(1)2}}{2} + \dots$$

$$\theta^{(1)}(\varphi) = \theta^{(1)}(z) + \varepsilon \frac{d\theta^{(1)}(z)}{dz}\varphi^{(1)} + \dots$$

At the same time $C^{(0)}(\varphi)=0$ and $C^{(1)}(\varphi)=0$, because the principal term of the pressure is constant along the wing. Substituting the expansions in equations (2.4), we shall have, after integration:

$$\varphi^{(1)}=0\,,\qquad \tau^{(0)}=-z-\alpha_1(\varphi')\,,$$

$$\tau^{(1)}=tg\left[z+\alpha_1(\varphi')\right]\int_{\varphi'}^{z}\frac{C^{(2)}(z)}{tg^2\left[z+\alpha_1(\varphi')\right]}\,dz\,,$$

$$\varphi^{(1)}=-\int_{\varphi'}^{z}\frac{\tau^{(1)}+\frac{\theta^{(1)2}}{2}\sin\left[z+\alpha_1(\varphi')\right]\cos\left[z+\alpha_1(\varphi')\right]}{\sin\left[z+\alpha_1(\varphi')\right]\cos\left[z+\alpha_1(\varphi')\right]}\,dz\,. \qquad (2.5)$$

It is clear from formulae (2.5) and (1.8) that it is enough to know the solution of [1] for the determination of $\tau^{(2)}$ and $\varphi^{(2)}$ in which we are interested. According to (2.5) the formulae for τ and φ will have the following form:

$$\tau=-z-\alpha_1(\varphi')+\varepsilon^2 tg\left[z+\alpha_1(\varphi')\right]\int_{\varphi'}^{z}\frac{C^{(2)}(z)}{tg^2\left[z+\alpha_1(\varphi')\right]}\,dz\,,$$

$$\varphi=z-\varepsilon^2\int_{\varphi'}^{z}\frac{\tau^{(2)}+\theta^{(1)2}(z)\sin\left[z+\alpha_1(\varphi')\right]\cos\left[z+\alpha_1(\varphi')\right]}{\sin\left[z+\alpha_1(\varphi')\right]\cos\left[z+\alpha_1(\varphi')\right]}\,dz \qquad (2.6)$$

The obtained relations enable to extend the uniform convergence of the initial solution to a small region in the surroundings of the singularity.

If we denote $d=\rho W\theta\psi$, then for the new variable Z we have:

$$\frac{\partial\varphi}{\partial z}=\frac{tg\tau}{\cos\theta}ctg\tau^0$$

The equation continuity (1.1-5) can be written in the form

$$\frac{\partial d}{\partial z}+2dctg\tau^0=0\,,$$

from which we obtain

$$d(\varphi', z) = d' \frac{\sin^2[\tau^0(z)]}{\sin^2 \tau^{0\prime}} ,$$

here ($'$) denotes that the value of the variable is taken on the shock wave or

$$\rho w \theta_r = \frac{\rho' w' \theta'_\psi \sin^2 \tau^0(z)}{\sin^2 \tau^0(\varphi')} ,$$

where, for example,

$$w' = w\big|_{z=\varphi'} .$$

After integration, it is possible to find the corrected formula for the line of flow

$$\theta = \varepsilon \sin\alpha \int_{\beta}^{\varphi'} \frac{w^0}{w^{0\prime 2}} R \frac{\sin[\tau^0(z)]}{\sin[\tau^0(z) + \varepsilon^2 \tau^{(2)}]} d\varphi' ,$$

$$R = 1 + (\theta^{*\prime} \cos\varphi' - \theta^{*\prime}_\varphi \sin\varphi') \operatorname{ctg}\alpha + \frac{\varepsilon}{\sin\alpha} (P_1^{*\prime} - P_1^* - P_2) ,$$

$$w^{0\prime} = w(\tau^0)\big|_{z=\varphi'} .$$

In this manner, the convergent solution in the whole outside region, including the critical surface and the small region around it, is performed uniformly.

3. To obtain the expansion in the whole region it is necessary to find the total inside solution.

The principal term for τ in the inside region has the form

$$\tau_i = \varepsilon^2 \tau_i^{(2)} = -\varepsilon^2 C_i^{(2)} . \qquad (3.1)$$

Consequently, $w = O(\varepsilon^2)$.

Using these relations in the exact equation (1.1) for the variables of the inside region, we obtain:

$$\frac{\partial d_i}{\partial \varphi} + \frac{2 d_i}{\varepsilon^2 \tau_i^{(2)}} = 0 \,, \qquad \frac{\partial P_i}{\partial \psi} = O(\varepsilon^2) \,,$$

$$\Delta_i = \Delta(\varphi') + O(\varepsilon^2) \,. \qquad (3.2)$$

It is clear from equation (3.2-2) that the pressure with an accuracy reaching ε^2 across the entropy layer is constant. Consequently, the value of $C_i^{(2)}$ can be determined by the pressure on the critical surface, i.e. by the value of the pressure in the surface solution, because $D_i^{(2)} \sim \varepsilon^2$ and only the term $B_i^{(2)}$ containing the pressure gradient, remains. These considerations can be applied also to the quantity $C^{(2)}$. If we investigate the asymptote from $\tau^{(2)}$ of (2.5), then on the critical surface, we have:

$$\tau^{(2)} \approx - C^{(2)}[\alpha, (\varphi')] \,.$$

So, the surface solution, performed by the method of PLG, is asymptotically coupled with the inside solution.

From equation (3.2-1), we obtain

$$d_i = d_r \exp\left[-\frac{2}{\varepsilon^2}\int_{\varphi_r}^{\varphi} \frac{d\varphi}{\tau_i^{(2)}}\right] \,,$$

Further we find that

$$\theta_i = \frac{1}{\varepsilon^2}\int_{\beta}^{\psi} \frac{d_r}{\rho \Delta \tau_i^{(2)}} \exp\left[-\frac{2}{\varepsilon^2}\int_{\varphi_r}^{\varphi} \frac{d\varphi}{\tau_i^{(2)}}\right] d\varphi \,, \qquad (3.3)$$

where d_r is determined from the condition of coupling with the surface solution in a certain section φ_r.

$$d_r = d' \exp\left[-2\int_{\varphi'}^{\Sigma_r} ctg\, \tau^\circ\, dz\right]$$

Substituting the formula for d_r in (2.9), we obtain

$$\theta_i = \frac{\sin\alpha}{\varepsilon}\int_{\beta}^{\varphi'} \frac{R}{\Delta \tau_i^{(2)}} \exp\left[-\frac{2}{\varepsilon^2}\int_{\varphi_r}^{\varphi} \frac{d\varphi}{\tau_i^{(2)}} - 2\int_{\varphi'}^{\Sigma_r} ctg\, \tau^\circ\, dz\right] d\varphi' \,, \qquad (3.4)$$

Further, taking into account (3.1) and (1.3), we will have

$$\tau_i^{(2)} = \frac{1}{\rho^{(1)} \Delta^{(0)}}\left[\sin 2\alpha \sin\varphi (\theta^* + \theta^*_{\varphi\varphi}) - P_{2\varphi}\right] \,. \qquad (3.5)$$

The calculation, performed by the formula (3.5), showed that the value of $\tau_i^{(2)}$ is negative and the first component in the square bracket is much larger than the value of $P_2\varphi$ which, in turn, is proportional to the variable φ . An analogous derivation can be obtained if the method of disturbance given in reference [1] is used for the determination of the form of the shock wave. Then, for the small values of φ , the equation of the shock wave and pressure gradient allow simple analogous representations, from which it follows that $P_2\varphi$ has a higher order of smallness in comparison to the first component in the square bracket of (3.5).

Now, taking into account (3.4) and (3.5), it is possible to draw a conclusion that $\theta_i > 0$ and $\theta_i, w \to 0$ when $\varphi \to 0$.

So, the performed solution, consisting of two asymptotic conjugated derivations, is valid in the whole region of the bad flow and totally satisfying the Fery's scheme.

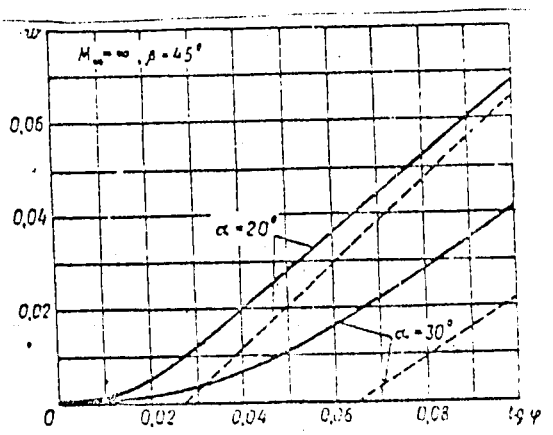

Fig. 3

The graphs of the transverse component of the velocity w at $\beta = 45°$, $M_\infty = \infty$, $\varkappa = 1.4$, $\alpha = 20°$ and 30° are shown in Fig. 3. They are calculated by formulae (2.6) and (3.5) (solid line) and by the corresponding formula of reference [1] (dashed line). The comparison shows that, without taking account of the entropy layer near the plane of symmetry, the velocity distribution on the wing at big angles of attack is appreciably decreased.

References

1. Gonor A.L. "Teoriya obtekaniya kryla giperzvukovym potokom" (Theory of hypersonic flow around a wing).--- PMM No. 3, 1970.

2. Sapunkov Ya.G. "Giperzvukovoe ovtekanie kruglogo konusa pod uglom ataki" (Hypersonic flow around a circular cone under an angle of attack).--- PMM, 27 (1), 1963.

3. Sapunkov Ya.G. "Kruglovoi konus pod uglom ataki v giperzbukovom potoke gaza" (Circular cone under an angle of attack in a hypersonic gas flow).--- PMM, 27 (5), 1963.

4. Van-Daik "Metody vozmushchenii v mekhanike zhidkosti" (Methods of disturbances in fluid mechanics).--- Mir, 1967.

5. Tsyan-Syue-Sen', "Metod Puankare-Laitkhilla-Go" (Method of PLG).--- Sb.: "Problemy mekhaniki", (Edited by Draiden and Karman); issue P, Moskva IL, 1959.

6. Cheng H.K. Hypersonic shock layer theory of a yawed cone and other three dimensional pointed bodies. WADC 2 TN, N 59-335, Dec., 1959.

7. Melnik R.E., R.A. Sheuing, Shock layer structure and entropy layers in hypersonic conical flows, progress Astronaut, and Roketry, Vol. 7, New-York-London, Acad. Press., pp. 379-420, 1962.

8. Munson A.G., The vortical layer an inclined cone, J. Fluid mech., 625-643, 20, 1964.

ABOUT THE MODE OF FLOW AROUND V-SHAPED WINGS WITH SUPERSONIC LEADING EDGES

By

V.I. Lapygin

It was shown by experimental investigations [1,2] that on flowing around V-shaped wings, a complex system of shock waves is formed in the field of the flow. In the present work, a system of shock waves formed on flowing around a V-shaped wing by an ideal gas, is investigated by means of performing numerical calculations on the EVM BESM-6, using the method discussed in reference [3]. We shall consider the flow around a V-shaped wing at an angle of attack α (Fig. 1). In the conical coordinates $\xi = \ln x$, $\zeta = y/x$, $\eta = z/x$ the system of equations of gas dynamics (for an ideal gas) in the divergent form will be as follows:

$$\frac{\partial f}{\partial \xi} + \frac{\partial}{\partial \zeta}(F^y - \zeta f) + \frac{\partial}{\partial \eta}(F^z - \eta f) + 2f = 0 \quad , \qquad (1)$$

where

$$f = \begin{Bmatrix} \rho u \\ p + \rho u^2 \\ \rho u v \\ \rho u w \\ E \end{Bmatrix} , \quad F^y = \begin{Bmatrix} \rho v \\ \rho u v \\ p + \rho v^2 \\ \rho v w \\ E v/u \end{Bmatrix} , \quad F^z = \begin{Bmatrix} \rho w \\ \rho u w \\ \rho v w \\ p + \rho w^2 \\ E w/u \end{Bmatrix} ,$$

$$E = \rho u \left(\frac{\varkappa p}{(\varkappa - 1)\rho} + \frac{u^2 + v^2 + w^2}{2} \right) , \quad \varkappa = c_p / c_v .$$

here u, v, w are the components of the velocity vector on the axes x, y, z; p and ρ are the pressure and density.

Using the condition that the supersonic flow around a V-shaped wing is a conical flow, the method of determining ξ with the use of the difference scheme proposed in reference [5] is used for the numerical integration of system (1). The calculations were performed for different values of χ and M_∞. The analysis of the performed

calculations allowed to reveal several modes of flow around as a function of the expansion angle of the V-shaped wing, with qualitatively different systems of shock waves from one shock wave attached to the leading edge of the wing to a system of four waves and more. In particular, the performed calculations showed that there are flow modes with a reflection of a strong shock from the symmetry plane of the wing. In the plane case, as it is known, a strong reflected shock is not realized. The marks used in the text are clear from the consideration of Fig. 1.

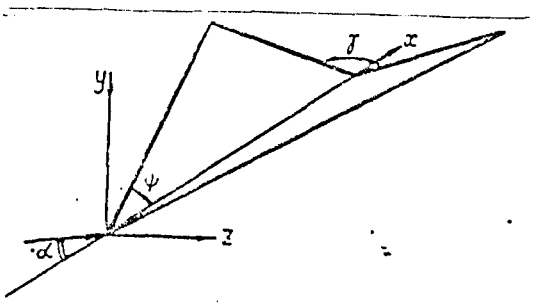

Fig. 1.

The results of the calculation for $\varphi = 29°30'$, $M_\infty = 3.95$, angles of γ from 100° to 150°, $\alpha = 15°$ and $\gamma = 160°$, $\alpha = 10°$, are represented in Figs. 2 and 3. The values of the parameters $\gamma = 160°$ and $\alpha = 10°$ correspond to a flow around with a mode close to the outgoing shock wave. The forms of the shock waves are given in Fig. 2, and the distribution of the pressure coefficient $C_p = (P - P_\infty)/q_\infty$ on the wall $(q_\infty = \frac{1}{2}\rho_\infty V_\infty^2)$. is given in Fig. 3. In the graphs, z is the distance from the plane of symmetry to the given point on the wall of the wing, R is the distance from the plane of symmetry to the leading edge.

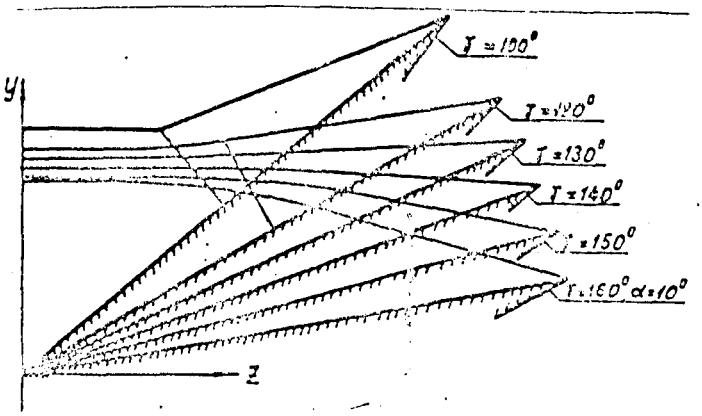

Fig. 2.

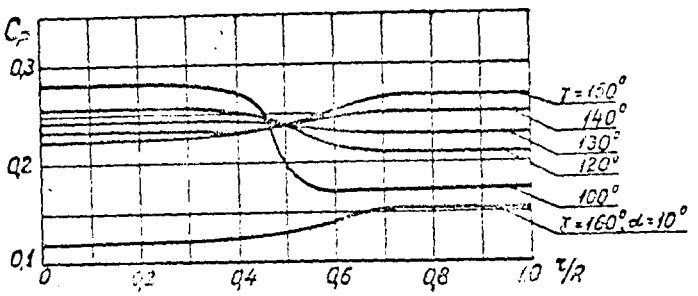

Fig. 3.

The values given below in the graphs and tables are dimensionless. These values are namely: the component of the velocity vector, relative to the modulus of the velocity vector of the undisturbed flow; the pressure, relative to the doubled dynamic pressure of the undisturbed flow; the density, relative to the density of the undisturbed flow.

On treating the results of the numerical calculations, the position of the shock wave is determined as the region of the sudden variation of the parameters of the flow. The results of the calculation of the configuration of the shock waves are represented in Fig. 2.

The relations of $Cp = f(r/R)$ are given in Fig. 3, and the analysis of the field of flow, performed for different angles of γ at $M_\infty = 3.95$, show that with decreasing γ, a transition from a flow around with a convex shock wave, through a mode of a plane shock [4], to a flow around with a concave shock wave occurs. In the case of the existence of the concave shock wave, an increase of the pressure takes place towards the center of the wing. At $\gamma = 120°$, this increase can already be identified by the presence of an internal shock wave; i.e., the flow around a V-shaped wing occurs with a formation of Mach configuration of the shock waves. The question about the formation of an internal shock wave at once at the transition from a mode of a flow around with a plane shock to a flow around with a concave shock wave, remains open. As an example, the field of the isobar for $\gamma = 120°$ and $\alpha = 15°$ is given in Fig. 4. The character of the isobar indicates the flow around with a Mach configuration of the shock waves. The position of the plane shock, formed on the leading edge, is represented by a dashed line in Fig. 4.

On decreasing the angle γ to 40°, the character of the isobars (Fig. 5a) indicates a regular reflection of the shock, incident from the leading edge, from the plane of symmetry of the wing. It is known that the reflection is theoretically possible with both a strong and weak reflected shock, but in the plane case, the reflection with a strong shock is not realized. In the present work, to determine

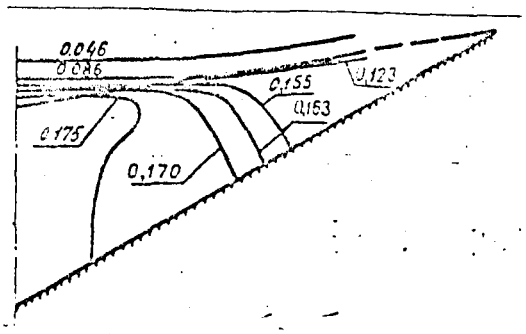

Fig. 4.

the type of the reflected shocks, and also the character of the reflection (regular or Mach), the results, obtained by numerical calculation, are compared with the calculation of the system of the shock waves performed by the formula of the oblique shock. Such analysis showed that for $\gamma = 40°$ and $\alpha = 15°$, a regular reflection of the plane shock, incident from the leading edge, from the plane of symmetry of the wing, occurs with a strong reflected shock. In this case, the values of the density and pressure, obtained in the numerical calculation and by the formula of the oblique shock, differ by not more than 2%. The system of the shock waves in that case is given in Fig. 5a by a dashed line.

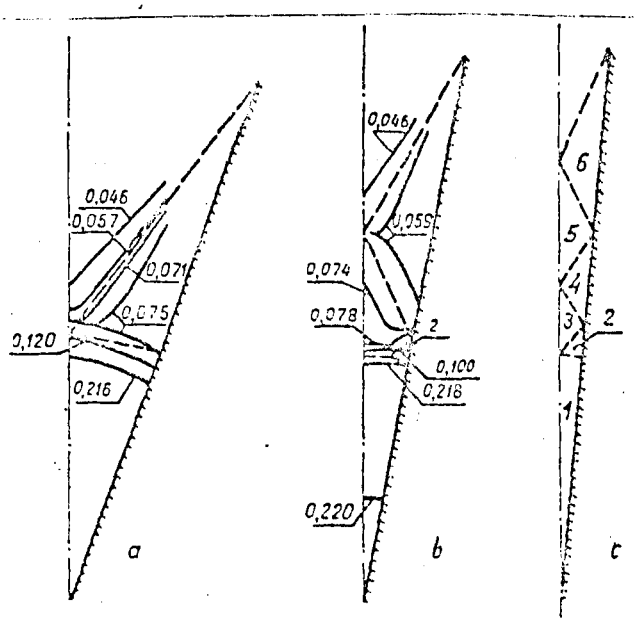

Fig. 5.

With decreasing the angle γ, the system of the shock waves, formed on flowing around the wing, is changed, and at $\gamma = 20°$, the field of the isobars (Fig. 5 b) indicates the presence of a shock wave, reflected from the plane of the wing. The comparison with the calculation performed by the formula of the oblique shock, showed that a system of shocks is realized. This system is represented in Fig. 5 b by the dashed lines, and namely: the incident shock wave, from the leading edge, is reflected from the plane of symmetry of the wing by the regular way with a weak wave which is regularly reflected from the plane of the wing with a weak reflected wave. The latter is reflected from the plane of symmetry with the formation of a Mach configuration. As for $\gamma = 40°$, the difference of the values of the veclocity, density and pressure obtained by the numerical means and by the formula of the oblique shock did not exceed 2%.

With further decrease of the angle γ ($\gamma = 10°$), the number of reflections from the plane of the wing and the plane of symmetry is increased. In this case, the last reflection from the plane of symmetry is regular with a strong reflected shock. All the rest reflections, observed in that case, are regular with weak reflected shocks. The system of the shock waves is given in Fig. 5 c. The difference of the values of velocity, density, pressure, obtained by the numerical means and by the formula of the oblique shock, as for the previous variant, did not exceed 2%. It is necessary to mention that in the numerical calculation, the region of the flow, designated in Fig. 5 b, c by the number 2, is poorly studied and is not practically defined in view of the small number of the points of the calculated net, falling in it. This case is caused by the small dimensions of the region 2, in comparison with the calculated region of the flow. As an example, the results of the numerical calculation are given in Table 1, and the results, obtained by the formula of the oblique shock are given in Table 2 for $\gamma = 10°$.

Table 1

Номер области ①	u	v	w	p	ρ
1	0,8946		0	0,223	3,004
2					
3	0,9500	-0,2143	0	0,0788	1,444
4	0,9838	-0,2278	-0,01994	0,0878	1,320
5	0,9574	-0,2394	0	0,0598	1,211
6	0,9617	-0,2494	-0,02183	0,0522	1,098

Key:
1) Region number.

Table 2

Номер области ①	u	v	w	p	ρ
1	0,8995	-0,00579	0	0,222	3,020
2	0,9472	-0,2017	-0,01759	0,0889	1,577
3	0,9507	-0,2169	0	0,0764	1,443
4	0,9544	-0,2283	-0,01998	0,0678	1,325
5	0,9576	-0,2403	0	0,0599	1,213
6	0,9617	-0,2494	-0,02184	0,0522	1,099

Key:
1) Region number.

As evident from the comparison of the tables, the coincidence of the results of the performed calculations is good, which allows to establish uniquely the system of the shock waves formed on flowing around a wing. The numbers of the regions mentioned in the tables, correspond to the numbers mentioned in Fig. 5 c. The values of u, v, w, p, ρ for the region 2 are not given. The values of components of the velocity v for the region 1 (Fig. 5 c) in Table 1 are not given, because in this region the velocity V smoothly decreases to v = 0 on the X-axis.

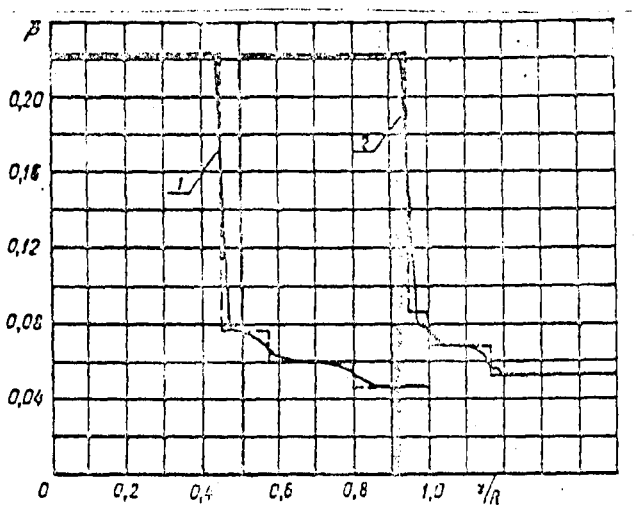

Fig. 6.

The relations $P = P/2q_\infty$ on the axis of symmetry (1) and on the wall of the wing (2), obtained in the numerical calculation, for $\gamma_1 = 10°$, $\alpha = 15°$, $\varphi = 29° 30'$, $M_\infty = 3.95$ are given in Fig. 6. In this figure, the ratio (x/A) for the axis of symmetry is the ratio of the distance from the intersection point of the planes of the wing to the flowing point on the axis of symmetry to the value of the projection of the leading edge on the plane of symmetry. The dashed lines represent the solution obtained by the formula of the oblique shock for the system of the shock waves shown in Fig. 5 c. The character of the curves confirms the existence of the system of the shock waves mentioned above.

The relation, given in Fig. 6, shows an enough big spreading of the fronts of the shock waves at the points of regular reflection. This is related, on one hand to the presence of two fronts, the spreading of which is increased approximately twice in comparison with a single front, and, on the other hand, to the small intensity of the shock waves.

Calculations of the flow around a V-shaped wing at $\gamma = 140°$, $\alpha = 15°$, at different values of Mach number M_∞, were also performed. The results of these calculations are not given here. The analysis of the calculations showed that with increasing the Mach number M_∞, a transition occurs from a flow around the wing with a convex shock wave to a flow around with a concave shock wave and Mach configuration, i.e., the transition is qualitatively as on flowing around at $M_\infty = \text{const}$ with decreasing γ and with values of γ that are not too small. In this case, at $\gamma = 140°$ a regular reflection is not observed for any Mach number M_∞ up to $M_\infty = \infty$, and a system of shock waves of Mach type is realized. In this manner, the performed analysis shows that at sufficient big angles of γ (in the considered case for $\varphi = 29° 30'$ the angle $\gamma \geq 80$–$100°$), a complex system of a large number of shock waves is not realized, and namely these angles are of greatest practical importance on constructing aircrafts with high aerodynamic quality.

The results obtained in the present work agree qualitatively well with the experimental investigations given in reference [1].

The author is grateful to A.L. Gonor for suggesting the problem and for his attention to the work.

References

1. Gonor A.L., A.I. Shvets. "Obtekanie V-obraznykh kryl'ev sverkhzvukovym potokom pri chisle M = 3.9" (Supersonic flow around V-shaped wings at Mach number M = 3.9). Izv. AN SSSR, MZhG, No. 6, 1967.

2. Gonor A.L., A.I. Shvets. "Issledovanie sistemy skachkov uplotneniya pri obtekanii zvevdoobraznykh tel" (Investigation of a system of shock waves on flowing around star-shaped bodies).--- Izv AN SSSR, MZhG, No. 3, 1966.

3. Lapygin V.I. "Raschet statsionarnogo obtekaniya v-obraznykh kryl'ev metodom ustanovleniya" (Calculation of stationary flow around V-shaped wings by the method of adjustment).--- Izv. AN SSSR, MZhG, No. 3, 1971.

4. Maikapar G.I. "O volnovom soprotivlenii neosesimmetrichnykh tel v sverkhzvukovom potoke" (About shock wave drag of non-axisymmetric bodies in a supersonic flow).--- PMM, vol. 23, No. 2, 1959.

5. Rusanov V.V. "Raschet vzaimodeistviya nestatsionarnykh udarnykh voln s prepyatstviyami" (Calculation of the interaction of nonstationary shock waves with obstacles).---Zh. vych. mat. i mat. phiz., vol. 1, No. 2, 1961.

QUASI-ONE-DIMENSIONAL THEORY OF THE INTERACTION OF A TURBULENT WAKE WITH A SUPERSONIC FLOW IN A CANAL AND JET

By

L.V. Gogish and G.Yu. Stepanov

Interactions of the turbulent layer of a flow with the outside flow are observed for outside flow around aircrafts, flow in canals, nozzles, diffusers, gratings of the blade engines. These interactions determine to a considerable degree the properties of these apparatus and installations.

Starting with the work of Krokko and Liz [1], the investigation of the interaction of the turbulent layer with the outside flow is performed by the integral methods of the theory of the boundary layer. These methods are used together with an assumption of the profile of the velocity in the turbulent layer. They secure a satisfactory coincidence of the calculated pressure distribution in the region of the interaction with the experimental data.

Due to the complexity of the phenomena, occurring during the interaction, the most simple of these phenomena are studied experimentally and theoretically, such as the flow around a step (projection) with a plane supersonic flow or the interaction of a shock with a turbulent layer, when the outside flow is represented by a simple wave (Prandtl-Maier flow). The respective theoretical solutions in which the outside nonviscous flow is described by the Prandtl-Maier functions are actually one dimensional, which considerably decreases the calculation difficulties connected with their derivation.

However, it is found that these simple solutions are insufficient for application. Great attention is paid to many practical problems, for example to the calculation of the interaction of flows arising from the flow around a step with a supersonic free jet (Fig. 1a) or in a canal at its sudden widening (Fig. 1b). In these cases, in the outside nonviscous flow, a complex and previously unknown structure of shocks and rarefaction waves exists. Such a structure interacts with the layer and determines its growth on the whole length up to the so-called choking cross-section (wake throat). The use of exact methods for the calculation of such nonviscous flows is associated with a big waste of time and effort and is inadequate for an approximate (essentially not one-dimensional) description of the flow in the layer.

A simple approximate method of the calculation of the flows, represented in Fig. 1 a and b, is discussed below. In this method, the average quasi-one-dimensional method of the description of complex nonviscous flow and the method of the one-parametric turbulent layer or wake* are used simultaneously.

---

* The wake differs from the more general case of the layer by the absence of friction on the wall limiting the flow.

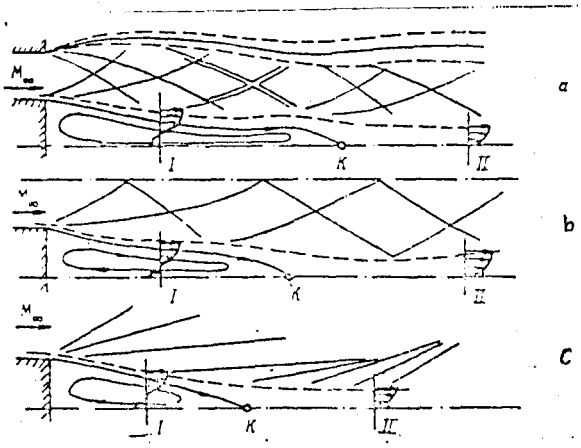

Fig. 1

To complete the discussion, the previously obtained solutions of the more simple limiting problem of flow around a step by a steady supersonic flow in the presence of a single shock or a rarefaction wave, incident on the neighbouring wake, and a blowing into the bottom region [2-6], are briefly described.

It was ascertained on the basis of the experimental data that, in the separating flows (Fig. 1) directly behind the end, an isobaric bottom region is arranged; the flow of interaction is strictly studied, starting from a certain arbitrary "lacing" cross-section I up to the choking cross-section, the wake throat II, behind which the whole flow can be considered supersonic. In the limits of the, integral methods of the boundary layer theory applicable here, one-parametric family of solutions is obtained. These solutions describe the flow of the interaction at a finite distance from the end. The condition of the selection of the real solution lies in the fact that this solution must be a singular one (must pass by the saddle point, corresponding to the physical throat of the wake).

1. The One-Parametric Turbulent Wake

In the general case, the turbulent wake is characterized by the profiles of the velocity and temperature. These profiles comprise a finite number of free parameters n_i ($i = 1, 2, \ldots$), the values of which determine the character of flow in the wake. As a result of the calculation of the interaction, the functions of the longitudinal coordinate x, the characteristic width of the wake $\delta(x)$, the parameters of the profile of velocity $n_i(x)$, the parameters of the outside nonviscous flow on the boundary of the wake, the value of the velocity $C(x)$ and its inclination to the X axis must be determined in the plane of flow.

In the integral methods of calculation, the turbulent wake is defined only by the integral values, generalized by the dimensionless widths of the displacement H_K^*, the loss of momentum H_K^{**} and the friction Δ_K ($K = 0, 1, 2, \ldots$). For the determination of the unknown functions, different integral relations of the boundary layer and other auxiliary equations, and in particular the conditions on the axis of symmetry of the wake, are used [2, 4]. The existence of a certain arbitrariness in the selection of the number of the parameters and the form of equations leads to a certain difference in the results, specially, if the number of the equations is small.

In the practice of the calculations in reference [4], a one-parametric profile of the velocity $\bar{u} = \bar{u}(\bar{y})$ in the free turbulent layer and wake was taken.

$$\frac{u}{u_\delta} = 1 - m f(\bar{z}), \quad f(\bar{z}) = \frac{u_\delta - u}{u_\delta - u_0}, \quad m = \frac{u_\delta - u_0}{u_\delta}, \quad \bar{z} = \frac{y}{\delta} . \qquad (1.1)$$

The indices "δ" and "0" refer to the parameters on the boundary of the wake $y = \delta$ and on its axis $y = 0$, respectively.

As most simple equations, describing the flow in the one-parametric turbulent wake, the equation of momentum and the condition on the axis of symmetry are taken:

$$(j+1)\frac{d}{dx}\ln\delta^{**} + (2 + H - M^2)\frac{d\ln C}{dx} = 0 , \qquad (1.2)$$

$$\rho_0 u_0 \frac{du_0}{dx} + \frac{dp}{dx} = (j+1)\left(\frac{\partial \tau}{\partial y}\right)_0 , \qquad (1.3)$$

in which $j = 0$ in the plane case, $j = 1$ in the axisymmetric case, $C = u/u_{max} = M\left(\frac{2}{\chi - 1} + M^2\right)^{-\frac{1}{2}}$ is the reduced velocity of the outside flow on the boundary of the wake $\delta(x)$. The turbulent tangential stress τ is expressed by the Prandtl formula.

$$\tau = \rho \nu_t \frac{\partial u}{\partial y} , \quad \nu_t = \varkappa (u_\delta - u_0)\delta , \quad \varkappa = const .$$

Taking account of (1.1)

$$\tau = -\rho_\delta u_\delta^2 \varkappa m^2 \frac{df(\bar{z})}{d\bar{z}} \frac{\rho}{\rho_\delta} , \quad \left(\frac{\partial \tau}{\partial y}\right)_0 = (-a\varkappa)\rho_\delta u_\delta^2 \frac{m^2}{\delta} \frac{1 - C^2}{1 - C^2(1-m)^2} . \qquad (1.4)$$

here $a = (d^2 f/d\zeta^2)_0$, the value $(-a\varkappa)$ is a free parameter (0.012 for the neighbouring plane wave). The parameter $H = H^*/H^{**}$, where

$$H^* = \left(\frac{\delta^*}{\delta}\right)^{j+1} = (j+1)\int_0^1 \left(1 - \frac{\rho u}{\rho_\delta u_\delta}\right)\zeta^j d\zeta$$ is the reduced

width (area) of the displacement,

$$H^{**} = \left(\frac{\delta^{**}}{\delta}\right)^{j+1} = (j+1)\int_0^1 \frac{\rho u}{\rho_\delta u_\delta}\left(1 - \frac{u}{u_\delta}\right)\zeta^j d\zeta$$ is the reduced

width (area) of the loss of momentum; all are tabulated functions of the parametric form m of the profile of velocity in the wake and of the numbers of C or M on its outside boundary.

It is suitable to select either the absolute width $\delta(x)$, or the integral width $\delta^*(x)$ of the displacement, as the characteristic width of the turbulent wake. These represent the principal parameter of the interaction of the viscous and nonviscous flow, since the surfaces $y = \delta(x)$ or $y = \delta^*(x)$ can be considered as lower boundaries for the outside nonviscous flow.

Equations (1.2) and (1.3), after transformation, take the form:

$$\frac{\partial \ln H}{\partial m}\frac{dm}{dx} + \left[\frac{\partial \ln H}{\partial \ln C} - (2 + H - M^2)\right]\frac{d\ln C}{dx} = (j+1)\frac{d\ln \delta^*}{dx}, \qquad (1.5)$$

$$\frac{dm}{dx} + \frac{m(2-m)}{(1-m)(1-C^2)}\frac{d\ln C}{dx} = -(j+1)(-a\varkappa)\frac{m^2}{1-m}\cdot\frac{(H^*)^{\frac{2-j}{2}}}{\delta^*}. \qquad (1.6)$$

In the two equations (1.2) and (1.3), there are three unknown functions of x: m, C and δ.

In order to close the problem, it is necessary to build an additional system of equations for the nonviscous flow. For this purpose, the equation of continuity in the form of Krokko-Liz [1] is used for the most simple case of an isoentropic plane Prandtl-Maier flow. This equation has the form:

$$\frac{d}{dx}\int_0^\delta \rho u\, dy = (\rho u)_\delta\left(\frac{d\delta}{dx} - \operatorname{tg}\theta_2\right), \qquad (1.7)$$

where $\theta = \nu(C_\infty) - \nu(C)$ is the angle of inclination of the nonviscous flow on the boundary of the viscous layer $\delta, \nu(C)$ is the Prandtl-Maier function.

Taking into account that $\int_0^\delta \rho u dy = (\rho u)_\delta (\delta - \delta^*)$, the equation (1.7) can be written in the form

$$\frac{d\delta^*}{dx} = (\delta - \delta^*) \frac{d \ln (\rho u)_\delta}{dx} + tg\, \theta_\delta \,. \qquad (1.8)$$

In this case equations (1.5), (1.6) and (1.8) form a closed system; its solutions describe the flow of interaction in the plane turbulent neighbouring wake.

Equation (1.8) differs from the known Prandtl equation:

$$\frac{d\delta^*}{dx} = tg\, \theta_{\delta^*} \,, \qquad (1.9)$$

which is usually applied to perform more accurate calculation of the velocity distribution on the outside limit of the boundary layer. It is possible to show that equations (1.8) and (1.9) agree with the accurate boundary layer theory.

From the point of view of calculation, the difference between the equations of Krokko-Luz (1.7) and Prandtl (1.9) is connected only with the selected boundary $y = \delta(x)$ or $\delta^*(x)$, for which the parameters of the nonviscous flow are given.

2. Flow Behind the Step in Unbounded Flow

In references [4, 5], a system of the equations (1.5), (1.6) (at $j = 0$) and (1.8) is applied for the investigation of plane flow in the turbulent neighbouring wake behind the step (Fig. 1 c). Solving this system of equations relative to the derivatives of the functions $\delta(x), m(x)$ and $C(x)$ we obtain:

$$\frac{d \ln \delta}{dx} = \frac{\Delta_1}{\Delta} \,, \quad \frac{dm}{dx} = \frac{\Delta_2}{\Delta} \,, \quad \frac{d \ln C}{dx} = \frac{\Delta_3}{\Delta} \,, \qquad (2.1)$$

where

$$\Delta = -\frac{\delta(1-m)}{(-\alpha\varkappa)m^2}\left[\Delta_2 + \frac{m(2-m)}{(1-m)(1-C^2)}\Delta_3\right]$$

$$\Delta_1 = -\left[\frac{\partial \ln H^{**}}{\partial m}\Delta_2 + \left(\frac{\partial \ln H^{**}}{\partial \ln C} + 2 + H - M^2\right)\Delta_3\right]$$

$$\Delta_2 = \frac{tg\,\theta}{(-\alpha\varkappa)m^2 H^*}\,\frac{m(2-m)}{1-C^2} + \frac{\partial \ln H}{\partial \ln C} - \left(\frac{1-M^2}{H^*} + H + 1\right)$$

$$\Delta_3 = -\left[\frac{tg\,\theta}{(-\alpha\varkappa)m^2 H^*}(1-m) + \frac{\partial \ln H}{\partial m}\right] .$$

The system of equations (2.1) is reduced to one differential equation concerning $m = m(c)$

$$\frac{dm}{d\ln C} = \frac{\Delta_2}{\Delta_3} \qquad (2.2)$$

and the two first integrals.

At the given parameters C_∞ and $(\alpha\varkappa)$ equation (2.2) has a singular solution, passing by the singular saddle point. The coordinates of this point in the plane (m, c) are determined by the equations $\Delta_2 = \Delta_3 = 0$ (Hereby, simultaneously, $\Delta_1 = \Delta = 0$) . As was shown in the work [4], the singular solution corresponds to the flow in the undisturbed neighbouring wake, and the singular point corresponds to its throat. The nonsingular integral curves of the system (2.1) or the equations (2.2) describe the flows of the interaction of the turbulent wake with the supersonic flow in the physical plane or in the plane (m, c) in the existence of isentropic shocks or rarefaction waves, disturbing the neighbouring wake.

The initial conditions for the system (2.1), $\varkappa = \varkappa^\circ$, $\delta = \delta^\circ$, $m = m^\circ$ and $C = C^\circ$, are determined as a result of the gluing in cross section I (Fig. 1) of the flow of the interaction in the wake with the isobaric flow of the displacement in the bottom region, on the basis of certain integral conditions. The

continuity of the absolute width δ of the layer and the displacements δ^* and also the conservation of the mass of the gas in the bottom region were taken in the works [4, 5] as such conditions. In this case, the initial value of the parametric form m°, the length of the isobaric bottom region x° and the initial width of the neighbouring wake δ° are determined as a function of the, beforehand, unknown bottom pressure p° and the given blowing parameter B by the equations:

$$\frac{1-H^*(m,C^\circ)}{G(m,C^\circ)} = \frac{1-H^*(1,C^\circ)}{H^{**}(1,C^\circ)} \frac{1}{1-B} , \qquad (2.3)$$

$$x^\circ = \left\{ \beta^\circ (\cos\theta^\circ)^{-1} H^{**}(1,C^\circ) \frac{H^*(m,C^\circ)}{G(m,C^\circ)} (1-B) + tg\,\theta^\circ \right\}^{-1} , \qquad (2.4)$$

$$\delta^\circ = \left[H^*(m,C^\circ) \right]^{-1} (1 - x^\circ tg\,\theta^\circ) \qquad (2.5)$$

In equations (2.3) – (2.5), B and G are denoted as follows:

$$B = \frac{(\rho u)_{BA}}{(\rho u)_\infty} \left[\beta^\circ H^{**}(1,C^\circ)(\cos\theta^\circ)^{-1} x^\circ \right]^{-1} ,$$

$$G = -\int_0^{z_*} \frac{\rho u}{(\rho u)_\delta} dz , \quad f(z_*) = m^{-1} ,$$

where G (m,c)— the relative rate of the returning flow in the wake $(0 < z < z_*)$, B – the blowing parameter, β — the empirical coefficient of the expansion of the isobaric turbulent jet.

The value of the bottom pressure p° (and its corresponding velocity C° of the outside flow) is found from the condition of the realization of the singular solution of equation (2.2), for which the initial condition m° is determined from equation (2.3).

For simplicity of calculation, it was assumed that there is no initial boundary layer in the step. The location of the outside boundary of the isobaric mixing layer $y_1 > 0$ with respect to the boundary streamline of the equivalent nonviscous flow (Y = 0) was simply determined, as for the ordinary boundary layer, by the formula $y_1 = \delta - \delta^*$ (for the unbounded flow behind the step, from the condition of the conservation of momentum $y_1 = \delta - \delta^* - \delta^{**}$; in the bounded flow, this condition is complicated and for supersonic velocities $(\delta^{**} \ll \delta^*)$ it can be disregarded.

If the equation of continuity (1.9) is used in the form of Prandtl, then the continuity of the width δ^{**} of the momentum loss must be used instead of the condition of continuity of the absolute width δ of the layer (taking account of the returning flows).

$$\delta H^{**}(m,C) = \delta(\cos\theta)^{-1} H^{**}(1,C) \times \qquad (2.6)$$

Then equation (2.3) will have the form:

$$H^{**}(m,C^{\circ}) = \frac{C(m,C^{\circ})}{1-B} \qquad (2.7)$$

Formulae (2.4) and (2.5) will be written in the previous form.

The value of the free parameter $(-a\varkappa)$ of essentially constant turbulence depends on the assumed equations, gluing conditions and the profile of the velocities. The above-mentioned value of $(-\varkappa) = 0.012$, was selected in work [4] from the comparison of the calculated and experimental data with respect to the bottom pressure P° behind a plane step in the condition of gluing of δ and with a profile of velocity (1.1) at $f(\eta) = 1 - 3\eta^2 + 2\eta^3$ [3].

For plotting the dependence of the relative bottom pressure p°/p_{∞} behind a plane step in an unbounded supersonic flow on the Mach number M_{∞} of the undisturbed flow and the blowing parameter $\bar{\rho}u = (\rho u)_{BA} / (\rho u)_{\infty}$, it is sufficient to use the family of the singular integral curves of the equation (2.2) $m_1(C, C_{\infty})$ and the family of the solutions of equation (2.3) or the curves of the initial conditions $m_2(C, B)$. The intersections of these curves determine the two-parametric relation $C^{\circ}(C_{\infty}, B)$ or $p^{\circ}/p_{\infty}(M_{\infty}, \bar{\rho}u)$ represented in Fig. 2.

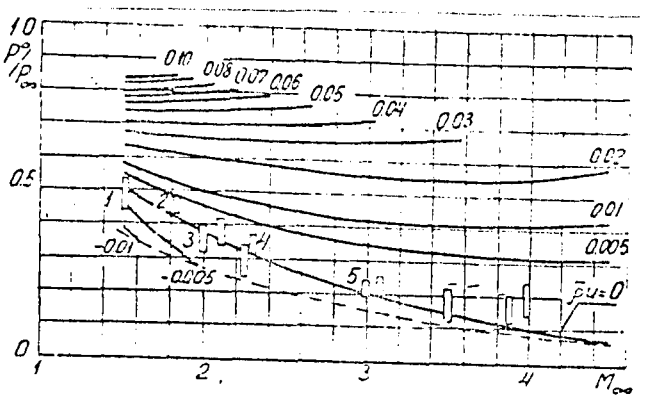

Fig. 2

The calculated curves of Fig. 2 satisfactorily agree with the experimental data in the case of existence of blowing ($\overline{\rho u} > 0$) or suction ($\overline{\rho u} < 0$), however, for clarity, the results of experiments (taking account of the dispersion of the data of the different authors), related only to flows with $\overline{\rho u} = 0$ are given in the graph, i.e., in the case of absence of blowing (suction). The curves in Fig. 2 are limited at certain maxima of blowing and suctions. The first limitation is related to the accepted assumption of the isobaric flow of the displacement in the zone of separation and, in principle, it can be removed if the interaction of supersonic and secondary subsonic flows is studied. The second limitation is more essential and is related to the existence of a limiting line for the solutions of the system (2.1) when the denominator in the right sides of the equations vanishes:

$$\Delta(m, c) = 0$$

or

$$\frac{\partial \ln H}{\partial \ln c} = \frac{1-M^2}{H^*} - 1 - H - \frac{m(2-m)}{(1-c^2)(1-m)} \frac{\partial \ln H}{\partial m} = 0 ,$$

which indicates the impossibility of the existence of separating flows, if the flow rate exceeds a certain critical value.

In Fig. 3, the calculated distributions of the pressures $p = p(x)$ on the axis of the neighbouring wake, are compared with the experimental data at different Mach numbers M_∞ of the supersonic flow in front of the step:

1 - $M_\infty = 1,56$ 2 - $M_\infty = 1,84$

3 - $M_\infty = 2,03$ 4 - $M_\infty = 2,30$

5 - $M_\infty = 3,02$

The numbers correspond to experimental data from the five different sources shown in the work [4].

The family of the nonsingular integral curves of equations (2.1) or (2.2) corresponds to the different flows in the neighbouring wake. These flows are disturbed by a shock or a rarefaction wave at finite distances from the beginning of the wake. They are represented by segments of nonsingular integral curves, which can be studied directly, or jointed with segments of other singular curves.

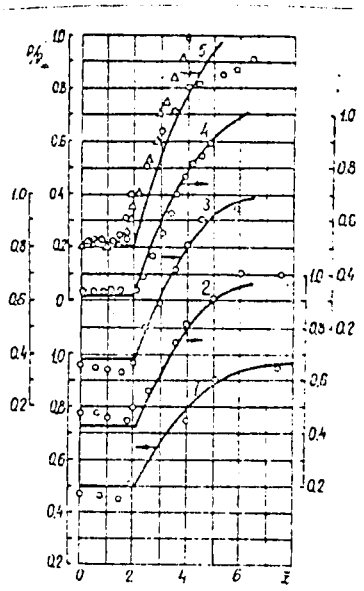

Fig. 3

The flow in neighbouring wake, disturbed by a shock wave of finite intensity $\delta_s > \delta_{s*}$, has two values. For given boundary conditions of the Mach number M_∞ in front of the step, the intensity of the shock δ_s and the place of its location in the wake x_s two possible flows exist in the neighbouring wake. These flows are characterized by the values of the bottom pressure p_1° and p_2° which can be arbitrarily called the strong and weak disturbances. This corresponds to hysteresis in physical flows of such a type. In the case of existence of blowing or suction in the bottom region, the flow in the neighbouring wake is two-valued in the whole range of the values of the bottom pressure $p_1^\circ < p^\circ < p_2^\circ$ The flow in a wake with blowing in the bottom region can be studied as quasi-steady, when the wake acts as a source or drain for the subsidiary flow rate, and the bottom region becomes a storage for the mass. On this basis, a series of change of the parameters of the bottom region was performed in the work [5]. This region supposedly characterizes the low-frequency oscillations in the wake. Such oscillations are really observed, and their amplitude and frequency in one example satisfactorily agreed with the calculated values.

3. Quasi-One-Dimensional Equations of the Supersonic Jet

For the approximate quasi-one-dimensional method of calculation of plane and axisymmetric thin jets, having a small curvature, of a nonviscous gas, all the parameters f of the flow (ρ, ρ the longitudinal u and transverse v velocity components) are assumed continuous and slightly changing across the

cross-section of the jet, x = const. At the boundaries of the jet the parameters at $y = y_0$ and $y = y_1$ are marked by f_0 and f_1, respectively. The variation of all tthe parameters $f - f_0$ and also the value of v are considered small of the first order.

Applying the operation of averaging to the analytical functions of the parameters of flow, it can be ascertained that the mean value of a function, correct up to the squares of the small quantities, is equal to the same function from the average values of the arguments. In particular, for the mean parameters with the mentioned exactness, the usual gas dynamic relations of one-dimentional flows hold; at the same time, taking into account the small value of v, it can be assumed that $\langle c \rangle^2 \approx (\langle u \rangle / \langle u_{max} \rangle)^2$

$$tg\,\theta_i = dy_i/dx = v_i/u_i \approx v_i/\langle u \rangle \qquad (i = 0,1) \quad etc.$$

The differential equations of motion after averaging with respect to y are reduced to the ordinary ones with respect to x, which is the main purpose of the developed approximate method. On the basis of a special investigation and of the practice of calculations, it was advisable to use the following system of equations (the signs of averaging are omitted):

equation of continuity

$$\frac{d}{dx}\left[(y_1^{j+1} - y_0^{j+1})\rho u\right] = 0 , \qquad (3.1)$$

equation of momentum in the longitudinal direction

$$\frac{d}{dx}\left[(y^{j+1} - y_0^{j+1})(p + \rho u^2)\right] = (j+1)\left[p_1 y_1^j \frac{dy}{dx} - p_0 y_0^j \frac{dy_0}{dx}\right] , \qquad (3.2)$$

equation of momentum in the transverse direction

$$\frac{d}{dx}\left[\rho u v (y_1^{j+1} - y_0^{j+1})\right] = (j+1)\left[(p - p_1) y_1^j - (p - p_0) y_0^j\right] , \qquad (3.3)$$

equation of the boundaries of the jet

$$dy_i/dx = v_i/u , \quad i = 0,1 \qquad (3.4), (3.5)$$

Equations (3.3), with the above-mentioned accuracy, can be divided into two equations with respect to dv_1/dx and dv_2/dx; (This physically corresponds to the division of the jet into two and to the application of each of them of the equation of momentum at the step change $v = v(y)$).

Performing this division and solving the equations with respect to the derivatives, we obtain, after some transformations, a system of six equations. This system describes the gas flow in the nonviscous curvilinear jet.

$$dy_0/dx = v_0/u \quad , \quad dy_1/dx = v_1/u \quad , \qquad (3.6),\ (3.7)$$

$$\frac{du}{dx} = (j+1)\,\frac{v_1\left(1+\frac{1}{\gamma-1}\frac{\pi_1}{\pi}\right)y_1^j - v_0\left(1+\frac{1}{\gamma-1}\frac{\pi_0}{\pi}\right)y_0^j}{\frac{\gamma}{\gamma-1}(M^2-1)\left(y_1^{j+1}-y_0^{j+1}\right)} \quad , \qquad (3.8)$$

$$\frac{da}{dx} = (j+1)\,\frac{v_0\left[\gamma M^2-\left(1-\frac{\pi_0}{\pi}\right)\right]y_0^j - v_1\left[\gamma M^2-\left(1-\frac{\pi_1}{\pi}\right)\right]y_1^j}{\frac{2\gamma}{\gamma-1}(M^2-1)\left(y_1^{j+1}-y_0^{j+1}\right)} \quad , \qquad (3.9)$$

$$\frac{dv_0}{dx} = -(j+1)\,\frac{1}{\alpha_0}\,\frac{a}{\gamma}\,\frac{\left(1-\frac{\pi_0}{\pi}\right)y_0^j}{M\left(y_1^{j+1}-y_0^{j+1}\right)} \quad , \qquad (3.10)$$

$$\frac{dv_1}{dx} = (j+1)\,\frac{1}{\alpha_1}\,\frac{a}{\gamma}\cdot\frac{\left(1-\pi_1/\pi\right)y_1^j}{M\left(y_1^{j+1}-y_0^{j+1}\right)} \quad . \qquad (3.11)$$

In the written equations, $c = M\left(2/(\gamma-1)+M^2\right)^{-1/2}$ is the reduced velocity, $M = u/a$, a is the velocity of sound, $\pi = (1-c^2)^{\gamma/(\gamma-1)} = \left[1+M^2(\gamma-1)/2\right]^{-\gamma/(\gamma-1)}$; $v = \alpha_1 v_1 + \alpha_2 v_2$

The coefficients α_i in the case of a circular jet are: $\alpha_0 = (y_1+2y_0)/3(y_1+y_0) = 1/3 \div 1/2$, $\alpha_1 = (2y_1+y_0)/3(y_1+y_0) = 2/3 \div 1/2$, and for a plane jet $\alpha_0 = \alpha_1 = 1/2$. The system of the six equations (3.6)-(3.11) is complete, because it contains eight functions of x, two of which (π_0 and π_1 or y_0 and π_1) are given. The initial conditions are known in the cross-section $x = 0$.

The obtained system of equations is used for the approximate construction of the boundaries of the nonviscous curvilinear jets $y_i(x)$ in the sections, where there are no strong shocks inside the jet and the angles of inclination of the boundaries to the axis of the jet are small. It is obvious that the greatest error in the determination of the boundary of a jet arises near the edge of the nozzle and the points of fall of the shocks, in which the boundary of the jet undergoes a sharp bend. Therefore, the reduced system can be used for the approximate calculation of the plane and circular curvilinear supersonic jets

at small degrees of unrated outflow. Examples of contours of plane curvilinear supersonic jets are shown in Fig. 4. These contours are obtained by means of the integration of the system (3.6)-(3.11). Examples of contours plotted by the method of the characteristic features for the most simple configuration of the jet, when $C_1 = C_\infty$ are given also in Fig. 4, (C_∞ is the reduced velocity in the first section of the jet).

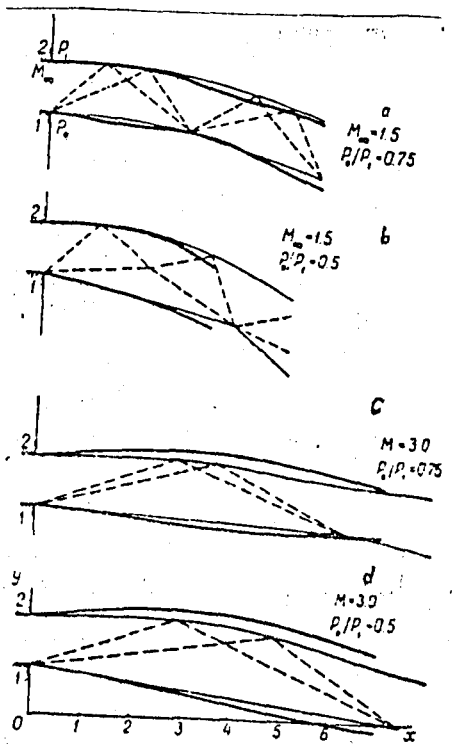

Fig. 4

In order to emphasize the wave (barrel-shaped) configuration of the jet in the quasi-one dimensional calculation, it was assumed that the nozzle has a small expansion angle $\lambda\,\theta_\infty = 0{,}2$. In the correct construction it was assumed for simplicity that $\theta_\infty = 0$. It is obvious that on the average, the boundaries of the correct and quasi-one-dimensional jets satisfactorily coincide. In the case of the most sharp bend of the boundary (Fig. 4 b) the quasi-one-dimensional jet is limited by the section $x \approx 3.5$ where M = 1.

As applied to the calculation of the flow of an interaction, we notice that only the integral properties of the complex outside flow up to the throat of the neighbouring wake are of interest. Examples of such properties are the number and the dimension of the "barrels" of the jet, which remain in one-dimensional approximation in a "spread" form. Moreover, the angles of inclination of the velocity vector of the outside flow on the boundary of the turbulent layer in the whole region of the interaction do not exceed 20°. So, the case of Fig. 4 b does not belong to the calculation of such a flow.

The discussed quasi-one-dimensional method of calculation is distinguished by sufficient simplicity, and it is similarly applicable for subsonic and supersonic nonviscous flows, both in the thin bounded jets and in the narrow canals. For the developed theory of interaction, it is particularly important that, by using this method, the problem as a whole obtains a closed analytical description that does not contain unnecessary informations about the flow and convenient for the programming of the numerical calculations.

4. Interaction of a Jet with a Wake

The flow of the interaction of a quasi-one-dimensional jet and one-parametric turbulent wake is described by a system of six equations for the nonviscous jet, (3.6)-(3.11), and two equations for the wake, (1.5) and (1.6). In the last two equations, one should assume that $\delta^* = y_0$ and $\frac{d\delta^*}{dx} = \frac{dy_0}{dx} = v_0^0$. It is necessary to add an auxiliary formula to the system of these equations for the determination of the length (surface) of the outside and inside boundaries of the nonviscous jet.

$$\frac{ds_i}{dx} = (j+1) y_i^j \sqrt{1 + (v_i/u)^2} \approx (j+1) y_i^j \,, \quad i = 0,1 \qquad (4.1)$$

This is necessary for the calculation of the width of the jet turbulent layer of the mixture.

The initial conditions of the neighbouring wake are determined, as previously, from the conditions of the gluing of the isobaric flow of the mixture in the bottom region with the flow of the interaction in the wake. On calculating the turbulent layer of the mixture behind the axisymmetric end, one should proceed from those approximate relations that exist in the plane flow: the profile of the velocity in the layer of the mixture is universal

$$\frac{df}{ds} = \beta(c) \,, \qquad (4.2)$$

where $f = (j+1) y_0^j \delta$ the area width of the cross-section of the zone of the mixture, β mixing coefficient

$$S_0 = (j+1) \int_0^x y_0^j \sqrt{1 + (v_0/u)^2}\, dx \approx (j+1) \int_0^x y_0^j \, dx \qquad (4.3)$$

is the area (length) of the ejector surface of the jet.

The conditions of continuity of δ and δ^* in the section of gluing and of conservation of mass in the stagnant region are written in the form:

$$y_0^{j+1}(x) + \beta^\circ S_0(x)[1 - H^*(1, C, 0)] = \delta^{j+1} , \tag{4.4}$$

$$y_0^{j+1}(x) = \delta^{j+1} H^*(m, C, j) , \tag{4.5}$$

$$\delta^{j+1} G(m, C, j) = (1-B)\beta^\circ H^{**}(1, C^\circ, 0) S_0(x) , \tag{4.6}$$

where

$$B = (\rho u)_{\delta_0} / (\rho u)^\circ \beta^\circ H^{**}(1, C^\circ, 0) S_0(x) ,$$

$$G(m, C, j) = -(j+1) \int_0^{z_*(m)} \frac{\rho u}{(\rho u)_\delta} z^j dz , \quad f(z_*) = m^{-1} .$$

The relative integral widths are expressed as functions of three arguments, the parametric form m, the reduced velocity C and the parameter j. The last argument, as shown previously, is equal to 0 or 1 in plane or axisymmetric layer, respectively.

From equations (4.4)–(4.6), it follows that the initial value of the parametric form m° is determined as a function of C° from an equation analogous to (2.3):

$$\frac{1 - H^*(m, C^\circ, 1)}{G(m, C^\circ, 1)} = \frac{1 - H^*(1, C^\circ, 0)}{H^{**}(1, C^\circ, 0)(1-B)} , \tag{4.7}$$

The coordinate $x = x^\circ$ of the section of gluing is determined from the equation

$$\frac{y_0^{j+1}}{S_0} - \beta(C^\circ) H^*(m, C^\circ, 1) \frac{1 - H^*(1, C^\circ, 0)}{1 - H^*(m, C^\circ, 0)} = 0 . \tag{4.8}$$

The calculation of the flows of the interaction, which are represented in Fig. 1 a and b, consists of two parts. Originally, for a given value of the bottom pressure P° (or C°), the flow on the isobaric region behind the step up to the section of gluing, determined by equation (4.8), is calculated by integrating the system (3.6)–(3.11), complemented by equation (4.1). Further, by the integration of the

same system of equations, the flow in the region of the interactions is calculated. The real value of the bottom pressure P° or C° and the actual flow of the interaction are determined, as in the most simple case in work [4], by the condition of passing the integral curve through the singular point (wake throat). The numerical construction of the singular solution in the neighbourhood of the saddle singular point, whose position is only determined in the operation of the calculation, is connected with known calculating difficulties. In practice, it seems sufficient to construct two nonsingular solutions related to the different families. The difference of the values of the bottom pressure in them is, beforehand, less than the given value, $|\bar{p}_2^{\circ} - \bar{p}_2^{\circ}| < 0.01$.

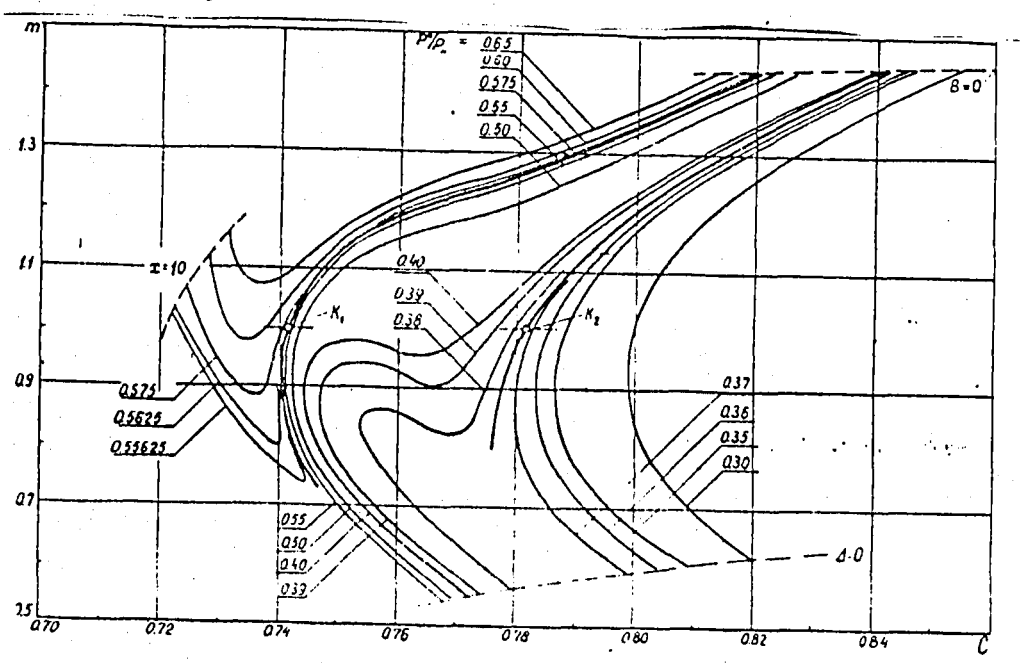

Fig. 5 a

The results of a successive integration (by the method of Rungo-Kutt) of the described system of equations for a plane flow at $M_\infty = 3.0$, $y_0 = 1$, $y_1 = 2$, $\theta_0 = -0.1$, $\theta_1 = 0.1$, $P_\infty/P_H = 0.6$ for different values of the relative bottom pressure P_0/P_H (P_H is the pressure in the outside medium) are represented in Fig. 5. The integral curves in the plane (m, c) are shown in Fig. 5 a. These curves characterize the change of the parameters in the viscous layer. The contours of the nonviscous jets are shown in Fig. 5 b. The lower boundary of the jets $y_0(x)$ in the region of the interaction corresponds to the width of the displacement of the viscous layer $\delta^*(x)$.

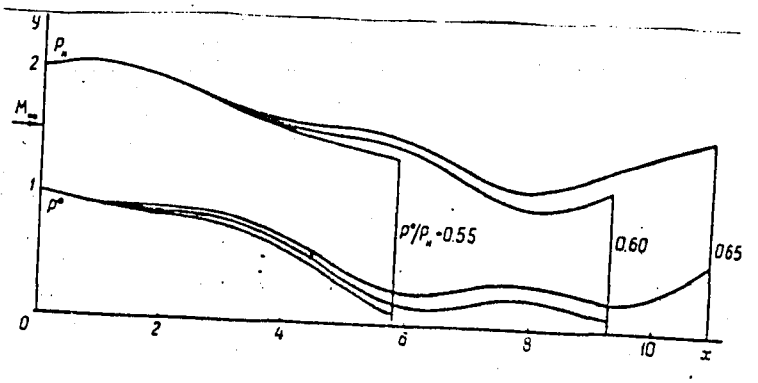

Fig. 5 b

The nonsingular integral curves, given in Fig. 5 a, do not correspond to any actual flow. All the curves begin on the line of the initial data (in the absence of blowing, B = 0), which is determined by equation (2.3). The right branches end on a limiting line which is determined by the condition $\Delta(m,C)=0$. The left branches are limited satisfactorily conditionally by the separated section $x = 10$, beyond which the solution has physically unreal singularities.

From the study of Fig. 5 a, it is obvious that, at given initial conditions, two singular curves are found. These two singular curves are plotted simply as averages between the nonsingular curves, related to the different families, and until these nonsingular curves are sufficiently close to each other. The two stationary flows of the interaction corresponding to them are represented in Fig. 6.

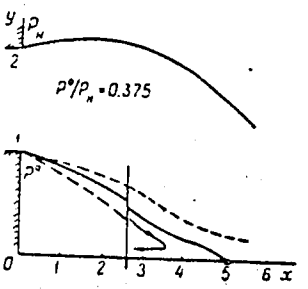

Fig. 6 a

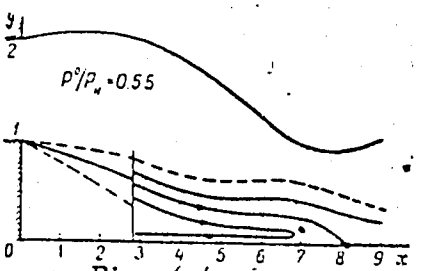

Fig. 6 b

As in the case of the interaction of a single shock with a wake, a flow with lower bottom pressure, $\bar{P}_1^\circ = 0.375$ and a flow with higher bottom pressure $\bar{P}_2^\circ = 0.55$, can be called weak and strong disturbances, respectively. The transition from one flow to the other is connected with the essential change of the configuration of the region of the returning flows and of the location of the critical points ($m = 1$) in the wake from $x = 5$ (at $\bar{P}_2^\circ = 0.375$) to $x = 8.2$ (at $\bar{P}^\circ = 0.55$).

The existence of the double-value in the flow of the interaction in the considered, more complex, case also attests the possibility of quasi-stationary ascillations with a relative amplitude:

$$2(\bar{P}_2^\circ - \bar{P}_1^\circ)/(\bar{P}_1^\circ + \bar{P}_2^\circ) \approx 0.38 .$$

5. Pseudoshock in a Canal

As shown in rectilinear long canals, a complex system of weak oblique shocks and flow separations, interacting with the turbulent layer near the wall, arises instead of a normal shock in such a way that the transition from a supersonic to a subsonic flow in the canal and the corresponding loss of the total pressure in the flow are distinguished by a viscous mechanism, which is commonly called pseudo-shock. Following work [7], we assumed that the effect of the shocks on the flow in the core of the canal, outside the layer of mixture, can be neglected, and this flow can be considered one-dimensional and isentropic. We assume also that the friction on the wall can be disregarded. The corresponding sketch of the pseudoshock is represented in Fig. 7.

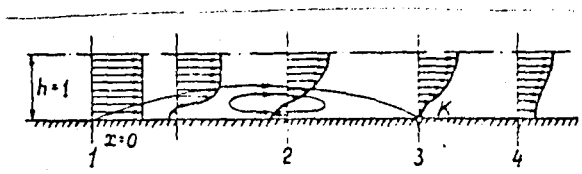

Fig. 7

In section 1, the flow consists of a uniform core and a thin ordinary turbulent boundary layer. This layer achieves a separating state under the action of the positive pressure gradient. Between sections 1 and 2, a layer of mixture with returning flows of fluid grows on the wall. In section 2, the layer of the mixture absorbs the isentropic core, after that a balancing of the flow takes place in the canal

A second critical point, behind which the asymptotic increase of the pressure to the maximum occurs, is located in section 3 when taking account of the friction on the walls in a certain section "4", the pressure reaches a maximum [8].

Since the effect of friction on the wall is not taken into account, the pseudoshoc can be considered as a flow of interaction of one-dimensional outside flow with a layer of mixture (with a wake).

In the layer of mixture between sections 1-4, a one-parametric profile of velocities of ordinary form (1.1) is received. The three unknown functions of the problem in the region 1-2 will be the reduced velocity $c(x)$ the width of the boundary layer $\delta(x)$ and the parametric form m (x), and in the region 2-4, where $\delta = 1$ will be the pressure p (x), we have as previously $c(x)$ and m (x). The original system of equations consists of two equations of conservation; the equation of continuity is:

$$(\rho u)_\infty = \rho u (1 - \delta H^*) = const \qquad (5.1)$$

and the equation of monentum is:

$$\frac{d}{dx} \ln(\delta H^{**}) + (2 + H - M^2) \frac{d \ln c}{dx} = 0 , \qquad (5.2)$$

and also the differential equation on the axis of the viscous layer is:

$$\rho_0 u_0 \frac{du_0}{dx} + \frac{dp}{dx} = \left(\frac{\partial \tau}{\partial y}\right)_0 \qquad (5.3)$$

In the case of the isentropic flow, we have in the core of the flow (in the section 1-2):

$$\delta^* = \delta H^* = 1 - q_\infty / q(c) , \quad q = \rho u / (\rho u)_* . \qquad (5.4)$$

For the calculation of the final increase of pressure in the pseudoshock, it is sufficient to use the equations of continuity and conservation of momentum. It is obvious that the mean parameters in the final and initial sections of the pseudoshock are connected with the relations of the normal shock.

For the calculation of the pressure distribution in a canal the equations of conservation, (5.1) and (5.2), should be used in the differential form.

The original system of equations of the pseudoshock for the region 1-2 with the isentropic core can be reduced to two ordinary differential equations of the first order with respect to m (x) and C (x):

$$-\left(\frac{\partial \ell n H}{\partial m}\right)\frac{dm}{dx}+\left(H+1+\frac{1-M^2}{1-q_\infty/q(C)}\cdot\frac{\partial \ell n H}{\partial \ell n C}\right)\frac{d\ell n C}{dx}=0\,, \qquad (5.5)$$

$$\frac{dm}{dx}+\frac{m(2-m)}{(1-m)(1-C^2)}\frac{d\ell n C}{dx}=\frac{(-a\varkappa)}{1-q_\infty/q(C)}\frac{H^* m^2}{1-m}\,. \qquad (5.6)$$

Equation (5.5) determines the integral curve m (C) in the plane (m, C)

$$\frac{dm}{dC}=\frac{1}{C}\,\frac{H+1+(1-M^2)/[1-q_\infty/q(C)]-\partial \ell n H/\partial \ell n C}{\partial \ell n H/\partial m}\,. \qquad (5.7)$$

From equation (5.6), the pressure distribution can be calculated in the physical plane C (x) or π (x):

$$(-a\varkappa)(x-x_1)=\int_C^{C_1}\left[1-q_\infty/q(C)\right]\frac{1}{H^* m^2}\left[(1-m)\frac{dm}{dC}+\frac{m(2-m)}{(1-C^2)C}\right]dC\,. \qquad (5.8)$$

Equations (5.5) and (5.6) are valid up to section 2 of the coupling viscous layers, where $\delta_2 = 1$, or

$$H_2^* = 1-\frac{q_\infty}{q(C_2)}\,. \qquad (5.9)$$

For the calculation of the balancing flow, one should proceed differently. The dependence of m on C_0 (C_0 is the reduced velocity on the axis of the canal) is more conviniently determined in this case from the transcendental equation, which is obtained from equations (5.1) and (5.2):

$$C_0\left[\frac{1-H^*(m,C_0)-H^{**}(m,C_0)}{1-H^*(m,C_0)}+\frac{\gamma-1}{2\gamma}\,\frac{1-C_0^2}{C_0^2}\,\frac{1}{1-H^*(m,C_0)}\right]=const\,. \qquad (5.10)$$

The value of the constant is determined from the data of integration of equation (5.7) in section 2.

The distribution of the velocity $C_0(x)$ is obtained from equation (5.6). The distribution of pressure $P(x)/p_0^*$ is calculated by the equation of momentum:

$$\frac{P}{P_0^*} = \frac{\pi_0[1-\gamma M_0^2(1-H^*-H^{**})]}{1+\gamma M_0^2(1-H^*-H^{**})} \quad . \qquad (5.11)$$

For the simplification of calculations, the integral parameters of the turbulent layer of the mixture were assumed to correspond to the linear profile of the velocity $f=1-\zeta$ in the nonviscous fluid:

$$H^* = m/2 \quad , \quad H^{**} = (m/6)(3-2m) \quad , \quad H = 3/(3-2m) \quad .$$

Then from equation (5.7) the following equation is obtained:

$$\frac{dm}{dC} = \frac{1}{C}\left\{\frac{3}{2} + \left(\frac{3}{2}-m\right)\left[\frac{1-M^2}{1-q_\infty/q(c)} + 1\right]\right\} \quad . \qquad (5.12)$$

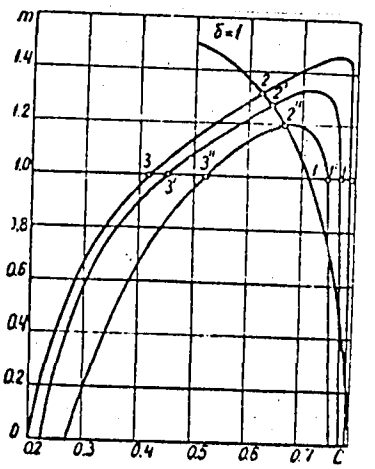

Fig. 8 a

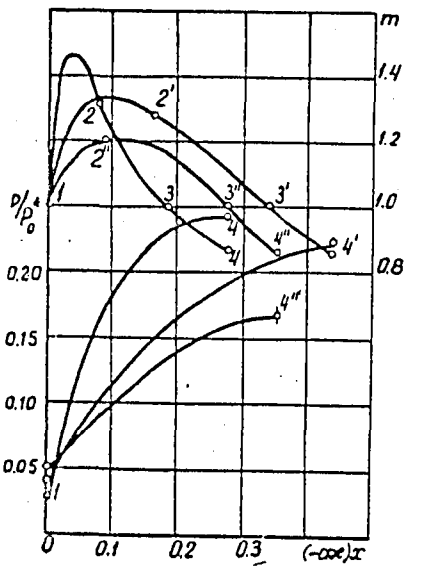

Fig. 8 b

The integral curves of equation (5.12) at $M_\infty = 3$ in the plane (m, C) are represented in Fig. 8 a. They are valid in the region 1-2 up to the section of the coupling of viscous layers at $\delta = 1$

The different curves correspond to different conditions in the initial section of pseudoshock 1 or to a different width of the displacement of the initial boundary layer δ_1^*. This consequently leads to a change of the initial parameters of the flow in the nonviscous core and of the mean-mass velocity of the flow in the section 1, λ_{m1} (Table 1).

The curve $\delta = 1$, corresponding to equation (5.9), is now determined by the equation:

$$m = 2\left[1 - \frac{q_\infty}{q_1(C)}\right]. \qquad (5.13)$$

The integral curves in the region 2-3-4 were plotted by the formula (5.10), taking account of the assumed simplifications.

The distribution of the pressures $p(x)$ and the parametric forms m (x) for three variants of calculation are shown in Fig. 8 b. It was assumed that $m_4 = 0.85$ in the final section of the pseudoshock. The obtained parameters of the flow in the pseudoshock and the comparison of its length with the experiment in work [8] are given in Table 1 (the linear dimensions are relative to the hight h, stated in Fig. 7).

Table 1

Вариант расчета (рис. 8) (1)	1 - 4	1' - 4'	1'' - 4''
Параметры потока в начальном сечении псевдоскачка: (2) δ_1^*	0,064	0,212	0,353
δ_1^{**}	0,016	0,053	0,088
λ_{m1}	1,82	1,76	1,5
(3) Длина псевдоскачка: расчет	22,5	36	29
эксперимент	22,5	38	29

Key:
1) Variant of calculation (Fig. 8); 2) Parameters of the flow in the initial section of the pseudoshock; 3) Length of the pseudoshock: calculation experiment.

It is obvious from the table that there is a totally satisfactory agreement between the experiment and the approximate calculation (at one and the same value of $m_4 = 0.85$).

6. The Final Remarks

In conclusion and first of all, one must emphasize that the essentially developed one-dimensional theory, in spite of the sufficiently rough initial assumptions and with the minimum number of the empirical constants, totally satisfactorily describes all the main properties of the investigated separating turbulent supersonic flows, including the hysteresis phenomena and the quasi-stationary oscillations. The good agreement of the calculated and experimental data is remarked also in other analogous works. This is explained, on one hand, by the existence of certain universal properties of the separating flows, slightly depending on the general configuration of the flows and enabling to use its simple calculating models, and on the other hand, by the smoothing characteristics of the integral methods of investigation. These methods guarantee at the same time the conservation of the principal properties of the phenomenon.

The first universal properties of the separation of the turbulent boundary layer and the combination of the turbulent wake at definite critical pressure ratios p_2/p_1 which are, with a high precision, functions only of the Mach number M_1 of the incident undisturbed flow, were ascertained experimentally in the works of I.P. Nekrasov, G.I. Petrov and other authors. The properties of the separation, taken phenomenologically, enabled to construct more complex flows by the investigation of the local separations and combinations of the turbulent flow in the case of achievement of the conditions of the critical increase of pressure or the critical angle of turn of the supersonic flow. These conditions obtained satisfactory explanation within the limits of the theory of nonviscous fluids, taking account of a definite reconstruction of the velocity profile of the separating or adjoining vortex layers and the satisfaction of the integral conditions of conservation of mass and momentum. Another explanation was connected with the assumption of conservation of the total pressure at the separating line of flow. This pressure, in the case of combination, must be more static for the magnitude of the increase of pressure in the region of combination. This assumption enabled Korst and Chepman to determine the bottom rarefaction behind the step in the plane flow, including the effect of the low blowing, in the case of good agreement with the experimental data. However, as the more detailed investigations in works [9,3] show, the method of Korst-Chepman is essentially connected with the local properties of the selected profile of velocity and of the flow of the nonviscous fluid along the line of flow of a constant rate, which must be considered the principal disadvantage of the method.

Further progress in the theory of the separating flows is due to Krokko and Liz [1] who extended the integral method of the theory of the boundary layer in the viscous fluid to these flows, taking into account the separating profiles of the velocity and the essential interaction of the layer with the outside

supersonic flow. Unlike the previous approach , this approach enabled to study in detail the growth of the layer, to obtain the pressure distribution and the location of the points of separation and combination, and to show the effect of the initial conditions, disturbances and friction in the flow.

The use of the integral methods of the theory of jets and wakes represents at present the most promising direction in the investigation of the separating flows.

Among the most important problems for further working out, one should point out the extension of the range of the investigation of Mach number M and Reynolds number Re; the consideration of the effect of the initial boundary layer and the friction on the walls; the study of the flow around more complicates space configurations; the introduction of consumption and thermal effects; the changes of the design model and working medium, corresponding to the conditions of the hypersonic velocities at high altitudes and to the cavitation flows of the incompressible fluid.

References

1. Krokko L., L. Liz "Teoriya smesheniya dlya opredeleniya vzaimodeistviya dissipativnogo i pochti izentropicheskogo potokov" (Theory of mixing for the determination of the interaction of dissipative and nearly izentropic flows).--- Vopr. raketnoi tekhniki, sb. perev., No. 2, 1953.

2. Gogish L.V., G.Yu. Stepanov" "Integral'nyi metod rascheta turbulentnykh otryvnykh techenii" (Integral method of calculation of the turbulent separating flows).--- Tretii vsesoyuznyi s"ezd po teoreticheskoi i prikladnoi mekhanike, Moskva, 1968.

3. Ginevskii A.S. "Teoriya turbulentnykh strui i sledov" (Theory of turbulent jets and wakes).--- "Mashinostroenie", 1969.

4. Gogish L.V., T.S. Sobaleva, G.Yu. Stepanov "Vzaimodejstvie turbulentnogo sleda s vneshnim potokom" (Interaction of a turbulent wake with outside flow).--- Izv. AN SSSR. MZhG, No. 3, 1969.

5. Gogish L.V. "Relaksatsionnye kolebaniya v turbulentnom blizhnem sledе" (Relaxation oscillation in the turbulent neighbouring wake).--- Izv, AN SSSR, MZhG, No. 6, 1969.

6. Gogish L.V. "Raschet kriticheskikh davlenii prisoedineniya i otryva turbulentnogo pogranichnogo sloya v sverkhzvukovom potoke" (Calculation of the critical pressures of the combination and separation of the turbulent boundary layer in the supersonic flow).--- Izv. AN SSSR, MZhG, No. 4, 1968.

7. Krokko L. "Odnomernoe rassmotrenie gazovoi dinamiki ustanovivskikhsya techenii" (One-dimensional investigation of the gas dynamics of steady flow).--- V. knige: Osnovy gazovoi dinamiki, IL, 1963.

8. Zubkov A.I. and L.I. Sorkie. "Vliyanie vyazkosti na techenie v oblasti pryamogo skachka uplotneniya" (The effect of viscosity on flow in the region of the direct shock wave).--- Izv. AN SSSR, Mekhanika i mashinostroenie, No. 1, 1961.

9. Gogish L.V. and G.Yu. Stepanov "K raschetu donnogo davleniya v dvumernykh sverkhzvukovykh techeniyakh" (Calculation of bottom pressure in two-dimensional supersonic flows).--- Izv. AN SSSR MZhG, No. 3, 1966.

OPTIMUM FORMS OF PLANE AND AXISYMMETRIC BODIES AT HYPERSONIC VELOCITIES

By

A.L. Gonor

The solution of a variational problem in a statement, using the resistance law of A. Buzeman, was proposed in the works [1-3]. However, as Kheiz had pointed out in work [2], in the more exact statement, the contour of a body of a minimum resistance must have a discontinuity of the inclination of the tangent at the end point. This is so because, according to the law of A. Buzeman, an infinite negative pressure is created at this point, which decreases the resistance in the final value. Physically, the pressure can not be negative, and the change of the inclination of the tangent at the end point in the supersonic flow must not ahead affect the pressure distribution and, consequently, the resistance. The mentioned discrepancy with the physics of the supersonic flow requires a new statement of the variational problem.

There are two possibilities. One of them is the use of the so-called the thrust ring and leads to the conception of the absolutely optimum body [2,3]. The second possibility involves an additional requirement of limiting the class of the bodies so that the pressure is positive everywhere on the contour. With such a statement the variational problem was strictly solved in work [4], for bodies of a given elongation and in work [6] for thin bodies with different boundary conditions. A number of questions, connected with the statement of these problems, is investigated in work [5]. The solutions of this problem in case of arbitrary isoperimetric conditions and without limitation on the thickness of the body are cited below.

§1. Problems with Arbitrary Isoperimetric Conditions

The solution of the variational problem about the form of a body of a minimum drag with a given length and diameter does not cover all the possible cases of interest for practice.

We shall take in consideration, beside the length of l and diameter, the following quantities: in the two-dimensional case—the area A, enveloped by the contour of the profile and the moment of inertia M of the contour; in the axisymmetric case—the wetted surface S and volume V. Their values are equal to:

$$A = 2\int_{x_0}^{x_1} y\,dx \quad ; \quad M = 2\int_{x_0}^{x_1} y^2 dx \; ;$$
$$S = 2\pi\int_{x_0}^{x_1} y\sqrt{1+y'^2}\,dx \quad ; \quad V = \pi\int_{x_0}^{x_1} y^2 dx \qquad (1.1)$$

Any two values are most frequently given, while the rest are considered free. For example l and V, V and S, t and S etc. The general problem is formulated as follows: find the minimum drag X_D in the condition that the pressure on the contour is non-negative and the values of (1.1) are given. The principal theorem of work [4] about the existence of a section of zero pressure on the optimum contour is, according to the argument method, not related to the form of the boundary conditions; therefore it can be extended without difficulty to the general case.

As a result, the problem is reduced to a detection of the minimum drag

$$X_D/q = 2\pi^n(n+1)\left[\frac{y_c^{n+1}}{n+1} - \frac{1}{(1+y_c'^2)^{1/2}}\int_{x_0}^{x_c}\frac{y^n y'\,dx}{(1+y'^2)^{1/2}}\right] \qquad (1.2)$$

in the condition of fulfilling, on the length $x_0 \leqslant x \leqslant x_c$, the inequality:

$$y'^2 + \frac{y''}{y^n(1+y'^2)^{1/2}}\int_0^x \frac{y^n y'}{(1+y'^2)^{1/2}}\,dx \geqslant 0 \qquad (1.3)$$

Here q – is the dynamic pressure; n = 0 and 1 for the plane and axisymmetric flows, respectively. The variable X– is the coordinate in the direction of the incident flow; y– in the perpendicular direction. The index 0– refers to the initial point, index 1– to the end point (Fig. 1). The drag arises only from the section OC of the contour. On the arc CF, called the free layer, the pressure is equal to zero.

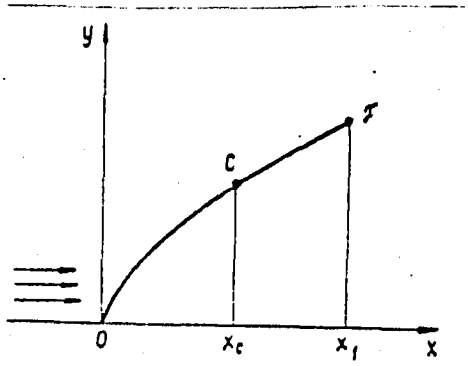

Fig. 1

Let us turn to the investigation of a set of curves of zero pressure. On this set, the inequality (1.3) converts to equality and represents a derivative from the formula.

$$\frac{y'}{(1+y'^2)^{1/2}}\int_a^x \frac{y'y^n dx}{(1+y'^2)^{1/2}} = const\ . \tag{1.4}$$

Hence, it follows in particular that it is impossible to carry out a contour of zero pressure from the initial point X = 0.

Eliminating the integral from the formulae (1.3) and (1.4), we obtain a simple differential equation of the second order for the function $y(x)$

$$y'^3 y^n + K y_c^{n+1} y'' = 0\ , \tag{1.5}$$

where y_c – is the ordinate of the corner point, and the parameter K is found from the formula

$$K = \frac{y_c'}{y_c^{n+1}(1+y_c'^2)^{1/2}}\int_{x_0}^{x_c} \frac{y^n y'}{(1+y'^2)^{1/2}}\, dx \tag{1.6}$$

As it is evident from (1.6), the geometry of the free layer depends on the geometry of the initial section, called the regular form. The general integral of equation (1.5) contains two arbitrary constants, which can be so determined that the free layer has no inclination y_c' in the point $C(x_c, y_c)$ and passes by the point (x_1, y_1) As a result we obtain the equation

$$\frac{y_1^{n+2} - y^{n+2}}{(n+1)(n+2)} + y_c^{n+1}\left(\frac{K}{y_c'} - \frac{1}{n+1}\right)(y_1 - y) - K y_c^{n+1}(x_1 - x) = 0\ , \tag{1.7}$$

determining the geometry of the free layer.

Applying (1.7) to the corner point, we obtain the relation

$$\frac{y_1^{n+2} - y_c^{n+2}}{(n+1)(n+2)} + y_c^{n+1}\left(\frac{K}{y_c'} - \frac{1}{n+1}\right)(y_1 - y_c) - K y_c^{n+1}(x_1 - x_c) = 0\ . \tag{1.8}$$

Taking into account (1.7), we rewrite the conditions (1.1) in a more suitable form:

$$S/2\pi = \int_{x_c}^{x_c} y\sqrt{1+y'^2}\, dx + s(x_c, y_c, y_c', x_1, y_1, K)\ ,$$

$$V/\pi = \int_{x_0}^{x_c} y^2 dx + v(K, x_c, y_c, y_c', x_1, y_1) \quad etc.$$

where j, V, ... – are known functions of their arguments.

Let us formulate the auxiliary functional

$$\mathcal{J} = x_D/\pi q\, 2\pi^n/(n+1) - \frac{1}{(1+y_c'^2)^{1/2}}\left\{\lambda_1 n\left[\int_{x_0}^{x_c} y(1+y'^2)^{1/2}dx + s(\kappa, x_c, y_c, \ldots)\right] + \right.$$
$$+\lambda_2 n\left[\int_{x_0}^{x_c} y^2 dx + V(\kappa, x_c, y_c, \ldots)\right] + \lambda_3(1-n)\left[\int_{x_0}^{x_c} y dx + a(\kappa, x_c, y_c, \ldots)\right] +$$
$$\left. +\lambda_4(1-n)\left[\int_{x_0}^{x_c} y^2 dx + m(\kappa, x_c, \ldots)\right]\right\}, \qquad (1.9)$$

where λ_i — constant numbers. The minimum functional of (1.2), in the above enumerated conditions, coincides with the minimum of (1.9). Hence the unknown solution must satisfy the condition $\delta\mathcal{J} = 0$. Expanding the latter, we obtain:

$$\delta\mathcal{J} = H\int_{x_0}^{x_c}(Fy - dFy'/dx)\delta y\,dx + \delta H\int_{x_0}^{x_c} F dx + H\left[(F - yFy')\delta x + \right.$$
$$\left. + Fy'\delta y\right]_{x_0}^{x_c} + \delta\sigma,$$

$$F = \frac{y^n y'}{(1+y'^2)^{1/2}} + \lambda_1^n y(1+y'^2)^{1/2} + \cdots, \qquad H = -\frac{1}{(1+y_c'^2)^{1/2}},$$

$$\sigma = \frac{y_c^{n+1}}{n+1} - \frac{1}{(1+y_c'^2)^{1/2}}\left[\lambda_1^n s(\kappa, x_c, y_c, \ldots) + \lambda_2^n V(\kappa, x_c, \ldots) + \right.$$
$$\left. + \lambda_3^{(1-n)} a(\kappa, x_c, \ldots) + \lambda_4^{(1-n)} m(\kappa, x_c, \ldots)\right].$$

Repeating the usual argument we find that the extremum satisfies the Euler equation, which assumes the first integral,

$$\left[n\lambda_2 + (1-n)\lambda_4\right]y^2 + \left[(1-n)\lambda_3 + n\lambda_1\frac{1+y'^2-y'}{(1+y'^2)^{1/2}} + \right.$$
$$\left. + \frac{ny'^3}{(1+y'^2)}\right]y + (1-n)\frac{y'^3}{(1+y'^2)^{3/2}} - C = 0. \qquad (1.10)$$

The condition of transversality is represented in the form

$$\delta H\int_{x_0}^{x_c} F dx + H\left[C\delta x + Fy\,\delta y\right]_{x_0}^{x} + \delta\sigma = 0. \qquad (1.11)$$

According to (1.6) and (1.10), the coefficient K depends on the arguments (y_0, y_c, y_c') ; consequently $\sigma = \sigma(y_0, x_c, y_c, y_c', x_1, y_1)$.

The form of integral (1.10) is such that the equation of the extremum in the general case can be written in quadratures. Actually, solving (1.10) with respect to the variable y and taking into account the parameter y', we obtain

$$y = f(y', C, \ldots); \qquad x = \int_{y_0'}^{y'} \frac{f_{y'}(y', C, \ldots)\,dy'}{y'} = \varphi(y', C, y_0', \ldots). \tag{1.12}$$

Writing (1.12-1) in the initial point* it is possible to express y_0' by the parameters in the point of conjugation and in the point (x_1, y_1) If equation (1.12-1) is now applied to the point of conjugation and C is eliminated, then the following relation will take place

$$\psi(x_c, y_c, y_c', x_1, y_1) = 0 . \tag{1.13}$$

The variation (1.13) gives the condition

$$\psi_{x_c}\delta x_c + \psi_{y_c}\delta y_c + \psi\,\delta y_c' + \psi_{x_1}\delta x_1 + \psi_{y_1}\delta y_1 = 0 . \tag{1.14}$$

The condition of transversality (1.11) is reduced to an analogous form. Investigating it together with (1.14), it is possible to eliminate any one variation and, by (1.13), the corresponding variable, for example, x_c . As a result we obtain a condition connecting four variations with coefficients that are dependent on four variables. Finally, the variation of the equation of the free layer (1.8) enables to decrease the number of the independent parameters to three. The latters are determined from the equality of the corresponding coefficients in the independent variations to zero. The discussed shceme gives the possibility to find the values of $x_c, y_c, y_c', x_1, y_1, y_0'$. The constants λ_i , entering in these parameters, are calculated from the relations (1.1) . Thus, the solution of the general problem is closed.

---

* If the extremum does not pass by the origin of the coordinates, when the class of the bodies with plane nose [5] is engaged in the investigation. The condition of the transversality gives an auxiliary relation for the elimination of the variable y_0'.

§2. Investigation of the General Solution

On performing the solution, certain moments, which require special investigation, were omitted. First, it was not proved that the inequality (1.3) will be realized for the regular form of the body. Second, it nowhere follows that the optimum contour contains a free layer only at the end and that it cannot be composed from some sections of the free layer and regular form. We shall carry out the proof of these situations for the case of a body with a given relative thickness. The correctness of the condition (1.3) is most easy to verify by a direct calculation of the pressure distribution on the nose of the contour. In the plane flow, the regular form is the wedge and the condition (3) is certainly fulfilled. In the axisymmetric flow, the pressure distribution is determined by the following formula:

$$C_p = p/q = 2\sin^2\alpha\left[1-\frac{1}{4}\sin^2\alpha-\frac{3}{8}\sin^4\alpha+\frac{3}{8}\frac{\sin^6\alpha}{\cos\alpha}\ln\operatorname{tg}\frac{\alpha}{2}\right], \text{ where } \operatorname{tg}\alpha = y'.$$

The corresponding graph, represented in Fig. 2, shows that a positive pressure is always realized in the regular form.

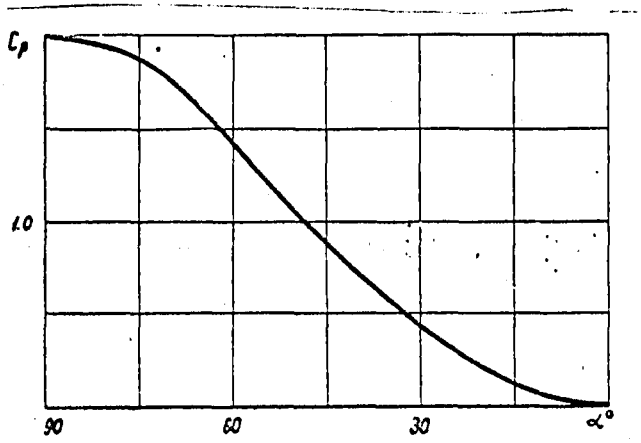

Fig. 2

Let us now determine the succession of the arcs of the regular form and free layer. As already shown, the extremum cannot start from the free layer. Therefore, the initial section is the regular form or the arc of the boundary extremum. One may ask: does the transition from a regular form to a free layer occur directly at the end or we have intermediate arcs of a free layer and regular form by means of which the conjugation of the initial and final sections takes place? If the latter situation is assumed, a reverse transition from the free layer to the regular form will certainly take place at a certain point. Such point is denoted by the letter C in Fig. 3; the arcs of the free layer are shown by the dashed lines and the arcs of the regular form by the solid lines.

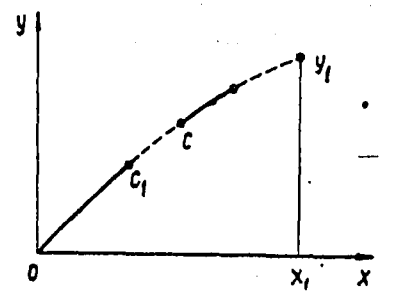

Fig. 3

To reduce the calculation, we shall limit the investigation to the plane problem. The drag coefficient of a body consisting of two arcs of the regular form (Fig. 3) is determined by the formula:

$$C_D = 2\left\{ y_{c_1} - \frac{1}{(1+y_{c_1}'^2)^{1/2}} \int_0^{x_{c_1}} \frac{y'\,dx}{(1+y'^2)^{1/2}} - y_c + \frac{1}{(1+y_c'^2)^{1/2}} \int_0^{x_c} \frac{y'\,dx}{(1+y'^2)^{1/2}} + \right.$$

$$\left. + y_{c_2} - \frac{1}{(1+y_c'^2)^{1/2}} \int_0^{x_{c_2}} \frac{y'\,dx}{(1+y'^2)^{1/2}} \right\} \frac{1}{\varsigma''} \qquad (2.1)$$

Calculating and equating the total variation (2.1) to zero, it is in particular received that at the point C, a condition of transversality of the following form must be fulfilled:

$$\delta H \int_0^{x_c} F\,dx + H\left[(F - y'F_{y'})\delta x + F_{y'}\delta y\right]_c + \delta\sigma = 0 \;;$$

$$H = \frac{1}{(1+y_c'^2)^{1/2}} \;;\; F = \frac{y'}{(1+y'^2)^{1/2}} \;;\; \sigma = y_c \;. \qquad (2.2)$$

On calculating the first term, it is necessary to take into account that the integral of the function F is taken both on the regular form and the free layer. As a result, (2.2) will have the form:

$$\left[\frac{y\,y_{c_1}'}{1+y_{c_1}'^2}\,\delta y' - \frac{y'^3}{1+y'^2}\,\delta x + \frac{(1+y'^2)^2 - 1}{1+y'^2}\,\delta y \right]_c = 0 \;. \qquad (2.3)$$

On the other hand, the equation of the free layer (1.7) reduces to the relation:

$$\frac{y_c^2 - y_{c_1}^2}{2} + y_{c_1}\left(\frac{K}{y_{c_1}'} - 1\right)\left(y_c - y_{c_1}\right) - K y_{c_1}\left(x_c - x_{c_1}\right) = 0 \;. \qquad (2.4)$$

Hence, the variations at the point C are related with the following condition:

$$\left\{\left[y(1+y_{c_1}'^2)-y_{c_1}y_{c_1}'^2\right]\delta y-y_{c_1}y_{c_1}'\delta x\right\}_c=0\ . \qquad (2.5)$$

It is easy to set also a relation including the variation of the angle of the inclination of the tangent at the point C. Therefore, changing beforehand th indices "1" to "C" and "C" to "C_1", we differentiate (1.7) with respect to the variable X. Then, we obtain the formula:

$$\left\{y'\left[y(1+y_{c_1}'^2)-y_{c_1}y_{c_1}'^2\right]-y_{c_1}y_{c_1}'\right\}_c=0\ , \qquad (2.6)$$

the variation of which gives the condition:

$$\left[(1+y_{c_1}'^2)y'\delta y+y(1+y_{c_1}'^2)-y_{c_1}y_{c_1}'^2\delta y_c'\right]_c=0\ . \qquad (2.7)$$

Equations (2.3), (2.5) and (2.7) form a linear one-dimensional system with respect to the variations. Therefore, the determinant from the coefficients must become zero. This leads to the relation:

$$\left\{y'^2\left[y(1+y_{c_1}'^2)-y_{c_1}y_{c_1}'^2\right]^2-2y'y_{c_1}y_{c_1}'(1+y'^2/2)\left[y(1+y_{c_1}'^2)-y_{c_1}y_{c_1}'^2\right]+\right.$$

$$\left.+yy_{c_1}y_{c_1}'^2(1+y'^2)\right\}_c=0\ .$$

We shall rewrite the latter in the form:

$$y_c'=\frac{y_{c_1}y_{c_1}'(1+y_c'^2/2)}{(1+y_{c_1}'^2)y_c-y_{c_1}y_{c_1}'^2}\left(1-\sqrt{1-\frac{y_c}{y_{c_1}}\frac{(1+y_c'^2)}{(1+y_c'^2/2)^2}}\right)\ . \qquad (2.8)$$

If we now consider (2.6) and (2.8) together, we have $y_c > y_{c1}$ at the point C, which contradicts the initial inequality $y_c > y_{c_1}$. In this way, it is proved that the free layer can not occupy the intermediate position and be alternated with the regular form.

§ 3. The Second Method of the Solution of Variational Problems with Inequalities

In work [6], the above discussed problems are reduced, in the case of thin bodies, to the solution of general problems of a variational calculation of the Mayer–Lagrange type. The principal idea of the solution is borrowed from work [7] and includes the insertion of an auxiliary function, enabling to replace the inequality by an equivalent relation. We extend this method to the case of bodies of arbitrary thickness. The strong and weak sides of the solution will be seen in the course of its performing.

Let us consider the general problem of minumum wave drag in the case of the inequality (1.3) and arbitrary initial and isoperimetric conditions. We shall write the formula of the drag in the form:

$$x_D/q = 2\pi^n(n+1)\left[\frac{y_1^{n+1}}{n+1} - \frac{1}{(1+y_1'^2)^{1/2}}\int_{x_0}^{x_1}\frac{y^n y'\,dx}{(1+y'^2)^{1/2}}\right]. \qquad (3.1)$$

According to [7], we replace the inequality (1.3) by the relation:

$$y'^2 + \frac{y^n}{y^n(1+y'^2)^{1/2}}\int_{x_0}^{x}\frac{y'y^n\,dx}{(1+y'^2)^{1/2}} - p^2 = 0\ , \qquad (3.2)$$

where p is a real variable

Differentiating (3.2) with respect to the variable X and eliminating the integral from the both relations, we obtain:

$$\frac{y'y^n(3+2y'^2)}{1+y'^2} + \left\{\frac{y^m}{y^n} - \frac{y'[n(1+y'^2)+yy^n]}{y(1+y'^2)}\right\}(p^2-y'^2) - 2pp' = 0\ . \qquad (3.3)$$

Introducing the designations:

$$y' = t\ ;\ y^n = s\ ;\ y^m = m\ .$$

the relation (3.3) will be equivalent to the following system:

$$\begin{cases} \varphi_0 \equiv \dfrac{ts(3+2t^2)}{1+t^2} + \left[\dfrac{m}{s} - \dfrac{ts}{1+t^2} - n\dfrac{t}{y}\right](p^2-t^2) - 2pp' = 0 \\ \varphi_1 \equiv y' - t = 0 \\ \varphi_2 \equiv t' - s = 0 \\ \varphi_3 \equiv s' - m = 0 \end{cases} \qquad (3.4)$$

As a result, we come to the formulation of the Lagrange problem: in the class of the functions $y(x), t(x), s(x), m(x), p(x)$ compatible with the conditions of the relation (3.4), the isoperimetric conditions (1.1) and the conditions on the end points, we find such a system of functions, which would be reduced to the minimum functional of (3.1).

We set up the auxiliary functional:

$$\mathcal{Y} = \frac{y_1^{n+1}}{n+1} - \frac{1}{(1+t_1^2)^{1/2}} \int_{x_0}^{x_1} F\,dx \quad ,$$

$$F = \frac{y^n t}{(1+t^2)^{1/2}} + \sum_{i=0}^{3} \lambda_i(x)\varphi_i + \lambda_4 n y^2 + \lambda_5 n y\sqrt{1+t^2} + \lambda_6(1-n)y + \lambda_7(1-n)y^2 \quad . \tag{3.5}$$

The vanishing of the function $\mathcal{Y}$ gives the following necessary conditions:

1. The Euler equations:

$$F_{y_\kappa} - \frac{d}{dx} F_{y'_\kappa} = 0 \quad . \tag{3.6}$$

takes place along the optimum contour.

2. The conditions of Weierstrass-Erdman:

$$(F_{y'_\kappa})_- = (F_{y'_\kappa})_+ \; ; \; \left(F - \sum_\kappa y'_\kappa F_{y'_\kappa}\right)_- = \left(F - \sum_\kappa y'_\kappa F_{y'_\kappa}\right)_+ \tag{3.7}$$

are achieved at the corner points.

3. Finally- the conditions of transversality are:

$$(y^n \delta y)_1 + \frac{t_1 \delta t_1}{(1+t_1^2)^{3/2}} \int_{x_0}^{x_1} F\,dx - \frac{1}{(1+t_1^2)^{1/2}} \left[\left(F - \sum_\kappa y'_\kappa F_{y'_\kappa}\right)\delta x + \sum_\kappa F_{y'_\kappa} \delta y_\kappa \right]_0' = 0 \quad ,$$

here:

$$x_0 = 0 \; , \; x_1 = \ell \; , \; y_1 = y \; , \; y_2 = t \; , \; y_3 = s \; , \; y_4 = m \; , \; y_5 = p \quad . \tag{3.8}$$

Expanding the Euler equations (3.6), we obtain the system:

$$\begin{cases} \dfrac{n y^{n-1} t}{(1+t^2)^{1/2}} + \lambda_0\left(p^2 - t^2 \dfrac{n t}{y^2}\right) + 2\lambda_4 n y + \lambda_5 n\sqrt{1+t^2} + \lambda_6(1-n) + 2\lambda_7(1-n)y - \lambda_1' = 0 \\ \dfrac{s y^n}{(1+t^2)^{3/2}} + \lambda_0\left\{\dfrac{s^2(3+3t^2+2t^4)}{(1+t^2)^2} - (p^2 - t^2)\left[\dfrac{s(1-t^2)}{(1+t^2)^2} - \dfrac{ns}{y}\right] - 2t\left[m - \dfrac{ts}{1+t^2} - n\dfrac{ts}{y}\right]\right\} - \\ - s\lambda_1 - \lambda_2 s' + \lambda_5 \dfrac{yts}{(1+t^2)^{1/2}} = 0 \end{cases}$$

$$\begin{cases} p\left[\lambda_0\left(m-\frac{ts^2}{1+t^2}-n\frac{ts}{y}\right)+\lambda_0' s\right]=0 \\ \lambda_0\left[\frac{s^2t(3+2t^2)}{1+t^2}-\left(m+\frac{ts^2}{1+t^2}\right)(p^2-t^2)\right]-\lambda_2 s^2-\lambda_3' s^2=0 \\ \lambda_0(p^2-t^2)-\lambda_3 s=0 \end{cases} \quad (3.9)$$

The absence of the independent variable enables to write out the first integral:

$$\frac{y^n t}{(1+t^2)^{1/2}}-\lambda_1 t-\lambda_2 s-\lambda_3 m+\lambda_4 n y^2+\lambda_5 y\sqrt{1+t^2}+\lambda_6(1-n)y+\lambda_7(1-n)y^2=C \quad (3.10)$$

Equation (3.9-3) enables to draw the conclusion that in the general case, the extremum can be discontinuous, and it consists of arcs, along which:

$$\lambda_0\left(m-\frac{ts^2}{1+t^2}-n\frac{ts}{y}\right)+\lambda_0' s=0 \quad \text{or} \quad p=0 . \quad (3.11)$$

We shall name the first arcs the regular forms, and the second arcs the free layers.

The conditions of (3.7) in the corner points necessitates that the multipliers λ_1, λ_2, λ_3 should be continuous and the constant C, of integration, should have the same value for all the arcs forming the extremum. Moreover,

$$(p\lambda_0)_- = (p\lambda_0)_+ . \quad (3.12)$$

The form of the conditions (3.8) depends on whether they are recorded in fixed points or in points of the natural type. In the last case we have:

$$c=0;\ \lambda_{10}=0;\ \lambda_{11}=y_1^n(1+t_1^2)^{1/2};\ \lambda_{20}=0;$$

$$\lambda_{21}(1+t_1^2)=t_1\int_0^{x_1} F\,dx;\ \lambda_{30}=\lambda_{31}=0;\ p_0\lambda_{00}=p_1\lambda_{01}=0 . \quad (3.13)$$

If the end points are fixed, then the first three conditions of (3.13) disappear. We shall illustrate further solution on the example of a plane contour with a given relative thickness.

The first equation of (3.9) in the case gives the integral $\lambda_1 = c_1$

In the point of conjugation of the regular form and the free layer, according to (3.13), the multiplier $(\lambda_0)_- = 0$.

The forms of equation (3.11) and of the boundary condition for the Lagrange multiplier $\lambda_0(x)$ enable to suppose that this multiplier is identically equal to zero along the regular form. Such supposition gives the possibility to solve the system (3.9) and satisfy all the boundary conditions. Actually, the second equation is written in the form:

$$(1+t^2)^{3/2} = 1/c_1 \qquad \text{or} \qquad y' = y_c' \ .$$

This solution satisfies the system (3.9) at any values of λ_2 and λ_3. We obtain the equation of the free layer from (3.3) at $P = 0$. Performing the integration, we have:

$$y'^3 + C_2 y'' = 0 \ .$$

The constant $C_2 = K y_c$. The functions λ_0, λ_2 and λ_3 along the arcs of the free layer are found from the solutions of the second, fourth and fifth equations of (3.9) at the conditions (3.12) and (3.13).

The composition of the arcs forming the optimum contour needs a special investigation, similar to that performed in § 2.

In conclusion, it is possible to draw the conclusion that both methods give an identical solution. Nevertheless, the second method, even in the most simple case, leads to the necessity of the investigation of a complex system of differential equations, the solution of which is performed in a heuristic way.

References

1. Gonor A.L. and G.G. Chernyi. O telakh naimen'shego soprotivleniya pri bol'shikh sverkhzvukovykh skorostyakh" (About bodies of minimum drag at high supersonic velocities).--- Izv. AN SSSR, OTN, No. 7, 1957.

2. Khejz U., R. Probstin "Teoriya giperzvukovykh techenii" (Theory of hypersonic flow).--- Izd. in. lit, 1962.

3. Chernyi G.G. "Techeniya gaza s bal'shoi sverkhzvukovoi skorost'yu" (Gas flow with a high supersonic velocity).--- fizmatgiz, 1959.

4. Gonor A.L. "Opredelenie formy tel minimal'nogo soprotivleniya pri bol'shikh sverkhzvukovykh skorostyakh" (Determination of the form of bodies of minimum drag at high supersonic velocities).--- PMM, 24 (6), 1960.

5. Kraiko A.N. "Ob opredelenii tel minimal'nogo soprotivleniya pri ispol'zovanii zakonov soprotivleniya N'yutona i Buzemana" (About the determination of bodies of minimum drag by using the laws of resistance of Newton and Busemann).--- PMM, 27 (3), 1963.

6. Miele A., A Study of slender shapes of minimum drag using the Newton-Busemann pressure coefficient law, AIAA Journal, I (I), 1963.

7. Valentine F.A., The problem of Lagrange with differential inequalities as added side conditions, Contributions to the calculus of variations, 1933-1937, The University of Chicago Press, Chicago, 1937.

BODIES OF MAXIMUM AERODYNAMIC QUALITY IN A HYPERSONIC FLOW

By

V.I. Lapygin

In the present work, the form of a conical body having the maximum value of aerodynamic quality is determined. It is supposed that the pressure distribution is determined by the Newton formula and that the coefficient of local friction is constant; the length and area of the mid-section of the body are given. However, such statement does not give the possibility to perform an analytical solution. An essential simplification of analysis was attained by auxiliary limitations for the class of the permissible surfaces. Till now, the procedure of Strend [8] has obtained the maximum spread. Strend solved the first problem about the form of a minimum-drag wing that is thin in both the longitudinal and transverse directions.

Subsequently, the optimization of the mentioned class of surfaces at different auxiliary conditions was investigated in the works [1, 9, 10]. In particular, the problem of a thin wing of maximum aerodynamic quality was discussed in detail in works [1, 10]. The simplicity of solution in such a statement is attained owing to the reduction of the three-dimensional problem of the form of the wing to the finding of the optimum profile in the longitudinal cross section. On the other hand, it is known that the form of the cross section of a wing strongly affects the value of aerodynamic quality [2, 11, 12]. Therefore, a more exact statement of a variational problem may give essentially new results for the optimum form of a hypersonic wing. In the below- cited solution of the variational problem of the form of a conical wing having a maximum quality, the assumption of the thinness of wing is removed.

The solution represented below was discussed initially in work [6]. At the moment of its completion, the investigations [13, 14], in which similar results are obtained, became known. However in contrast to work [14], the results of the given work are obtained for a more general statement of the problem, not limited by an auxiliary assumption of the form of the lee of the wing. Work [14] involves the same trend. In this work, for the first time, the method of the local variations is used for the variational problem of a wing in the Newtonian approximation.

1. Derivation of the Calculating Formulae, Statement of the Variational Problem

We shall consider the hypersonic flow of gas around a conical body. Let the axis of the cylindrical coordinate system ρ, φ, x, be selected along the flow, the velocity of which is U (Fig. 1). The surface of the conical body in the assumed coordinate system is given in the form:

$$\rho = \frac{x z(\varphi)}{l} \tag{1.1}$$

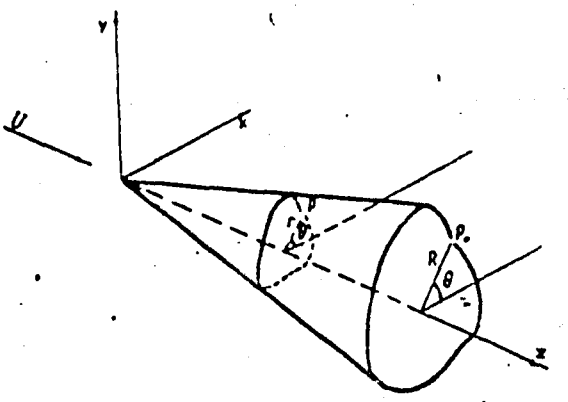

Fig. 1.

We shall consider that the total drag of the body consists of two parts: the wave drag and the frictional drag. We shall neglect the portion of the frictional force in the lift force. We shall determine the pressure distribution on the body by the Newton formula

$$C_p = k\cos^2(\bar{n}, \bar{U}), \tag{1.2}$$

where C_p – the coefficient of pressure on the body, relative to the dynamic pressure of the incident flow.

K – the proportionality constant.

$\bar{n}$ – the normal to the surface of the body.

Below, we shall assume that $k = 2$, $\ell = 1$.

We assume that the value of the local coefficient of friction is constant along the surface. With the assumed allowances, we obtain the following formulae for the coefficients of the aerodynamic forces (in view of the symmetry of the problem with respect to the plane $\varphi = 0$, the half of the body, $0 \leqslant \varphi \leqslant \pi$, is investigated):

$$SC_x = \int_0^{\pi} \left\{ \frac{z^4}{1+z^2+z'^2/z^2} + az\sqrt{1+z'^2/z^2} \right\} d\varphi \,, \tag{1.3}$$

$$SC_y = \int_0^{\pi} \frac{z^3(\cos\varphi + z'/z \sin\varphi)}{1+z^2+z'^2/z^2}\, d\varphi \,, \tag{1.4}$$

where $a = \frac{1}{2} C\tau$,

$S = \int_0^{\pi} z^2 d\varphi$ – is the area of the stern cross section of the body.

$C\tau$ – is the local coefficient of friction.

On investigating thin bodies, these formulae are simplified. Actually, at $\tau^2 \ll 1$ introducing a new dependent variable, $\tau = \alpha^{1/3} y$ we obtain:

$$I_1 = C_x \alpha^{-2/3} S_1 = \int_0^{\pi} \left(\frac{y^6}{y'^2 + y^2} + \sqrt{y^2 + y'^2} \right) d\varphi \quad , \tag{1.5}$$

$$I_2 = C_y \alpha^{-1/3} S_1 = \int_0^{\pi} y^4 \frac{y \cos\varphi + y' \sin\varphi}{y'^2 + y^2} \, d\varphi \quad , \tag{1.6}$$

$$S_1 = S\alpha^{-2/3} = \int_0^{\pi} y^2 \, d\varphi \quad . \tag{1.7}$$

The coefficient C_τ evidently does not enter in the right sides of formulae (1.5) and (1.6), which simplifies the investigation.

The statement of the problem: to find the function $y(\varphi)$ at the given value of (1.7), along which the ratio

$$\lambda = \frac{I_2}{I_1} \tag{1.8}$$

takes the maximum value.

The coupling between λ and the aerodynamic quality of the body is given by the relation

$$K = \lambda \alpha^{-1/3} \tag{1.9}$$

2. The Algorithm of the Numerical Solution and the Results of the Calculation

The analytical investigation of the problem encounters considerable difficulties connected with the fact that the Eulerian equation in this case is essentially nonlinear and has a second order.

A direct method is used for the solution of the problem. It is known by the name "method of local variations" [6, 3], in which the isoperimetric condition, $S_1 = \text{const}$, is fulfilled in every step. The convergence of the method in the case of absence of the isoperimetric condition is shown in work [5]. Because S_1

is maintained constant in the process of calculation, it is possible to hope that the used method coincides with the Eulerian equation for this case also; the calculations confirm this assumption.

The calculations were performed on the EVM- BESM-3M. The interval of φ was selected to be 4°, the initial value of the variation of the radius h = 0.01.

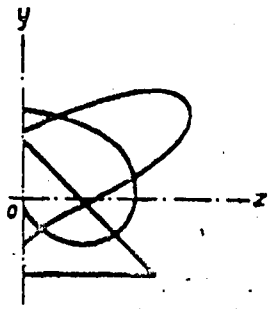

Fig. 2

For checking the convergence of the method to the unique solution, the contours shown in Fig. 2 are selected as a first approximation. These contours have the same area, but they differ in the form and the position of the maximum radius y_{max}. We denote the angle corresponding to the maximum radius by φ^*. It was found that the angle φ^* at a sufficient big number of interaction (h in the process of the calculation is decreased in 8 times), remains as it was in the initial approximation, with the exception of the case of the triangular contour. The forms of the contours are obtained qualitatively similar. For the explanation of this condition, some contours were selected. These contours are close in form to the optimum, and have the same area, but they differ in the angle φ^*. It was found that the dependence of quality on φ^* in the vicinity of the optimum angle is very weak (Table 1).

Table 1

φ^*	72°	64°	60°	56°	48°	36°
λ	0,3904	0,3977	0,4018	0,4015	0,3963	0,3739

Analogous dependence of λ on φ^* takes place at other values of S_1. The fact of variance of the angle φ^* at S_1 = const is evidently due to the insufficient accuracy of calculation (at a moderate number of interaction).

One must mention that the velocity of the convergence to the solution essentially depends on the selection of the initial approximation.

In the calculation, the value of the aerodynamic quality is determined considerably more quickly, than the contour of a transverse cross-section, and, starting from a certain moment, is changed extremely insignificantly. Therefore the obtained dependence $\lambda(S_1)$ has a high accuracy; the forms of the optimum contours are found with less accuracy. We notice that in the process of the calculation, a decrease of the interval of φ was not performed, because the time of the calculation considerably increases in this case, and the accuracy of the determination of λ is practically not changed.

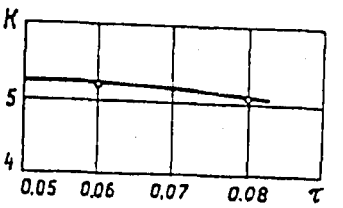

Fig. 3

The dependence of the optimum aerodynamic quality K at $C_\tau = 10^{-3}$ on the parameter of the volume $\tau = \sqrt{V}/S^{3/2}$ where V— is the volume of the body, and S— is the area in the plane, is shown in Fig. 3. The maximum values of K for V-shaped wings [2] are given by the small circles in the graph. The value of K for the V-shaped wing practically coincides with the value of K for the optimum body. We notice that these points correspond to wings with a cross-section close to a triangle, the base of which is directed to the windward side.

Let us cite data on the value of the aerodynamic quality of the bodies, investigated in works [11, 12]. At a given length of a half-cone body with a cross-section in the form of a semicircle has a quality K = 3.6 at $C_\tau = 10^{-3}$ and $V/\ell^3 = 0.0727$; with an elliptical cross-section, the maximum increase of the quality is 2%; with a sine cross-section—12.5%; with a triangular cross-section with the lateral sides facing the flow, the quality approaches the value for optimum bodies; for all the remaining cases, the increase is noticeably less. If we consider the triangle cross-section, with the base turned to the side of the flow, then, as the calculation shows (Fig. 4), the quality of the optimum body will practically coincide with the quality of the body of the mentioned form.

We notice that the triangular contour, with the base facing the windward side, consists of the extrema of the Eulerian equation for the investigated problem. However, this contour is not the solution because in the place of conjugation of the two arcs of the extrema (half-line and straight line, parallel to the OZ axis), the condition of Weierstrass- Erdman is not fulfilled. The forms of the optimum transverse contours as a function of S_1 are represented in Figs. 5 and 6.

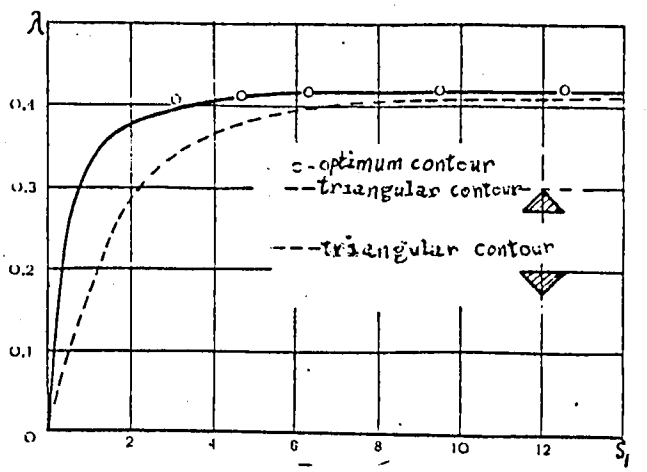

Fig. 4

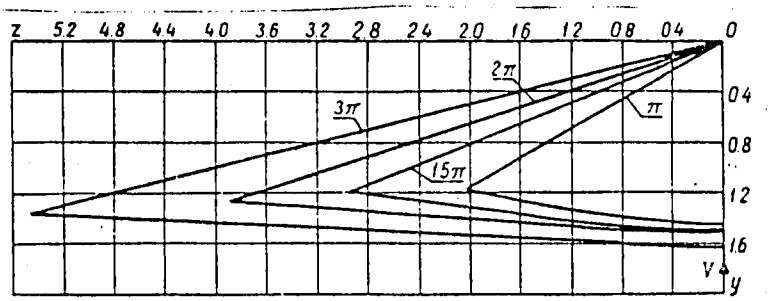

Fig. 5

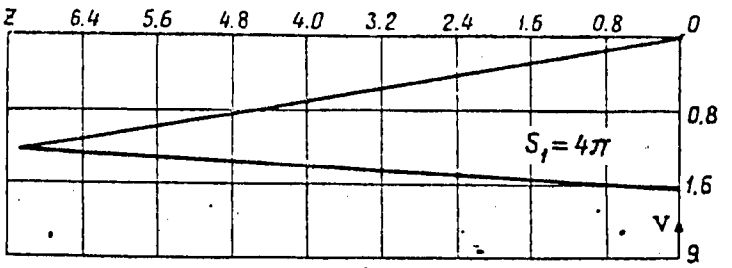

Fig. 6

It is noteworthy that the whole volume of the body is limited from above by surfaces representing, within the limits of the calculation error, two planes located along the flow. The lower surface of the wing, receiving the whole load, has a small convexity to the side of the incident flow. In the vicinity of the angle $\varphi=\pi$ there is a very small elevation, the hight of which decreases with increasing the number of iteration. The obtained numerical results confirmed with high accuracy the hypothesis that the upper surfaces of the optimum wing are planes located in the flow. As a whole, the form of an optimum transverse contour is close to a triangle, with the base facing the windward side. Hence, it becomes clear whey the quality of a wing with an optimum triangular cross-section almost coincides with the quality of the optimum.

For checking, a calculation was performed with the use of formulae (1.3) and (1.4) for $S = \pi \cdot 10^{-2}$; $S = 2\pi \cdot 10^{-2}$; $S = 4\pi \cdot 10^{-2}$ at $a = 10^{-3}$, without an assumption about the thinness of the body. The results are obtained identical with the above-mentioned. In particular, the form of the body and the value of the aerodynamic quality for the same values of S are practically the same.

3. Remark About the Convergence of the Solution

The problem under consideration is equivalent to the problem of the absolute extremum of the functional: $I = \int_0^{\pi} \Phi d\varphi$,

where

$$\Phi = y^4 \frac{y\cos\varphi + y'\sin\varphi}{y^2 + y'^2} - \lambda\left\{\frac{y^6}{y^2+y'^2} + \sqrt{y^2+y'^2}\right\} + \mu y^2 ,$$

$\mu = const$.

If the obtained solution will satisfy, with the given accuracy, the Eulerian equation for the function Φ and the boundary conditions, then the numerical convergence of the method does not arouse doubts. In order to be convinced by this, it is necessary to check:

1. The fulfillment of the boundary conditions at the extremum.

2. The fulfillment of the Eulerian equation.

3. The fulfillment of the conditions of the conjugation of extremum arcs in the corner point.

A direct numerical check of these conditions was performed for $S_1 = \pi$, $\varphi^* = 60°$.

1. The boundary conditions at the points $\varphi = 0$, $\varphi = \pi$ (the condition of the transversality) $\Phi_{y'}(0) = \Phi_{y'}(\pi) = 0$ are fulfilled exactly, because $y'(0) 0$ $y(\pi) = 0$.

2. The fulfillment of the Eulerian equation was checked only in the interval $0 < \varphi < \varphi^*$, because the half-line of $\varphi = \varphi^*$ is an extremum. At every point of the contour the value of 2μ was calculated in the interval $(0, \varphi^*)$. The results of calculation are represented in Fig. 7. For $0 < \varphi \leqslant 48°$, the deviations from the mean value do not exceed 6.5%; in the vicinity of $\varphi = 60°$, the variance of the values is slightly increased, which is explained by the difference of the actual angle φ^*_{opt} from the assumed angle in the calculation $\varphi^* = 60°$. (As shown in Table 1, $56° < \varphi^*_{opt} < 60°$).

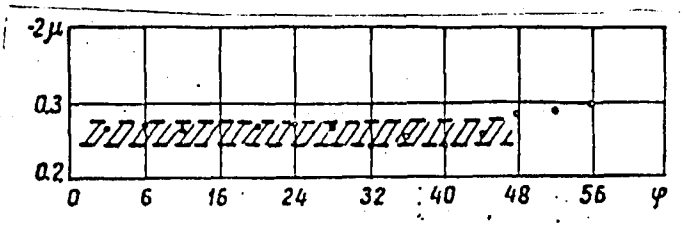

Fig. 7

3. The conditions at the corner point:

The condition $\Delta[\Phi_{y'}] = 0$ is satisfied with an accuracy of 3%; the condition $\Delta[\Phi_{-y'}, \Phi_{y'}] = 0$ is satisfied with an accuracy of 10%.

Here $\Delta[\ldots]$ denotes the difference of the values on the left and right from the corner point.

In conclusion, we mention that the accuracy of the method, as clear from the result of work [4], has the order of the interval of φ. In the performed calculations, the interval of φ was equal to 0.0698. Thus, the obtained above valuations of the convergence of the solution coincide with the accuracy of the method.

References

1. Maikapar G.I. "Krylo s maksimal'nym aerodinamicheskim kachestvom pri giperzvukovykh skorostyakh" (A wing with maximum aerodynamic quality at hypersonic velocities).--- PMM, 30 (1), 1966.

2. Gonor A.L., A.I. Shvets "Obtekanie V-obraznykh kryl'ev sverkhzvukovym potokom gaza" (Supersonic flow of gas around V-shaped wings).--- (Report of the Institute of Mechanics) MGU, No. 613, 1966.

3. Chernous'ko F.L. "Metod lokal'nykh variatsii dlya chiclennogo resheniya variatsionnykh zadach" (Method of local variations for the numerical calculation of the variational problems).--- Zh. vych. mat. i mat. fiz., 5 (4), 1965.

4. Krylov I.A., F.L. Chernous'ko "Reshenie zadach optimal'nogo upravleniya metodom lokal'nykh variatsii" (The solution of the problem of optimum control by the method of the local variations).--- Zh. vych. mat. i mat. fiz., 6 (2), 1966.

5. Banichuk N.V., V.M. Petrov, F.L. Chernous'ko "Metod lokal'nykh variatsii dlya variatsionnykh zagach s neadditivnymi funktsionalami" (The method of local variations for the variational problems with nonadditive functionals).--- Zh. vych. mat. i mat. fiz., 9, (3), 1969.

6. Gonor A.L., N.A. Ostatsenko, V.I. Lapygin "Obtekanie i optimal'naya forma konicheskogo kryla pri giperzvukovykh skorostyakh" (Flow around and optimum form of a conical wing at hypersonic velocities).--- Otchet Instituta mekhaniki (Report of the Institute of mechanics) MGU, No. 981, 1969.

7. Perminov V.D. "Kryl'ya s optimal'nymi kharkteristikami v giperzvukovom potoke" (Wings with optimum characteristics in the hypersonic flow).--- Izv. AN SSSR, MZhG, No. 6, 1969.

8. Strand T., Wings and bodies of revolution of minimum drag in newtonian flow, Convair, Rep. N ZA-303, 1958.

9. Hull, D.G. and Miele A., Three-dimensional shapes of minimum total drag in Newtonian flow. J. Astronaut. Sci., 12 (2), 1965.

10. Miele A. Maximum lift-to-drag ratio of a slender wing at hypersonic speeds, Z. Flugwise, 15 (7), 1967.

11. Lustu, A.H., Jr. and Miele A., Bodies of maximum lift-to-drag ratio i., hypersonic flow. AIAA Journal, 4 (12), 1966.

12. Miele A., Lift-to-drag ratio of slender bodies at hypersonic speeds. J. Astronaut. Sci., 13.6.1966.

13. Miele A., Heideman J.C., Pritchard R.E., Conical bodies of given length and volume having maximum lift-to-drag ratio at hypersonic speeds, Part 1 —Direct Methods, J. Ast. S., XY (2), 1968.

14. Ho-Yi Huang, Conical bodies of given length and volume having maximum lift-to-drag ratio at hypersonic speeds, Part 2 - Variational Methods, J. Astronaut. S., XY (3), 1968.

SUPERSONIC FLOW OF AIR AROUND A RECTANGULAR PLATE

By

M.P. Falunin

A considerable quantity of works is dedicated to the aerodynamics of wings of different forms at high velocities. An extensive bibliography of this problem is comprized in the works [1- 4].

In the present work, the pressure distribution on the windward side of a rectangular plate of infinite elongation is experimentally investigated, a study of the spectra of the flow around is also carried out on wide angles of attack for a wide range of change of elongation values ($0.025 \leqslant \lambda \leqslant 40$).

§ 1. Pressure Distribution on the Windward Side of an Infinite Rectangular Plate

The study of the pressure distribution on a rectangular plate with cutters on the ends, decreasing the influence of the end effects, permitted the determination of the diagrams of the pressures along the chord of the plate, and also the location of the center of the pressure of the plate. The pressure was measured in three cross-sections in the central part of the plate. These cross-sections are located at a distance of 15 mm from each other. In each cross-section, 6 drains were located. The distance between the drain points along the cross-section was equal to 5 mm; the distance from the edge of the plate was equal to 2.5 mm. A sketch of the location of the drain points is represented in Fig. 1.

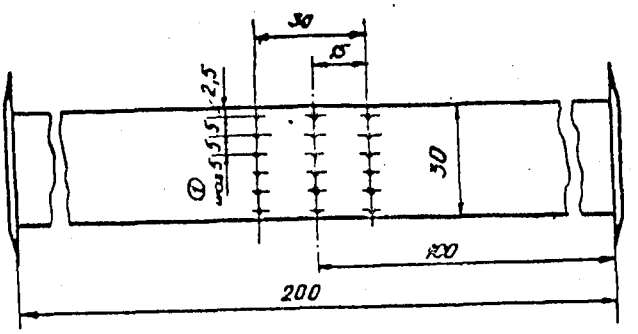

Fig. 1.

Key:
1) Distance.

The experiments were carried out at an incident flow velocity corresponding to a Mach number of M = 3.0. The obtained results shown in Figs. 2- 4 indicate the following:

1. The pressure at the drain points located at the same distance from the leading edge is the same in all three cross-sections. Therefore in the graphs, the pressures are shown at one point for every value of $\bar{h}$ (the distance along the chord from the leading edge relative to the length of the chord).

2. At narrow angles of attack ($\alpha \leqslant 30°$), the pressure along the chord practically does not change and agrees with the theoretical value for a rectangular plate of infinite speed at the corresponding angle of attack (Fig. 2).

3. Beginning from $\alpha \approx 35°$, when the leading wave withdraws from the leading edge, the pressure at that edge obviously increases, and by increasing the angle of attack, it approaches the value of the stagnation pressure behind the normal shock at M = 3. The pressure at the trailing edge slightly increases. The pressure distribution has an unsymmetrical form (Fig. 3, I- V).

4. By increasing the angle of attack, the zone of the increased pressure shifts from the leading edge to the middle of the plate, and at $\alpha = 90°$, the maximum pressure corresponds to $\bar{h} = 0.5$ (Fig. 3, VI). The pressure near the zone of the increased pressure begins to decrease in proportion to the displacement of this zone from the leading edge. At the angles of attack $35° \leqslant \alpha < 90°$, near the trailing edge (at a distance $\approx$ 0.1 of the chord), the pressure is less than that at the leading edge at the same distance. As the drop between the maximum pressure on the windward side and the pressure on the leeward side of the plate is supercritical, the velocity and pressure at the edges themselves must be critical.

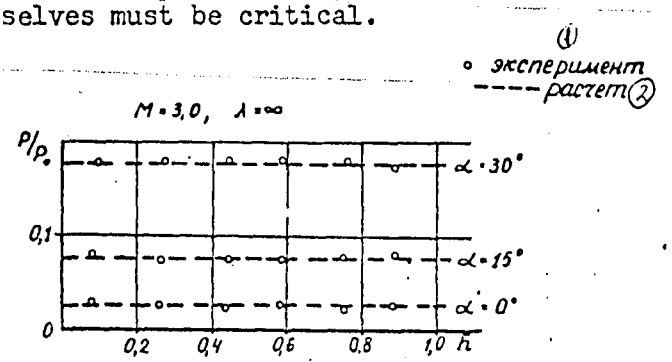

Fig. 2.

Key:
1) Experimental; 2) Calculated.

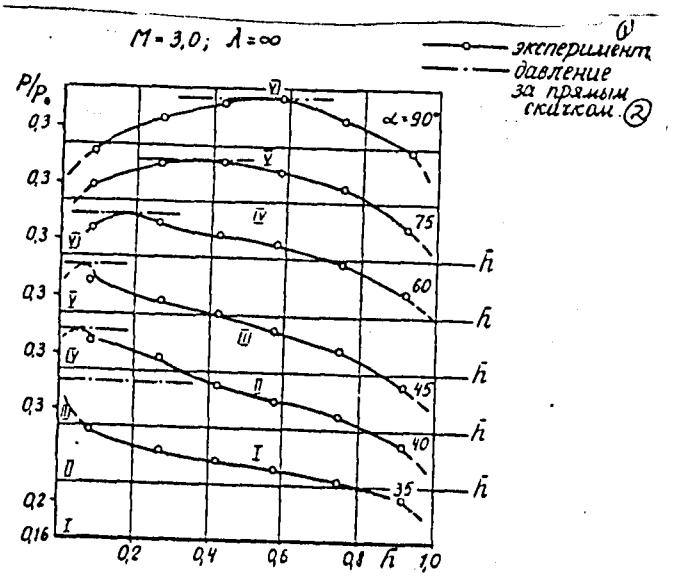

Fig. 3

Key:
1) Experimental; 2) Pressure behind the normal shock.

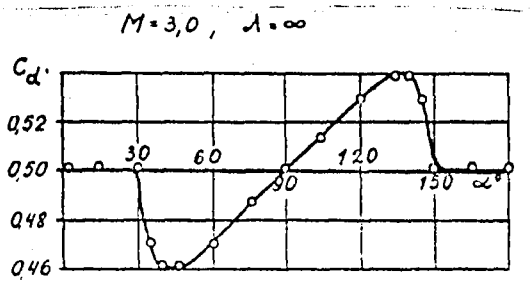

Fig. 4.

5. Owing to the change and displacement of the region of the increased pressure, the center of the pressure (in the condition that considers the pressure on the leeward side is equal to zero) also shifts from the center line of the plate to the side of the increased pressure. The graph of the relation $C_d(\alpha)$ is represented in Fig. 4. The data are obtained for the angle of attack α such that $0° \leqslant \alpha \leqslant 90°$. It is obvious that as long as the leading wave is attached to the leading edge, the pressure on all the faces is the same, and the center of the pressure is located on the central line of the plate ($C_d = 0.5$). After the detachment of the shock wave from the leading edge and the appearance of the zone of the increased pressure near it, the center of pressure shifts forward by about 8% ($C_{d\,min} \approx 0.46$; $\alpha \approx 35-45°$). On further increase of the angle of attack, the center of pressure shifts to the middle of the plate, at $\alpha = 90°$, $C_d = 0.5$. The increase of the angle of attack from 90° to 140° leads to the displacement of the center of pressure to the trailing edge ($C_{d\,max} \approx 0.54$). The attachment of the shock wave to the trailing edge of the plate necessitates the decrease of C_d to 0.5. Thus, the relative coordinate of the center of pressure of the forces acting on the windward side of the rectangular plate may be changed for the range of the angles of attack $0° \leqslant \alpha \leqslant 180°$ by about 15-17%.

6. The dependence of the relative coordinate of the point of maximum pressure $\bar{h}^*$ on the angle of attack is represented in Fig. 5. In Figs. 4 and 5, the curves for the angles of attack, $90° \leqslant \alpha \leqslant 180°$, are drawn on the basis of the symmetry of the flow around the plate at angles of attack $\alpha°$ and $180° - \alpha°$.

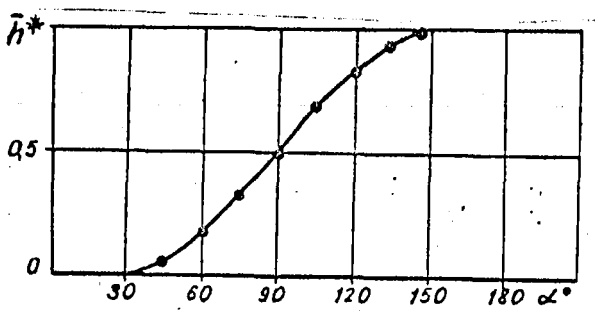

Fig. 5.

§ 2. Spectra of Supersonic Flow Around Rectangular Plates at Large Angles of Attack

The study of the spectra of supersonic flow around rectangular plates was carried out within a wide range of change of the angles of attack from 20° to 90° and of elongation from 0.025 to 40.

General remarks on the form of the shock wave: The analysis of the spectra of flow around and their quantitative treatment point to a sharp qualitative difference in the form of the shock wave* for small and big elongations. First of all, for such characteristic features of the form of the shock wave, it is possible to refer to the following (Fig. 6):

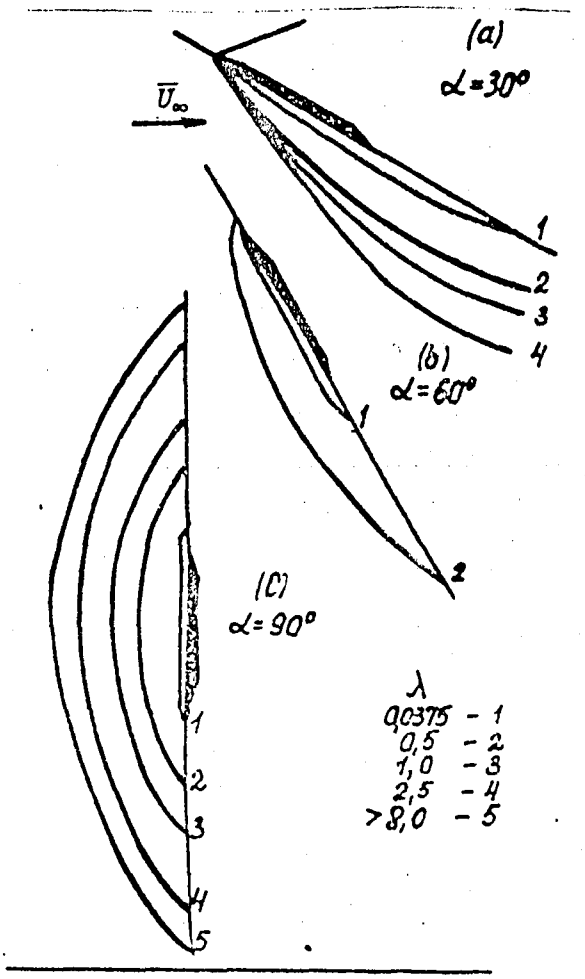

Fig. 6.

* All the data shown in the sketch graphs and tables are relative to the vertical plane of symmetry.

a) The presence of two straight segments of shock wave in the case of plates of small elongation and narrow angles of attack; one segment is attached to the leading edge, the other—at a certain distance from it. In the case of a plate with an elongation of the order of one or more, there is only one straight segment adjacent to the leading edge. b) At wide angles of attack, when the shock wave is totally detached, the shock wave is curvilinear in the case of plates of big elongation while it is, for the most part, equidistant from the windward side of the plate in the case of plates of small elongation.

The values of the quantities from which it is possible to judge the form of the shock wave and its variation with the angle of attack α and the elongation $\lambda = b/h$ are given in Table 1, where b is the length (spread) of the plate, and h is its height (chord). All the quantities are relative to the height of the plate h. The quantities in Table 1 correspond to the following geometric characteristic of the shock wave (Fig. 7).

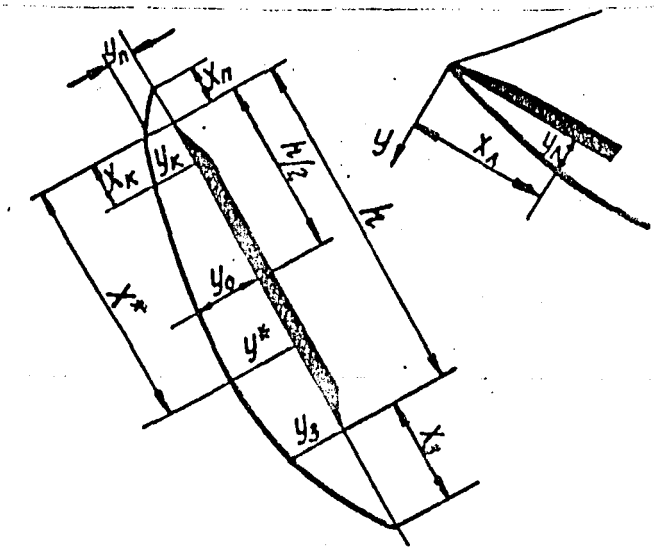

Fig. 7.

1) X_n, 2) y_n — the distance from the leading edge of the plate to the shock wave along the plate, upstream and in the perpendicular direction, respectively; 3) y_c — the distance from the center of the plate to the shock wave perpendicular to the plate direction; 4) $X_з$, 5) $y_з$ — the distance from the trailing edge of the plate to the shock wave along the plate, downstream and in the perpendicular direction, respectively; 6) $X_л$, 7) $y_л$ — the coordinates of the end of the straight segment of the attached shock wave with respect to the leading edge; 8) $X_к$, 9) $y_к$ — the coordinates of the end of the

curvilinear segment of the detached shock wave with respect to the leading edge; 10) X*, 11) y^* - the point grid reference of the shock wave with maximum departure from the surface of the windward side of the plate, with respect to the leading edge.

For illustration, the graphs of the quantities 1- 11 (except 6 and 7) are represented in Figs. 8 and 9 for a plate with an elongation $\lambda = 0.0375$. The numbering of the curves corresponds to the enumerated quantities.

Model No. 2 $\lambda = 0.0375$; h = 80 mm; M = 3.0

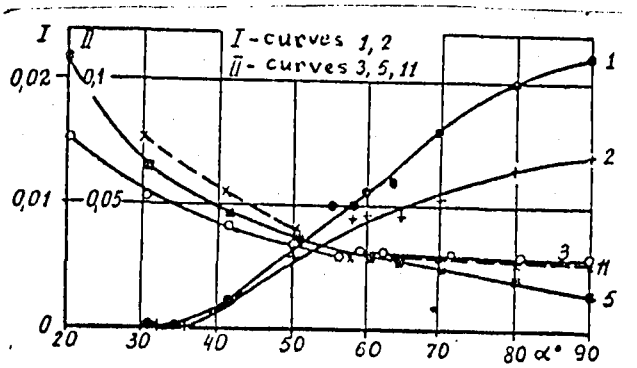

Fig. 8

Key:
1) Curves.

We have to do some explanations in connection with the quantity $X_к$: a) if the curvilinear segment of the shock wave, adjacent to the leading edge, converts afterwards to a rectilinear one, which, in its turn, is already curved because of the effect of the trailing edge, then $X_к$ denotes the distance from the leading edge to the projection of the end of the first curvilinear segment on the windward surface of the plate; b) if the shock wave is totally curvilinear, then the quantities $X_к$ and X* coincide; c) in the case of a symmetric flow around a plate ($\alpha = 90$), the quantities of $X_к$ and X* coincide. The dash in Table 1 denotes that the corresponding quantities could not be measured in the limits of the visual field. This refers to the quantities $X_з$, $X_л$, $y_л$, $X_к$, $y_к$, X*, y^*. In individual cases, this denotes the absence of truthworthy data about the corresponding quantities ($X_п$, $y_п$).

Model No. 2; 0.0375, h = 80 mm; $M = 3.0$

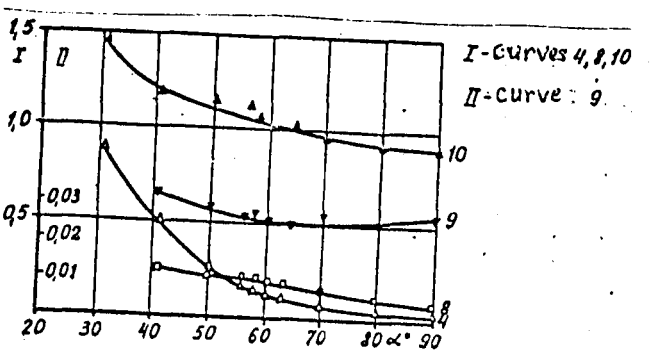

Fig. 9.

Key:
1) Curves.

Analysis of the straight segment of the shock wave:: The straight segment adjacent to the leading edge of the plate corresponds to flow around a plate with attached shock wave. In this case, in the vertical plane of symmetry, the straight segment of the wave proportionally increases with increasing the elongation of the plate, until one achieves the elongation of the length at which disturbance from the trailing edge reaches the wave more quickly than from the lateral ends. At $M = 3.0$ and angle of attack $\alpha = 30°$, the proportionality is broken for $\lambda > 0.75$, and at the angle of attack $\alpha = 20°$ — for $\lambda > 0.125$ (see Table 1 and Fig. 10). Lines 1', 2', 3' in Fig. 10 correspond to the experimental data for the relative length of projection of the straight segment of the shock wave on the plane of the plate. The solid lines were calculated with Mach disturbances from the lateral ends of the leading edge.

The results of the analysis of the spectra of flow around indicate that the rectilinearity of the attached shock wave in the vertical plane of symmetry is broken at values of $X_\wedge$ that are smaller than implied from the mentioned calculation.

Dependence of the form and dimensions of the leading shock wave on the angle of attack and edge effects: The angle of attack and the elongation of the plate essentially influence all the geometric structure of the shock wave, namely the length of the straight segment, the magnitude of withdrawal, its departure from the leading and trailing edges of the plate, etc.

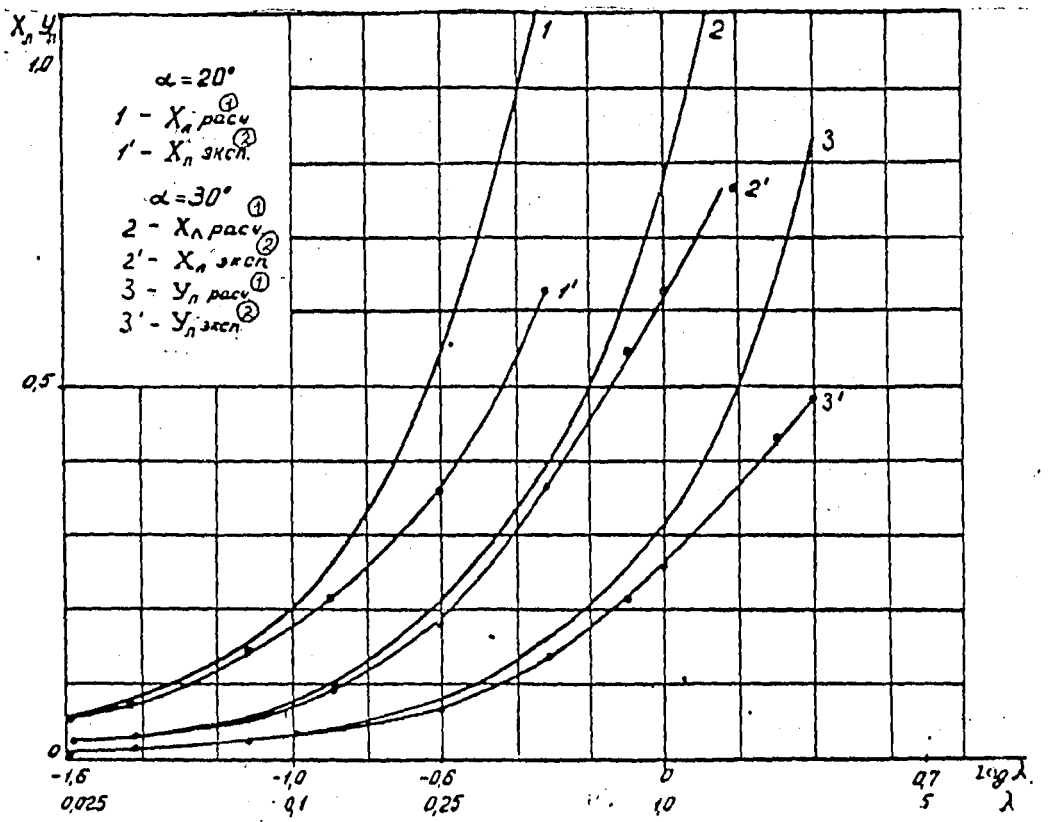

Fig. 10.

Key:
1) Calculated; 2) Experimental.

The corresponding data are given in Table 1. In the case of narrow angles of attack, when the shock wave is attached to the leading edge, plates with an elongation exceeding a few units will be flowed around in the central part of the windward side by a translational flow along the whole height. The shock wave has one straight segment, which is curved because of the disturbances running from the trailing edge. This bend of the wave is observed downstream at a considerable departure from the plate. The slope of the straight segment corresponds to the calculation. In the case of plates with small elongation ($\lambda < 0.1$), the structure of the shock wave at certain angles of attack is different: the translational flow occupies a small segment adjacent to the leading edge; the shock wave at the edge is rectilinear, then it is strongly curved, converting to the second straight segment, which is almost parallel to the face of the plate (Fig. 6a).

At angles of attack, occupying an intermediate location between the normal flow around ($\alpha = 90°$) and different angles of attack, the sharp difference in the form of the shock wave is retained for plates of different elongation when the wave is attached to the leading edge. In the case of plates with an elongation $\lambda \lesssim 0.5$, the shock wave in the plane of symmetry is totally curved. The distance from the windward side to the shock wave in the perpendicular direction is variable: it is minimum at the leading edge, and maximum at the trailing edge. It is characteristic for plates of small elongation ($\lambda < 0.1$) at the mentioned angles of attack that, for the most part, the shock wave is equidistant from the force; at the same time, the distance between them is approximately the same as in the case of symmetric flow around ($\alpha = 90°$, see Fig. 6b and Table 1).

At last, the difference in the form of the shock wave for a plate with small and big elongation, in the case of flow around perpendicular to the windward surface is shown in Fig. 6C, Plates with small elongation have a straight segment of shock wave on the whole extension, with the exception of the range adjacent to the edges. In connection with the influence of the finite dimensions of a plate on the form of the shock wave, we should add that in the case of narrow angles of attack, this influence may be extended to considerable distances. At angles of attack $\alpha = 60–90°$, the ends of the plate exert an influence on the form of the shock wave at a departure approximately equal to 4– 3 times the magnitude of the spread (width) of the plate, respectively. Therefore, if $\lambda > 8$ or $\lambda < 1/8$, the middle part of the plate will exhibit a flow around as a plate of infinite spread. That is to say, the relative geometric parameters of the shock layer will not depend on the location of the fairing segment of that part of the plate.

Determination of the magnitude of the withdrawal of a shock wave in the case of a flow around a plate which is perpendicular to the flow: We shall relate the magnitude of the withdrawal of the shock wave to the height (chord) or to a side of a square equivalent in area to the plate. If at a fixed height of a plate, its elongation is changed, the relation of the magnitude of the withdrawal of the wave to the height of the plate ($\bar{\delta}$) gives a clear idea about the dependence of this relation on the elongation. In particular, in the case of elongation exceeding 6– 8, the quantity $\bar{\delta}$ approaches a constant value. The corresponding data are given in Table 1 and in Fig. 11 (solid line). If we relate the magnitude of withdrawal to the square root of the area of the plate, this quantity ($\bar{\delta}'$) will enable to reveal the equality of withdrawal of the shock wave for the quantities λ and $1/\lambda$. The maximum is attained at $\lambda = 1$ (Fig. 11, the dashed line). In connection with the great range of change of the elongation of plate, the relations $\bar{\delta}(\lambda)$ and $\bar{\delta}'(\lambda)$ are represented in a logarithmic scale on the axis of λ . According to the data (Table 1, Fig. 11), in the case of the change of the elongation of the plate from 0.025 to 0.125, the value of $\bar{\delta}$ is linearly changed, and at $\lambda \geq 8$, it remains constant and is equal to ≈ 0.72. Thus, in the case of the change of elongation by more than two orders, the withdrawal of the shock wave changes forty times. The maximum value of $\bar{\delta}'$ is one half of $\bar{\delta}_{max}$.

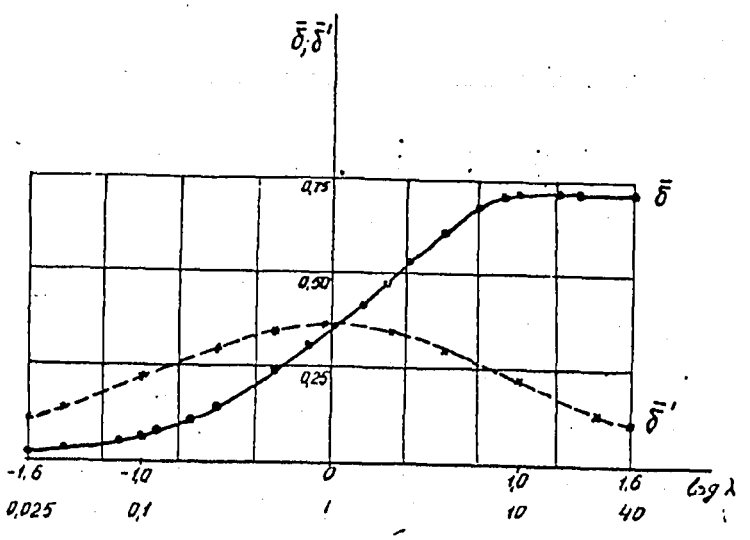

Fig. 11

On the basis of the given discussion, it is possible to draw the following conclusions. In the case of a supersonic flow around a rectangular plate, the structure of the shock wave strongly depends on the elongation of the plate and the angle of attack. In particular, in the case of a perpendicular flow around a plane plate, the withdrawal of the shock wave may be changed by ten times.

In the case of narrow angles of attack, the influence, of the leading and trailing edges may be transferred to comparatively great distances downstream. At angles of attack close to $\alpha = 90°$, this influence is extended along the plate to distances exceeding its width by three–four times. Plates with elongation $\lambda \lesssim 1/8$ and $\lambda \gtrsim 8$ are flowed around in their central part as infinite plates.

In the case of an attached leading wave, the center of pressure of the forces acting on the windward side of a rectangular plate with infinite length is located at the centeral line. In the case of a detached wave, the center of pressure is shifted to the side facing the flow. The magnitude of the displacement of the center of the pressure may attain 15– 17%.

In conclusion, the author expresses sincere thanks to G.S. Ul'yanov, A.F. Mosin, A.A. Makshin and L.V. Filyand for their help in carrying and working out the experiments.

Table 1

λ	$\alpha°$	① Характеристики ударной волны										
		$x_п$	$y_п$	$y_о$	$x_з$	$y_з$	$x_л$	$y_л$	$x_к$	$y_к$	x^*	y^*
		1	2	3	4	5	6	7	8	9	10	11
0,025	21	0	0	0,064	–	0,094	0,048	0,018	–	–	–	–
	30,5	0	0	0,038	0,700	0,046	0,027	0,008	–	–	1,260	0,054
	41	–	–	0,020	0,280	0,026	–	–	–	–	1,083	0,028
	50	0,0020	0,0010	0,018	0,150	0,018	–	–	0,220	0,018	1,046	0,021
	60,5	0,0052	0,0033	0,019	0,110	0,017	–	–	0,130	0,017	0,021	0,018
	66	0,0080	0,0045	0,018	0,065	0,016	–	–	0,120	0,016	1,000	0,019
	68	0,0085	0,0048	0,018	0,052	0,015	–	–	0,090	0,017	0,978	0,018
	70,5	0,0087	0,0052	0,018	0,044	0,014	–	–	0,080	0,018	0,957	0,018
	71	0,0090	0,0064	0,017	0,040	0,014	–		0,070	0,018	0,950	0,017
	80	0,0110	0,0080	0,018	0,030	0,012	–	–	0,065	0,017	0,945	0,018
	90	0,0150	0,0096	0,018	0,015	0,010	–	–	0,065	0,018	0,935	0,018
0,0375	20,5	0	0	0,079	–	0,113	0,069	0,024	–	–	–	–
	30,5	0	0	0,053	0,890	0,067	0,034	0,013	–	–	1,480	0,078
	41	0,0022	–	0,041	0,500	0,048	–	–	0,250	0,033	1,200	0,056
	50	0,0072	0,0061	0,037	0,260	0,038	–	–	0,240	0,030	1,170	0,040
	56	0,0100	0,0087	0,032	0,170	0,032	–	–	0,220	0,026	1,130	0,032
	58	0,0110	0,0092	0,031	0,150	0,032	–	–	0,180	0,027	1,060	0,031
	60	0,0120	0,0092	0,030	0,130	0,031	–	–	0,160	0,026	1,043	0,031
	64	0,0130	0,0094	0,028	0,110	0,028	–	–	0,130	0,026	1,030	0,030
	70	0,0150	0,0105	0,028	0,065	0,024	–	–	0,150	0,027	0,957	0,030
	80	0,0200	0,0130	0,027	0,035	0,020	–	–	0,130	0,026	0,935	0,028
	90	0,0220	0,0140	0,027	0,022	0,014	–	–	0,097	0,027	0,903	0,027

λ	α°	1	2	3	4	5	6	7	8	9	10	11
	70	0,040	0,030	0,100	0,39	0,111	–	–	0,72	0,102	0,87	0,115
	80	0,075	0,050	0,107	0,22	0,104	–	–	0,67	0,111	0,67	0,111
	90	0,125	0,072	0,116	0,125	0,072	–	–	0,5	0,116	0,5	0,116
0,25	20	0	0	0,154	–	0,235	0,360	0,140	–	–	–	–
	30	0	0	0,138	–	0,198	0,180	0,054	1,100	0,196	1,76	0,23
	34	0	0	0,130	–	0,172	0	0	1,070	0,174	1,65	0,19
	36	0,012	0,083	0,127	–	0,166	–	–	1,070	0,170	1,56	0,19
	38	0,017	0,015	0,130	–	0,165	–	–	1,040	0,170	1,54	0,19
	40	0,018	0,018	0,133	–	0,164	–	–	1,020	0,170	1,46	0,19
	60	0,031	0,032	0,139	0,740	0,163	–	–	0,70	0,160	1,17	0,17
	90	0,187	0,107	0,154	0,187	0,107	–	–	0,5	0,154	0,5	0,154
0,50	20	0	0	0,162	–	0,292	0,630	0,260	–	–	–	–
	30	0	0	0,180	–	0,280	0,370	0,143	–	–	–	–
	34	0	0	0,190	–	0,276	0,174	0,089	–	–	–	–
	36	0,013	0,008	0,192	–	0,273	–	–	–	–	–	–
	38	0,015	0,009	0,193	–	0,288	–	–	1,22	0,276	1,70	0,322
	40	0,018	0,018	0,196	–	0,264	–	–	1,17	0,265	1,59	0,290
	60	0,070	0,067	0,221	1,150	0,260	–	–	1,00	0,260	1,15	0,260
	90	0,345	0.186	0,243	0,345	0,186	–	–	0,5	0,243	0,5	0,243
0,75	30	0	0	0,194	–	0,324	0,566	0,215	–	–	–	–
	34	0	0	0,215	–	0,336	0,262	0,132	–	–	–	–
	38	0,021	0,017	0,225	–	0,325	–	–	–	–	–	–
	90	0,490	0,250	0,310	0,474	0,251	–	–	0,5	0,310	0,5	0,310
1,0	30	0	0	0,206	–	0,383	0,630	0,254	–	–	–	–
	34	0	0	0,240	–	0,383	0,087	0,063	–	–	–	–
	38	0,026	0,034	0,262	–	0,390	–	–	–	–	–	–
	90	0,590	0,0315	0,365	0,590	0,312	–	–	0,5	0,365	0,5	0,365

λ	α°	I	2	3	4	5	6	7	8	9	I0	II
0,075	20	0	0	0,104	–	0,157	0,168	0,052	–	–	–	–
	30	0	0	0,072	–	0,100	0,065	0,025	–	–	1,52	0,122
	39,5	–	–	0,060	0,860	0,076	–	–	0,410	0,056	1,28	0,087
	46	0,001	0,001	0,054	0,490	0,064	–	–	0,380	0,055	1,15	0,064
	48	0,001	0,001	0,053	0,435	0,060	–	–	0,360	0,054	1,12	0,060
	50	0,002	0,004	0,055	0,420	0,060	–	–	0,340	0,054	1,10	0,055
	60	0,005	0,006	0,054	0,240	0,060	–	–	0,320	0,055	1,07	0,055
	70	0,012	0,014	0,054	0,165	0,057	–	–	0,270	0,055	0,97	0,055
	80	0,028	0,020	0,053	0,111	0,047	–	–	0,220	0,054	0,93	0,054
	90	0,045	0,032	0,054	0,045	0,036	–	–	0,200	0,055	0,80	0,055
0,125	20	0	0	0,121	–	0,175	0,217	0,074	–	–	–	–
	30	0	0	0,102	–	0,127	0,087	0,037	–	–	1,59	0,152
	38	0,001	0,001	0,092	1,180	0,112	–	–	0,68	0,089	1,41	0,104
	40	0,004	0,004	0,092	1,140	0,105	–	–	0,50	0,092	1,35	0,113
	42,5	0,008	0,007	0,090	0,940	0,098	–	–	0,48	0,090	1,28	0,098
	50	0,008	0,009	0,088	0,820	0,096	–	–	0,43	0,087	1,18	0,094
	60	0,015	0,011	0,088	0,480	0,093	–	–	0,39	0,085	1,06	0,093
	70	0,032	0,024	0,087	0,250	0,085	–	–	0,37	0,087	0,94	0,089
	80	0,076	0,035	0,088	0,160	0,072	–	–	0,35	0,088	0,87	0,088
	90	0,101	0,050	0,088	0,101	0,050	–	–	0,34	0,088	0,67	0,088
0,875	20	0	0	0,181	–	0,213	0,288	0,095	–	–	–	–
	30	0	0	0,145	–	0,162	0,130	0,060	–	–	–	–
	38	0,001	0,001	0,113	1,310	0,142	–	–	0,90	0,135	1,39	0,150
	40	0,010	0,010	0,107	1,25	0,140	–	–	0,86	0,128	1,37	0,148
	44	0,020	0,020	0,107	1,04	0,119	–	–	0,82	0,115	1,32	0,133
	50	0,020	0,020	0,093	0,82	0,110	–	–	0,80	0,103	1,22	0,122
	60	0,031	0,030	0,098	0,51	0,110	–	–	0,77	0,103	0,98	0,118

λ	α°	1	2	3	4	5	6	7	8	9	10	11
1,5	30	0	0	0,214	–	0,403	0,76	0,363	–	–	–	–
	34	0	0	0,270	–	0,447	0	0	–	–	–	–
	38	0,036	0,058	0,309	–	0,479	–	–	–	–	–	–
	90	0,706	0,350	0,406	0,706	0,350	–	–	0,5	0,406	0,5	0,406
2,0	30	0	0	0,218	–	0,431	0,95	0,434	–	–	–	–
	34	0	0	0,284	–	0,490	0	0	–	–	–	–
	38	0,042	0,052	0,341	–	0,532	–	–	–	–	–	–
	90	0,87	0,400	0,485	0,87	0,400	–	–	0,5	0,460	0,5	0,460
2,5	30	0	0	0,230	–	0,447	1,1	0,480	–	–	–	–
	34	0	0	0,309	–	0,524	0	0	–	–	–	–
	38	0,048	0,066	0,383	–	0,594	–	–	–	–	–	–
	90	1,020	0,502	0,542	1,02	0,500	–	–	0,5	0,542	0,5	0,542
0,050	90	0,040	0,023	0,036	0,040	0,023	–	–	0,5	0,036	0,5	0,036
0,055	90	0,042	0,026	0,040	0,042	0,026	–	–	0,5	0,040	0,5	0,040
0,063	90	0,050	0,029	0,044	0,050	0,029	–	–	0,5	0,044	0,5	0,044
0,071	90	0,057	0,033	0,051	0,057	0,033	–	–	0,5	0,055	0,5	0,051
0,084	90	0,067	0,039	0,060	0,067	0,039	–	–	0,5	0,060	0,5	0,060
0,100	90	0,080	0,047	0,072	0,080	0,047	–	–	0,5	0,072	0,5	0,072
0,125	90	0,100	0,054	0,088	0,100	0,054	–	–	0,5	0,088	0,5	0,088
0,167	90	0,119	0,065	0,065	0,119	0,065	–	–	0,5	0,115	0,5	0,115
0,250	90	0,165	0,095	0,150	0,165	0,095	–	–	0,5	0,150	0,5	0,150
0,400	90	0,275	0,170	0,210	0,275	0,170	–	–	0,5	0,210	0,5	0,210
0,50	90	0,313	0,192	0,245	0,313	0,192	–	–	0,5	0,245	0,5	0,245
0,667	90	0,428	0,254	0,280	0,428	0,254	–	–	0,5	0,280	0,5	0,280
1,000	90	0,556	0,261	0,360	0,556	0,261	–	–	0,5	0,360	0,5	0,360
1,5	90	0,644	0,386	0,416	0,644	0,388	–	–	0,5	0,416	0,5	0,416

λ	α°	1	2	3	4	5	6	7	8	9	10	11
2,0	90	0,835	0,480	0,485	0,835	0,480	–	–	0,5	0,480	0,5	0,480
2,5	90	0,870	0,486	0,542	0,870	0,486	–	–	0,5	0,542	0,5	0,542
4,0	90	1,010	0,575	0,616	1,010	0,575	–	–	0,5	0,610	0,5	0,610
6,0	90	1,180	0,590	0,690	1,180	0,590	–	–	0,5	0,654	0,5	0,654
8,0	90	1,220	0,625	0,720	1,220	0,625	–	–	0,5	0,720	0,5	0,720
10,0	90	1,220	0,625	0,720	1,220	0,625	–	–	0,5	0,720	0,5	0,720
12,0	90	1,220	0,625	0,720	1,220	0,625	–	–	0,5	0,720	0,5	0,720
14,0	90	1,220	0,625	0,720	1,220	0,625	–	–	0,5	0,720	0,5	0,720
16,0	90	1,220	0,625	0,720	1,220	0,625	–	–	0,5	0,720	0,5	0,720
18,0	90	1,220	0,625	0,720	1,220	0,625	–	–	0,5	0,720	0,5	0,720
20,0	90	1,220	0,625	0,720	1,220	0,625	–	–	0,5	0,720	0,5	0,720

Key:
1) Characteristics of shock waves.

References

1. Chernyi, G.G. "Kryl'ya v giperzvukovom potoke". (Wings in hypersonic flow).--- PMM, 29 (4), 1965.

2. Dzhons, P. and D. Koen. "Aerodinamika kryl'ev pri bol'shikh skovostyakh". (Aerodynamics of wings at high velocities).--- Review article in the book "Aerodinamika chastei samoleta pri bol'skikh shorostyakh", 1957.

3. Issledovaniya v oblasti mekhaniki zhidkostei i gaza" (Investigations in the field of the mechanics of liquids and gases).--- Materialy k istorii TsAGI, 1968.

4. "Mekhanika v SSSR za 50 let", vol. 2, 1970.

SUPERSONIC FLOW AROUND PENETRABLE PLATES AT NARROW ANGLES OF ATTACK

By

G.S. Ul'yanov

The development of the aviation and space technology raises a whole series of important scientific-technical problems in the stabilization, deceleration, descent and landing of different objects. For these purposes, parachutes of different constructions and other stopping devices acting at supersonic velocities are used to a large extent. The supersonic flow around penetrable bodies has a whole series of specific aspects and peculiarities, to which the works [1 - 3] are dedicated. However, a whole series of problems are still open at the present time. For example, in the case of supersonic flow around a penetrable plate with a finite thickness under an angle of attack, the necessity arises to estimate and point out when one should take into account the tangential component of the aerodynamic force. For this purpose, it is necessary to determine experimentally the value of the tangential component relative to the normal component, its dependence on the degree of penetrability, angle of attack, Mach number M, and relative geometric dimensions. This enables to work out in a physically substantiated way the equations of conservation of momentum and energy for the penetrable surface.

The present work is dedicated to experimental study of supersonic flow around penetrable plates at narrow angles of attack.

1. Models and Techniques of the Experiments

Squares plates of 100 x 100 mm with a thickness of 2.5 mm and symmetrically sharp leading and trailing edges, were investigated. The perforation of the plates was attained by uniform boring of holes of diameter 3 mm along the whole surface of the plate. The penetrability of the plates was as follows: 0, 8.5, 16.0, 25.5, 51.5%. The ratio of the sum of the areas of the holes S_o to the total area S is known as the penetrability factor W of the plate δ ($W = (S_o/S)\ 100\ [\%]$).

The experiments were carried out in a supersonic wind tunnel at Mach numbers M of the flow from 1.5 to 3.0 and Reynolds numbers $Re_\ell = 2.5 - 4.10^6$ ($\ell = 0.1$ m).

The gravimetric investigations of the penetrable plates were carried out in the range of angles of attack from 0 to 17°. The plates were fastened in the working section of the wind tunnel on two belt suspensions. The aerodynamic coefficients C_x and C_y — were determined. The correction for the suspension device was determined by a separate experiment, in which the belt suspensions were blown through without plate. The calculation of interference had not been considered. The relative error in measuring the drag force X and lifting force Y was in the limits of 0.5 - 3%.

2. Results of the Experiments and their Analysis

We consider that the aerodynamic coefficients C_x and C_y are determined, with the forces X and Y related to the total area of the plate, and the coefficients with index "P" (C_{xp} , C_{yp})— to the area taking account of the degree of penetrability. The coefficients C_n and C_τ for the normal and tangential components of the aerodynamic force were determined by recalculation and were related to the total area of the plate.

The relations $C_{xp}(\alpha)$ and $C_{yp}(\alpha)$ at the Mach number M = 2.5 and at different values of the penetrability parameter W are represented in Figs 1 and 2. It is obvious from the given graphs that the resistance coefficients C_{xp} (C_x) nonlinearly increase with increasing the angle of attack. A similar pattern of monotonic nonlinear increase of the resistance coefficients with increase of the angle of attack was observed in the range of Mach number M = 1.5—3.0.

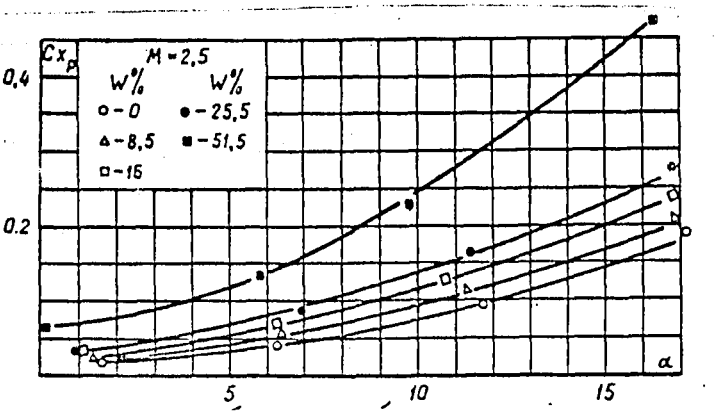

Fig. 1

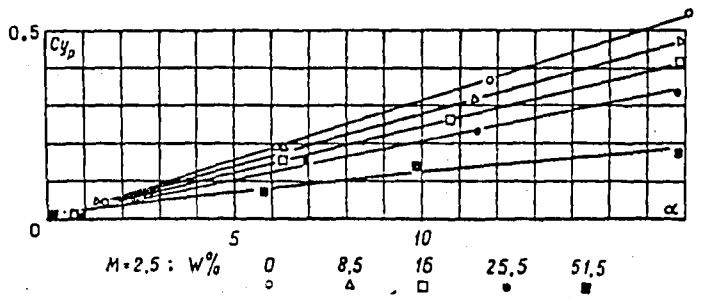

Fig. 2.

The aerodynamic coefficients of the lifting force $C_{y_p}(C_y)$ for the penetrable plates are linear functions of the angle of attack of the plate. Their values are conveniently calculated by the following formula:

$$C_y = K_{c_y}(W, M)\cdot\alpha \ ,$$

where α is in radiants and the coefficients K_{c_y} and $K_{c_{y_p}}$ are given in Table 1.

Table 1

$C_y = K_{c_y}(W,M)\cdot\alpha$										
M	1,5					2,0				
W%	0	8,5	16,0	25,5	51,5	0	8,5	16,0	25,5	51,5
K_{c_y}	2,522	2,064	1,662	1,204	0,401	2,064	1,662	1,318	1,032	0,344
$K_{c_{y_p}}$	2,522	2,236	1,948	1,605	0,917	2,064	1,834	1,548	1,376	0,745
	2,5					3,0				
W%	0	8,5	16,0	25,5	51,5	0	8,5	16,0	25,5	51,5
K_{c_y}	1,834	1,490	1,146	0,860	0,287	1,433	1,146	0,86	0,688	0,229
$K_{c_{y_p}}$	1,834	1,605	1,376	1,204	0,631	1,433	1,261	0,974	0,8599	0,516

The graphs of the aerodynamic quality $K = \frac{C_y}{C_x} = f(\alpha)$ for plates with different penetrability parameters W and Mach number M = 2.5 are given in Fig. 3. It is obvious from these graphs that the quality of the penetrable plates strongly depends on the degree of penetrability. For example, the plate with a penetrability W = 51.5% has a maximum quality approximately eight times less than that of the solid plate. The maximum aerodynamic quality for penetrable plates at a Mach number M = 2.5 is observed approximately at angles of attack α = 6– 7°. One should also notice that $K_{max}(\alpha)$ slowly depends on the degree of penetrability. Similar relationships in the behavior of the aerodynamic quality are observed at other Mach numbers M. The values of $K_{max}(\alpha)$ for Mach numbers M = 1.5– 3.0 and plate penetrabilities W = 0– 51% are given in Table 2.

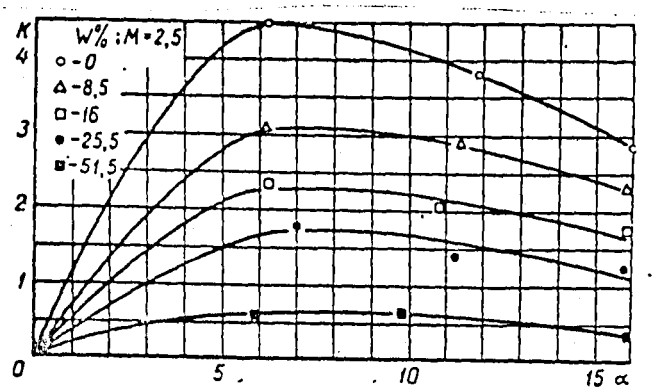

Fig. 3

Table 2

	W %	0	8,5	16	25,5	51,5
$K_{max}(\alpha)$	M=1,5	4,65	3,55	2,95	2,05	0,55
	2,0	4,55	3,45	2,60	1,80	0,55
	2,5	4,45	3,05	2,25	1,70	0,55
	3,0	3,70	2,80	2,10	1,55	0,55

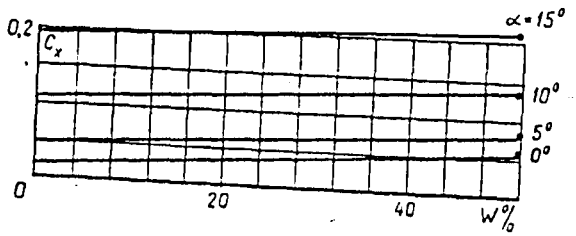

Fig. 4

The relations C_x (w) and C_y (w) at different values of the parameter α and Mach number M = 2.0 are shown in Figs. 4 and 5. The increase of the degree of penetrability of the plate at a fixed angle of attack strongly decreases the lifting force coefficient and slightly increases the resistance coefficient. The influence of the degree of penetrability on the resistance coefficient C_{xp} at narrow angles of attack is more strong than in the case of wide angles. For example, for M = 1.5 and angle of attack $\alpha = 5°$, the value of C_{xp} increases five times with the increase of the penetrability factor from 0 to 51.5%, and at $\alpha = 15°$ — only by two times. One should also notice that the coefficient C_x (w) is a linear function of W. As a consequence of linearity, the resistance coefficient C_x (w) can be calculated by the formula:

$$C_x = K_{c_x}(M, \alpha) \cdot W + B_{c_x} .$$

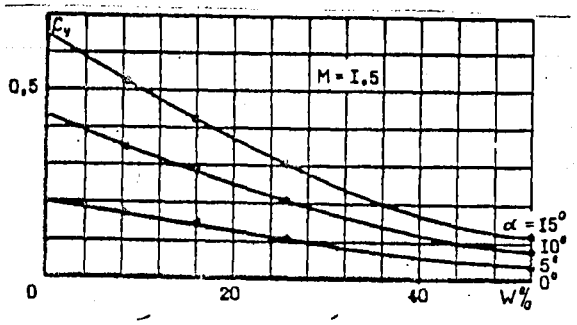

Fig. 5.

In the mentioned formula, the penetrability factor of the plate is taken in the form of the ratio $\frac{S_{\omega}}{S}$. The values of the coefficients K_{c_x} and B_{c_x} are given in Table 3.

Table 3

$C_x = K_{c_x}(M, \alpha) \cdot W + B_{c_x}$								
M	1,5				2,0			
α	0	5	10	15	0	5	10	15
K_{c_x}	0,06	0,06	0,08	0,04	0,10	0,07	0,06	0,05
B_{c_x}	0,020	0,045	0,105	0,195	0,025	0,045	0,095	0,165
M	2,5				3,0			
α°	0	5	10	15	0	5	10	15
K_{c_x}	0,035	0,050	0,070	0,090	0,025	0,040	0,080	0,100
B_{c_x}	0,010	0,030	0,085	0,155	0,015	0,035	0,065	0,115

With increasing the Mach number M, the aerodynamic coefficients C_x and C_y of the penetrable plates, at constant angle of attack and degree of penetrability, decrease in a linear fashion (Figs. 6 and 7).

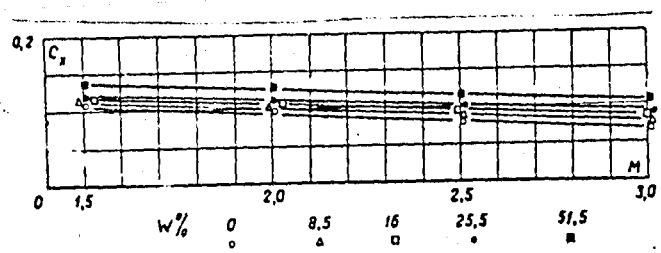

Fig. 6

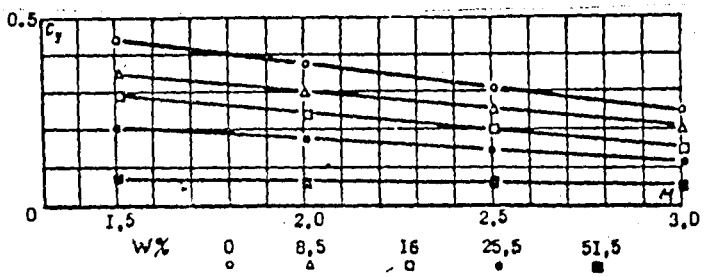

Fig. 7.

The relations C_x (M) and C_y (M) for different values of the penetrability parameter W and at an angle of attack $\alpha = 10°$ are shown in Figs. 6 and 7. For other angles of attack, the observed relationships are similar. The quantity C_y (M) can be calculated by the formula:

$$C_y = -K_{c_y}(W,\alpha)\cdot M + B_{c_y}$$

Table 4

$C_y = -K_{c_y}(W,\alpha)\cdot M + B_{c_y}$						
W %		0	8,5	16,0	25,5	51,5
$\alpha° = 5$	K_{c_y}	0,047	0,040	0,033	0,027	0,013
	B_{c_y}	0,280	0,240	0,200	0,150	0,070
10	K_{c_y}	0,127	0,097	0,093	0,070	0,008
	B_{c_y}	0,630	0,480	0,430	0,280	0,080
15	K_{c_y}	0,180	0,147	0,120	0,093	0,033
	B_{c_y}	0,910	0,740	0,605	0,440	0,145

The polars $C_y = f(C_x)$, for penetrable plates at a Mach number M = 1.5, and $C_{yp} = f(C_{xp})$, at a Mach number M = 3, are shown in Figs. 8 and 9. One should notice some peculiarities in the behavior of the integral carachteristics of C_n and C_τ for the penetrable plates. In the case of the penetrable plates, with increasing the degree of penetrability and angle of attack, the coefficient of the tangential component of the aerodynamic force C_τ increases and approaches in value the coefficient of the normal component C_n, and even exceeds it. For example, for the penetrability W = 51.5%, $\alpha = 15°$ and Mach number M = 3.0, C_τ is approximately twice C_n. The coefficient C_τ nearly does not depend on the Mach number M and it is a linear function of the penetrability (W) of the plate. It can be approximately calculated by the formula:

$$C_\tau = K_{c_\tau}\cdot W + 0{,}025,$$

where $K_{c\tau} = 0.32$ for $\alpha = 15°$; 0.23– 10°; 0.19– 5°; 0.08– 0°.

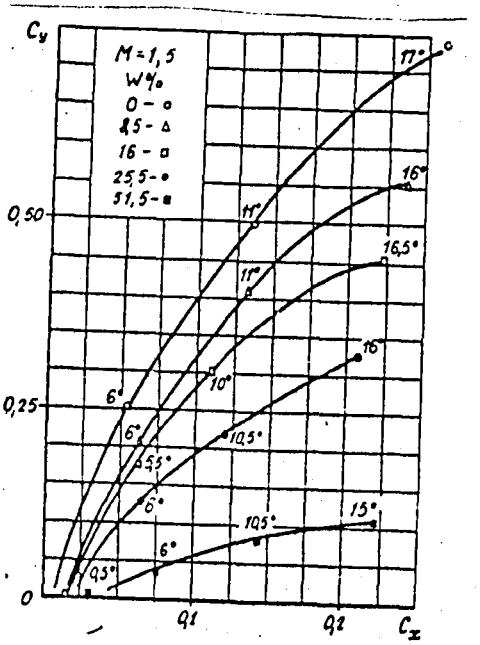
C_y
M = 1,5
W%
0 - ○
8,5 - △
16 - □
25,5 - ●
51,5 - ■
0,50
0,25
0
q1
q2
C_x
17°
16°
16,5°
11°
10°
6°
10,5°
15°
9,5°

Fig. 8.

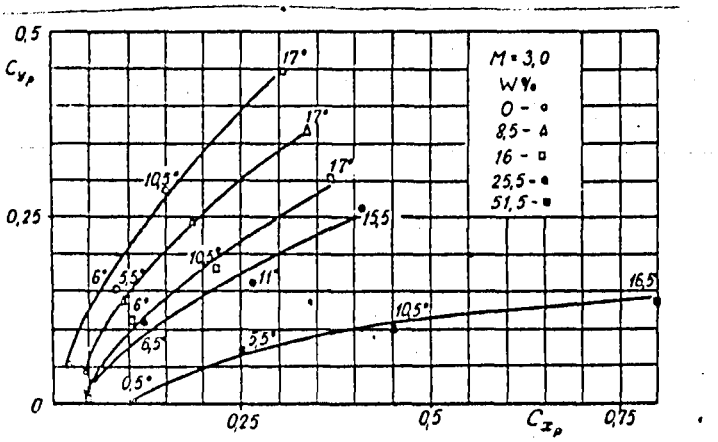
0,5
C_{y_p}
0,25
0
0,25
0,5
C_{x_p}
0,75
M = 3,0
W%
0 - ○
8,5 - △
16 - □
25,5 - ●
51,5 - ■
17°
10,5°
6°
5,5°
15,5
11°
16,5
8,5°
0,5°

Fig. 9

The relations $C_n(\alpha)$ and $C_\tau(\alpha)$ for different values of the penetrability parameter W at a Mach number M = 2.0 are shown for illustration in Figs. 10 and 11. The values of the coefficients C_n and C_τ for the mentioned ranges of the Mach numbers M, angles of attack and penetrability of the plates, are given in Table 5. The obtained experimental data show that in the case of supersonic flow around penetrable plates under an angle of attack, it is impossible to neglect the value of the coefficient C_τ, in comparison with C_n. The appearance of the tangential component of the aerodynamic force is connected with some physical peculiarities which take place in the case of flow around a penetrable plate under an angle of attack.

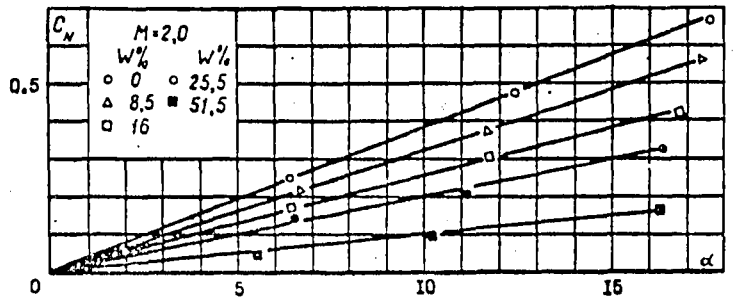

Fig. 10

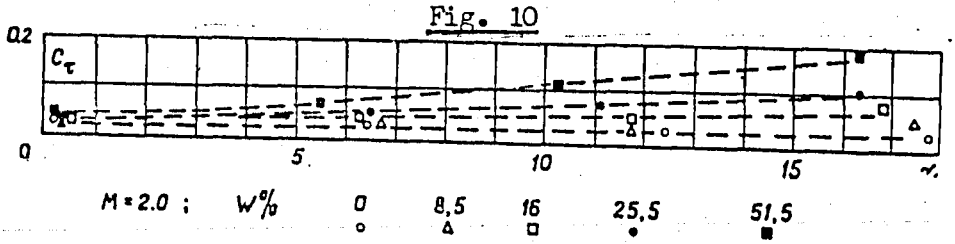

Fig. 11

The essential pecularities are the following : on the passage of gas through the holes of a plate, the velocity of the flow changes in value and direction and as a result, an auxiliary force arises. The increase of the thickness of the penetrable plate leads to an appreciable reconstruction of the flow and to a change of the pressure distribution on the walls of the holes.

Table 5

M		1,5				2,0				2,5				3,0			
	α°	0°	5°	10°	15°	0°	5°	10°	15°	0°	5°	10°	15°	0°	5°	10°	15°
C_n	W = 0 %	0	0,20	0,38	0,69	0,00	0,19	0,38	0,57	0,00	0,17	0,32	0,48	0,00	0,14	0,28	0,39
	8,5 %	0,00	0,19	0,38	0,57	0,00	0,16	0,32	0,48	0,00	0,14	0,28	0,41	0,00	0,11	0,21	0,22
	16,0 %	0,0	0,16	0,31	0,47	0,00	0,13	0,26	0,38	0,00	0,12	0,23	0,33	0,00	0,08	0,17	0,25
	25,5 %	0,0	0,12	0,21	0,38	0,00	0,10	0,20	0,30	0,00	0,08	0,17	0,26	0,00	0,06	0,12	0,19
	51,5 %	0,0	0,05	0,10	0,16	0,00	0,05	0,10	0,15	0,00	0,04	0,08	0,12	0,00	0,03	0,05	0,07
C_x	0 %	0,02	0,03	0,035	0,04	0,02	0,02	0,025	0,03	0,01	0,015	0,025	0,03	0,02	0,02	0,025	0,03
	8,5 %	0,02	0,035	0,045	0,055	0,02	0,03	0,04	0,05	0,02	0,03	0,04	0,05	0,02	0,03	0,04	0,05
	16,0 %	0,025	0,04	0,06	0,065	0,025	0,04	0,055	0,07	0,025	0,035	0,05	0,065	0,02	0,04	0,05	0,065
	25,5 %	0,030	0,05	0,07	0,09	0,030	0,05	0,075	0,10	0,03	0,045	0,07	0,10	0,025	0,05	0,07	0,09
	51,5 %	0,05	0,08	0,13	0,18	0,045	0,075	0,125	0,175	0,035	0,065	0,11	0,175	0,03	0,07	0,105	0,14

References

1. Rakhmatulin, Kh. A. "Obtekanie pronitsaemogo tela" (Flow around penetrable bodies).--- Vestnik MGU, Seriya Fiz- Mat. i estestv. nauk, issue no. 2, No. 3, 1950.

2. Kalinin, E.M. "Obtekanie pronitsaemogo konusa pod uglom ataki" (Flow around penetrable cones under an angle of attack).--- Izv. AN SSSR, MZhG, No. 1, 1966.

3. Grodzovckii, G.L., A.A. Nikol'skii, G.P. Svishchev and G.I. Taganov. "Cverkhzvukovye techeniya gaza v perforirovannykh granitsakh" (Supersonic flow of gas in perforated boundaries).--- Izd "Mashino- stroenie", Moskva, 1967.

PART II

MOVEMENT OF GAS WITH EXOTHERMIC REACTIONS

FORMATION OF PLANE DETONATION WAVE AT THE DECAY OF DISCONTINUITY IN FUEL GAS

By

S.A. Medvedev

The problem of the formation of a detonation wave in an inflammable medium with a finite reaction rate and instantaneous energy release in a finite or semi-finite volume of reacting gas, is solved.

The problem of the decay of the initial discontinuity in a fuel gas [1] is one of the problems whose solution is necessary for the answer of the question about the possibility of formation of detonation waves from physically practicable initial conditions. The self-similar problem of the decay of arbitrary discontinuity, in the case when a heat supply takes place in infinitely thin fronts of the combustion or detonation waves, was solved in the work [2]. In the present work we use a model of an inflammable medium in which the ignition decay is taken into account, and the heat release is described by relaxation equation in which the characteristic time of the heat release may depend on the gas-dynamical parameters. The finite difference numerical method is used for solving the system of equations of the gas dynamics and chemical kinetics. This method enables the direct calculation of the discontinuities and their interactions. The calculations, which were performed for the cases when the density of the energy supply in the case of instantaneous heat release ("explosion") is comparable with the density of the energy release in a gas with a finite reaction rate, showed that the intensity of the initial shock wave generated as a result of the decay of the discontinuity is less than the intensity of the leading front of the detonation wave in Chapman - Jouguet system. They showed also that the detonation wave in the undisturbed gas is formed as a result of the fusion of the shock wave with the heat-release zone formed on the contact surface, with the initial shock wave. From the obtained numerical solutions for the cases when the specific energy of the explosive gas is less or equal to the specific energy of a gas with a finite reaction rate and when the dependence of the rate of the heat release on the pressure is taken into account, it follows that the shock wave generated behind the initial shock, with a reaction zone behind it on fusion with the initial shock, is more intensive for small energies of explosion than a similar wave at high specific energy of explosion. The velocities and pressures behind the fronts

It consists of simple waves, progressive flows and crossed simple waves. The trajectory of the shock wave consists of rectilinear and curvilinear parts. If the rarefaction wave did not succeed to prevent the ignition on the contact surface, then during the expansion of the gas in the combustion process, compression waves (or shock waves) should be formed. These waves propagate on both sides from the place of ignition through the products of the explosion and through the heated gas of the initial shock wave. The detonation wave, generally speaking, may appear before the compression wave (or the shock wave of the reaction [8]) reaches the initial shock wave (and in such case may not be fully compressed). Investigation of the flow, after co-flowing of the wave of reaction occurs with the initial shock wave, is of special interest.

The model of the medium, which is used for solving the problem of the formation of detonation during the decay of discontinuity in a fuel gas, is set in the following system of equations:

$$\frac{d\rho}{dt} + \rho \operatorname{div} \bar{V} = 0 \qquad \frac{d\bar{V}}{dt} + \frac{\operatorname{grad} p}{\rho} = 0$$

$$\frac{d\varepsilon}{dt} + \frac{p}{\rho} \operatorname{div} \bar{V} = 0 \qquad \varepsilon = \frac{p}{\rho(\gamma-1)} - Q\beta$$

$$\frac{dC}{dt} = a\rho^{m-1} e^{-\frac{E}{RT}} \qquad \frac{d\beta}{dt} = \rho^{\alpha} \frac{1-\beta}{\Gamma} I(C-1)$$

$$I(C-1) = \{0,\ C<1\ ;\ 1,\ C \geq 1\}\ . \qquad (1)$$

Here ν – the concentration of the fictitious component determining the time of induction ($0 \leq C \leq 1$); β – the concentration of the product of the reaction determining the heat supply $Q \cdot \beta(t)$ to the mass unit ($0 \leq \beta \leq 1$), Q – the calorific power of the unit mass of the gas, Γ – the characteristic time of recombination, m and α – constants characterizing the order of the reaction, a – factor, E – activation energy. The remaining signs are standard ones. As follows from system (1), the transfer process is neglected.

Let us calculate the velocity of the propagation of the primary shock wave M_θ and consider some properties of the solution of the stationary progressive wave type [7].

As we assumed that the density and pressure before the explosion on the right and left from the membrane are equal, the Mach number of the shock wave M_θ is found from the following equation:

$$\frac{(\gamma-1)(M_\theta^2-1)}{M_\theta(\gamma+1)\sqrt{\gamma(\gamma-1)\bar{Q}+1}} + \left[\frac{2\gamma M_\theta^2-(\gamma-1)}{(\gamma+1)[\gamma(\gamma+1)\bar{Q}+1]}\right]^{\frac{\gamma-1}{2\gamma}} - 1 = 0\ , \qquad (2)$$

where

$$\bar{Q} = Q/a_1^2\ , \quad M_\theta = D_\theta/a_1$$

D_0 - the velocity of the initial shock wave,

a_1 - the velocity of sound in front of the initial shock wave.

The relations $M_0 = M_0(\gamma, \bar{\theta})$, obtained by solving this equation, are drawn in Fig. 2.

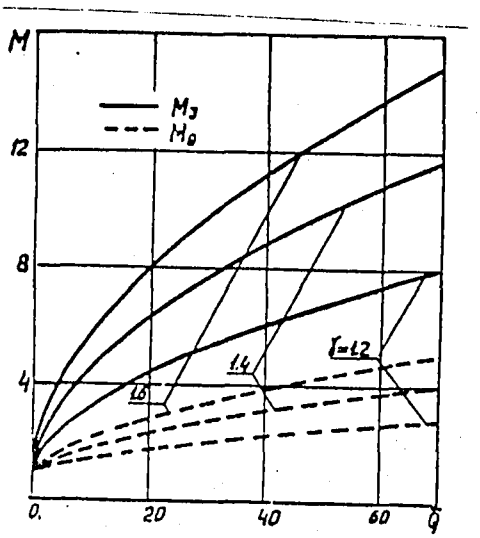

Fig. 2.

Let us now calculate the velocity of the detonation wave, which is the solution of equation (1). Let a plane shock wave with Mach number M_1 propagate in the fuel gas. After the transformation of equations (1) to a coordinate system moving with the shock wave, for a stationary one-dimensional flow behind the shock, the following equation is valid:

$$\frac{dv}{d\lambda} = \left(\frac{\gamma-1}{\gamma+1}\bar{Q}\right) : \left(\frac{\gamma M_1^2+1}{(\gamma+1)M_1} - v\right)$$

This equation combines the velocity v relative to the shock with the concentration of the product λ. By integrating this equation and satisfying the conditions for the shock, the following relation is received:

$$v = \frac{\gamma M_1^2+1}{(\gamma+1)M_1} - \sqrt{\left[\frac{M_1^2-1}{(\gamma+1)M_1}\right]^2 - 2\frac{\gamma-1}{\gamma+1}\bar{Q}\lambda} \quad ,$$

From this equation, it follows that in the case of a complete heat release, a steady state solution behind the shock wave may be present only for Mach number $M_1 \geq M_y$, where M_y is the Mach number in Ch.-J. system, and is determined by the formula:

$$M_y = \sqrt{[1+(\gamma^2-1)\bar{Q}] + \sqrt{[1+(\gamma^2-1)\bar{Q}]^2 - 1}} \quad .$$

Thus, the distribution of the parameters inside the detonation wave depends only on the specific form of kinetics, whereas the velocity of propagation of the stationary wave of Ch.-J. depends only on γ and $\bar{Q}$. In particular, the velocity of propagation of the stationary double-front wave in the Chapman-Jouguet system at given values of γ and $\bar{Q}$ coincides with the velocity of the wave of Ch.-J. with a distributed heat release. The stationary progressive wave with any number of reactions has a similar property.

The relation $M_y = M_y(\gamma, \bar{Q})$ is drawn in Fig. 2 together with the relation $M_\theta = M_\theta(\gamma, Q)$.

2. To obtain a quantitative information about the formation of detonation and about the gas movement after sufficiently big intervals of time, it is necessary to integrate numerically system (1) at the corresponding initial and boundary conditions. The one-dimensional equations reduced to the dimensionless form, in Lagrangian coordinates, are written in the form:

$$\frac{\partial x}{\partial t} = u \quad , \qquad \frac{\partial u}{\partial t} + \frac{\partial p}{\partial x_0} = 0 \quad , \qquad \rho = \frac{\partial x_0}{\partial x} \quad ,$$

$$\frac{\partial \varepsilon}{\partial t} + p\,\frac{\partial \partial x/\partial x_0}{\partial t} = 0 \quad , \quad \varepsilon = \frac{p\,\partial x}{(\gamma-1)\partial x_0} - \bar{Q}\beta \quad ,$$

$$\frac{\partial c}{\partial t} = \left(\frac{\rho}{\rho_\theta}\right)^{m-1} \exp\left(\frac{\bar{E}\rho_\theta}{p_\theta} - \frac{\bar{E}\rho}{p}\right), \quad \frac{\partial \beta}{\partial t} = \left(\frac{\rho}{\rho_\theta}\right)^{\alpha} \frac{1-\beta}{\bar{\tau}}\, I(c-1) \, .$$

Initial conditions:

$$0 < x_0 < L \qquad c(0, x_0) = \beta(0, x_0) = 1$$

$$L \le x_0 < \infty \qquad c(0, x_0) = \beta(0, x_0) = 0$$

$$0 < x_0 < \infty \qquad u(0, x_0) = 0 \, , \quad \varepsilon(0, x_0) = \frac{1}{\gamma(\gamma-1)} \, , \quad x = x_0 \, .$$

The boundary conditions : $u(t, 0) = 0$.

The dimensionless quantities are expressed in dimensional quantities (maked by dashes)in the form:

$$u = u'/a_1 \ , \quad t = t'\beta \ , \quad x = x'\beta/a_1 \ , \quad \rho = \rho'/\rho_1 \ ,$$

$$p = p'/\gamma P_1 \ , \quad \bar{\varepsilon} = \varepsilon'/a_1^2 \ , \quad \bar{Q} = Q'/a_1^2 \ , \quad \bar{E} = E/\gamma RT_1 \ ,$$

$$L = L'B/a_1 \ , \quad \bar{\Gamma} = \Gamma' B \ .$$

Here, a_1, ρ_1, P_1, T_1 – are the velocity of sound, density, pressure and temperature in the undisturbed gas on the right, respectively.

$$B = \alpha P_\theta^{m-1} \exp^{-1}\left(\frac{\bar{E}\rho_\theta}{\rho_\theta}\right)$$

The quantities behind the primary shock wave are marked by index θ. The velocity of this wave is calculated by formula (2) for $\bar{Q}_0$ on the left, equal to $\bar{Q}_1$ on the right. The relation $Q_0/Q_1 = K$ is also a characteristic parameter of the problem. Thus, the formulated one-dimensional nonstationary problem contains the following dimensionless determining parameters:

$$\gamma \ , \ m \ , \ \alpha \ , \ \bar{E} \ , \ \bar{Q} \ , \ K \ , \ L \ , \ \bar{\Gamma} \ .$$

The one-dimensional variant of the conservative obvious numerical scheme of the second order of accuracy with direct calculation of the discontinuities was used in the calculations after it was fitted to problem with distributed heat supply. This one-dimensional variant was worked out in the works [9 and 10] for the solution of the elastic-plastic problems and problems of gas dynamics.

The unknown quantities are calculated by the formulae:

$$u_\kappa^{n+1/2} = u_\kappa^{n-1/2} - \frac{\Delta t}{\Delta x_0}\left(\hat{p}_{\kappa+1/2}^{\,n} - \hat{p}_{\kappa-1/2}^{\,n}\right) \ , \quad x_\kappa^{n+1} = x_\kappa^n + \Delta t \cdot u_\kappa^{n+1/2} \ ,$$

$$\hat{p}_{\kappa+1/2}^{\,n} = p_{\kappa+1/2}^{\,n} + q_{\kappa+1/2}^{\,n-1/2} \ , \quad p_{\kappa+1/2}^{\,n} = \frac{\Delta x_0(\gamma-1)}{x_{\kappa+1}^n - x_\kappa^n}\left[\varepsilon_{\kappa+1/2}^{\,n} + \bar{Q}\lambda_{\kappa+1/2}^{\,n}\right] \ ,$$

$$q_{\kappa+1/2}^{\,n-1/2} = \left\{ d^2 \Delta x_0 \left(\frac{u_{\kappa+1}^{n-1/2} - u_\kappa^{n-1/2}}{x_{\kappa+1}^n - x_\kappa^n}\right)^2 , \ u_{\kappa+1}^{n-1/2} \geq u_\kappa^{n-1/2} ; \ 0 , \ u_{\kappa+1}^{n-1/2} < u_\kappa^{n-1/2} \right\} \ ,$$

$$\varepsilon_{\kappa+1/2}^{\,n+1} = \varepsilon_{\kappa+1/2}^{\,n} + \frac{\Delta t}{\Delta x_0}\left(u_\kappa^{n+1/2} - u_{\kappa+1}^{n+1/2}\right)\left(\rho_{\kappa+1/2}^{\,n} + q_{\kappa+1/2}^{\,n+1/2}\right) \ ,$$

$$C^{n+1}_{K+1/2} = C^{n}_{K+1/2} + \left(\frac{P^{n}_{K+1/2}}{\rho_0}\right)^{m-1} \Delta t \cdot \exp\left\{\frac{\bar{E}\rho_0}{P_0} + \frac{\bar{E}\left(u^{n+1/2}_{K} - u^{n+1/2}_{K+1}\right)}{P^{n}_{K+1/2}} \frac{\Delta t}{\Delta x_0}\right\},$$

$$\beta^{n+1}_{K+1/2} = \beta^{n}_{K+1/2} + \Delta t \left(\frac{P^{n}_{K+1/2}}{\rho_0}\right)^{\alpha} \frac{1-\beta^{n}_{K+1/2}}{\dot{r}} I\left(C^{n}_{K+1/2} - 1\right).$$

The integral lower indices are given to the boundaries of the particles, the half-integral— to the particles. The upper indices designate the numbers of the temporary layers. The quantities x and u are determined for the boundaries of the particles, the quantities ξ, C, β - inside the particles. The velocity is calculated at half-integral instants.

The interval of time was selected from the requirements of the stability of calculation.

3. The calculations were carried out at $\bar{E} = 10$, $\bar{Q} = 24$, $\bar{\Gamma} = 0.3$, $m = 1$, $L = 3$ for $\alpha = 0$ and $\alpha = 1$ and for $K = 0.8$, $K = 1.0$, $K = 1.5$. The value of γ was taken equal to 1.4. From 100 to 150 particles were placed in the section with length L. The coefficient of the artificial viscosity d^{ℓ} was equal to five. All the particles in the calculating range were originally the same.

The slightly smoothed profiles of the velocities for different instants in the case of $\alpha = 1$, $K = 1$ were given in Fig. 3. At $t = 0.146$, the profile consists of a compression shock on the right, linear part in the rarefaction wave on the left, and constant velocity between the shock and the rarefaction wave. At $t = 0.767$ this simple distribution is disarranged because heat release started on the contact discontinuity (marked by circles) and it led to the generation of an internal shock wave (the mark * indicates where the time of induction elapsed) in the gas behind the initial shock wave, whereas in the strongly heated products of combustion, where the density is small and the velocity of sound is high, a compression wave propagates. As a result of the compression wave, which is propagated in the gas behind the initial shock wave until the second shock wave arises, the velocity level between the shock waves is higher than the value $U_0 = 1.77$ obtained by the exact formulae of the decay of the discontinuity. On the velocity profile at $t = 1.236$, two shocks of velocity corresponding to two shock waves are recorded. The second shock wave is the leading front of the formed detonation wave and behind it there is a heat release zone. The particle, in which $0.5\,\bar{Q}$ was separated out is marked by a pointer, and the particle, in which $0.9\,\bar{Q}$ was separated out — a pointer with two lines. The heat supply between the contact surface and the wave front leads to the intensification of the compression wave going from the zone of the heat supply to the products of the explosion. Therefore, the velocity of the gas flowing from the zone of explosion decreases and a gap appears on the velocity profile. The curve of $t = 1.439$ represents the distribution of the velocities after the occurrence of interaction between the initial shock wave and the shock wave with the following zone of heat supply behind it, and the shock wave with the zone of release behind it went out in the stationary gas. We notice that the velocity behind the shock exceeds the velocity behind the shock front of the wave of Ch.-J.,

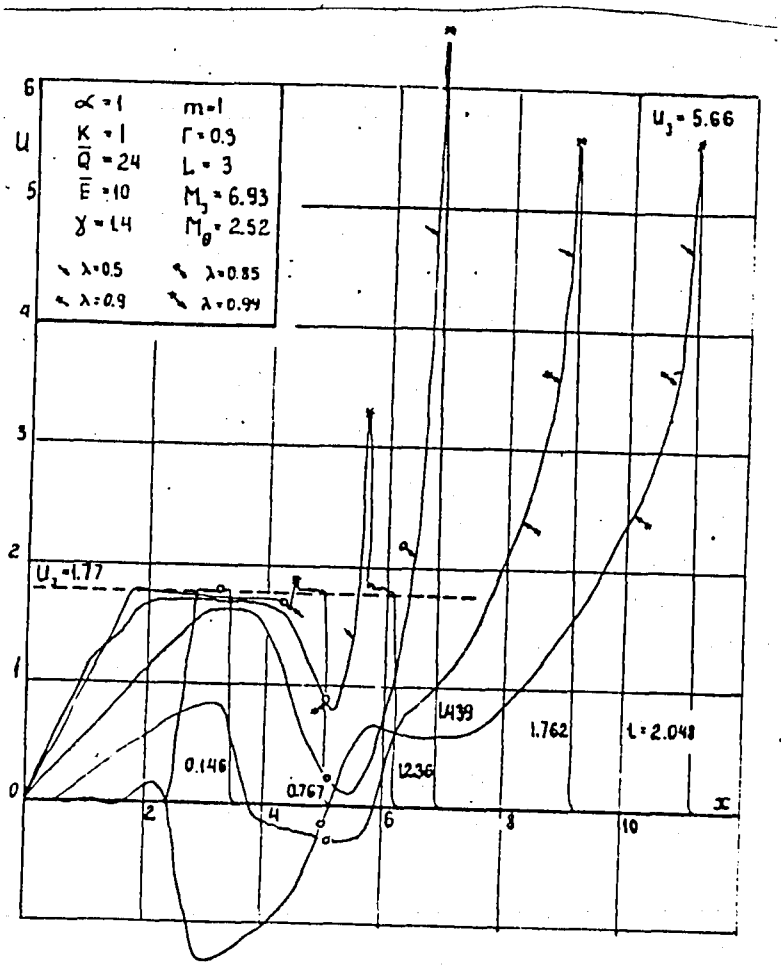

Fig. 3

and the products of the explosion by then slowed down still more strongly. At t = 1.762 and t = 2.048, the velocity behind the shock is practically equal to the velocity behind the front of the wave of Ch.-J., and a portion of the products of detonation and explosion has a negative, that is to say, the gas flows in the opposite direction. The steepness of the parts of negative slope in the profiles of the velocity increases with increasing the time. Taking into account the relatively high temperature of the products of the explosion and the established artificial viscosity in the scheme, it is possible to consider that the retonation shock wave was formed at the moment t = 2.048.

A fragment of the graph in Fig. 3, where all the boundaries of the units are drawn, is represented without smoothing in Fig. 4. This fragment gives a concept about the magnitude and character of the oscillations of numerical nature for the investigated wave propagated in the Ch.-$\bar{v}$. system.

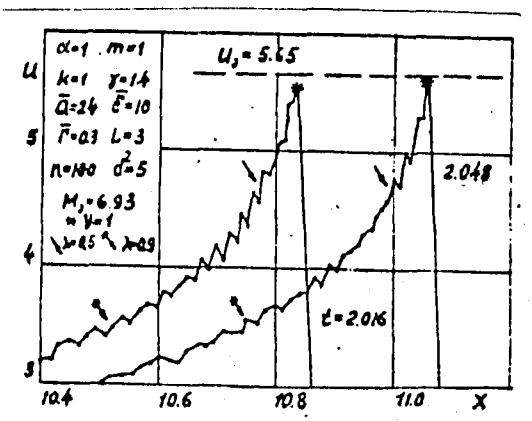

Fig. 4.

The x-t diagrams for the shock waves and the leading edges of the detonation waves (points or points connected by lines), of the contact surface $\ell(t)$ (triangles) and of the trajectory $r(t)$ of the retonation wave (rhombs) are shown in Figs. 5-9. The dependence of the pressure and velocity behind the front of the shock and detonation waves on time, $P_D(t)$ and $U_D(t)$, are also drawn in these figures and are marked by crosses and circles, respectively. In the figures, there are also the reference values of the velocity U_y and pressure P_y behind the detonation wave in Ch.-J. system, and the velocity U_θ and pressure P_θ behind the initial shock wave, which are obtained from the exact relation. The initial slope of the trajectory of the contact surface is drawn by dot-dash line; the exact slope of the trajectory of the initial shock wave - by double dots-dash line; the slope of the trajectory of the detonation wave in the stationary gas in the Ch.-J. system — solid line. Let us return to Fig. 5. The aupper succession of the black points represents the trajectory of the initial shock wave. On the lower series of the points and triangles, the finned pointer shows the place, where for the first time on the contact surface, the time of induction elapsed and the combustion started. Since that moment, the contact surface begins to lag behind the trajectory of the ignition, on which the time of induction elapses; however, the shock wave with the zone of heat release behind it, does not still arise for some time. The formation and acceleration of the shock wave with heat supply begins there,

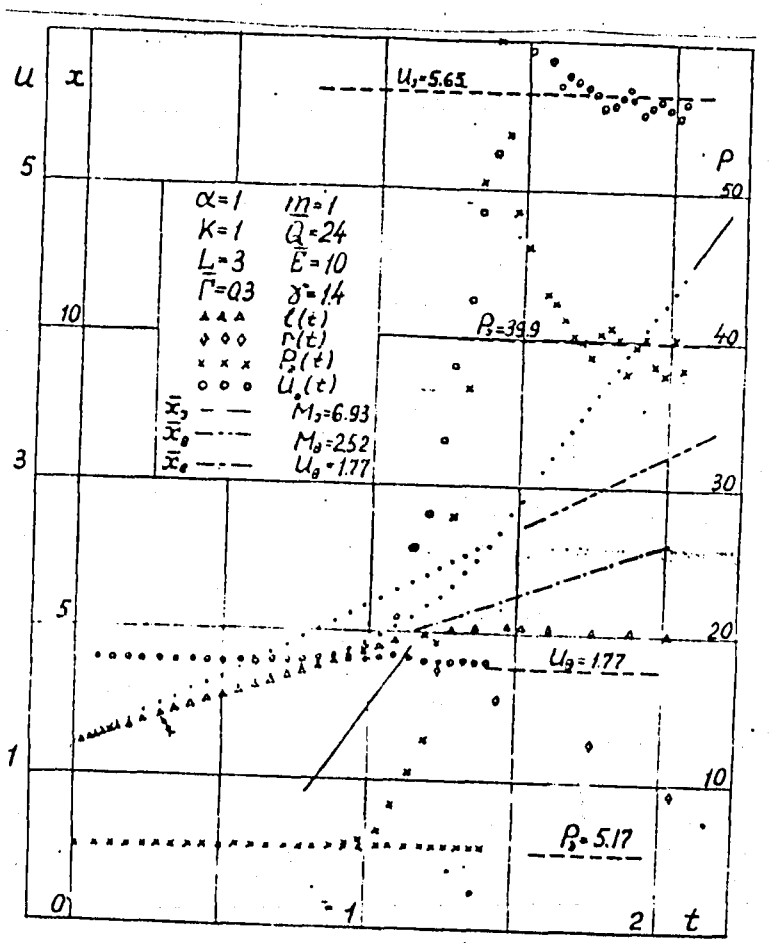

Fig. 5

where the graphs of the pressures and velocities behind the initial wave and on the trajectory of the ignition bifurcate. Till that instant, the greater part of the yielded energy is carried away from the zone of heat supply by the compression waves going in the direction of the light products of the explosion, which are stopped at that time. After the generation of the internal shock wave with a sufficient intensity in the compressed gas behind the initial shock wave, the time of induction of the particles quickly elapses on passing through this internal wave and the movement of that wave gets a self-accelerating character. The trajectory of the shock wave with heat release behind it is bent upwards and intersects with the trajectory of the initial wave; after that only the shock with heat release behind it (detonation wave) remains. Here, the graphs

of u and p behind the initial shock are cut off. In the graphs for the shock wave with heat supply, it is obvious that the pressures and velocities are greater behind the front of that wave than behind the front of the wave of Chapman–Jouguet in the stationary gas. However, they rapidly decrease to the values corresponding to the parameters behind the front of the wave of Ch.–J. as soon as the detonation wave goes out in the stationary gas.

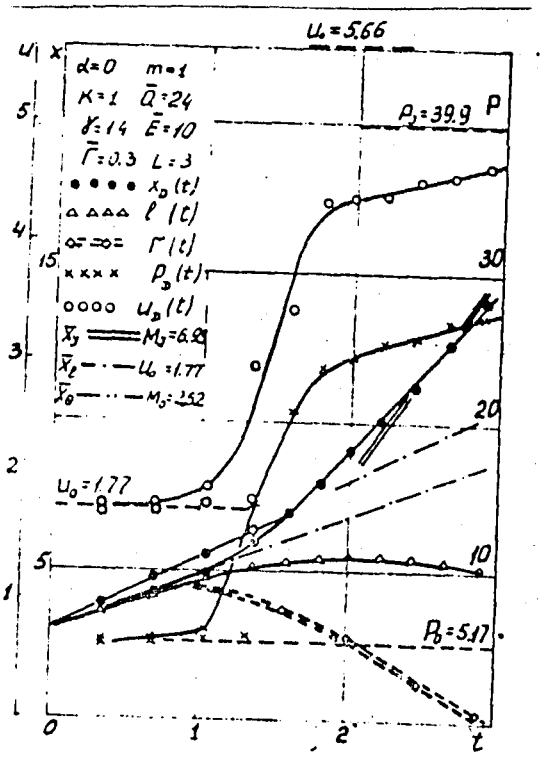

Fig. 6.

The trajectory of the shock and detonation waves, of the contact surface and retonation wave, and also the graphs $P_D(t)$ and $U_D(t)$ for the case of $\alpha = 0$, $K = 1$ are drawn in Fig. 6. It is obvious from the given data that although the internal shock with zone of heat supply behind it is generated at the same time as in the case of $\alpha = 1$, $K = 1$, it is accelerated afterwards more slowly than in the case of $\alpha = 1$, $K = 1$, and at the fusion with the

initial shock, the developed detonation wave does not form. In the graphs $P_D(t)$ and $U_D(t)$, there are no bursts of pressure and velocity, and subsequently a relatively slow acceleration of the shock wave with zone of heat supply behind it is observed. In the investigated section of time, the velocity of the shock and the velocity and pressure behind it are still far from the corresponding values for the wave in the Ch.-J. system.

We notice that even in that case, when the resulting wave is relatively slow, the retonation compression wave did not succeed yet to reflect from the wall, and thus it is possible to neglect the influence of the wall on the flow in the neighbourhood of the shock with heat release behind it.

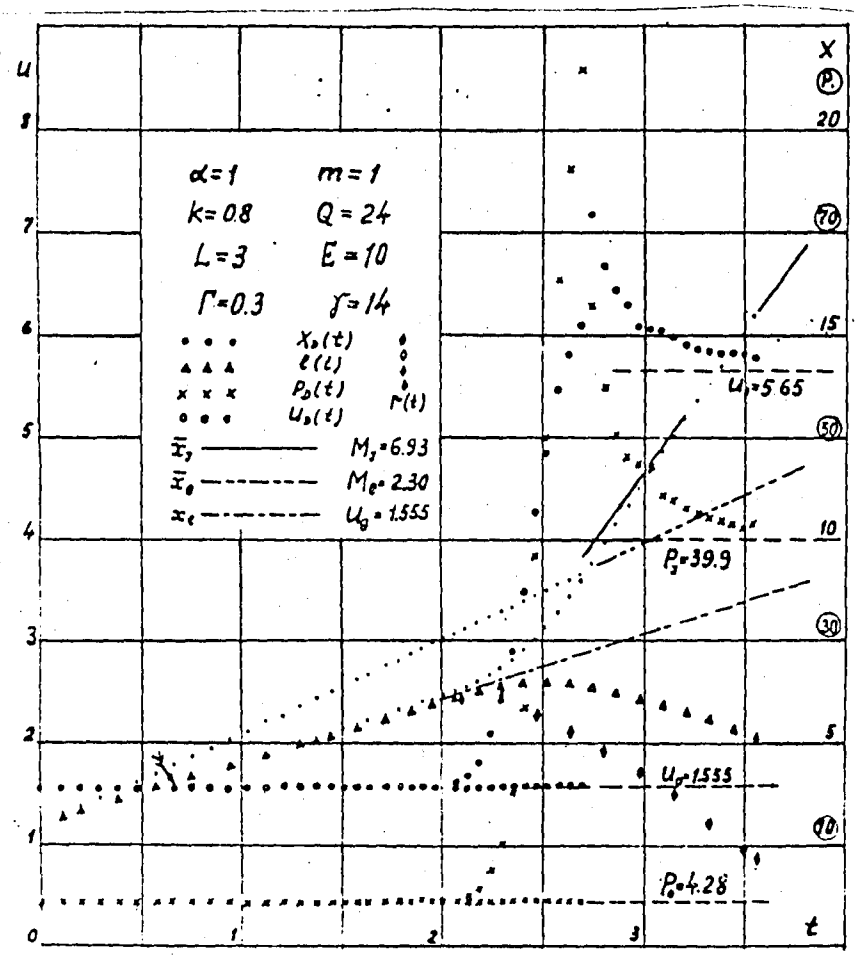

Fig. 7

The x-t diagrams and the graphs $P_D(t)$ and $U_D(t)$ for the case of $\alpha = 1$, $K = 0.8$ are given in Fig. 7. As was expected, the beginning of the heat release on the contact surface (finned pointer) is protracted in comparison with the case of $\alpha = 1$, $K = 1$. The beginning of the generation of the internal shock with zone of heat release behind it is accordingly drawn back. In consequence, the generated internal wave with heat supply behind it may be for a sufficiently long time accelerated in the gas behind the initial shock wave before it flows with it. At that time, a detonation wave generates with a leading front that is more intense than that in the case of $\alpha = 1$, $K = 1$. It is obvious from the comparison of Figs. 5 and 7 that the waves of pressure and velocity generated behind the front exceed the corresponding values for the case of $\alpha = 1$, $K = 1$. As in the case of $\alpha = 1$, $K = 1$, after the exit in the stationary gas, the velocity of the detonation wave rapidly decreases down to the velocity of the wave of Ch.-J., and the velocities and pressures behind the front of the wave approach to the corresponding values behind the front of the wave of Ch.-J.

The x- t diagrams and the graphs of $P_D(t)$ and $U_D(t)$ for $\alpha = 1$, $K = 1.5$ are given in Fig. 8. In this case, the initial shock wave is the most intense and the internal shock with heat supply generates more quickly than at $K = 0.8$ and $K = 1$. However, its intensity by the moment of the fusion with the initial

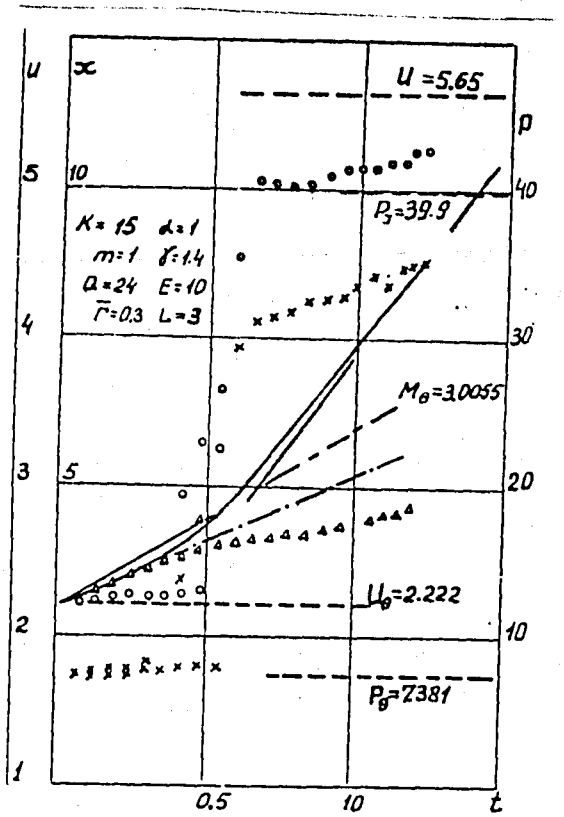

Fig. 8

shock wave, as in the case of $\alpha = 0$, $K = 1$, is insignificant, and the detonation wave goes out in the undisturbed gas with a leading front is more slow than that in the system of Chapman-Jouguet. Subsequently, the velocity of the detonation wave of $\alpha = 1$, $K = 1.5$, increases more rapidly than that for the case of $\alpha = 0$, $K = 1$. We notice also a different form of the trajectories of the contact discontinuities for the two cases.

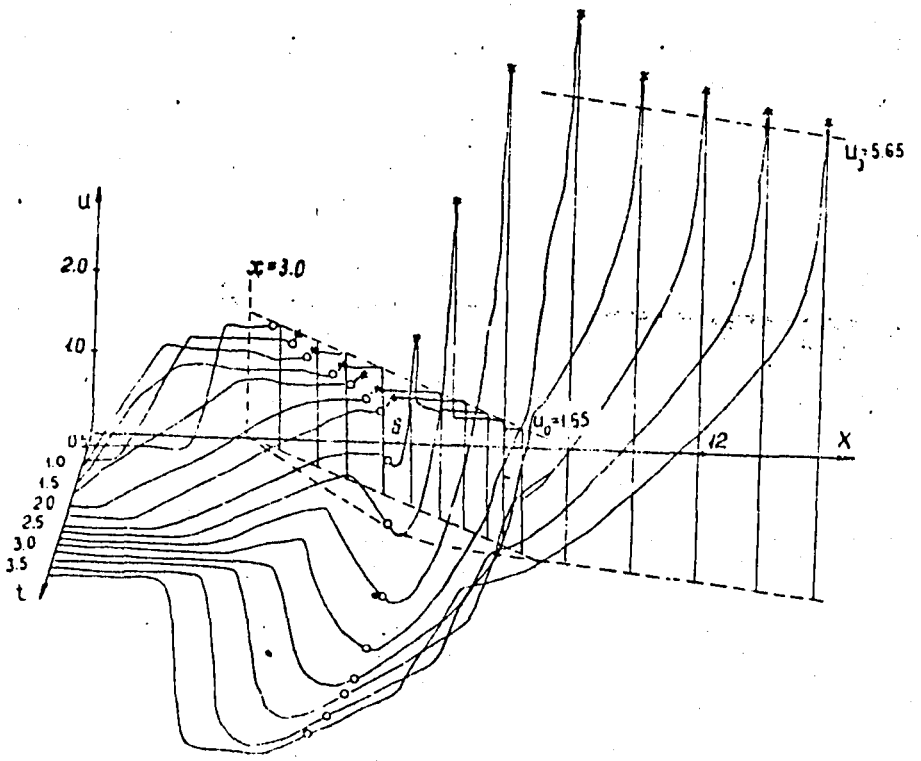

Fig. 9

4. The relief of the velocity in x, t coordinates for the case of $\alpha = 1$, $K = 0.8$ is given in Fig. 9. It is clear how the internal detonation wave arises, and how also the retonation compression wave, from which the retonation shock wave is subsequently formed, arises. Finally, it is clear how the detonation wave transits to the system of Ch.-J. after going out in the stationary gas.

This pattern may serve as one of the illustrations of the process of the formation of detonation on the ignition of the gas at the closed end of the tube and as an example of the autonomous flow which arises in the unconstrained gas in the absence of external influences owing to the released energy in the chemical reaction which is characteristic for the movement occurring in the self-sustaining detonation waves.

References

1. Bishimov E., V.P. Korobeinikov, V.A. Levin, and G.G. Chernyi. "Odnomernye nestatsionarnye techeniya goryuchei smesi gasov s uchetom konechnoi skorosti khimicheskikh reaktsii" (One-dimensional nonstationary flow of fuel mixtures of gases, taking account of the finite velocity of the chemical reactions).--- Izv. AN SSSR, MZhG, No. 6, 1968.

2. Bam-Zelikovich G.M. "Raspad proizvol'nogo razryva v garyuchei smesi" (Decay of arbitrary discontinuity in fuel mixture). --- Sb. "Teoreticheskoya gidromekhanika" pod red. akademika L.I. Sedova, vynusk pervyi (Sbornik statei, No. 4, Oborongiz, 1949).

3. Chernyi G.G. "Vozniknovenie kolebanii pri oslablenii voln detonatsii" (Formation of oscillations in the attenuation of the detonation waves).--- PMM, T. XXIII, v. 3, 1969.

4. Medredev S.A. "Ob oslablenii pereszhatykh voln s konechnoi skorost'yu reaktsii" (About the attenuation of supercompressed detonation waves with finite reaction rates).--- Izv. AN SSSR, MZhG, No. 3, 1969.

5. Medvedev S.A. "Vozniknovenie kolebanii i ustoichivost' rasprostraneniya detonatsionnoi volny s konechnoi skorost'yu reaktsii" (Formation of oscillations and stability of propagation of detonation waves with finite reaction rates).--- Institut mekhaniki MGU, nauchnaya konferentsiya, tezisu dokladov, M., 1970.

6. Korobeinikov V.P., V.A. Levin, S.A. Medvedev, and G.G. Chernyi "Odnomernye neustanovivshiesya dvizheniya goryuchikh smesei gazov s obrazovaniem voln tipa detonatsionnykh" (One-dimensional unsteady movement of fuel gas mixtures with the formation of waves of the detonation type).---Vestnik MGU, No. 2, 1970.

7. Zel'dovich Ya.B., and A.C. Kompaneets. "Teoriya detonatsii" (Theory of detonation).--- GITTL. M., 1955.

8. Gilbert R.B., and R.A. Strehlow. Theory of Detonation Initiation Behind Reflected Shock Waves. AIAA Journal, v. 4, No. 10. 1966.

9. Wilkins M.L. Calculation of Elastic-Plastic Flow. University of California, LRL UCRL - 7322, 1966.

10. Wilkins M.L. Finite Difference Scheme for Calculating Problems in Two Space Dimentions and Time. University of California, LRL UCRL - 71724, 1966.

EXPLOSION IN FUEL MIXTURE OF GASES

By

V.P. Korobeynikov, V.A. Levin, V.V. Markov

Let in an infinite mass of stationary gas, in which chemical reactions may proceed, instantaneous energy release E_0 occurs at a point along a plane or straight line. Let us consider that the gas is ideal, nonviscous and non-heat-conducting. The density ρ_0 and pressure P_0 in the stationary gas are constants. One-dimensional motions of the gas with different forms of symmetry are investigated.

The strong shock wave generated as a result of the energy release initiates the chemical reactions in the fuel mixture of gases. On calculating the combustion process, a model is assumed, which takes into account the time delay of ignition and the subsequent simultaneous proceeding of the direct and reverse reactions.

The equations describing the proceeding of the chemical reactions are taken in the form of Arrhenius relations. The reaction determining the period of induction is described by the equation in [1, 8, 9].

$$\frac{dc}{dt} = -K f(\mu,\rho) e^{-\frac{E}{RT}} , \qquad (1)$$

and the reaction with heat release - by the equation in reference [2]:

$$\frac{d\beta}{dt} = -K_1 \beta^{m_1} p^{n_1} \rho^{l_1} e^{\left(-\frac{E_1}{RT}\right)} + K_2 (1-\beta)^{m_2} p^{n_2} \rho^{l_2} e^{-\frac{E_1+Q}{RT}} , \qquad (2)$$

where C - virtual concentration, β - mass portion of the unburned gas, Q - calorific power of the unit mass of the fuel mixture, E - activation energy of the induction period, E_1 - activation energy of the direct reaction, R - universal gas constant, $K > 0$, $k_1 > 0$, $k > 0$; m_1, n_1, l_1, m_2, l_2 —are constants. The quantity $C = 1$ is on the front of the shock wave. The vanishing of C denotes the end of the period of induction and beginning the reaction with heat release.

The motion of the fuel gas generated as a result of the explosion, will be described by equations (1) and (2) together with the equations of motion:

$$(r^{\nu-1}\rho)_t + (r^{\nu-1}\rho v)_r = 0 , \qquad (3)$$

$$(r^{\nu-1}\rho v)_t + (r^{\nu-1}\rho v^2 + p)_r = (\nu-1)p \quad , \qquad (4)$$

$$\left\{r^{\nu-1}\left[\frac{1}{2}\rho v^2 + \rho h - p\right]\right\}_t + \left\{r^{\nu-1}\rho v\left[\frac{1}{2}v^2 + h\right]\right\}_r = 0 \quad . \qquad (5)$$

Here $h = \frac{\gamma}{\gamma-1}\frac{p}{\rho} + \beta Q$, $p = \rho R T$, $\nu = 1, 2, 3$ - for motion with plane, cylindrical and spherical waves, respectively. The parameters of the gas must also satisfy the boundary conditions in the center of the explosion and on the shock wave. The velocity vanishes in the center of the explosion, and the following relations are fulfilled for the shock wave:

$$\rho_0 D = \rho_1 (D - v_1) \quad ,$$

$$\rho_0 D^2 + \frac{\gamma}{\gamma-1}\frac{p_0}{\rho_0} = \frac{1}{2}(D-v_1)^2 + \frac{\gamma}{\gamma-1}\frac{p_1}{\rho_1} \quad ,$$

$$\rho_0 D^2 + p_0 = \rho_1 (D - v_1)^2 + p_1 \quad , \qquad (6)$$

where D - the velocity of the shock wave, and the indices 0 and 1 are related to the values of the parameters before and after the shock wave, respectively.

The system of equations (1) - (5) is linear, and the problem in the given statement is not self-similar. Therefore, it is possible to carry out the complete investigation only by the method of numerical integration of the equations in partial derivatives.

Similar to work [2], we shall study the motion of the gas at an instant near to the initial motion.

It is possible to obtain an approximate analytical formula for the time of induction. In order to do that, we write the thermodynamic functions in adiabatically expanding particle behind the shock wave in the form given in work [4]:

$$\frac{1}{T} = \frac{1}{T_*} + \frac{\alpha}{T_*}\ln\left(\frac{t}{t_*}\right) , \quad \rho = \rho_*\left(\frac{t_*}{t}\right)^{2\beta} , \quad p = p_*\left(\frac{t_*}{t}\right)^{2\beta\gamma} , \qquad (7)$$

where the index * - is related to the value of the function at the moment of passing by the particle of shock wave, which is marked by t_*, a and β - are constants.

An analytical solution of the problem about a strong point explosion was used for the determination of a and b. The values of a and b were determined from the condition of equality of the first derivatives with respect to V, from the exact solution and formulae (7). The values of a and b for certain ν and γ are given in the table:

ν / γ	1		2		3	
	a	β	a	β	a	β
1,1	0,085	0,476	0,141	0,703	0,168	0,839
1,2	0,163	0,455	0,264	0,661	0,314	0,785
1,3	0,261	0,435	0,374	0,624	0,442	0,750
1,4	0,333	0,417	0,472	0,590	0,556	0,694
3,0	1,000	0,250	1,250	0,313	1,400	0,350

Substituting formula (7) in equation (1) and integrating it, we obtain:

$$c = 1 - \frac{t_*}{\tau_0(t_*)A}\left[1 - \left(\frac{t_*}{t}\right)^A\right] , \qquad (8)$$

where

$$A = 2\beta(\gamma n + \ell) + \frac{aE}{RT_*} - 1 , \quad \tau_0(t_*) = \frac{e^{E/RT_*}}{K \rho_*^{\ell} p_*^{n}} .$$

If t_0 is the instant at which C vanishes, the difference $t_0 - t_*$ gives the value of the period of induction τ_* as a function of t_*. From (8) we obtain:

$$\tau_*(t_*) = t_*\left\{\left[1 - \tau_0(t_*)A/t_*\right]^{-1/A} - 1\right\} . \qquad (9)$$

Previously, for example in work [7], the following formula taken from work [1] was used for the induction time:

$$t_{ind} = \frac{N_1}{p} \exp(E/RT) . \qquad (10)$$

Below, for the investigation of the initial stage of the explosion, the next formula is used, following work [3]:

$$t_{ind} = \frac{N_2}{3\rho} \exp(E/RT), \qquad (11)$$

where N_1, N_2 – are constants. Both these formulae give the value of the period of induction on combustion of stoichiometric mixture of hydrogen with oxygen, initiated by a shock wave.

Fig. 1 is presented for the comparison of the graph of the dimensionless values of τ_* ($\bar{\tau}_*$), calculated by formula (9) (curve 1) with those obtained by integrating equation (1), taking account of (11) along the streamline and using the exact solution of the problem about a strong point explosion (curve 2), for the case of $\gamma = 1.3$ and $\nu = 3$. It is obvious that the approximate formula is in good agreement with the calculation.

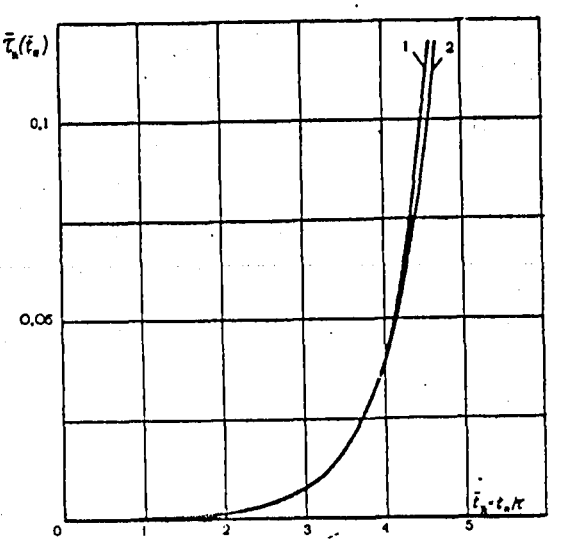

Fig. 1

The performed analysis showed that already at the instant close to the initial, the time of the ignition delay abruptly increases, which leads to the separation of the ignition zone from the shock wave.

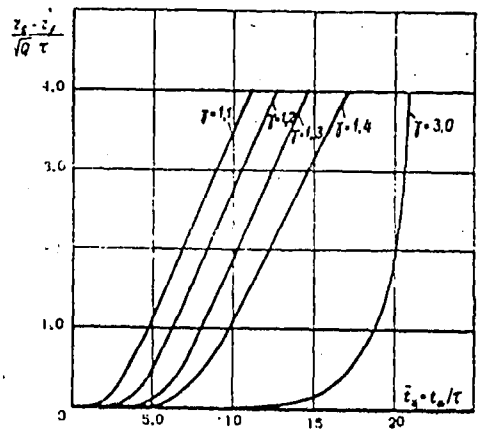

Fig. 2

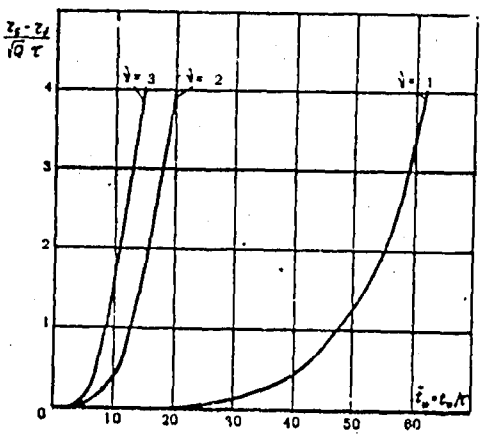

Fig. 3

The results of the calculations showing the influence of the different determining parameters of the problem on the withdrawal of the ignition front from the shock wave front are represented in figs. 2-4. The value of the time, at which the shock wave passes through the particle, relative to the characteristic time of induction is plotted on the abscissa. The dimensionless distance from the shock wave, at which the period of induction is completed in that particle, is plotted on the ordinate.

Fig. 2 illustrates the influence of the adiabatic index γ on the decay of the detonation front for the case of $\nu = 3$, $E_0 = 10^{10}$ erg, $(E/Q) = \sigma = 10$. The dependence of this process on the form of the symmetry for $\gamma = 1.3$, $E_0 = 10$ erg/cm$^{3-\nu}$ and $\sigma = 10$ is represented in Fig. 3. The influence of the magnitude of the energy E of explosion and the activation energy E of the induction period when $\gamma = 1.3$ and $\nu = 3$ is represented in Fig. 4. The curves 1, 2, 3 are for ($E_0 = 10^{10}$ erg, $\sigma = 13$), ($E_0 = 10^{10}$ erg, $\sigma = 10$), and ($E_0 = 10^{11}$ erg, $\sigma = 10$), respectively.

Two curves are shown for comparison in Fig. 5. One, represented by solid line, is obtained in the present work by the formula for the time of induction (11), and the other, dotted, — in work [5], on the basis of formula (10). In the initial stage of the explosion, it is possible to obtain a distribution of all the unknown functions on the coordinate at certain instants. Such distribution

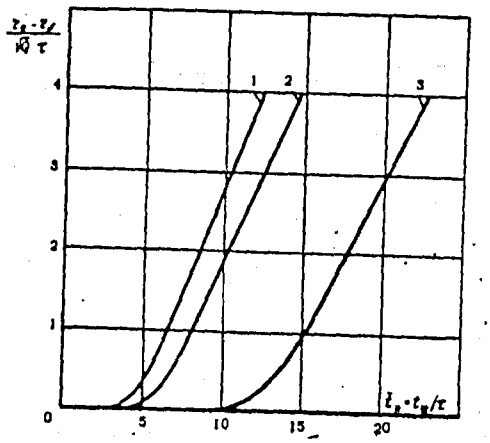

Fig. 4

is necessary for the continuation of the solution at still later instants, at which it is already impossible to neglect the influence of the energy released by the reaction and of the pressure in the undisturbed gas. The calculation of the initial distribution shows that the value of C monotonically decreases from 1 to 0.

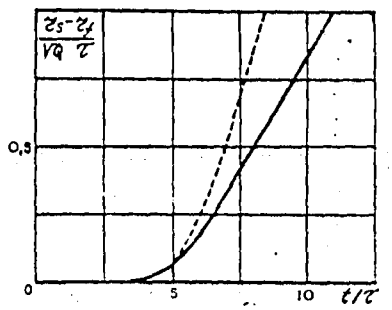

Fig. 5

The value of β rapidly decreases at once after the ignition front, and then it increases to the equilibrium value in the center of the explosion, which is calculated by the formula:

$$\frac{K_1}{K_2} = \frac{(1-\beta)^2}{\beta^2} \qquad (12)$$

The mode of the curve of β is represented in Fig. 6.

The calculation of the later stages of the explosion, taking account of the energy released by the chemical reaction and the conterpressure, was carried out for the case of the cylindrical symmetry using the differential method of S.K. Godunov [6]. Direct application of this method near the center of the explosion is difficult because of the high temperatures. Therefore we are obliged here to carry out the calculation by another method. The central interval, representing the standard calculating unit, is introduced in the investigation; one of the boundaries of this unit coincides with the center of the explosion. On this boundary, besides the condition of the equality of gas velocity to zero, some other conditions are set out. The value of β is supposed to be equal to the value calculated by (12), density- to zero, pressure— to the pressureffrom the lower temporary layer. The validity ofthe first two conditions is secured by the fact that the equality of the density to zero and the infinity of the temperature in the center of the explosion remain at all the time of the gas motion, because this takes place in the case of ordinary explosion with counterpressure in view of the conservation of entropy in the zone of continuous flow [7]. In our case, because of the chemical reactions, the entropy may only increase (it is assumed that the reactions as a whole are exothermic). The dimensions of the neighbourhood of the center of the explosion were automaticaly selected so that a small amount of mass and energy was included in it. The ignition front was included in the boundary of the calculated unit. Its position was determined so that the values of the modulus C extrapolated to it from the neighbouring units was smaller than the small positive number δ. Equations (1-5) were solved for the dimensionless functions: $\bar{P}=\frac{P}{a\rho_0}$, $\bar{\rho}=\frac{\rho}{\rho_0}$, $\bar{v}=\frac{v}{\sqrt{a}}$ and the variables: $\bar{t}=\frac{t}{\tau}$, $\bar{r}=\frac{r}{\sqrt{a}\tau}$. The parameters, by which the numerical calculation were carried out by the differential method, were as follows:

$$E_0 = 10^{10}\ erg/cm$$

$$Q = 7 \cdot 10^{10}\ cm^2/sec^2$$

$$\rho_0 = 10^{-3}\ g/cm^3$$

$$P_0 = 10^6\ dine/cm^2 = 1\ atm$$

$$\sigma_0 = \tau K \rho_0^{\ell+n} Q^n = 10^3$$

$$\sigma_1 = 10$$

$$\sigma_2 = \tau K_1 \rho_0^{\ell_1+n_1} Q^{n_1} = 20$$

$$\sigma_3 = E_1/Q = 2.5$$

$$\sigma_4 = \tau K_2 \rho^{\ell_2+n_2} Q^{n_2} = 20$$

$$\ell = \ell_1 = \ell_2 = 0$$

$$m_1 = m_2 = 2$$

$$n_1 = n_2 = 2 \quad n = 1$$

$$\bar{\rho}_0 = 1,\ \bar{P}_0 = 0{,}01429,\ \bar{v}_0 = 0 \qquad (13)$$

Control of calculation was carried out by the laws of conservation of mass and energy. The values of the relative errors ε_E and ε_M were calculated:

$$\varepsilon_E = \frac{\bar{E}_1 - \bar{E}_0}{\bar{E}_0},$$

$$E_1 = 2\pi \int_0^{\bar{r}_s} \left[\bar{\rho}\frac{\bar{v}^2}{2} + \frac{1}{\gamma-1}\left(\frac{\bar{p}}{\bar{\rho}} - p_0\right)\bar{\rho} + (\beta-1)\bar{p}\right]\bar{r}\,d\bar{r}$$ — the total energy of the gas being in motion after the deduction of the internal energy of the original state.

E_0 — the dimensionless energy of the explosion.

$$\varepsilon_M = \frac{\bar{M}_1 - \bar{M}_0}{\bar{M}_0},$$

where $M_1 = 2\pi \int_0^{\bar{r}_s} \bar{\rho}\,\bar{r}\,d\bar{r}$ — the mass of the disturbed gas, $M_0 = \pi \bar{r}_s^2$ — the mass of the undisturbed gas in the volume limited by the shock wave.

The calculation was carried out from $\bar{t} = 10$ to $\bar{t} = 500$. It was discovered that beginning from the instant $\bar{t} = 19$, the ignition front merges with the streamline and then it follows together with it. Oscillations of the ignition front were observed beginning from the instant $t = 50$. Some results of the calculation are shown in Figs. 6-7. It is possible to judge about the calculation accuracy of the gas dynamical functions from the following data. The initial error ($t = 10$): $\varepsilon_E = -3.4\%$; $\varepsilon_M = -0.14\%$. The error at the instant $t = 19$; $\varepsilon_E = -3.3\%$; $\varepsilon_M = -0.06\%$. For still later instants, the error did not increase.

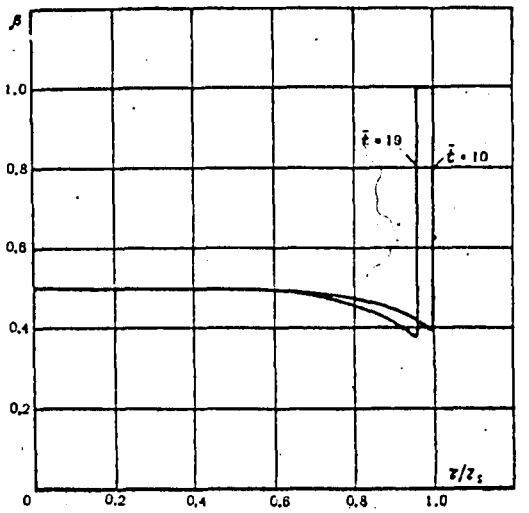

Fig. 6

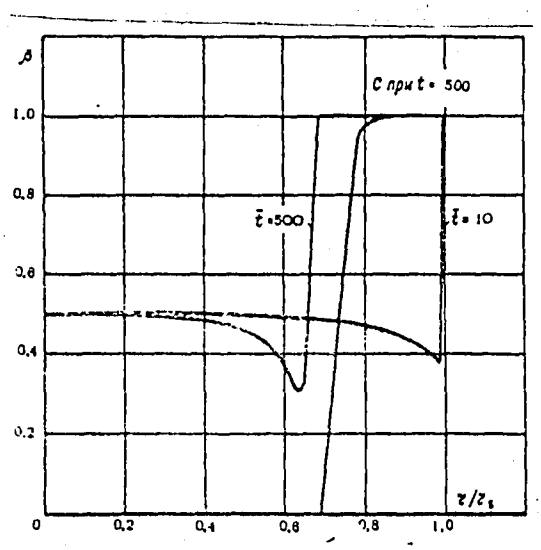

Fig 7

Thus the motion of the gas, in which exothermic chemical reactions, generated as a result of the instantaneous release of energy E_o in a point, can proceed on a straight line or a plane can be divide into two stages. The first stage is that where the quantity of the energy released in the region bounded by the front of the flame is small compared to the energy E_o of the explosion. In this stage, the flow is described by the formulae giving the solution of the problem of a strong point explosion. The chemical reactions occur at the background of this flow. At the same time, in the case of explosion, the generated supercompressed wave of detonation decays on the ordinary shock wave and ignition front. The increase, with time, of the distance between the shock wave and the ignition fronts essentially depends on the form of the symmetry, the energy E_o of the explosion, the activation energy E for the induction period, and the adiabatic index γ .

The second stage differs by the fact that it is necessary to take into account the energy released by the chemical reaction. The numerical investigation of the flow in this stage for the values of the parameters mentioned above (13) showed that in spite of the energy supply, the ignition front continues to lag behind the shock wave and flows together with the trajectory of a determined particle of the gas, i.e. in the present case, the detonation combustion is not regenerated.

References

1. Soloukhin R.I. "Metody izmereniya i osnovnye rezul'taty v eksperimentakh na udarnykh trubakh" (Methods of measurements and main results of experiments on shock tubes).--- Novosibirsk, 1969.

2. Korobeinikov V.P., V.A. Levin "Sil'nyi vzryv v goryuchei smesi gazov" (Strong explosion in fuel gas mixtures).--- Mekhanika zhidkosti, gaza, No. 6, 1969.

3. Sedov L.I. "Metody podobiya i razmernosti v mekhanike" (Similarity and dimensional methods in mechanics).--- Izd. 6, Moskva, "Nauka", 1967.

4. Zel'dovich Ya.B., and Yu.P. Raizer "Fizika udarnykh voln i vysokotemperaturnykh gidrodinamicheskikh yavlenii". (Physics of shock waves and high-temperature hydrodynamic phenomena).--- Fizmatgiz, 1963.

5. Chernyi G.G. i.dr. "Vzryv v goryuchei smesi gazov" (Explosion in fuel gas mixtures).--- otchet No. 1000. Institut mekhaniki MGU, 1970.

6. Godunov S.K., A.V. Zabrodin, and G.P. Prokopov. "Raznostnaya skhema dlya dvumernykh nestatsionarnykh zadach gazovoi dinamiki i raschet obtekaniya s otoshedshei udarnoi volnoi" (A difference scheme for two-dimensional nonstationary problems of gas dynamics and calculation of flow around with a withdrawable shock wave).--- Zh. vych. mat. i mat. Fiz., No. 6, 1961.

7. Okhotsimskii D.E., I.L. Kondrat'eva, Z.P. Vlasov, and R.K. Kazakova. "Raschet tochechnogo vzryva s uchetom protivodavleniya" (Calculation of point explosion taking account of counterpressure).--- Trudy matem. instituta im. V.A. Steklova, 50, Moskva, 1967.

8. Perri A., P. Libby and V. Zakkay Theoretical and experimental investigation supersonic combustion Polytech. Inst. of Brooklyn and General Appl. Science Lab. Inc. 1962.

9. Gilbert R.B. and R.A. Strehlow. Theory of detonation initiation behind reflected shock waves, AIAA Journal v. 4, No. 10, 1966.

ONE-DIMENSIONAL NONSTATIONARY MOTIONS OF A FUEL MIXTURE OF GASES IN CASE OF SMALL HEAT EFFECTS OF THE CHEMICAL REACTIONS

By

L.I. Zak and V.A. Levin

The one-dimensional unstationary motions of a fuel mixture of gases, accompanied by the presence of shock waves, and n involving exothermic chemical reaction mechanisms are investigated. As a result of the proceeding of the chemical reactions in the gas flow behind the shock wave, heat is released. This heat affects the motion of the shock wave and the gas flow behind it. The quantity of the heat energy reserved in a unit mass of the fuel gas mixture is supposed to be a sufficiently small value. In an analogous statement, the propagation of a shock wave in an ideally- dissociable gas was investigated in work [5], in which the problem of a piston moving with a constant velocity was solved.

Movement of a Piston in a Fuel Mixture of Gases

Let at the initial instant a piston starts to move in a stationary gaseous fuel medium. A shock wave is formed in front of the piston. This wave initiates the chemical reactions occurring with a release of heat. We shall consider the case when the heat effect of the chemical reactions exerts a small influence on the gas motion. This assumption will be achieved in the case of impoverished fuel mixtures. If Q denotes the quantity of the heat energy released by complete combustion of a unit mass of the fuel, then, in the present case, the following relation must be fulfilled:

$$\frac{\rho_x^\circ Q}{\rho^\circ a_\circ^2} \ll 1 \qquad (1)$$

Here ρ_x° - the density of the burning gas, ρ° - the total density, $a_\circ$ - sound velocity behind the shock wave. The superscript "O" corresponds to the parameters of the gas in front of the shock wave.

It is necessary to mention that the unequality (1) will be also fulfilled in the case of piston movement with a sufficiently high velocity and for high-grade fuel mixtures.

Let us write the system of the equations describing the motion of the gas in the form:

$$\frac{\partial \rho}{\partial t} + u\frac{\partial \rho}{\partial x} + \rho\frac{\partial u}{\partial x} = 0 \quad , \quad \rho\left(\frac{\partial u}{\partial t} + u\frac{\partial u}{\partial x}\right) + \frac{\partial P}{\partial x} = 0 \, ,$$

$$\rho\left(\frac{\partial h}{\partial t} + u\frac{\partial h}{\partial x}\right) - \left(\frac{\partial P}{\partial t} + u\frac{\partial P}{\partial x}\right) = 0 \quad ,$$

$$h = \frac{\gamma}{\gamma-1}\frac{P}{\rho} + \beta Q \quad . \qquad (2)$$

Here h, P, ρ - the enthalpy, pressure and velocity of the medium, respectively, β - the mass concentration of the unreacted gas, Q - the total heat release in the unit mass of the gas and assumed to be of a small value in the above-mentioned sense;; γ - the adiabatic index.

Let us write the equation simulating the proceeding of the chemical reactions in the form:

$$\frac{d\beta}{dt} = \frac{\partial \beta}{\partial t} + u\frac{\partial \beta}{\partial x} = -K_1(P,\rho)\beta^{m_1} + K_2(P,\rho)(1-\beta)^{m_2} \quad . \qquad (3)$$

For the investigation of the gas motion, it is convenient to convert from the Euler variables x, t to the Lagrange variables t, τ , where τ - the instant at which the given particle is set in motion when the shock wave passes through it. With these variables, the system (2,3) has the form:

$$\frac{\partial x}{\partial t} = u \quad , \quad \rho\frac{\partial x}{\partial \tau} = \rho^{\circ} D(\tau) \quad ,$$

$$\rho^{\circ} D(\tau)\frac{\partial u}{\partial t} + \frac{\partial P}{\partial \tau} = 0 \quad , \quad \frac{\partial P}{\partial t} - \frac{\gamma P}{\rho}\frac{\partial \rho}{\partial t} + \rho(\gamma-1)Q\frac{\partial \beta}{\partial t} = 0 \qquad (4)$$

$$\frac{\partial \beta}{\partial t} = -K_1(P,\rho)\beta^{m_1} + K_2(P,\rho)(1-\beta)^{m_2} \quad . \qquad (5)$$

Here D(t)— the velocity of the shock wave front. The parameters of the flow must satisfy the conditions on the shock wave at $t = \tau$

$$u_s = \frac{2D}{\gamma+1}\left(1 - \frac{a^{\circ 2}}{D^2}\right) \quad , \quad P_s = -\frac{\gamma-1}{\gamma+1}P^{\circ} + \frac{2}{\gamma+1}\rho^{\circ} D^2 \quad ,$$

$$\rho_s = \rho^{\circ}\frac{\gamma+1}{\gamma-1}\left(1 + \frac{2}{\gamma-1}\frac{a^{\circ 2}}{D^2}\right)^{-1} \qquad (6)$$

and the condition on the piston at $\tau = 0$

$$u(t,0) = U_*(t) \quad .$$

Let the velocity of the movement of the piston slightly differs from the constant value U_0 , i.e.,

$$U_n(t) = U_0[1+\varepsilon V_1(t)] \quad (\varepsilon \ll 1) .$$

In connection with this, we shall seek the solution of the system (4, 5) in the form:

$$u = U_0(1+\varepsilon u_1) , \quad P = P_0(1+\varepsilon P_1) ,$$

$$\rho = \rho_0(1+\varepsilon \rho_1) , \quad \beta = \beta_0 + \varepsilon \beta_1 ,$$

$$D = D_0(1+\varepsilon D_1) . \qquad (7)$$

The values with the subscript "0" correspond to the common gas-dynamical flow from a piston moving with a constant velocity, and are determined by the formulae:

$$U_0 = \frac{2D_0}{\gamma+1}\left(1-\frac{a^{*2}}{D_0^2}\right) , \quad P_0 = -\frac{\gamma-1}{\gamma+1}P^0 + \frac{2}{\gamma+1}\rho^0 D_0^2 ,$$

$$\rho_0 = \rho^0 \frac{\gamma+1}{\gamma-1}\left(1+\frac{2}{\gamma-1}\frac{a^{*2}}{D_0^2}\right)^{-1} . \qquad (8)$$

Substituting formula (7) in equation (4) and using the assumption $\frac{P}{\rho_0} \sim \varepsilon$ we obtain for the values u_1, P_1, ρ_1 .

$$\frac{\partial u_1}{\partial \tau} + \frac{D_0 \rho^0}{\rho_0 U_0}\frac{\partial \rho_1}{\partial t} = 0 , \quad \frac{\partial u_1}{\partial t} + \frac{P_0}{\rho^0 D_0 U_0}\frac{\partial P_1}{\partial \tau} = 0 ,$$

$$\frac{\partial P_1}{\partial t} - \gamma\frac{\partial \rho_1}{\partial t} + \gamma(\gamma-1)\frac{\partial \beta_0}{\partial t} = 0 . \qquad (9)$$

At the same time the chemical reactions will proceed in the given field of the gas-dynamical parameters, and, instead of equation (5), we have the equation:

$$\frac{\partial \beta_0}{\partial t} = -\varphi(\beta_0, P_0, \rho_0) . \qquad (10)$$

For the parameters of the gas on the shock wave at $t = \tau$, we obtain:

$$u_{1s} = \frac{M_0^2+1}{M_0^2-1} D_1 \quad , \quad P_{1s} = \frac{4\gamma M_0^2}{2\gamma M_0^2-(\gamma-1)} D_1 \quad ,$$

$$\rho_{1s} = \frac{4}{(\gamma-1)M_0^2+2} D_1 \quad ; \quad \beta_0 = 1 \quad . \qquad (11)$$

On the piston at $\tau = 0$, the following condition will be fulfilled

$$u_1(t,0) = V_1(t) \quad .$$

The equation describing the proceeding of the chemical reaction is integrated irrespective of system (9), and its solution, taking account of the boundary condition on the shock wave, will be $\beta_0 = F(t-\tau)$. The specific form of the function $F(t-\tau)$ depends on the constants m_1 and m_2 entering in equation (5).

Excluding the parameters P_1 and ρ_1 in equations (9), we obtain the following equation for the quantity u_1

$$\frac{\partial^2 u_1}{\partial t^2} - \frac{2\gamma M_0^2-(\gamma-1)}{(\gamma-1)M_0^2+2} \frac{\partial^2 u_1}{\partial \tau^2} = (\gamma-1) \frac{2\gamma M_0^2-(\gamma-1)}{2(M_0^2-1)} \frac{\partial^2 \beta_0}{\partial t \partial \tau} \quad . \qquad (12)$$

The general solution of this equation will be:

$$u_1(t,\tau) = f_1(\omega t+\tau) + f_2(\omega t-\tau) + \mu F(t-\tau) \quad , \qquad (13)$$

where

$$\omega^2 = \frac{2\gamma M_0^2-(\gamma-1)}{(\gamma-1)M_0^2+2} \quad , \quad \mu = (\gamma-1)\frac{2\gamma M_0^2-(\gamma-1)}{2(M_0^2-1)(\omega^2-1)} \quad .$$

For pressure P_1 we obtain

$$P_1(t,\tau) = \frac{2\gamma(M_0^2-1)}{2\gamma M_0^2-(\gamma-1)} \left[-\omega f_1(\omega t+\tau) + \omega f_2(\omega t-\tau) + \mu F(t-\tau)\right]. \qquad (14)$$

Using the boundary conditions on the shock wave, (11) we find that:

$$f_1(\xi) = \frac{\omega(M_0^2+1)-2M_0^2}{2\omega(M_0^2-1)} D_1\left(\frac{\xi}{\omega+1}\right) - \frac{\omega-1}{2\omega}\mu \quad ,$$

$$f_2(\xi) = \frac{\omega(M_0^2+1)+2M_0^2}{2\omega(M_0^2-1)} D_1\left(\frac{\xi}{\omega-1}\right) - \frac{\omega+1}{2\omega}\mu \quad . \qquad (15)$$

Using the relations (15), it is easy to obtain the relation between the functions f_1 and f_2 :

$$f_1(\xi) = -\frac{2M_0^2 - \omega(M_0^2+1)}{2M_0\sqrt{(M_0^2+1)}} f_2\left(\frac{\omega-1}{\omega+1}\xi\right) - \frac{\mu(M_0^2-1)}{2M_0^2+\omega(M_0^2+1)} \quad . \qquad (16)$$

This relation shows how the disturbance of the pressure changes when it is reflected from the shock wave. The quantity $\lambda = [2M_0^2 - \omega(M_0^2+1)]/[2M_0^2+\omega(M_0^2+1)]$ is called the reflection coefficient of small disturbances, and it concides with the corresponding coefficient on reflection of disturbances from the shock wave in the common gas dynamics [1-3].

Substituting formulae (15) in formulae (13) and (14), we express the increment of the gas velocity and pressure by the increment of the shock wave velocity:

$$u_1(t,\tau) = \frac{2M_0^2+\omega(M_0^2+1)}{2\omega(M_0^2-1)} D_1\left(\frac{\omega t-\tau}{\omega-1}\right) - \frac{2M_0^2-\omega(M_0^2+1)}{2\omega(M_0^2-1)} D_1\left(\frac{\omega t+\tau}{\omega+1}\right) - \mu[1-F(t-\tau)] ,$$

$$p_1(t,\tau) = \frac{2\gamma(M_0^2-1)}{2\gamma M_0^2-(\gamma-1)} \left\{ \frac{2M_0^2+\omega(M_0^2+1)}{2(M_0^2-1)} D_1\left(\frac{\omega t-\tau}{\omega-1}\right) + \right.$$

$$\left. + \frac{2M_0^2-\omega(M_0^2+1)}{2(M_0^2-1)} D_1\left(\frac{\omega t+\tau}{\omega+1}\right) - \mu[1-F(t-\tau)] \right\} . \qquad (17)$$

For finding the function $D_1(\xi)$, we use the condition for the piston: $u(t,0) = V_1(t)$. From this condition, we find the functional equation which is satisfied by the increment of shock wave velocity:

$$D_1(\xi) - \lambda D_1\left(\frac{\omega-1}{\omega+1}\xi\right) = \frac{2\omega(M_0^2-1)}{2M_0^2+\omega(M_0^2+1)} \left\{ \mu\left[1-F\left(\frac{\omega-1}{\omega}\xi\right)\right] + V_1\left(\frac{\omega-1}{\omega}\xi\right) \right\} . \qquad (18)$$

Thus, the problem of a piston movement with a nearly constant velocity in the fuel mixture of gases is reduced to the solution of a functional equation. The solution of this equation, as shown in [2], can be written in the form:

$$D_1(\xi) = \frac{2\omega(M_0^2-1)}{2M_0^2+\omega(M_0^2+1)} \left\{ \mu \sum_{n=0}^{\infty} \lambda^n \left[1-F\left(\frac{\omega-1}{\omega}K^n\xi\right)\right] + \right.$$

$$\left. + \sum_{n=0}^{\infty} \lambda^n V_1\left(\frac{\omega-1}{\omega}K^n\xi\right) \right\} \qquad \left(K = \frac{\omega-1}{\omega+1}\right) . \qquad (19)$$

The solution consists of two absolutely convergent series. The first sum ensures the change of the velocity of the shock wave owing to the heat release in the gas flow, and the second—owing to the change of the velocity of movement of the piston (as in common gas dynamics). Let us consider in more detail that component of the increment of the velocity of the shock wave which is caused by the proceeding of the chemical reaction. For that, we put $V_1(\xi_0) \equiv 0$ in (19). In t at case, it is easy to obtain the limiting increment of the velocity from (18), with transition to the limit at $\xi_0 \longrightarrow \infty$

$$D_1(\infty) = \frac{2\omega(M_0^2-1)}{2M_0^2+\omega(M_0^2-1)} \mu \frac{[1-F(\infty)]}{1-\lambda}, \qquad (20)$$

where $F(\infty) = \beta_e$ — the equilibrium value of the concentration which is the solution of the algebraic equation:

$$K_2(\rho_0, p_0)(1-\beta_e)^{m_2} - K_1(\rho_0, p_0)\beta_e^{m_1} = 0. \qquad (21)$$

Thus, the limiting increment of the velocity of the shock wave is determined by the equilbrium value of the concentration of the component participating in the reaction. The knowledge of the function $F(\xi_0)$ is necessary for the detailed distribution of the gas-dynamical parameters with respect to the coordinate and time. For example, at $m_1 = m_2 = 1$, the solution of equation (10) has the form:

$$\beta_0 = \beta_e\left[1 - e^{-(K_1+K_2)(t-\tau)}\right] + e^{-(K_1+K_2)(t-\tau)}, \qquad (22)$$

and thereby the form of the function $F(\xi)$ is determined. For that case, the limiting value of the increment of the shock wave velocity as a function of the Mach number of the shock wave of the main flow M_0 at $\gamma = 1.3$ is represented in Fig. 1. The change of the increment of the shock wave velocity with the time $\bar{t} = (k_1 + k_2)\, t$ for some values of M_0 is shown in Fig. 2. It is obvious from the graph that the velocity monotomically tends to its limiting value. The change of the pressure on the piston with time is represented in Fig. 3. That change is nonmotonic. There is an obviously expressed maximum of pressure, which was also discovered on the body, on calculating the supersonic flow of a fuel mixture of gases around a cone [4].

Let a shock tube in the form of a canal of a constant cross-section be filled with two stationary gases separated by a diaphragm. On the left from the diaphragm, there is an inert gas with a high pressure, the so-called "driver gas", and the right part of the tube is filled with a fuel mixture of gases with a high pressure. After the rupture of the diaphragm, a shock

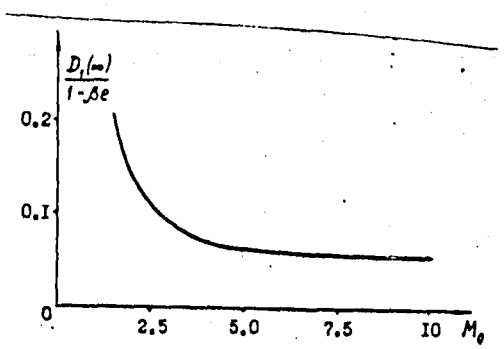

Fig. 1

wave will propagate in the fuel mixture and ignite it. Heat will be released in the gas flow behind the shock wave, and the motion of the shock wave as well as of the contact surface becomes nonuniform. A Riemannian central wave of rarefaction propagates with high pressure in the gas. In contrast to the classical problem of the decay of the arbitrary discontinuity, this wave will not be self-similar.

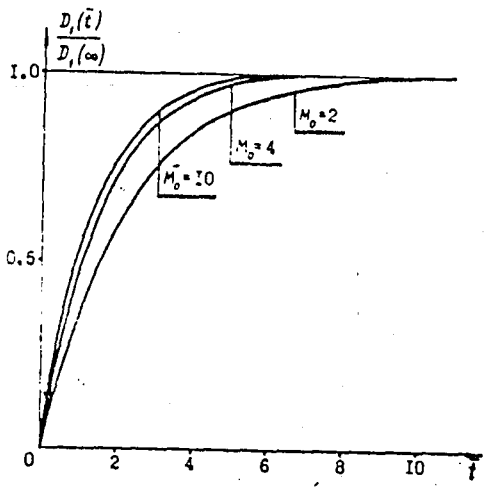

Fig. 2

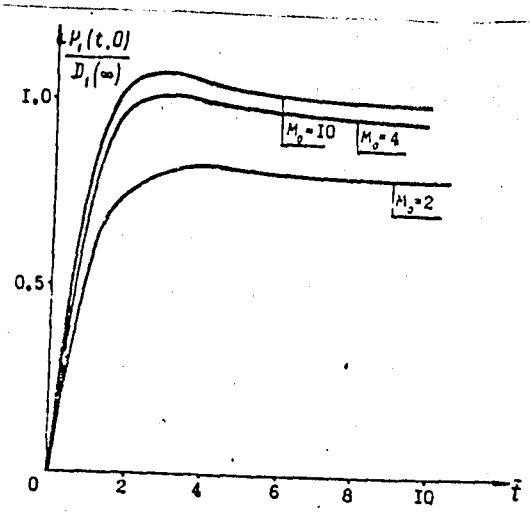

Fig. 3

Movement of a fuel mixture of gases in a shock tube.

The flow in the rarefaction wave is described by the formulae:

$$p = p_*\left(1 - \frac{\gamma_* - 1}{2}\frac{u}{a_*}\right)^{\frac{2\gamma_*}{\gamma_* - 1}}, \quad \rho = \rho_*\left(\frac{p}{p_*}\right)^{\frac{1}{\gamma_*}},$$
$$a = a_* - \frac{\gamma_* - 1}{2}u, \quad x = \varphi(u) - \left(a_* - \frac{\gamma_* + 1}{2}u\right)t. \qquad (23)$$

Here $\varphi(u)$ - tunknown function determined by the continuity conditions of the velocity and pressure on the contact surface. The subscript * corresponds to the state of the stationary gas with high pressure.

Let us use the general solution (17), obtained previously, for the description of the movement of the fuel mixture of gases. The following condition must be fulfilled on the contact surface.

$$p_*\left[1 - \frac{\gamma_* - 1}{2}\frac{v_0(1+\varepsilon u_1(t))}{a_*}\right]^{\frac{2\gamma_*}{\gamma_* - 1}} = p_0(1+\varepsilon p_1(t)), \qquad (24)$$

$$\varphi[v_0(1+\varepsilon u_1(t))] = \int_0^t v_0(1+\varepsilon u_1(t))dt + \left[a_* - \frac{\gamma_* + 1}{2}v_0(1+\varepsilon u_1(t))\right]t. \qquad (25)$$

Reforming condition (24) and expanding in a series through orders of the small parameter ε, we find the relation between the increment of the pressure and the increment of the velocity of the contact discontinuity in the form:

$$p_1(t) + \frac{\frac{2\gamma_* M_0}{\gamma+1}\left(1 - \frac{1}{M_0^2}\right)\frac{a^\circ}{a_*}}{1 - \frac{\gamma_* - 1}{\gamma + 1}\frac{a^\circ}{a_*}M_0\left(1 - \frac{1}{M_0^2}\right)}u_1(t) = 0. \qquad (26)$$

Here the value of M_0 is a function of the decrease of the pressure and temperature and it is determined by the relation:

$$\frac{p_*}{p_0}\left[1 - \frac{\gamma_* - 1}{\gamma + 1}\frac{a^\circ}{a_*}\left(M_0 - \frac{1}{M_0}\right)\right]^{\frac{2\gamma_*}{\gamma_* - 1}} = \frac{2\gamma}{\gamma+1}M_0^2 - \frac{\gamma - 1}{\gamma + 1}. \qquad (27)$$

Substituting the corresponding formulae for $P_1(t)$ and $u_1(t)$ in the condition (26), we obtain the functional equation for the unknown function $D_1(\xi)$.

$$D_1(\xi) - \lambda\lambda_1 D_1\left(\frac{\omega-1}{\omega+1}\xi\right) = \frac{2\omega\Delta(M_0^2-1)}{2M_0^2+\omega(M_0^2+1)}\left[1-F\left(\frac{\omega-1}{\omega}\xi\right)\right], \tag{28}$$

where:

$$\lambda_1 = \frac{\Omega-\omega\dfrac{2\gamma(M_0^2-1)}{2\gamma M_0^2-(\gamma-1)}}{\Omega+\omega\dfrac{2\gamma(M_0^2-1)}{2\gamma M_0^2-(\gamma-1)}} \qquad \Omega = \frac{\dfrac{2\gamma_* M_0}{\gamma+1}\left(1-\dfrac{1}{M_0^2}\right)\dfrac{a^0}{a_*}}{1-\dfrac{\gamma_*-1}{\gamma+1}\dfrac{a^0}{a_*}\left(M_0-\dfrac{1}{M_0}\right)},$$

$$\Delta = \mu\,\frac{\Omega+\dfrac{2\gamma(M_0^2-1)}{2\gamma M_0^2-(\gamma-1)}}{\Omega+\omega\dfrac{2\gamma(M_0^2-1)}{2\gamma M_0^2-(\gamma-1)}}.$$

Using the equations (13) and (14), we find the relation between the function f_1 and f_2 on the contact discontinuity:

$$f_2(\xi) = -\lambda_1 f_1(\xi) - \Delta\cdot F\left(\frac{\xi}{\omega}\right). \tag{29}$$

From this relation, the physical meaning of the quantity λ_1 becomes clear. It is the coefficient of reflection of the compression wave going backward from the shock wave, from the contact surface of the wave.

The solution of the functional eqaution (28) will be:

$$D_1(\xi) = \frac{2\omega\Delta(M_0^2-1)}{2M_0^2+\omega(M_0^2+1)}\sum_{n=0}^{\infty}(\lambda\lambda_1)^n\left[1-F\left(\frac{\omega-1}{\omega}K^n\xi\right)\right]. \tag{30}$$

For the limiting increment of the velocity of the shock wave, we obtain:

$$D_1(\infty) = \frac{2\omega\Delta(M_0^2-1)}{2M_0^2+\omega(M_0^2+1)}\cdot\frac{1-\beta_e}{1-\lambda\lambda_1}. \tag{31}$$

The final velocity of the shock wave, both in this case and in the case of the movement of a piston, is determined by the equilibrium concentration of the component participating in the reaction. The change of the velocity of the shock wave with time for the values $\gamma_* = 1.66$; $\gamma = 1.3$ and for some Mach numbers M_0 at the temperature drop $\frac{a_0^*}{a_0} = \frac{1}{2}$ is represented in Fig. 4. The velocity of the shock wave monotonically tends to its limiting value. The change of the velocity of the contact discontinuity and the pressure on it with time are shown in Figs. 5 and 6. The velocity of the contact discontinuity nonmonotonically decreases. It has a velocity minimum. The character of the change of the pressure is the same as on the piston, i.e. the pressure nonmonotonically increases, tending to its limiting value.

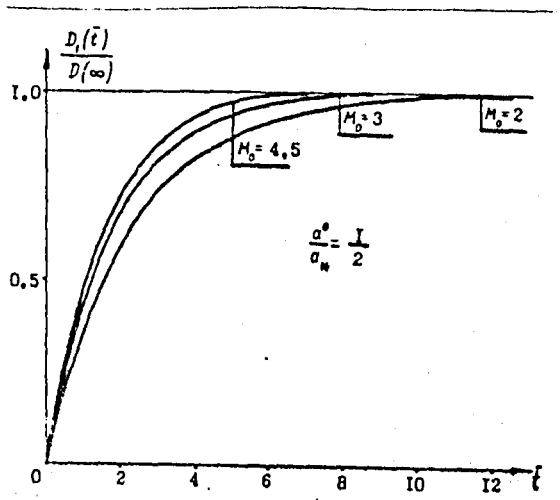

Fig. 4

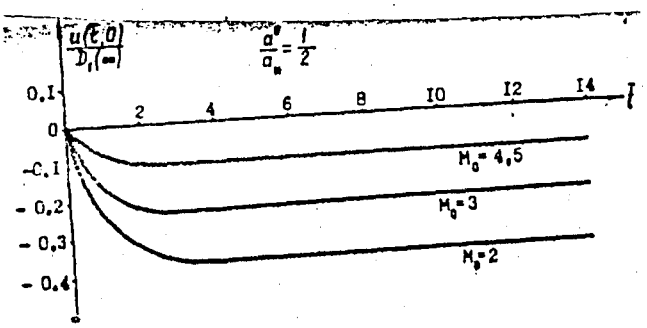

Fig. 5

The knowledge of the increment of the shock wave velocity in the experiment enables to determine some functional relations between the constants determining the proceeding of the chemical reactions. Thus, in the case of a single reaction of type (3), it is possible to determine the affinity constant from the relation (31). One should also mention that the discussed method of the construction of solution can be generalized for the cases of many chemical reactions proceeding both simultaneously and successively.

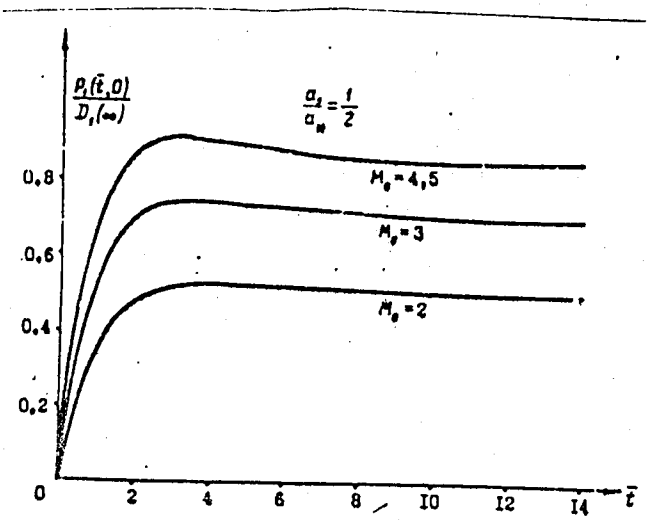

Fig. 6

References

1. Chernyi G.G. "Neustanovivshiesya dvizheniya gaza v kanalakh s pronitsaemymi stenkami. Ob ustoichivosti skachka uplotneniya v kanalakh" (Unsteady motion of gas in canals with penetrable walls. On the stability of shock waves in canals).--- Trudy TsIAM, No. 224, 1953.

2. Chernyi G.G. "Techeniya gaza s bol'shoi sverkhzvukovoi skorost'yu" (Gas flow with a high supersonic velocity).--- Fizmat., 1959.

3. Kraiko A.N. "Nekotorye voprosy geometricheskoi akustiki odnomernykh nestatsionarnykh i dvumernykh statsionarnykh techenii" (Some problems of the geometric acoustics of one-dimensional nonstationary and two-dimensional stationary flow).--- MZhG, No. 5, 1967.

4. Chushkin P.I. "Sverkhzvukovoe obtekanie tel goryuchim gazom" (Supersonic fuel gas flow around bodies by fuel gas).--- Fizika goreniya i vzryva, 5 (2), 1969.

5. Spence D.A. Unsteady shock propagation in relaxing gas. Proc. Roy. Soc., A264, pp. 221-233, 1961.

HYPERSONIC NONSTATIONARY FLOW OF A FUEL MIXTURE OF GASES IN THE NEIGHBOURHOOD OF THE CRITICAL LINE OF A BLUNTED BODY

By

S.M. Gilinskii

On shooting a body with high velocities in hydrogen–air and hydrogen–oxygen mixtures, some characteristic modes of flow around were observed: stationary—with plain shock and thermal fronts; nonstationary—of pulsating character with a strictly periodic structure of the combustion region in the form of circular waves; modes with a complex structure, with the formation of internal exploisons interacting with the leading shock wave and bending it. The theoretical investigation of the stationary modes was carried out previously, and the main results are discussed in [6].

In the present work, the pulsating nonstationary modes of combustion generated at hypersonic flow around the leading part of blunted bodies are investigated. The investigation is carried out numerically. The flow is studied in the neighbourhood of the critical line. The method of "termination of series" is used and the solution is searched for in the form of a first approximation. The integration of the two-dimensional equations in partial derivatives is carried out by the finite difference method with the use of the characteristic relations for discontinuities and for the contour of the body. The initial stationary flow is determined from the solution of the boundary-value problem for the system of ordinary differential equations by the method of iteration.

The growth of finite disturbances artificially inserted in the boundary and initial conditions, and also of the small disturbances generated because of numerical errors is studied with time. It is ascertained that the inserted disturbances lead to the formation of the oscillations of the leading shock wave and the parameters of the gas behind it. The amplitude and frequency of oscillations depend on the magnitude of the activation energy.

The detected modes are near to self-oscillating ones with constant amplitude and frequency. The region of stability, with respect to the small and finite disturbance, for the two-dimensional flow is significantly larger than that in the case of the propagation of one-dimensional detonation.

§ 1. Let a supersonic flow of a fuel mixture of gases with the parameters: velocity V_∞, pressure P_∞ and temperature T_∞, runs against an axisymmetric

blunted body. We shall assume that ignition does not occur in the incident flow, and that an exothermic irreversible reaction A → B proceeds behind the shock wave because of the increase of temperature and pressure according to Arrhenius law:

$$\frac{d\beta}{dt} = -L\beta^m p^{m-1} e^{-E/RT} = \omega(p,T) . \qquad (1.1)$$

Here, as usual, β – the concentration of the unreacted gas, m – order of reaction, E – activation energy, L – reaction rate constant, R – gas constant,

The system of gas dynamic equations together with the kinetic one (1.1) for the axisymmetric flow can be written in Eulerian variables in the following form:

$$\frac{\partial \rho}{\partial t} + \frac{\partial(\rho u)}{\partial r} + \frac{1}{r}\frac{\partial(\rho v)}{\partial \theta} + \frac{\rho}{r}(2u + v\,ctg\,\theta) = 0 ,$$

$$\frac{\partial u}{\partial t} + u\frac{\partial u}{\partial r} + \frac{v}{r}\frac{\partial u}{\partial \theta} - \frac{v^2}{r} = -\frac{1}{\rho}\frac{\partial p}{\partial r} ,$$

$$\frac{\partial v}{\partial t} + u\frac{\partial v}{\partial r} + \frac{v}{r}\frac{\partial v}{\partial \theta} + \frac{uv}{r} = \frac{1}{\rho r}\frac{\partial p}{\partial \theta} ,$$

$$\frac{\partial p}{\partial t} + u\frac{\partial p}{\partial r} + \frac{v}{r}\frac{\partial p}{\partial \theta} - \rho\left(\frac{\partial h}{\partial t} + u\frac{\partial h}{\partial r} + \frac{v}{r}\frac{\partial h}{\partial \theta}\right) = 0 ,$$

$$\frac{\partial \beta}{\partial t} + u\frac{\partial \beta}{\partial r} + \frac{v}{r}\frac{\partial \beta}{\partial \theta} = -L\beta^m p^{m-1} exp(-E\rho/p) ,$$

$$h = \frac{\gamma}{\gamma-1}\frac{p}{\rho} + \beta Q , \qquad (1.2)$$

where r, θ – the polar coordinates with the origin in the center of the curvature of the body in the critical point at zero time; u, v – the projections of the velocity vector $\vec{W}$ in the direction r and θ as shown in Fig. 1, p, ρ, h, T – the pressure, density, enthalpy and temperature, respectively; γ – adiabatic index, Q – energy release of the reaction.

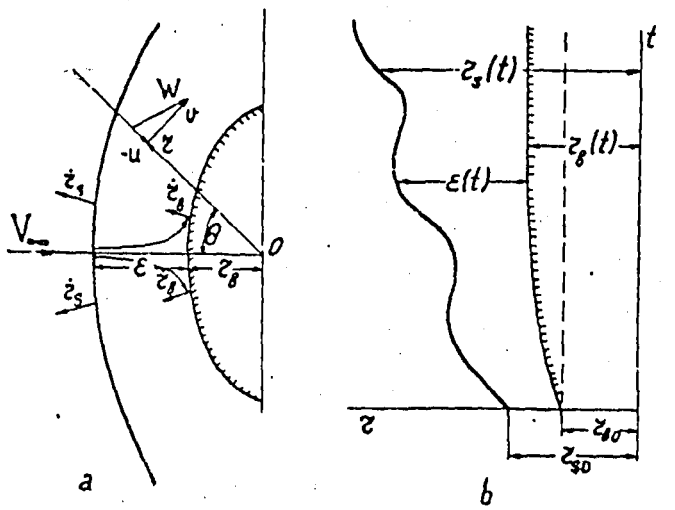

Fig. 1

We interpolate the dimensionless variables (with index 1), with the help of the following relations:

$$r' = \frac{r}{R_\beta^\circ} \quad , \quad t' = \frac{V_{max}}{r_\beta^\circ}\, t \quad ,$$

$$u' = \frac{u}{V_{max}^\circ} \quad , \quad v' = \frac{v}{V_{max}^\circ} \quad ,$$

$$\rho' = \frac{\rho}{\rho_\infty^\circ} \quad , \quad p' = \frac{p}{\rho_\infty^\circ V_{max}^{\circ 2}} \quad ,$$

$$E' = \frac{E}{V_{max}^{\circ 2}} \quad , \quad q' = \frac{q}{V_{max}^{\circ 2}} \quad ,$$

$$L' = L\, r_\beta^\circ (\rho_\infty^\circ)^{m-1} (V_{max}^\circ)^{in} \quad , \quad T' = \frac{T}{T_\infty^\circ} \quad . \qquad (1.3)$$

Here the subscript "∞" refers to the parameter of the incident flow, and the superscript "O" denotes that the value of the parameter is considered at zero time, V_{max} — the maximum velocity of the gas in front of the shock wave.

The form of equations (1.2) remains in the dimensionless variables (below we shall omit the index "1"). The boundary conditions on the surface of the body are given - conditions of non-flowing and in the incident flow for V_∞, P_∞, T_∞ and γ. The shock wave is considered a discontinuity, where Hugoniot relations are fulfilled.

Thus, the solution of the problem in the dimensionless variables is determined by five main parameters M_∞, γ, q, E, L, and the parameters characterizing the disturbance. The heat release q of the reaction at a fixed Mach number M_∞ characterizes the degree of the supercompression of the stationary detonation wave. It is coupled with the ordinary used contraction coefficient f by the relation:

$$q = \frac{1}{2(\gamma^2-1)} \frac{(M_\infty^2 f - 1)^2}{(M_\infty^2 f + \frac{2}{\gamma-1}) M_\infty^2 f}, \quad f = \frac{M_y^2}{M_\infty^2}, \tag{1.4}$$

where M_y - the minimum Mach number M of the propagation of the detonation wave (Mach number M of Chapman-Jouguet).

The integration of the three-dimensional equations (1.2) can be reduced to a successive integration of two-dimensional equations if we use the so-called method of "termination of series" suggested by Van-Dike. This method was used in a number of works for the calculation of the flow of viscous [1] and ideal gases [2].

Let us represent the unknown functions in the neighbourhood of the critical line in the form of series with various powers of $\sin\theta$. Taking account of the eveness of the functions we shall have:

$$\begin{aligned}
p(t,z,\theta) &= p_1(t,z) + p_2(t,z)\sin^2\theta + p_3(t,z)\sin^4\theta + \dots \\
u(t,z,\theta) &= -u_1\cos\theta + u_2\cos\theta\sin^2\theta + \dots \\
v(t,z,\theta) &= v_1\sin\theta + v_2\sin^3\theta + \dots \\
\rho(t,z,\theta) &= \rho_1 + \rho_2\sin^2\theta + \dots \\
\beta(t,z,\theta) &= \beta_1 + \beta_2\sin^2\theta + \dots
\end{aligned} \tag{1.5}$$

The first "termination" (the term "termination" is universally recognized) includes all the first terms of expansion (1.5), with the exception of the expansion for pressure in which the first two terms are taken; the second "termination"- the first two expansion terms of (1.5) plus three- in the expansion for pressure, etc.

The first "termination" is substituted in the system of equations (1.2), and in each equation the coefficients with powers of $\sin\theta$ are equated to zero. A system of equations concerning the variables t and τ is obtained for the coefficients of expansions (1.5). This system contains seven equations with six unknown functions. Following work [1], we shall omit the equation, obtained by equating the coefficients with $\sin^2\theta$ in the energy equation to zero.

The final system of the equations of the first "termination" in the variables t and ξ is:

$$\xi = \frac{\tau - \tau_g(t)}{\varepsilon(t)}, \quad \varepsilon(t) = \tau_s(t) - \tau_g(t)$$

can be written in the following form:

$$\frac{\partial \rho_1}{\partial t} - A\frac{\partial \rho_1}{\partial \xi} = \gamma\rho_1\left[\frac{1}{\varepsilon}\frac{\partial u_1}{\partial \xi} - 2\frac{(v_1-u_1)}{\tau_g+\xi\varepsilon}\right] - (\gamma-1)q\rho\left[\frac{\partial \beta_1}{\partial t} - A\frac{\partial \beta_1}{\partial \xi}\right],$$

$$\frac{\partial \beta_1}{\partial t} - A\frac{\partial \beta_1}{\partial \xi} = -L\beta_1^m \rho_1^{m-1} \exp(-E\rho_1/\rho_1),$$

$$\frac{\partial u_1}{\partial t} - A\frac{\partial u_1}{\partial \xi} = \frac{1}{\rho_1\varepsilon}\frac{\partial p_1}{\partial \xi},$$

$$\frac{\partial \rho_1}{\partial t} - A\frac{\partial \rho_1}{\partial \xi} = \rho_1\left[\frac{1}{\varepsilon}\frac{\partial u_1}{\partial \xi} - \frac{2(v_1-u_1)}{\tau_g+\xi\varepsilon}\right],$$

$$\frac{\partial v_1}{\partial t} - A\frac{\partial v_1}{\partial \xi} = -\frac{2p_2}{(\tau_g+\xi\varepsilon)\rho_1} - \frac{v_1(v_1-u_1)}{\tau_g+\xi\varepsilon},$$

$$\frac{\partial p_2}{\partial \xi} = -\frac{1}{2}\left(\frac{\partial p_1}{\partial \xi} - \rho_1 u_1\frac{\partial u_1}{\partial \xi} - 2\varepsilon\rho_1 v_1\frac{v_1-u_1}{\tau_g+\xi\varepsilon}\right), \quad A = \frac{u_1+\dot{\tau}_g+\xi\dot{\varepsilon}}{\varepsilon}, \tag{1.8}$$

Here, $\tau_s = \tau_s(t)$ and $\tau_g = \tau_g(t)$ — are the equations of the contour of the shock wave and the body respectively.

The system of equations (1.6) has the following characteristics:

a) along the "trajectory"

$$\frac{d\xi}{dt} = -A \quad , \tag{1.7}$$

$$\frac{dp_1}{dt} - \frac{\gamma p_1}{\rho_1}\frac{d\rho_1}{dt} + (\gamma-1)q\rho_1\frac{d\beta_1}{dt} = 0 \quad , \tag{1.8}$$

$$\frac{dv_1}{dt} + \frac{2p_2}{(\tau_s+\xi\varepsilon)\rho_1} + \frac{v_1(v_1-u_1)}{\tau_s+\xi\varepsilon} = 0 \quad , \tag{1.9}$$

$$\frac{d\beta_1}{dt} = -L\beta^m\rho_1^{m-1}\exp(-E\rho_1/\rho_1) \quad ; \tag{1.10}$$

b) along the characteristics C^+ and C^-

$$\frac{d\xi}{dt} = -A \pm \frac{a_1}{\varepsilon} \quad , \quad a_1^2 = \frac{\gamma p_1}{\rho_1} \quad , \tag{1.11}$$

$$a_1\frac{du_1}{dt} \pm \frac{1}{\rho_1}\frac{dp_1}{dt} \pm 2a_1^2\frac{v_1-u_1}{\tau_s+\xi\varepsilon} \pm (\gamma-1)Lq\beta_1^m\rho_1^{m-1}\exp(-E\rho_1/\rho_1) \quad , \tag{1.12}$$

c) along the characteristic:

$$\frac{dt}{d\xi} = 0 \quad , \tag{1.13}$$

$$\frac{dp_2}{d\xi} + \frac{1}{2}\left(\frac{dp_1}{d\xi} - \rho_1 u_1\frac{du_1}{d\xi} - 2\varepsilon\rho_1 v_1\frac{v_1-u_1}{\tau_s+\xi\varepsilon}\right) = 0 \quad . \tag{1.14}$$

The boundary conditions on the contour of the body take the form:

$$\text{at} \quad z = z_B(t) \qquad \text{or} \qquad \xi = 0 \qquad u_1 + \dot{z}_B = 0 \ . \tag{1.15}$$

For the calculation of the functions behind the shock wave, it is necessary to substitute expansions (1.5) in the Hugoniot relations, using the scheme of "termination" described above. Analogous expansion should be written for the contour of the shock wave and the body:

$$\begin{aligned} z_s(t,\theta) &= z_{s_1}(t) + z_{s_2}(t)\sin^2\theta + \dots \\ z_B(t,\theta) &= z_{B_1}(t) + z_{B_2}(t)\sin^2\theta + \dots \end{aligned} \tag{1.16}$$

We shall be limited by the first two terms in expansions (1.16) and shall assume that the coefficient with $\sin^2\theta$ does not depend on time. This is equivalent to the assumption that the shock wave (and body) in any point in the neighbourhood of the critical line moves in the direction of the normal with the same velocity, and that it is near to a sphere.

The relations coupling the parameters of the gas in front of and behind the shock wave (at $\xi = 1$) are as follows:

$$\begin{aligned} u_1 &= \frac{\gamma-1}{\gamma+1}\left[\left(V_\infty + \dot{z}_{s_1}\right) + \frac{2\gamma}{\gamma-1}\frac{p_\infty}{\rho_\infty}\left(V_\infty + \dot{z}_{s_1}\right)^{-1}\right] - \dot{z}_{s_1} \ , \\ p_1 &= \frac{2}{\gamma+1}\rho_\infty\left(V_\infty + \dot{z}_{s_1}\right)^2 - \frac{\gamma-1}{\gamma+1}p_\infty \ , \\ \rho_1 &= \rho_\infty \frac{V_\infty + \dot{z}_{s_1}}{u_1 + \dot{z}_{s_1}} \ , \\ p_2 &= \frac{\gamma-1}{2\gamma}\rho_1\left(u_1 - V_\infty\right)\left(u_1 + V_\infty - \dot{z}_{s_1}\right) \ , \\ v_1 &= V_\infty - \left(V_\infty - u_1\right)2z_{s_2}/z_{s_1} \ , \quad \beta = 1 \ . \end{aligned} \tag{1.17}$$

For the solution of the system of equation (1.6) with the boundary conditions (1.15) and (1.17), it is necessary to know all the functions at zero time.

The main calculations were carried out from the distributions obtained by solving the stationary equations (1.6). The system of the stationary equations for the system (1.6) is solved with respect to the derivatives of

$$\frac{du_1}{d\xi} = \frac{\varepsilon_0}{a_1^2 - u_1^2}\left[2a_1^2\frac{v_1 - u_1}{1+\xi\varepsilon_0} - (\gamma-1)L q \rho_1 \beta_1^m \rho_1^{m-1} \exp(-E\rho_1/\rho_1)\right],$$

$$\frac{d\beta_1}{d\xi} = \frac{L\varepsilon_0}{u_1}\beta_1^m \rho_1^{m-1}\exp(-E\rho_1/\rho_1),$$

$$\frac{dv_1}{d\xi} = \frac{\varepsilon_0}{u_1}\left[\frac{2p_2}{\rho_1(1+\xi\varepsilon_0)} + \frac{v_1(v_1-u_1)}{1+\xi\varepsilon_0}\right],$$

$$\frac{d\rho_1}{d\xi} = \frac{\rho_1}{u_1}\left[2\varepsilon_0\frac{v_1-u_1}{1+\xi\varepsilon_0} - \frac{du_1}{d\xi}\right], \quad \frac{dp_2}{d\xi} = \varepsilon_0\rho_1 u_1\frac{v_1-u_1}{1+\xi\varepsilon_0} - \frac{dp_1}{d\xi},$$

$$\frac{dp_1}{d\xi} = -\rho_1 u_1 du_1/d\xi \quad . \qquad (1.18)$$

(1.18)

The solution of the boundary value problem for the system of the ordinary differential equations (1.18) is obtained by the iteration method. The Cauchy problem is repeatedly solved from the initial data behind the shock wave before the body. The unknown parameter ε_0 is determined by the Newton method from the condition of non-flowing (1.15). The indeterminate form in the point $\xi = 0$. for some equations of (1.18) is treated by extrapolation of the functions from a certain distance from the body. The integration of equations (1.18) is carried out according to the clear Eulerian scheme.

The system of the nonstationary equations (1.6) with the boundary conditions (1.15) and (1.16) is solved by the finite-difference method within the interval $0 \leq \xi \leq 1$ and with using the characteristic relations (1.7-1.14) for the determination of the functions at the boundary points. The space interval (0.1) is divided to (N + 1) nodal points at equal intercepts, and the values of the functions for the following time-layer in the internal points are determined by the clear scaling circuit of Lax with a second order of accuracy (Fig. 2 a). At first, the values of the functions in the two half-integral points 5 and 6 are calculated for the layer $(j + \frac{1}{2})$ and then, by the obtained values of the functions in the half-integral points, all the functions in point 4 on the layer (j + 1) are obtained.

The calculation of P_2 in the half-integral and integral nodal points are performed by the solution of the ordinary differential equation (1.14) along each time layer, using the clear Eulerian scheme.

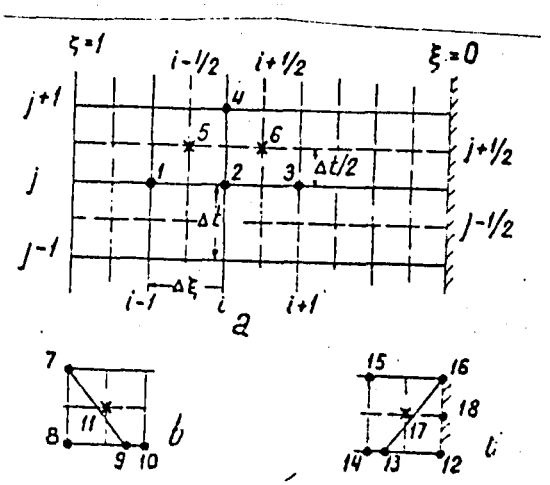

Fig. 2

The withdrawal ξ of the shock wave from the body and its relative velocity $\dot{\xi}$ on the following layer is found by the Newton iteration method. The trajectory of the shock wave within one time interval is approximated by a parabola, and the value of $\dot{\xi}$ is the solution of the characteristic equation along the characteristic C drawn backwards from the boundary nodal point of the upper layer (Fig. 2 b). The scheme of the second order of accuracy is investigated and the value of the functions in the intersection point of the characteristic with the j- m layer is calculated by equations (1.11-1.12). The parameters in the point 9 are determined by linear or quadratic interpolation from the values of the functions in the nearest nodal points.

On the surface of the body (Fig. 2 B), the calculation is performed as follows. The pressure P_2 is originally calculated on the layer (j + 1) in the point 16 by integrating equation (1.14) at the end of the interval (0.1). The pressure P_1 and the velocity components are calculated from equation (1.6), taking account of the boundary condition (1.15) from the clear formulae, and the density is calculated by the iteration method from the equation that is a consequence of the relations along the trajectory and the C^+ characteristic drawn backwards from point 16. The values of the functions in point 13 are determined by linear or quadratic interpolation.

After the calculation of the density, the concentration B_i is determined from relation (1.8) along the trajectory by the clear formula.

§2- The algorithm, described in § 1, was programed on EVM-BESM-3M. A standard net with a number of nodal points N = 40 in the space variable ξ was used in most of the calculations. Besides the standard net, a net with numbers of nodal points N = 80 and 120 was used to estimate the accuracy of the individual variants.

The main calculations were carried out at $M_\infty = 5$, $\gamma = 1.4$, $q = 0.3$ and 0.4. The activation energy E and the reaction rate L were simultaneously varied so that the relative width of the nonequilibrium zone of the stationary solution comprised about half of the width of the whole shock layer. The value of the withdrawal of the shock wave is close to that observed in the experiments in work [7] and obtained in the calculations of stationary flow around bodies [6].

For the purpose of studying the influence of the Mach number M_∞ and comparison with the known investigations of "one-dimensional flows, the following values of the parameters were also considered: $M_\infty = 7.6$, $q = 0.615$ ($f = 1.6$), $\gamma = 1.2$, $E = 0.5$-1.25. These conditions were partially considered in work [8], where the growth of the disturbances with time in the one-dimensional flow in front of the piston was investigated. The values of $E = 0.5$ and 0.6 correspond to the steady and unsteady modes of flows according to the linear theory [9].

Two forms of disturbances of stationary flow were investigated. A strong disturbance was originally inserted in the initial distribution. It led to the assignment of constant values of the functions of P_1, ν_1, P_2, ρ_1 and of a linear distribution for the velocity u_1 with respect to ξ. The boundary conditions on the shock wave and on the body were satisfied, and the value of the withdrawal $\varepsilon_0 = 0.2$ is arbitrarily given.

The calculation was carried on from these initial data to the setting of the stationary flow. The results of such calculations are represented in Fig. 3. Here, for convenience, the dimensionless time $\tau = t \times (1.62)^{-1}$ was introduced. This is related to the number of the time intervals, through which the results were delivered to the printing of the EVM.

In the case of a perfect gas, and for small activation energies ($E \leq 0.5$), steadiness rapidly occurs. Slowly decaying oscillations with a nearly constant frequency are observed with the increase of the activation energy. Irrespective of the reaction rate, at E = 1.0, the generated oscillations due to the strong initial disturbance gradually decay, after that the flow is described by the stationary solution (1.18).

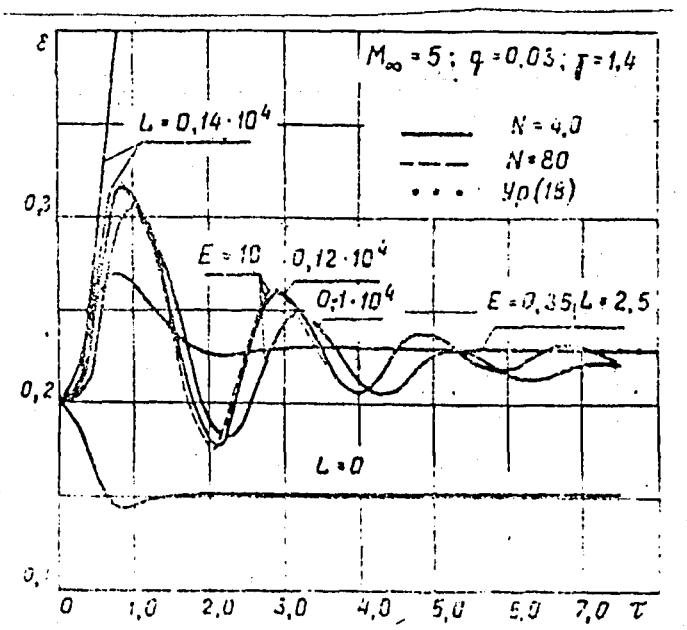

Fig. 3

The change of the velocity of the incident flow by the law:

$$M_\infty(t) = M_\infty^\circ + \ell \frac{t}{t_0} e^{-t/t_0}, \quad \begin{matrix} \ell = const \\ t_0 = const \end{matrix} \tag{2.1}$$

at constant density and pressure was with another form of the given disturbance.

The growth of the distrubance (19) with time for some values of the activation energies and for different Mach numbers M is shown in Figs. 4 and 5.

In the first case, at $M_\infty^\circ = 5$ and for an activation energy E = 1.0, the oscillations always decay with time, so that this range of the values of E can be considered as belonging to the region of steadiness with respect to the finite disturbance. For an activation energy E = 1.5, the oscillations intensify with time.

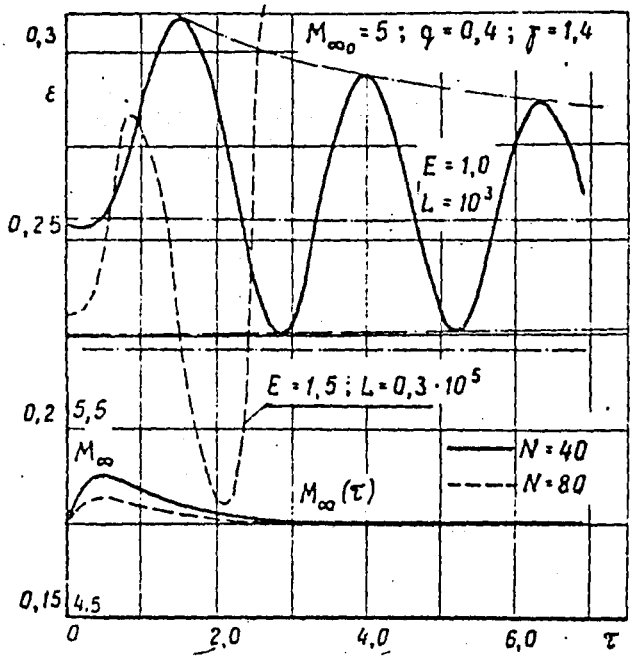
$M_{\infty_0} = 5$; $q = 0,4$; $\gamma = 1,4$
ε
0,3
0,25
0,2
0,15
$E = 1,0$
$L = 10^3$
$E = 1,5$; $L = 0,3 \cdot 10^5$
5,5
4,5
M_∞
$M_\infty(\tau)$
$N = 40$
$N = 80$
0
2,0
4,0
6,0
τ

Fig. 4

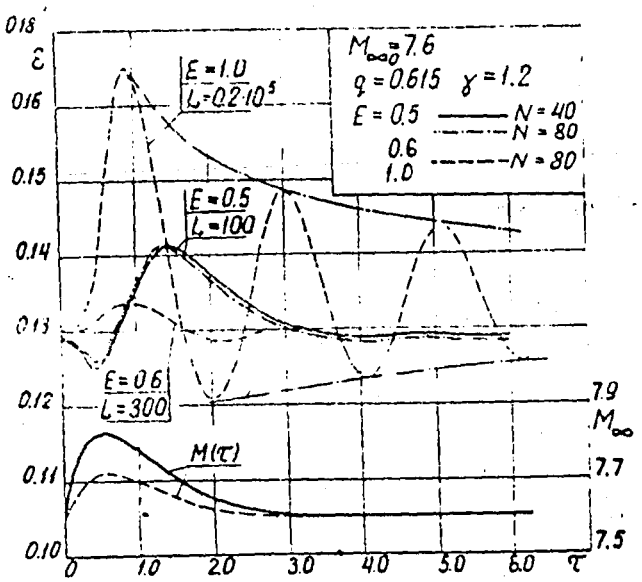
$M_{\infty_0} = 7.6$
$q = 0.615$ $\gamma = 1.2$
$E = 0.5$ $N = 40$
$N = 80$
0.6
1.0 $N = 80$
$E = 1.0$
$L = 0.2 \cdot 10^5$
$E = 0.5$
$L = 100$
$E = 0.6$
$L = 300$
$M(\tau)$
ε
0.18
0.16
0.15
0.14
0.13
0.12
0.11
0.10
7.9
7.7
7.5
M_∞
0
1.0
2.0
3.0
4.0
5.0
6.0
τ

Fig. 5

An analogous result was obtained at $M_\infty = 7.6$. When the activation energy E was ≤ 1.0, the oscillations decayed, and at $E \geq 1.25$ they intensified with time. It should be noted that the calculations in the last case were carried out on a comparatively short time interval. This is connected with the fact that for great values of the activation energy, lying in the region of unsteadiness, the numerical errors increase owing to the increase of the gradients of the functions. For the continuation of calculations, a decrease of the interval of time and space from a certain moment was required.

We investigated also the growth of very small disturbances connected with the increase of the numerical errors. For that, the calculation was performed from the stationary solution of equations (1.18) without introducing any artificial disturbances.

For values of the activation energy from the steady region with respect to the finite disturbance, very weak oscillations are observed near the stationary solution. These oscillations practically do not increase by widely changing E from 0 to 1. The deviation does not exceed $\sim 0.3\%$. For values of E from the unsteady region, a relatively rapid formation of considerable oscillations of the leading shock wave and the whole flow behind it is observed. The amplitude of the oscillations of the shock wave (Fig. 6) grows slowly with time, and the frequency remains almost constant. The qualitative character of the curve does not change by using a more fine net. The change of the profile of pressure from the shock wave to the body at $\xi = 1 - \xi$ with time, shown in the same figure, illustrates the oscillatory character of the whole flow in the shock layer.

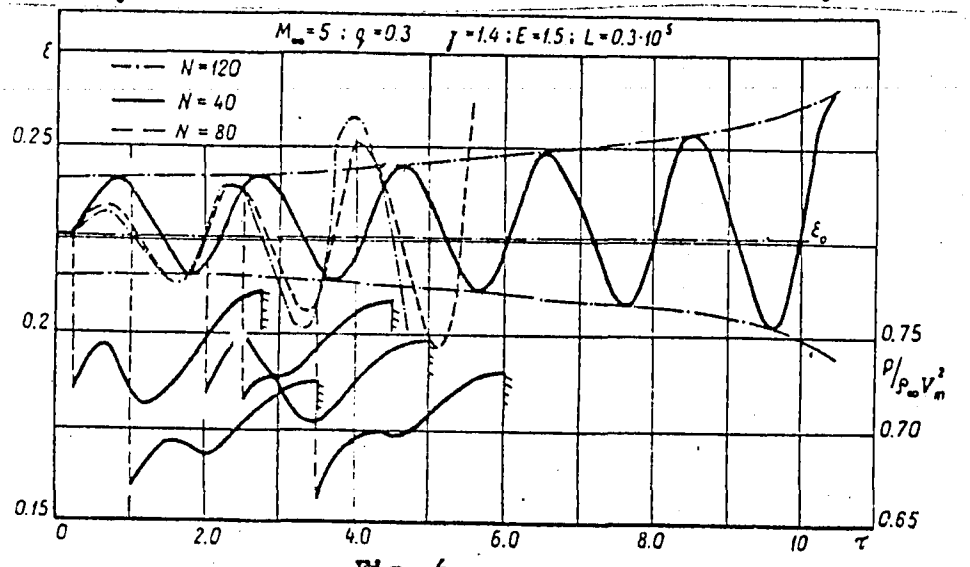

Fig. 6

In order to exclude the influence of the errors of the numerical method on qualitative conclusions about the growth or decay of the disturbances, a great consideration in the process of performance of work was given to the control of the calculation accuracy.

For the values of the parameters lying in the region of steadiness, besides the comparison of the results obtained with different space nets, the comparison with the stationary solution of equations (1.18) served as a criterion for the accuracy of the numerical scheme. The small fluctuations of the parameters of the nonstationary but near-stationary solution insignificantly depend on the value of E ($\sim 0.3\%$) for sufficiently large instants. The comparison of the results obtained with the standard space net and with a net with half interval gives approximately the same evaluation (see for example, Fig. 5).

In some cases, the calculation with the standard net led to a physically unreal result. Thus, Fig. 3 represents the result of the calculation at E = 1.0 and $L = 0.14 \cdot 10^4$, obtained with N = 40 (solid line) and N = 80 (dotted line). In the first case, the shock wave monotonically moves away from the body, in the second-the oscillations decay with time.

In the unsteady region at E = 1.5 ($M_\infty = 5$), the nonstationary solution, on the average, has fluctuations near the stationary. At the same time for the standard net, the deviation of the maxima of the fluctuations, as a rule, is greater than the deviations of the minima. The relative error, as follows from the comparison of the results with N = 40, 80 and 120, is the greatest in th neighbourhood of the maxima. On decreasing the space intergal, the curves are shifted to the side of smaller values of τ . In this case one should evaluate the maximum error from the difference of the corresponding maxima. This evaluation gives a value of $\sim 5.7\%$ for the first three fluctuations.

The numerical errors arise in the first place from the inaccuracy of the calculation of the kinetic equations (1.6) and (1.10), where the product of the big (L) and the small (exponent) multipiliers is involved in the velocity of the process. In the case of the big gradients, these errors rapidly increase, which leads to the physically unreal result.

In order to exclude the influence of these errors, an additional series of calculations with a still more simple kinetic model was carried out. It is assumed that the mixture burns instantaneously in the detonation front, and the heat release q of the reaction depends on the velocity of the flow in a system of coordinates connected with this front.

$$q = q_{max}\,\varphi(M) .$$

Such an enthalpy function changes the explicit kinetic process in the gas (distributed heat supply, ignition delay, and others) to an implicit one and serves as if it is an average characteristic of that process. The form of that function is determined by the parameters of the incident flow V_∞ , P_∞ , T_∞ and the dimensions of the body.

According to theory and experiment, the form of that function is qualitatively determined as represented in the left upper angle of Fig. 7. Here, a narrow range of the Mach number M is only shown, where the flow is reconstructed from an adiabatic one without heat release to a detonation one with a complete combustion of the mixture in a relatively narrow zone.

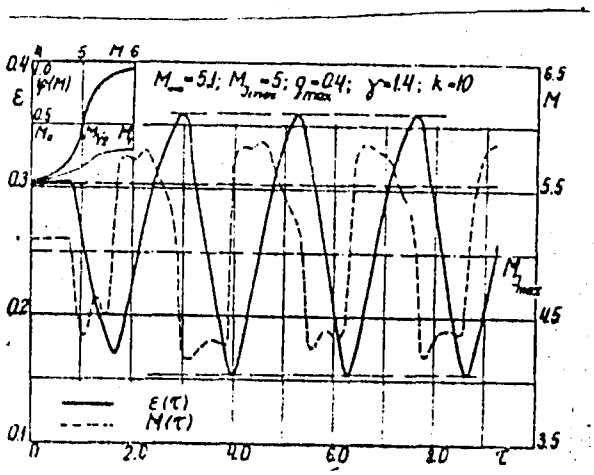

Fig. 7

By carrying out concrete calculations of the function $\varphi(M)$, it is possible to approximate the analytic relation:

$$\varphi(M) = \frac{1}{2}\left[1 + \frac{2}{\pi}\operatorname{arctg} K(M - M_{1/2})\right]$$

The curves of the drop-out of the shock wave and the Mach number M of the incident flow in a coordinate system connected with the shock wave are plotted in Fig. 7 for the following values of the parameters: $M_\infty = 5.1$, $q_{max} = 0.4$, $\gamma = 1.4$, $K = 10$, $M_{y\,max} = 5$ corresponds to $q_{max} = 0.4$ at $\varphi = 1$.

The stationary solution with such parameters corresponds to a flow with a detonation wave, in which the mixture completely burns with the heat release: $q = -\frac{3}{4} - q_{max} = 0.3$. Thus, such solution will be near to the limiting one at $L \longrightarrow \infty$ for the case represented in Fig. 7; the difference here is in Mach number M_∞ .

It is obvious that owing to the numerical errors at $\tau \sim 0.75$, the solution of the system of equations (1.6) becomes essentially nonstationary. It is interesting that in this case, self-oscillations with constant frequency and amplitude of the leading detonation wave take place. The mechanism of the maintainance of such oscillations is similar to that described in the experimental work [3].

Owing to some reasons, the stationary flow is led out from the equilibrium state at which, for example, the shock wave begin to move in the direction of the body. At that time, the thermodynamic parameters, pressure and temperature behind the shock wave, begin to fall in view of the decrease of its intensity. Accordingly and because of the high activation energy of the fuel mixtures, the heat release sharply decreases and the shock wave acceleratingly moves to the body. Then its retardation takes place because of the compression of the gas in the shock layer "the reflection". As a result, a peak of pressure and temperature is formed; the mixture again "ignites" and the shock wave maintained by ignition moves away from the body. Farther, because of the radial expansion of the flow, it begins to attenuate and it stops at a certain distance. After that, the process described above is renewed.

All these moments of the process are represented in Figs. 7 and 8. The three-dimensional diagram of the pressure as a function of the two variables t and ξ is plotted in Fig. 8.

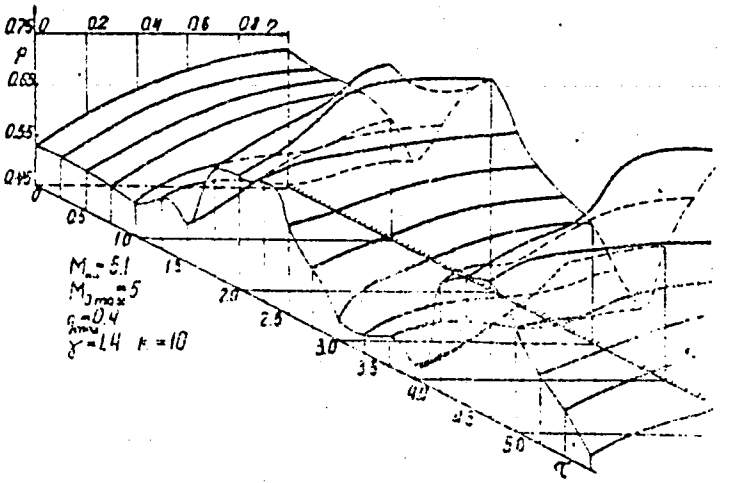

Fig. 8

The described mechanism of the pulsation of the leading shock wave with the periodic generation of the waves of the burnt gas, which after that are carried away downstream, can serve in some cases as explanation of the presence of a strictly periodic wave structure of the combustion front. The latter in the supersonic part degenerates in surface, separating the burnt and unburnt parts of the gas.

In conclusion, we mention that the values of the activation energy of a mixture, corresponding to the neutral oscillations in the investigated two-dimensional flow, are lying far in the region of unstability for one-dimensional flows in front of a piston. This follows from comparison with the results of the linear and nonlinear stability theory both for the strongly-compressed [8, 9] and weakly-compressed [4, 5] detonation waves. This effect is explained by the stabilizing influence of the spreading of gas along the surface. In this case, disturbances, do not succeed to develop and are carried away downstream.

References

1. Kao "Giperzvukovoe vyazkoe techenie vblizi kriticheskoi linii toka zatuplennogo tela" (Hypersonic viscous flow near the critical streamline of a blunted body).--- Part I and II Russian translation "Raketnaya tekhnika i kosmonavtika" (Rocket engineering and stronautics), No. 11, 1964.

2. Paskonov V.M., and L.Ya. Shlyapochnik "Raschet techeniya ideal'nogo gaza v okrestnosti linii tormozheniya zatuplennogo tela" (Calculation of the flow of an ideal gas in the neighbourhood of the stagnation line of a blunted body), Sb. "Chislennye metody v gazovoi dinamike"---vyp. XI, izd-vo, MGU, 1968.

3. Soloukhin R.I. "Pul'siruyushchee gorenie gaza za udarnoi volnoi v sverkhzvukovom potoke" (Pulsating combustion of gas behind a shock wave in a supersonic flow).--- PMTF, No. 5, 1961.

4. Chernyi G.G. "Bozniknovenie kolebanii pri oslablenii pereszhatykh detonatsionnykh voln" (Formation of oscillations on attenuation of supercompressed detonation waves).--- PMM, No. 3, 1969.

5. Medvedev S.A. "Ob oslablenii pereszhatykh detonatsionnykh voln s konechnoi skorost'yu reaktsii" (On the attenuation of supercompressed detonation waves with finite reaction rates).--- Izv. AN SSSR, MZhG, No. 3, 1969.

6. Gilinskii S.M. and G.G. Chernyi "High velocity motion of solid bodies in combustible gas mixtures", Astronautica Acta, v. 16, 1970.

7. Chernyi G.G. Supersonic flow around bodies detonation and deflagration fronts. Astronautica Acta 13, 1968.

8. Fickett W., and W.W. Wood. "Flow calculations for pulsating one-dimensional detonations", Phys. Fluids, v. 9, No. 5, 1966.

9. Erpenbeck J.J. "Stability of idealized one-reaction detonations". Phys. Fluids, v. 7, No. 5, 1964.

USE OF THE BOUNDARY LAYER METHOD FOR SOLVING THE PROBLEMS OF THE MOTION OF GAS MIXTURES WITH EXOTHERMIC REACTIONS

By

S.M. Gilinskii, and M.L. Khaykin

A great number of works [1, 5-8] is dedicated to the analytical investigation of the motion of nonequilibrium reaction or relaxation media.

In the present work, a hypersonic nonequilibrium flow of a mixture of gases near a wedge or a cone, and also in front of a moving piston is investigated by the boundary layer method [2]. The obtained solutions can be simply used for the evaluation of the influence of the oscillatory relaxation or the nonequilibrium dissociation.

§ 1. Hypersonic nonequilibrium flow of a fuel mixture of gases around a wedge or cone

Let the heat supply to the gas takes place in a combustion wave of a finite width and let this process be arbitrarily described by one irreversible reaction [3]:

$$\frac{d\beta}{dt} = -L\beta^m \rho^{m-1} \exp\left(-\frac{E}{RT}\right), \qquad (1.1)$$

where β - the relative concentration of the original reacting components of the mixture, m - the order of reaction, ρ - pressure, T - temperature, E - activation energy, R - the universal gas constant.

We shall be limited to the investigation of plane and axisymmetric flows. Following work [2] for the variables of the boundary layer, where x' - the coordinate along the contour and ψ' - the flow function, we shall write the gas-dynamical equation system

$$\rho u \frac{\partial u}{\partial x'} + \rho v \frac{\partial v}{\partial x'} + \frac{\partial p}{\partial x'} = 0 ,$$

$$\frac{1}{1+y'/R_s} \frac{\partial v}{\partial x'} - \frac{u}{R_s + y'} = -\tau_1^{\nu-1} \frac{\partial p}{\partial \psi'} ,$$

$$\frac{\partial}{\partial x'}\left(\frac{u^2+v^2}{2} + \frac{\gamma}{\gamma-1}\frac{p}{\rho} + \beta Q\right) = 0 ,$$

$$\frac{u}{1+y'/R_s}\frac{\partial \beta}{\partial x'} = -L\beta^m \rho^{m-1} \exp\left(-\frac{E'\rho}{p}\right), \quad E' = \frac{E}{M} . \qquad (1.2)$$

Here, y^1 — coordinate, orthogonal x^1; u, v — the components of the velocity vector in the directions x^1, y^1; R_β — radius of the curvature of the flow line, $\nu = 1,2$, for plane and axisymmetric flows, M — molecular weight of the mixture, Q — quantity of heat supplied to the unit mass of gas at complete combustion. For the axisymmetric flows, τ_1 — the distance from the axis of symmetry to the considered point of the shock layer, τ — the distance from the axis of symmetry to the point of the contour (Fig. 1). The flow function is interpolated by the relations:

$$\frac{\partial y^1}{\partial \psi^1} = \frac{1}{\rho u \tau_1^{\nu-1}}, \qquad (1.3)$$

$$\frac{\partial y^1}{\partial x^1} = \left(1 + y^1/R_\beta\right)\frac{v}{u}. \qquad (1.4)$$

The solution of (1.3), (1.4) is written in the form of series of powers of the small parameter $\varepsilon = \frac{\gamma-1}{\gamma+1}$

$$y^1 = \varepsilon y_0^1 + \ldots \qquad \rho = \rho_0 + \varepsilon\rho_1 + \ldots$$

$$u = u_0 + \varepsilon u_1 + \ldots \qquad \rho = \frac{\rho_0}{\varepsilon} + \rho_1 + \ldots$$

$$v = \varepsilon v_0 + \ldots \qquad \beta = \beta_0 + \varepsilon\beta_1 + \ldots \qquad (1.5)$$

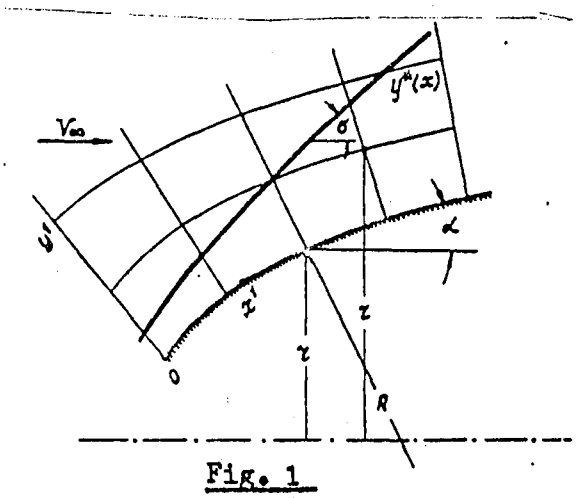

Fig. 1

The variables of the boundary layer; diagramatic pattern of flow near the body.

After the performance of the standard operations for the determination of the first terms of the series, we get a system of equations:

$$\frac{\partial y_0'}{\partial \psi'} = \frac{1}{\rho_0 u_0 z^{\nu-1}}, \quad v_0 = u_0 \frac{\partial y_0'}{\partial x'},$$

$$\frac{\partial u_0}{\partial x'} = 0, \quad \frac{u_0}{R} = z^{\nu-1} \frac{\partial p_0}{\partial \psi'},$$

$$\frac{\partial}{\partial x'}\left[\frac{\gamma}{\gamma+1}\frac{p_0}{\rho_0} + \beta Q\right] = 0,$$

$$u_0 \frac{\partial \beta_0}{\partial x'} = -L \beta_0^m p_0^{m-1} \exp\left(-\frac{E' p_0}{\rho_0}\right), \quad E' = \frac{E'}{\varepsilon}, \tag{1.6}$$

and for the determination of the functions u_1, P_1, ρ_1, β_1 — we have:

$$\rho u_0 \frac{\partial u_1}{\partial x'} + \frac{\partial p_0}{\partial x'} = 0,$$

$$\frac{\partial v_0}{\partial x'} - \frac{u_1}{R} = -\frac{u_0}{R}\left[\frac{y_0}{R} + (\nu-1)\frac{y_0'}{z}\cos\alpha\right] - z^{\nu-1}\frac{\partial p_1}{\partial \psi'},$$

$$\frac{\partial}{\partial x'}\left[\frac{\gamma}{\gamma+1}\left(\frac{p_1}{\rho_0} - \frac{p_0 \rho_1}{\rho_0^2}\right) + u_0 u_1 + \beta_1 Q\right] = 0,$$

$$u_0 \frac{\partial \beta_1}{\partial x'} + \left(u_1 - \frac{u_0 y_0}{R}\right)\frac{\partial \beta_0}{\partial x'} = -L\left[m \beta_0^{m-1} \beta_1 p_0^{m-1} + \right.$$

$$\left. + (m-1)\beta_0^m p_0^{m-2} p_1 - E' \beta_0^m p_0^{m-1}\left(\frac{p_1}{\rho_0} - \frac{p_0 \rho_1}{\rho_0^2}\right)\right] \exp\left(-\frac{E' p_0}{\rho_0}\right). \tag{1.7}$$

The representation of the concentration β in the form of (1.5) is a consequence of the assumption that the limiting flow at $\varepsilon \to 0$ is a non-equilibrium one, and this enables to take into account, as a first approximation, the effect of the nonequilibrium state.

The arbitrary functions should be determined from the boundary conditions on the given contour

$$y' = 0 \qquad \text{at} \qquad \psi' = 0 \tag{1.8}$$

and on the shock wave, where all the functions are expanded in power series of the form of (1.5).

The relations for the shock wave in the considered case coincide with those given in work [2] for the ordinary adiabatic flow, and it is necessary only to add the conditions of concentration (the index S will be attached to the parameters directly behind the shock wave).

$$\beta_{0s} = 1 \;, \quad \beta_{1s} = 0 \qquad \text{at} \qquad \psi' = \psi'^{*}(x')$$

$$\psi'^{*}(x') = \psi_0'^{*} + \varepsilon \psi_1'^{*} + O(\varepsilon^2) \;. \tag{1.9}$$

The systems of equations (1.6) and (1.7) are integrated in quadratures, but unlike the case of the adiabatic flow this procedure is more complicated, and the solution is more cumbersome.

We introduce the dimensionless variables x, y and ψ as follows:

$$x' = L^{-1} u_\infty \rho_\infty^{1-m} x \;, \quad y' = L^{-1} u_\infty \rho_\infty^{1-m} y \;,$$

$$\psi' = \frac{\rho_\infty V_\infty}{\nu} \left(L^{-1} u_\infty \rho_\infty^{1-m} \sin\alpha \right)^{\nu} \psi \;, \tag{1.10}$$

In this form, the function $x^{*}(\psi)$ on the shock wave becomes $\psi^{1/\nu}$.

For a wedge and cone, the integration of the last two equations of (1.6) along the line $\psi = \text{const}$ gives:

$$\psi^{1/\nu} - x = \int_1^{\beta_0} \frac{\exp\left(\frac{B}{c-t}\right)}{t^m}\, dt = \mathcal{J}_m(\beta_0) - \mathcal{J}_m(1) \;, \tag{1.11}$$

where

$$B = \frac{\gamma}{\gamma+1} \frac{\tilde{E}}{Q} \;, \quad c = 1 + \frac{\gamma}{\gamma+1} \frac{\rho_{0s}}{\rho_{0s} Q} \;. \tag{1.12}$$

In the most simple case at $m = 1$, for which all the results will be reduced for shortness, the integration of (1.11) gives (see [4]).

$$\mathcal{J}_1 = e^{\alpha} Ei(\zeta-\alpha) - Ei(\zeta) \quad ,$$

$$Ei(\zeta) = \ln\zeta + \sum_{\kappa=1}^{\infty} \frac{\zeta^{\kappa}}{\kappa\cdot\kappa!} \quad , \quad \zeta > 0 \quad , \quad \zeta - \alpha > 0 \quad . \tag{1.13}$$

Formula (1.11) gives an unclear dependence of the concentration β_0 on the coordinates of the point (x, ψ) in the shock layer to zero, and only in the case when the activation energy E equals zero ($\beta = 0$), it is possible to solve this relation with respect to β_0.

When the activation energy differs from zero, it is necessary to select, as independent variables, the value of the concentration β_0 inside the shock layer and the value of the concentration β_0^0 on the contour in such a way that the coupling of the old and new variables will be given by the equations:

$$x = \mathcal{J}_1(1) - \mathcal{J}_1(\beta_0^0)$$
$$\psi = \left[\mathcal{J}_1(\beta_0) - \mathcal{J}_1(\beta_0^0)\right]^{\nu} . \tag{1.14}$$

Further, it is necessary to express all the unknown functions in the variables β_0 , β_0^0 in an obvious form, and then, for example, plot graphically the dependence on x and ψ . It appears that all the unknown functions of the first and second approximations are expressed in a combination of exponential integrals, transcendental and rational algebraic functions of β_0 and β_0^0.

The calculation of these functions reduces to a partial differentiation, or integration along the coordinate lines x = const, ψ = const.

Finally, we obtain for a wedge in zero-approximation:

$$u_0 = V_\infty \cos\alpha \quad , \quad p_0 = \rho_\infty V_\infty^2 \sin^2\alpha \quad , \quad \rho_0 = \frac{\rho_\infty \sin^2\alpha}{q(c-\beta_0)} \quad ,$$

$$v = \frac{V_\infty q}{\sin\alpha}(\beta_0 - \beta_0^0) \quad , \quad y_0 = \frac{2q}{\sin 2\alpha}\left[\Phi_1(\zeta) - \Phi_1(\zeta_0)\right] \quad ,$$

$$\Phi(\zeta) = c\left[e^{\alpha} Ei(\zeta-\alpha) + (\alpha-1)Ei(\zeta) - \frac{\alpha e^{\zeta}}{\zeta}\right] \quad ,$$

$$\zeta_0 = \frac{\alpha c}{c+\beta_0^0} \quad , \quad q = \frac{\gamma}{\gamma+1}\frac{Q}{V_\infty^2} \quad ,$$

$$y_0^* = \frac{2q}{\sin 2\alpha}\left[\Phi_1(\zeta_s) - \Phi_1(\zeta_0)\right] \quad , \quad \zeta_s = \frac{\alpha c}{c-1} \quad , \tag{1.15}$$

where $y_0^*(x)$ determines the form of the shock wave.

In the first approximation, we shall have:

$$u_1 = u_{1s}(\psi) = -\frac{V_\infty q}{\cos\alpha}\left[c - \beta_0^{\circ *}(\psi)\right],$$

$$p_1 = \rho_\infty V_\infty^2 q\left\{2c - 1 - \beta_*^\circ - \beta_0^\circ \exp\left[-a/(1-\beta_0^\circ/c)\right] \times \right.$$

$$\left. \times\left[\mathcal{J}_1(\beta_0) - \mathcal{J}_1(1)\right]\right\} - \rho_\infty V_\infty^2 \sin^2\alpha - p_\infty , \qquad (1.16)$$

$$\beta_1 = \beta_0 \exp\left[a/(1-\beta_0/c)\right]\left[\Phi(-\xi) - \Phi(-\xi_s)\right],$$

$$p_1 = \frac{\rho_\infty \sin^2\alpha}{q^2(c-\beta_0)^2}\left[\frac{p_1}{\rho_0 V_\infty^2} + \beta_1 q - f_{s\kappa\lambda}(\psi)\right],$$

where $$\Phi(-\xi) = \frac{a}{c}\left[1 + q^{-1} f_{s\kappa\lambda}(\psi)\right]\left[e^{-a}Ei(a-\xi) - \frac{e^{-\xi}}{a}\right] -$$

$$- \frac{q}{\cos^2\alpha}\left[c - \beta_0^{\circ *}(\psi)\right]\left[e^{-a}Ei(a-\xi) - Ei(-\xi)\right]$$

$$\xi > 0$$

$$f_{s\kappa\lambda}(\psi) = \frac{1}{V_\infty^2}\left[\frac{p_{1s}}{\rho_{0s}} - \frac{\rho_{0s}\rho_{1s}}{\rho_{0s}^2}\right]. \qquad (1.17)$$

It is obvious from the formula that the concentration β_0 along the flow line monotonically decreases from one to zero (Fig. 2).

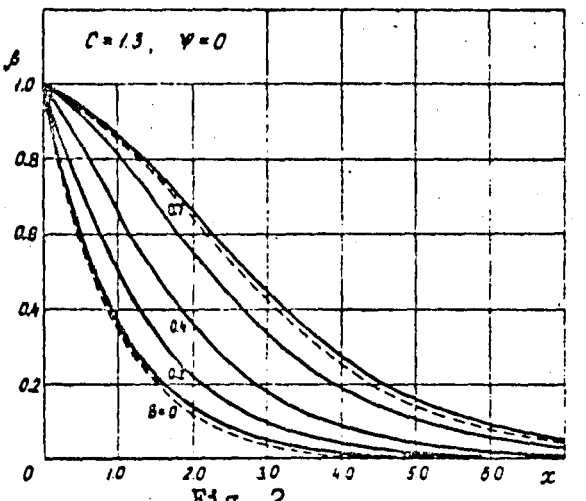

Fig. 2

Distribution of the concentration β (x) along the generating line of the body

——— first approximation

– – – – – – second approximation taken into account

In the first approximation, we shall have:

$$u_1 = u_{1s}(\psi) = -\frac{V_\infty q}{\cos\alpha}\left[c - \beta_0^{\circ *}(\psi)\right],$$

$$p_1 = \rho_\infty V_\infty^2 q\left\{2c - 1 - \beta_s^\circ - \beta_0^\circ \exp\left[-a/(1-\beta_0^\circ/c)\right] \times \right.$$

$$\left. \times\left[\mathcal{J}_1(\beta_0) - \mathcal{J}_1(1)\right]\right\} - \rho_\infty V_\infty^2 \sin^2\alpha - p_\infty , \qquad (1.16)$$

$$\beta_1 = \beta_0 \exp\left[a/(1-\beta_0/c)\right]\left[\Phi(-\xi) - \Phi(-\xi_s)\right],$$

$$\rho_1 = \frac{\rho_\infty \sin^2\alpha}{q^2(c-\beta_0)^2}\left[\frac{p_1}{\rho_0 V_\infty^2} + \beta_1 q - f_{s_{KA}}(\psi)\right],$$

where

$$\Phi(-\xi) = \frac{a}{c}\left[1 + q^{-1} f_{s_{KA}}(\psi)\right]\left[e^{-a}Ei(a-\xi) - \frac{e^{-\xi}}{a}\right] -$$

$$- \frac{q}{\cos^2\alpha}\left[c - \beta_0^{\circ *}(\psi)\right]\left[e^{-a}Ei(a-\xi) - Ei(-\xi)\right]$$

$$\xi > 0$$

$$f_{s_{KA}}(\psi) = \frac{1}{V_\infty^2}\left[\frac{p_{1s}}{\rho_{0s}} - \frac{\rho_{0s}\rho_{1s}}{\rho_{0s}^2}\right]. \qquad (1.17)$$

It is obvious from the formula that the concentration β_0 along the flow line monotonically decreases from one to zero (Fig. 2).

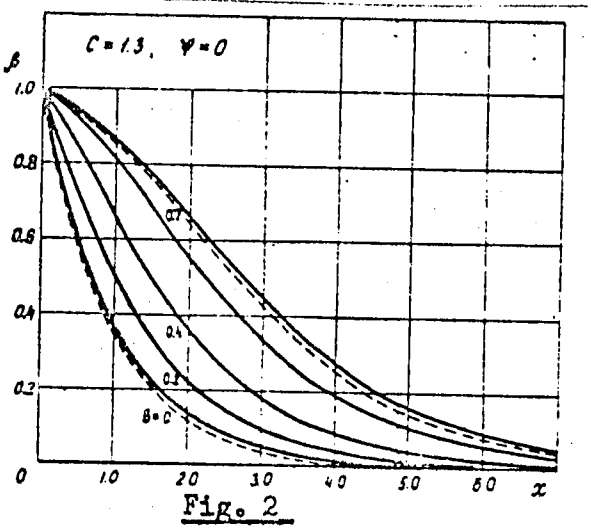

Fig. 2

Distribution of the concentration β (x) along the generating line of the body

——— – first approximation

– – – – – – second approximation taken into account

Formulae (1.15) and (1.16) are essentially simplified and become evident with respect to x, ψ when the activation energy is equal to zero. For shortness, we shall not give these formulae here, since analogous formulae will be written out below.

It should be noticed that the pressure and velocity in the zero approximation are calculated by the Newton formula. Taking account of the first approximation, the velocity u is constant along the flow line, but it changes across the shock layer. The pressure changes nonmonotonically and it has a maximum. On increasing the activation energy this maximum increases and shifts to the equilibrium region of flow. The curves $p_1'/p_e' = f(x)$ along the wall of the wedge are plotted in Fig. 3 for the values of B = 0 and 0.7; C = 1.3:

$$f(x) = 1-(2C-1)^{-1}\beta_0^{\circ}\left\{1+\exp\left[\alpha/(1-\beta_0^{\circ}/C)\left[J_1(\beta_0^{\circ})-J_1(1)\right]\right]\right\}. \qquad (1.18)$$

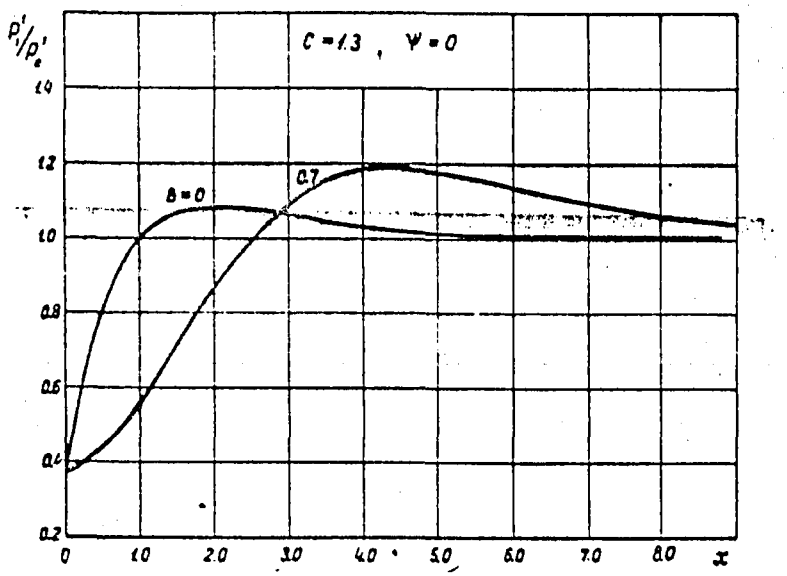

Fig. 3

Pressure distribution along the side of the wedge for two values of the dimensionless parameter β

Taking account of the first approximation, the density and concentration monotonically decrease along the line ψ = const. For the determination of the function $y_0(\beta_0, \beta_0^{\circ})$ we have:

$$y_0 = \frac{2q}{\sin 2\alpha}\int_{\beta_0^*}^{\beta_0}(c-t)t^{-1}\left[x + J_1(t) - J_1(1)\right]\exp\left(\frac{B}{c-t}\right)dt = \qquad (1.19)$$

$$= \frac{2q}{\sin 2\alpha}\left[\chi(\zeta) - \chi(\zeta_0)\right] ,$$

where $\chi(\zeta) = a^2 c\left\{A\left[a^{-1}e^{a}Ei(\zeta-a) - 2Ei(\zeta) + \frac{e^{\zeta}}{\zeta}\right] + \frac{1}{2a}\left[e^{a}Ei(\zeta-a) - Ei(\zeta)\right]^2 + \right.$

$$\left. + \frac{1}{2}Ei^2(\zeta) - \frac{e^{\zeta}}{\zeta}Ei(\zeta) + 2Ei(2\zeta) - \frac{e^{2\zeta}}{\zeta} - e^{a}J^{\circ}\right\}$$

$$A = \left[x - e^{a}Ei(\zeta_s - a) + Ei(\zeta_s)\right] , \quad J^{\circ} = \int \frac{Ei(\zeta-a)\,e^{\zeta}}{\zeta^2}\,d\zeta \qquad (1.20)$$

We present the function ζ^{-2} in an integrand of the unstationary integral J in the form of a power series in the neighbourhood of the point a. Performing a term-by-term integration of this series we shall have:

$$J^{\circ} = \frac{e^{a}}{a^2}\sum_{\kappa=1}^{\infty}(-1)^{\kappa-1}\frac{\kappa}{a^{\kappa}}J'_{\kappa} , \qquad (1.21)$$

where J'_{κ} is calculated by the recurrent relations:

$$J'_{\kappa} = (\zeta-a)^{\kappa-1}e^{\zeta-a}Ei(\zeta-a) - (\kappa-1)J'_{\kappa-1} - J''_{\kappa-1} ,$$

$$J'_1 = e^{\zeta-a}Ei(\zeta-a) - Ei(2(\zeta-a)) ,$$

$$J'_2 = \frac{1}{2}e^{2(\zeta-a)} , \quad J''_{\kappa} = \frac{1}{2}\left[(\zeta-a)^{\kappa-1}e^{2(\zeta-a)} - (\kappa-1)J''_{\kappa-1}\right] . \qquad (1.22)$$

The component of the velocity v_0 is calculated as follows:

$$v_0 = -V_{\infty}\left\{\frac{y_0}{x}\cos\alpha + \frac{q}{x\sin\alpha}\left[\beta_0(\psi^{1/2} - x) - \beta_0^{\circ}x - \right.\right.$$

$$\left.\left. - a^2c\left(Ei(\zeta - \frac{e^{\zeta}}{\zeta}) + a^2c\left(Ei(\zeta_0) - \frac{e^{\zeta_0}}{\zeta_0}\right)\right]\right\} . \qquad (1.23)$$

The position and inclination of the shock wave to the x direction are determined as follows:

$$y_0^{*} = \frac{2q}{x \sin 2\alpha}\left[\chi(\zeta_s) - \chi(\zeta_*)\right], \qquad (1.24)$$

$$y_0^{*'} = V_\infty \sin 2\alpha \frac{\rho_\infty}{\rho_{0s}} - \frac{u_0}{v_0} \qquad (1.25)$$

In the zero approximation, the difference of the solution for a wedge and cone appears only in the form of the shock wave and the value of the velocity v_0 and the velocity u_0 ; the pressure, density and concentration in these solutions coincide.

It follows from system (1.16) that in the first approximation for a reaction of the first order, the parameters p_1, ρ_1, u_1, ρ_1 are determined for a cone from the same differential equations recorded along the flow line for a wedge, with an accuracy up to the coefficients which depend on φ and are determined in the shock wave. Therefore, for these functions we shall not give here the tedious formulae in the case of $B \neq 0$.

We shall write out the more simple formulae for the case of $B = 0$, when all the functions are evidently expressed in x, φ.

zero approximation

$$u_0 = V_\infty \cos\alpha, \quad \rho_0 = \rho_\infty V_\infty^2 \sin^2\alpha, \quad \beta_0 = \exp(\psi^{1/2} - x),$$

$$\rho_0 = \rho_\infty\left[K + q(1 - e^{\psi^{1/2} - x})\right]^{-1},$$

$$y_0 = \frac{1}{x \sin 2\alpha}\left\{K \sin^2\alpha \cdot \psi + q\left[\psi - 2e^{-x}(1+x)\left(e^{\psi^{\frac{1}{2}}}(\psi^{1/2} - 1) + 1\right)\right]\right\} \qquad (1.26)$$

first approximation

$$u_1 = -\frac{V_\infty}{2\cos\alpha}\left\{K \sin^2\alpha + q\left[1 - 2\frac{1 - e^{-\psi^{1/2}}(1 + \psi^{1/2})}{\psi}\right]\right\},$$

$$p_1 = \rho_\infty V_\infty^2 \sin^2\alpha K\left(\frac{5}{4} - \frac{\psi^2}{4x^4}\right) - \left(\rho_\infty V_\infty^2 \sin^2\alpha + p_\infty\right) +$$

$$+ \rho_\infty V_\infty q\left\{\frac{5}{4} - \frac{\psi^2}{4x^4} - \frac{2(1 - e^{-x} - xe^{-x})}{x^2} + \right.$$

$$+ \frac{e^{-x}(x^2 + 2x + 2)}{x^4}\left[e^{\psi^{1/2}}(\psi - 3\psi^{1/2} + 3) + \frac{\psi}{2} - \right.$$

$$\left.\left. - e^{x}(x^2 - 3x + 3) - x^2/2\right]\right\},$$

$$\beta_1 = \frac{1}{2\cos^2\alpha}\left\{K\sin^2\alpha + q\left[1 - \frac{2\left(1 - e^{-\psi^{1/2}} - \psi^{1/2}e^{-\psi^{1/2}}\right)}{\psi}\right]\right\} e^{\psi^{1/2}}\left(\psi^{1/2} - x\right)$$

$$\rho_1 = \frac{\rho_\infty \sin^2\alpha}{\left[K\sin^2\alpha + q\left(1 - e^{\psi^{1/2} - x}\right)\right]^2}\left\{\frac{P_1}{\rho_\infty V_\infty^2} + \beta_1 q - f_{s\,хол}(\psi)\right\} \qquad (1.27)$$

The behaviour of the gas-dynamical parameters in the shock layer near a cone, taking account of both approximations, is qualitatively similar to the behaviour of the corresponding parameters near a wedge.

As an illustration, a comparison of the position of the shock waves for a wedge and cone with the same expansion angle $2\alpha = 60°$ at $M_\infty = \infty$, $q = 0.5$ is drawn in Fig. 4. The shock waves for frozen and equilibrium flows are shown by the dotted and dash-dotted lines, respectively.

The pressure distribution along the wall of the wedge and the generatrix of the cone for these conditions is represented in Fig. 5. It is obvious that at the same activation energy the pressure on the wedge tends more rapidly to its equilibrium value than on the cone.

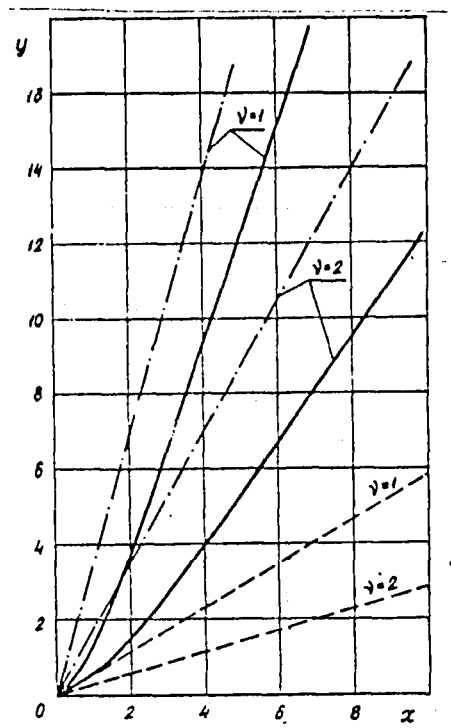

Fig. 4

Form of the shock wave for a wedge ($\nu = 1$) and a cone ($\nu = 2$) with expansion angle $2\alpha = 60°$, $M_\infty = \infty$, $q = 0.5$.

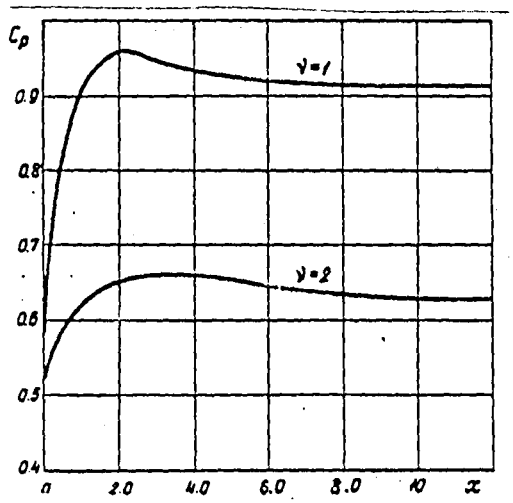

Fig. 5

Pressure coefficients for a wedge and a cone at $2\alpha = 60°$, $M_\infty = \infty$, $q = 0.5$.

In the case of $\beta = 0$, the pressure on the wedge and cone is calculated by the formulae:

$$C_{p_{кл.}} = \frac{p - p_\infty}{\rho_\infty V_\infty^2/2} = 2\sin^2\alpha\left\{1 + \frac{\gamma-1}{\gamma+1}\left[1 + \frac{2}{(\gamma-1)M_\infty^2\sin^2\alpha} + \right.\right.$$

$$\left.\left. + \frac{q}{\sin^2\alpha}\left(1 - e^{-x} + xe^{-x}\right)\right]\right\} \qquad (1.28)$$

$$C_{p_{кон}} = 2\sin^2\alpha\left\{1 + \frac{\gamma-1}{\gamma+1}\left[\frac{1}{4}\left(1 + \frac{2}{(\gamma-1)M_\infty^2\sin^2\alpha}\right) + \frac{q}{\sin^2\alpha}\left(\frac{5}{4} - \frac{2(1 - e^{-x} - xe^{-x})}{x^2} - \right.\right.\right.$$

$$\left.\left.\left. - \frac{(x^2+2x+2)(x^2-3x+3-3e^{-x}+x^2e^{-x}/2)}{x^4}\right)\right]\right\}, \qquad (1.29)$$

which convert to the known formulae for the adiabatic flow around a wedge or cone, if we put in them $q = 0$ (see [2]).

§ 2. Nonequilibrium flow of a fuel mixture of gases, caused by a piston moving with a high supersonic velocity

Similar to § 1, it is possible to investigate the problem of the motion of a mixture of gases, generated when a piston moves with a high supersonic velocity. The original system of equations in Lagrangian variables has the form:

$$\frac{\partial R}{\partial m} = \frac{1}{\rho R^{\nu-1}}$$

$$\frac{\partial^2 R}{\partial t^2} = -R^{\nu-1}\frac{\partial P}{\partial m}\,,$$

$$\frac{\partial P}{\partial t} = -K\beta^m P^n \rho^e \exp\left\{-\frac{E}{P/\rho}\right\}\,,$$

$$\frac{\partial}{\partial t}\left(\frac{P}{\rho^\gamma}\right) = -\rho^{1-\gamma}(\gamma-1)Q\frac{\partial \beta}{\partial t}\,, \qquad (2.1)$$

where γ – the initial distance of a particle of the gas, by which the shock wave did not pass yet, to the plane of the axis of symmetry;

Q – the quantity of heat released on complete combustion of a unit mass of the gas,

ρ^0 – density, P^0 – pressure of the unburned gas.

We shall introduce the parameter $\varepsilon = \frac{\gamma-1}{\gamma+1}$, following [2] we shall seek for the solution of (2.1) by the method of the boundary layer in the form of the following series:

$$R = R_0 + \varepsilon R_1 + O(\varepsilon^2)\,,$$

$$P = P_0 + \varepsilon P_1 + O(\varepsilon^2)\,,$$

$$\rho = \frac{\rho_0}{\varepsilon} + \rho_1 + O(\varepsilon)\,,$$

$$\beta = \beta_0 + \varepsilon\beta_1 + O(\varepsilon^2)\,. \qquad (2.2)$$

The boundary values for the zero terms are obtained by the analoguous expansion of the boundary values of the unknown functions. For the zero and first terms of series (2.2), we obtain certain systems of equations.

For the zero terms:

$$\begin{aligned}
&\frac{\partial R_0}{\partial m} = 0 \quad , \\
&\frac{\partial^2 R_0}{\partial t^2} = -R_0^{\nu-1}\frac{\partial P_0}{\partial m} \quad , \\
&\frac{\partial}{\partial t}\left(\frac{P_0}{\rho_0}\right) = -2Q\frac{\partial \beta_0}{\partial t} \quad , \\
&\frac{\partial \beta_0}{\partial t} = -\bar{K}\beta_0^{\gamma}\rho_0^{\alpha}\rho_0^{\varepsilon}\exp\left\{-\frac{E\varepsilon^{-1}}{P_0/\rho_0}\right\} \quad ,
\end{aligned} \tag{2.3}$$

where $\bar{K} = K\cdot\varepsilon^{-\ell}$. From (2.3), it follows that $R_0 = R_0(t)$. As $R_0(t)$, we shall take the law of motion of the shock wave. Then the equality $R_1 = 0$ is fulfilled on the shock wave. Let us turn from the Lagrangian variable m to the Lagrangian variable τ using the relation.

$$m = \frac{\rho^* R_0^{\nu}(\tau)}{\nu} \quad .$$

From this relation, it is obvious that τ is the time of passage of the shock wave by the particle with the coordinate m. The system of equations for the first terms has the following form:

$$\begin{aligned}
&\frac{\partial R_1}{\partial m} = \frac{1}{\rho_0 R_0^{\nu-1}} \quad , \\
&R_0^{\nu-1}\frac{\partial P_1}{\partial m} = (\nu-1)\frac{\ddot{R}_0}{R_0}R_1 - \frac{\partial^2 R_1}{\partial t^2} \quad , \\
&Q\frac{\partial \beta_1}{\partial t} = \frac{1}{2}\frac{\partial}{\partial t}\left[\frac{1}{\rho_0}\left(P_1 - P_0\frac{\rho_1}{\rho_0}\right) = \frac{P_0}{\rho_0}\right] - \frac{P_0}{\rho_0^2}\frac{\partial \rho_0}{\partial t} \quad , \\
&\frac{\partial \beta_1}{\partial t} = \frac{\partial \beta_0}{\partial t}\left[m\frac{\beta_1}{\beta_0} + n\frac{\rho_1}{\rho_0} + \ell\frac{\rho_1}{\rho_0} - \frac{E\varepsilon^{-1}}{P_0/\rho_0}\left(\frac{\rho_1}{\rho_0} - \frac{P_1}{P_0}\right)\right] .
\end{aligned} \tag{2.4}$$

Let us write the system for the zero and first terms in a dimensionless form:

$$\bar{K}^{*}=K\cdot\varepsilon^{-\ell}T\rho^{*\ell}(\rho^{*}a^{*2})^{n}\ ;\quad \bar{p}=\frac{p}{\rho^{*}a^{*2}}\ ;\quad \bar{Q}=\frac{Q}{a^{*2}}\ ;$$

$$\bar{E}=\frac{E}{a^{*2}}\ ;\quad \bar{\rho}=\frac{\rho}{\rho^{*}}\ ;\quad \bar{R}=\frac{R}{a^{*}T}\ ;$$

$$\bar{t}=\frac{t}{T}\ ;\quad \bar{\tau}=\frac{\tau}{T}\ ,$$

where T — a certain characteristic time. After simple conversions, the system for the "zero" terms will have the following form:

$$\bar{p}_{o}=\bar{R}_{o}^{2}+\frac{\bar{R}_{o}\cdot\ddot{\bar{R}}_{o}}{\nu}-\frac{\ddot{\bar{R}}_{o}}{\nu\bar{R}_{o}^{\nu-1}}\bar{R}^{\nu}(\bar{\tau})$$

$$\bar{\rho}_{o}=\left[\frac{\bar{p}_{o}}{\bar{c}(\bar{\tau})-(\gamma+1)\bar{Q}\beta_{o}}\right]^{1/\gamma}\ ,\ \text{where}\quad \bar{c}(\bar{\tau})=(\gamma+1)\bar{Q}+\bar{R}_{o}^{2}\left[1+\frac{2}{\gamma-1}\frac{1}{\bar{R}_{o}^{2}}\right]^{\gamma}$$

$$\frac{\partial\beta_{o}}{\partial\bar{t}}=-\bar{K}\beta_{o}^{m}\bar{p}_{o}^{n+e}\left[\bar{c}(\bar{\tau})-(\gamma+1)\bar{Q}\beta_{o}\right]^{-\frac{\ell}{\gamma}}\exp\left\{-\frac{\bar{E}\varepsilon^{-1}}{\bar{p}_{o}/\beta_{o}}\right\}$$

$$\bar{R}_{n}=\bar{R}_{o}-\varepsilon\frac{1}{\bar{R}_{o}^{\nu-1}(\bar{t})}\int_{o}^{\bar{t}}\frac{1}{\rho_{o}}\bar{R}_{o}^{\nu-1}(\bar{\tau})\dot{\bar{R}}_{o}(\bar{\tau})\,d\bar{\tau}\ . \qquad (2.5)$$

Here $\bar{R}_{n}$ — the law of the movement of the piston. The third and forth equations of (2.5) are an integral-differential system of equations with respect to the unknown functions β_{o} and $\bar{R}_{o}$. For solving this system, the approximate method of solution was used, which is algorithmically realized on the computer as follows: the iteration method was used, in which the value of $\bar{R}_{n}$ was taken as the zero approximation for $\bar{R}_{o}$; β_{o} was determined from the third equation, and then the following approximation for $\bar{R}_{o}$ was determined from the forth equation. The K approximation for $\bar{R}_{o}$ is expressed by the formula

$$\bar{R}_{o}^{(\kappa)}(\bar{t})=\bar{R}_{n}(\bar{t})+\varepsilon\frac{1}{(\bar{R}_{o}^{(\kappa-1)}(\bar{t}))^{\nu-1}}\int_{o}^{\bar{t}}\frac{1}{\bar{\rho}_{o}}\dot{\bar{R}}_{o}^{(\kappa-1)}(\bar{\tau})\left(\bar{R}_{o}^{(\kappa-1)}(\bar{\tau})\right)^{\nu-1}d\bar{\tau}\ .$$

Let us write the system for the zero and first terms in a dimensionless form:

$$\bar{R}^{*} = K \cdot \varepsilon^{-\ell} T \rho^{*\ell} (\rho^{*} a^{*2})^{n} \; ; \quad \bar{P} = \frac{P}{\rho^{*} a^{*2}} \; ; \quad \bar{Q} = \frac{Q}{a^{*2}} \; ;$$

$$\bar{E} = \frac{E}{a^{*2}} \; ; \quad \bar{\rho} = \frac{\rho}{\rho^{*}} \; ; \quad \bar{R} = \frac{R}{a^{*} T} \; ;$$

$$\bar{t} = \frac{t}{T} \; ; \quad \bar{\tau} = \frac{\tau}{T} \; ,$$

where T — a certain characteristic time. After simple conversions, the system for the "zero" terms will have the following form:

$$\bar{P}_{0} = \bar{R}_{0}^{2} + \frac{\bar{R}_{0} \cdot \ddot{\bar{R}}_{0}}{\nu} - \frac{\ddot{\bar{R}}_{0}}{\nu \bar{R}_{0}^{\nu-1}} \bar{R}^{\nu}(\bar{\tau})$$

$$\bar{\rho}_{0} = \left[\frac{\bar{P}_{0}}{\bar{c}(\bar{\tau}) - (\gamma+1)\bar{Q}\beta_{0}} \right]^{1/\gamma} \; , \text{ where } \; \bar{c}(\bar{\tau}) = (\gamma+1)\bar{Q} + \bar{R}_{0}^{2} \left[1 + \frac{2}{\gamma-1} \frac{1}{\bar{R}_{0}^{3}} \right]^{\gamma}$$

$$\frac{\partial \beta_{0}}{\partial \bar{t}} = -\bar{K} \beta_{0}^{m} \bar{P}_{0}^{n+\ell} \left[\bar{c}(\bar{\tau}) - (\gamma+1)\bar{Q}\beta_{0} \right]^{-\frac{\ell}{\gamma}} \exp\left\{ - \frac{\bar{E}\varepsilon^{-1}}{\bar{P}_{0}/\beta_{0}} \right\}$$

$$\bar{R}_{n} = \bar{R}_{0} - \varepsilon \frac{1}{\bar{R}_{0}^{\nu-1}(\bar{t})} \int_{0}^{\bar{t}} \frac{1}{\bar{\rho}_{0}} \bar{R}_{0}^{\nu-1}(\bar{\tau}) \dot{\bar{R}}_{0}(\bar{\tau}) d\bar{\tau} \; . \qquad (2.5)$$

Here $\bar{R}_{n}$ — the law of the movement of the piston. The third and forth equations of (2.5) are an integral-differential system of equations with respect to the unknown functions β_{0} and $\bar{R}_{0}$. For solving this system, the approximate method of solution was used, which is algorithmically realized on the computer as follows: the iteration method was used, in which the value of $\bar{R}_{n}$ was taken as the zero approximation for $\bar{R}_{0}$; β_{0} was determined from the third equation, and then the following approximation for $\bar{R}_{0}$ was determined from the forth equation. The K approximation for $\bar{R}_{0}$ is expressed by the formula

$$\bar{R}_{0}^{(\kappa)}(\bar{t}) = \bar{R}_{n}(\bar{t}) + \varepsilon \frac{1}{(\bar{R}_{0}^{(\kappa-1)}(\bar{t}))^{\nu-1}} \int_{0}^{\bar{t}} \frac{1}{\bar{\rho}_{0}} \dot{\bar{R}}_{0}^{(\kappa-1)}(\bar{\tau}) \left(\bar{R}_{0}^{(\kappa-1)}(\bar{\tau}) \right)^{\nu-1} d\bar{\tau} \; .$$

The iteration process was cut off on achievement of the condition:

$$|\bar{R}_0^{(\kappa)}(\bar{t}) - \bar{R}_0^{(\kappa-1)}(\bar{t})| < \delta \cdot \bar{R}_n \ ,$$

where δ — a certain constant.

After that, the third equation is solved with the found $\bar{R}_0^{(K)}$, which is taken as the law of motion of the shock wave, i.e. $\beta_0^{(K)}$ is found, and then the remaining terms of the zero approximation are found.

The system of equations of the first approximation has the following forms:

$$\bar{R}_1 = -\frac{1}{\bar{R}_0^{\nu-1}(\bar{t})}\int_0^{\bar{t}} \frac{1}{\bar{\rho}_0}\bar{R}_0^{\nu-1}(\bar{\tau})\,d\bar{\tau} \ ,$$

$$\bar{P}_1 = -(\gamma-1)\frac{\ddot{\bar{R}}_0}{\bar{R}_0^{\nu}}\int_{\bar{\tau}}^{\bar{t}} \bar{R}_1\cdot\dot{\bar{R}}_0(\bar{\tau})\bar{R}_0^{\nu-1}(\bar{\tau})\,d\bar{\tau} + \frac{1}{\bar{R}_0^{\nu-1}}\int_{\bar{\tau}}^{\bar{t}} \frac{\partial^2\bar{R}_1}{\partial\bar{t}^2}\dot{\bar{R}}_0(\bar{\tau})\,d\bar{\tau} - \left[\frac{1}{\Gamma} - \dot{\bar{R}}_0^2(\bar{t})\right] \ ,$$

$$\frac{\bar{P}_1}{\bar{\rho}_0} = \left(\gamma\frac{\bar{P}_0}{\bar{\rho}_0}\right)^{-1}\left[\frac{\bar{P}_1}{\bar{\rho}_0\Gamma} - \frac{\bar{P}_1}{\bar{\rho}_0\Gamma}\Big|_{\bar{t}=\bar{\tau}} - (\gamma+1)^2\bar{Q}\int_{\bar{\tau}}^{\bar{t}}\frac{\partial\beta_0}{\partial\bar{t}}m\bar{\rho}_0\,d\bar{t} + \bar{Q}(\gamma+1)\beta_1\right] \ ,$$

$$\frac{\partial\beta_1}{\partial\bar{t}} = \frac{\partial\beta_0}{\partial\bar{t}}\left[m\frac{\beta_1}{\beta_0} + \left(n + \frac{\bar{E}\varepsilon^{-1}}{\bar{P}_0/\bar{\rho}_0}\right)\frac{\bar{P}_1}{\bar{P}_0} + \left(\ell - \frac{\bar{E}\varepsilon^{-1}}{\bar{P}_0/\bar{\rho}_0}\right)\left\{\left(\gamma\frac{\bar{P}_0}{\bar{\rho}_0}\right)^{-1}\left[\frac{\bar{P}_1}{\bar{\rho}_0\Gamma} - \frac{\bar{P}_1}{\bar{\rho}_0\Gamma}\Big|_{\bar{t}=\bar{\tau}} - \right.\right.\right.$$

$$\left.\left.\left. - \bar{Q}(\gamma+1)^2\int_{\bar{\tau}}^{\bar{t}}\frac{\partial\beta_0}{\partial\bar{t}}m\bar{\rho}_0\,d\bar{t} + \bar{Q}(\gamma+1)\beta_1\right]\right\}\right] \ .$$

For simplicity, calculations were carried out for the case of piston movement with a constant velocity.

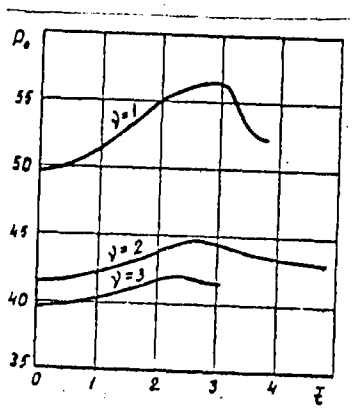

Fig. 6

Dependence of the pressure on the piston upon the dimensionl time $\bar{t}$. ν = 1, 2, 3 — plane, cylindrical and spherical cases, respectively.

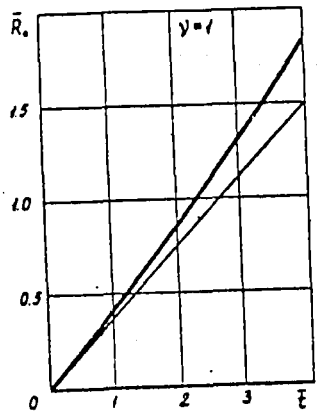

Fig. 7

Law of motion of a plane piston.

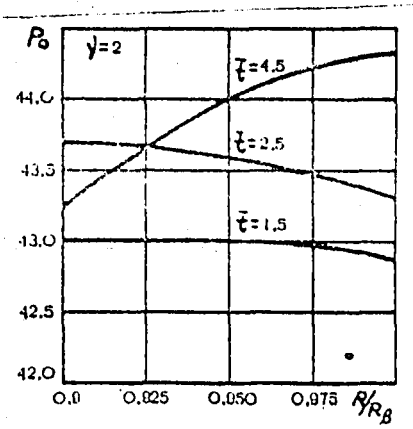

Fig. 8

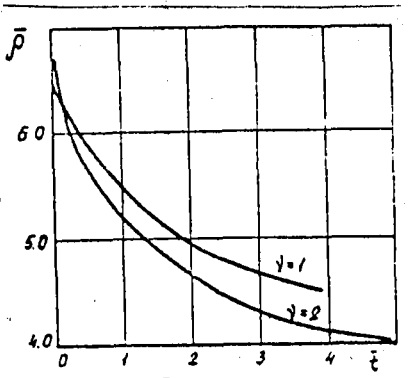

Fig. 9

Dependence of the density on the piston upon time.

The graph of the distribution of the pressure on the piston at different ν values is shown in Fig. 6. The graph of the law of motion of the shock wave at different ν values — in Fig. 7. The distribution of the pressure at a fixed instant on the $\bar{R}$ coordinate — in Fig. 8. The heat distribution on the piston at different ν values — in Fig. 9.

The problem was solved for the following numerical values of the parameters

$$m=2;\ \ell=n=0;\ \dot{\bar{R}}_n=6;\ \bar{Q}=30;\ \bar{E}=10;\ T=10^{-9}\ \text{sec}.$$

For the investigated case ($R_o = Dt$), from (2.3) we have:

$$P_o=\rho^o\dot{R}_o^2+\rho^o\frac{R_o\ddot{R}_o}{\nu}-\frac{\ddot{\bar{R}}_o}{\bar{R}_o^{\nu-1}}m=\rho^o D^2,$$

$$\frac{P_o}{\rho_o}=-2Q\beta_o+C(\tau),\ \text{where}\ C(\tau)=2Q+\dot{R}_o^2\left(1+\frac{2}{\gamma-1}\frac{a^2}{\dot{R}_o^2}\right)$$

$$\rho_o=P_o/(C(\tau)-2Q\beta_o).$$

Substituting ρ_o in the forth equation of (2.3), we iobtain an equation for the determination of β_o

$$\frac{\partial\beta_o}{\partial t}=-\bar{K}\beta_o^m P_o^{n+\ell}(C-2Q\beta_o)^{-\ell}\exp\left\{-\frac{E\varepsilon^{-1}}{C-2Q\beta_o}\right\}.$$

The boundary condition for the shock wave is as follows:

$$t=\tau\qquad \beta_o(\tau,\tau)=1$$

Since $R_o = Dt$, then $C(\tau)$ is a constant quantity. It is obvious from the equation that $\beta_o=\beta_o(t-\tau)$ therefore all the values of the zero approximation are functions of $t-\tau$. In the zero form β_o is expressed by the following relation:

$$\int_1^{\beta_o}\frac{\exp\left\{-\frac{E\varepsilon^{-1}}{C-2Q\beta_o}\right\}}{\beta_o^m(C-2Q\beta_o)^{-\ell}}d\beta_o=-\bar{K}\int_\tau^t P_o^{n+\ell}dt. \qquad (2.6)$$

At a fixed τ and $t \longrightarrow \infty$ the integral on the right side is dropped, therefore the integral on the left is also dropped. At $m \geqslant 1$ (this case will be investigated) this is possible when at a fixed τ and $t \to \infty$ we have $\beta_0 \to 0$, i.e. any particle burns for an infinite time. From the fact that $\beta_0 = f(t-\tau)$, it follows that for any particle the process of combustion will equally proceed if only we take $t = \tau$ as the start of the account of time for the particle. As the integral on the right side of (2.6) is not taken in an evident form, then for finding β_0 we take advantage of the approximation method, using the following consideration. As $\beta_0(t-\tau) \to 0$ at a fixed value of τ and $t \longrightarrow \infty$, then it follows that for any value of τ and φ, there is such a value of t that at $t > \tau + t'$ it follows that $\beta_0 < \varphi$, t' does not depend on τ and $\beta_0(\tau, \tau + t') = \varphi$. In particular, we take $\varphi = \varepsilon^2$. Therefore, at $t > t' + \tau$ it is possible to neglect β_0 in comparison with 1. Then for such values of t we obtain the following equation for the determination of β_0

$$\frac{\partial \beta_0}{\partial t} = -\bar{K} \beta_0^m \rho_0^n \rho_0^\ell \exp\left\{-\frac{E\varepsilon^{-1}}{\tau}\right\} . \qquad (2.7)$$

here $\rho_0 = \text{const}$. Integrating equation (2.7), we have:

$$\beta_0 = \left\{\left[\bar{K} \rho_0^{n+\ell} (t-\tau) + z\right] \frac{m-1}{C^\ell \exp\left\{\frac{E\varepsilon^{-1}}{C}\right\}} + \varphi^{1-m}\right\}^{\frac{1}{1-m}} .$$

here z - a known function of t'. At the interval $\tau \leqslant t \leqslant \tau + t'$ we approximate β_0 to a parobla:

$$\beta_0 = a(t-\tau)^2 + b(t-\tau) + z .$$

a, b, Z, t' are unknowns. We designate

$$\bar{K} \rho_0^n \rho_0^\ell \exp\left\{-\frac{E\varepsilon^{-1}}{C}\right\} = \zeta .$$

Then the four conditions for the determination of the four unknown constants take the form:

$$1)\ t = \tau \Rightarrow \beta_0 = 1 ,$$

$$2)\ t = \tau + t' \Rightarrow \beta_0 = \varphi ,$$

$$3)\ \left.\frac{\partial \beta_0}{\partial \tau}\right|_{t=\tau+t'} = -\zeta \varphi^m ,$$

$$4)\ \left.\frac{\partial \beta_0}{\partial t}\right|_{t=\tau} = \left.-\bar{K} \rho_0^n \rho_0^\ell \exp\left\{-\frac{E\varepsilon^{-1}}{C - 2Q\beta_0}\right\}\right|_{\beta_0 = 1} .$$

moreover, $t' = \tau + \tau_0$, where τ_0 — a known constant.

From equation (2.4), it follows that at $\nu = 1$ the following relation is fulfilled:

$$\rho_1 = 2\rho^\circ Q(\beta_0 - 1) - \rho^\circ - \rho^\circ \mathcal{D}^2 .$$

The third equation of (2.4) is integrated at once if the following equality is taken into account:

$$\frac{\rho_0}{\rho_0^2}\frac{\partial \rho_0}{\partial t} = 2Q\frac{\partial \beta_0}{\partial t} .$$

so that

$$\frac{1}{2}\left[\frac{1}{\rho_0}\left(\rho_1 - \rho_0\frac{\rho_1}{\rho_0}\right) - \frac{\rho_0}{\rho_0}\right] - 2Q\beta_0 = -Q\beta_1 + f_1(\tau) ,$$

where

$$f_1(\tau) = \frac{1}{2}\left[\left(\frac{\rho_1}{\rho_0}\right)_{t=\tau} - \left(\frac{\rho_0}{\rho_0}\right)_{t=\tau}\right] - 2Q .$$

Let us express ρ_1 from the given relation in β_1 and substitute the known "zero" and "first" terms in the forth equation of (2.4). We then obtain an equation for the determination of β_1

$$\frac{\partial \beta_1}{\partial t} = \frac{\partial \beta_0}{\partial t}\left[\frac{m}{\beta_0} + \left(\ell - E\varepsilon^{-1}/\frac{\rho_0}{\rho_0}\right)\frac{\rho_0}{\rho_0} 2Q\right]\beta_1 -$$

$$- \frac{\partial \beta_0}{\partial t}\left\{\frac{\rho_1}{\rho_0}(n+\ell) + \left(\ell - E\varepsilon^{-1}\frac{\rho_0}{\rho_0}\right)\cdot\left[\frac{\rho_0}{\rho_0}\frac{\rho^\circ}{\rho^\circ \mathcal{D}^2}(c - 2Q) + 1\right]\right\} .$$

The solution of this equation at $\beta_1 /_{t=\tau} = 0$ has the form

$$\beta_1 = C_1(t,\tau)\frac{\partial \beta_0}{\partial t} ,$$

where

$$C_1(t,\tau) = -\frac{\ell+n}{\rho_0}(2\rho^\circ Q + \rho^\circ + \rho^\circ \mathcal{D}^2)(t-\tau) + \ell(t-\tau) + \frac{\ell+n}{\rho_0}\rho^\circ 2Q \cdot$$

$$\times \int_\tau^t \beta_0\, dt - E\varepsilon^{-1}\int_\tau^t \frac{\rho_0}{\rho_0}\, dt + \ell(c-2Q)\int_\tau^t \frac{\rho_0}{\rho_0}\, dt - (c-2Q)E\varepsilon^{-1}\int_\tau^t \left(\frac{\rho_0}{\rho_0}\right)^2 dt .$$

Here the formula for β_1 is not given because of its tediousness. With respect to β_1 we only mention that as $\frac{\partial \beta_0}{\partial t} = -\varkappa \beta_0^m$ at $t > \tau + \tau_0$ then $\beta_1 \to 0$ for any fixed τ and $t \to \infty$. The law of motion of the piston $R_n(t)$ is determined as follows:

$$R_n(t) = (R_0 + \varepsilon R_1)_{\tau=0} = \mathcal{D}t - \varepsilon \frac{c}{\mathcal{D}} t + \varepsilon \frac{2Q}{\mathcal{D}} \int_0^t \beta_0(t,\tau)\, d\tau$$

$$\lim_{t\to\infty} R_n(t) = \mathcal{D} - \varepsilon \frac{c}{\mathcal{D}} = const .$$

Let us consider now some qualitative peculiarities of the found solution. We shall show that after the lapse of time τ_0 from the beginning of combustion, the characteristics of flow with an accuracy up to ε^2 become constants equal for all the particles:

$$\rho_0 = \rho^\circ \mathcal{D}^2 ; \qquad \rho_1 = -\rho^\circ - \rho^\circ \mathcal{D}^2 - 2\rho^\circ Q + O(\varepsilon^2) ;$$

$\beta_0 < \varepsilon^2$ at $t > \tau + \tau_0$ and $\beta_1 = O(\varepsilon^2)$; $\rho_0 = \frac{\rho_0}{c} + O(\varepsilon^2)$;

$\rho_1 = const + O(\varepsilon^2)$; because $\rho_1 = f(\beta_1, \beta_0, \rho_0, \rho_1)$;

$u(\tau,t) = \frac{\partial R}{\partial t} = \mathcal{D} - \varepsilon \frac{c}{\mathcal{D}} + \varepsilon \frac{2Q}{\mathcal{D}^2} \beta_0$ at $t > \tau + \tau_0$, i.e.

$u(\tau,t) = \mathcal{D} - \varepsilon \frac{c}{\mathcal{D}} + O(\varepsilon^2)$.

It should be noticed that since all the functions depend only on the argument $t - \tau$, then after the combustion of the particles the flow (with an accuracy up to ε^2) will be isentropic. The equation of the line in the plane R, t, by the attainment of which all the characteristics of flow become constants with an accuracy up to ε^2, is written in the form:

$$\begin{cases} R = R(t,\tau) \\ t = \tau + \tau_0 \end{cases} \quad \text{or} \quad R = R(t, t-\tau_0) , \quad \text{from which}$$

$$R = \mathcal{D}t + \varepsilon \frac{2Q}{\mathcal{D}^2}\left(\frac{\alpha}{3}\tau_0^3 + \frac{\beta}{2}\tau_0^2 + \tau_0\right) - \varepsilon \frac{c}{\mathcal{D}} \tau_0 .$$

The given line (we shall call it AB) is parallel, in the plane R, t, to the line representing the shock wave (Fig. 10). In the region lying on the right side of AB, it is possible to establish an isentropic flow, assuming that the gas is definitely burnt. In order that the solution can be plotted in the region ABC, realization of one of the following conditions is necessary:

1) The line AB must be a characteristics as the characteristics in the region ABC must not intersect the line AB, because all the functions are constants in it. The relation:

$$R = u + a \ ,$$

is realized for the characteristics in the region ABC. Hence, it follows that on the line R = D:

$$D = u + a \quad \text{and}$$

$$a_{AB} = \sqrt{\gamma \frac{P'}{\rho}} = \sqrt{\gamma}\left(1 + \frac{\varepsilon}{2}\right)\sqrt{\varepsilon C} + O(\varepsilon^2)$$

$$u_{AB} = D - \varepsilon \frac{C}{D} \ ,$$

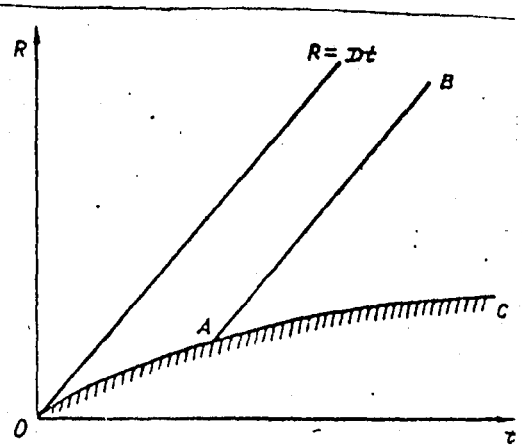

Fig. 10

where a— the velocity of sound. Thus, the velocity of the shock wave, at which the line AB is a characteristic, is uniquely determined:

$$D_+^2 = \frac{(\gamma - 1)\left[2Q + \frac{2}{\gamma - 1} a^{o2}\right]}{2\gamma^2 + 1 - \gamma} \qquad (2.8)$$

In such a case, instead of the interval AC, it is possible to take another law for the motion of the piston, and the solution in the region ABC will be a simple rarefaction wave;

2) The line AB may not be a characteristic. It is possible to plot the flow in the region ABC by the use of the characteristics, and as the piston in the case of $t > \tau_0$ moves with a constant velocity with an accuracy up to ε^2, then this flow will be a progressive one. In this case the characteristics will intersect the line AB. In order that the inclination of these characteristics was larger than the inclination of AB, it is necessary that the following inequality is realized:

$$D < \frac{dR}{dt} = u + a \qquad \text{or} \qquad D^2 \geq \frac{(\gamma-1)\left[2Q + \frac{2}{\gamma-1}a_0^2\right]}{2\gamma^2+1-\gamma} \qquad D^2 \geq D_+^2, \text{ i.e.}$$

In the present case there is an analogy with the detonations, when the mixture instantly burns in the shock wave. From the great number of possibilities of the propagation velocities of the detonation wave, given by detonation adiabat, the velocity of the propagation of the wave of Ch.-J. is minimum. Therefore, it is possible to make an analogy between the velocity of Ch.-J, and the velocity of the shock wave, which is given by (2.8). Since in the case of $K \to \infty$ the time of the combustion of the mixture approaches zero, then the obtained solution must change to the solution of the problem of the motion of a plane detonation wave, and the velocity determined by (2.8) must change to the velocity of the wave of Ch.-J. In the case when the counter-pressure is not taken into account we have:

$$D_y^2 = 2(\gamma^2-1)Q .$$

In our case, the velocity of the wave is calculated as follows:

$$D_*^2 = \frac{2(\gamma^2-1)Q}{2\gamma^2+1-\gamma} \quad \text{and} \quad \frac{D_y^2}{D_*^2} = (\gamma+1)(2\gamma^2+1-\gamma)$$

where

$$\gamma \to 1: \quad \frac{D_y}{D_*} \to 2 .$$

This discrepancy shows that the method used for the solution of the problem is, generally speaking, unfit when the velocities of motion of the shock waves are near to the velocity of the wave of Ch.-J. For the highly supercompressed waves, the heat release exerts a lesser influence on the character of flow. Therefore, the solution obtained by the method of the boundary layer [2] for such velocities of propagation of the shock wave will give smaller difference from the exact solution with a detonation. The velocity obtained after the combustion of a substance can be used for the calculation of the limits of applicability of the boundary layer method in the case of the solution of a problem with chemical reactions. Thus, it is sufficient to compare this velocity with the velocity formed behind the ordinary detonation wave. The velocity behind the detonation wave in the exact solution is:

$$u = \frac{D(1-\varepsilon) + D\sqrt{(1-\varepsilon)^2 - \frac{8Q}{D^2}\varepsilon}}{2} \qquad (2.9)$$

The value of u_y corresponds to the wave of Ch.–J.

$$u_y = \frac{D_y(1-\varepsilon)}{2} .$$

In the case under consideration the velocity of the gas after its combustion, with an accuracy up to ε^2, is determined by the formula:

$$u_+ = D(1-\varepsilon) - \varepsilon\frac{2Q}{D} . \qquad (2.10)$$

It is easy to see that in this case when:

$$\frac{\gamma-1}{\gamma+1}\left(\frac{8Q}{D^2} + \frac{\gamma+3}{\gamma+1}\right) << 1 \qquad (2.11)$$

formulae (2.9) and (2.10) coincide with an accuracy up to ε^2, i.e. the velocities behind the detonation wave and behind the region in which the mixture burns asymptotically approach each other at $\gamma \to 1$. Since $\gamma \leq 1.4$ in problems of the considered type, then $\varepsilon \leq \frac{1}{6}$. Thus, inequality (2.11) can be considered as the criterion of the applicability of the boundary layer method [2] in solving problems of the considered class.

In conclusion, it is worth noting that the law of propagation of the shock wave in the case of spherical and cylindrical symmetry, corresponding to the steady mode (R_n = const), has the form:

$$D^2 = \frac{2Q(\gamma-1)}{(\gamma+1)\nu - (\gamma-1)} \quad \text{and} \quad \frac{D_y^2}{D^2} = (\gamma+1)^2\left(\nu - \frac{\gamma-1}{\gamma+1}\right) .$$

Thus, the deviation from the mode of Ch.–J. increases with the increase of the value of ν.

References

1. Tkalenko, R.A. "Sverkhzvukovoe neravnovesnoe techenie gaza okolo tonkikh tel vrashcheniya" (Supersonic nonequilibrium flow of gas near thin rotation bodies).--- PMTF, No. 2, 1964.

2. Chernyi, G.G. "Techenie gaza s bol'shoi sverkhzvukovoi skorost'yu" (Flow of gas with high supersonic velocity).--- Fizmatgiz, 1959.

3. Zel'dovich, Ya.B. and A.S. Kompaneets. "Teoriya detonatsii" (Theory of detonation).--- Gostekhizdat, Moskva, 1955.

4. Gradshtein, I.S. and I.M. Ryzhik. "Tablitsy integralov, summ, ryadov i proizvedenii" (Tables of integrals, sums, series and products).--- Fizmatgiz, 1962.

5. Moore, F.K. and W.E. Gibson. Propagation of weak disturbances is a gas subject to relaxation effects. JAS, No. 2, 1960.

6. Vincenti, W.G. Nonequilibrium flow over a wavy wall. J. Fluid Mech., Vol. 6, p. 4, 1959.

7. Clarke J.F. Relaxation effects on the flow over slender bodies. J. Fluid Mech., Vol. 11, p. 4, 1961.

8. L. and R. Hypersonic nonequilibrium flow near thin bodies. J. Fluid Mech., v. 22, p. 3, 1965.

LINEARIZED SUPERSONIC NONEQUILIBRIUM FLOW OF A FUEL MIXTURE OF GASES NEAR A WEDGE

By

S.M. Gilinskii

Let us consider a supersonic flow of a fuel mixture around a wedge. We shall assume that the maximum quantity of heat, which may be released as a result of a chemical reaction, is much smaller than the total enthalpy of the mixture in the incident flow. In this case, the nonequilibrium flow will slightly differ from the adiabatic flow near the wedge, and the problem of the flow around can be solved analytically in a linear approximation.

If we consider the profile near to the wedge, the disturbances caused by the bend of the profile will interact with the disturbances related to the nonequilibrium release of heat in the flow. In the linear approximation, the total disturbance is determined by a simple superposition of these disturbances. Therefore it is sufficient to study independently the two problems of the nonequilibrium flow around the wedge and the adiabatic flow around the profile near to the wedge.

The first problem was investigated in works [1-3, 6, 7], the second- in works [4, 5, 8, 9].

The solution of the problem of a flow of a fuel mixture around a wedge is given below, taking into account the proceeding of one irreversible exothermic reaction. In the general case the solution is presented in the form of a series. For certain particular values of the order of the reaction, this series is summed up, and the solution is expressed by finite algebraic functions. The latter enabled to analyze the influence of the different laws of supply of heat to the gas on the character of the flow behind the shock wave. In particular, it is discovered that the solution may have an oscillatory character. The amplitude and frequency of these oscillations decrease downstream. In the extreme case of hypersonic flow around a thin wedge, the qualitative character of the solution essentially depends on the order m of the reaction. Thus at $m = 0$ and $M_\infty = \infty$, $\gamma \to 1$, $(\gamma - 1)\, Q \longrightarrow C$, the amplitude and frequency of these oscillations increase. The amplitude of the oscillations approaches a finite limit, and the frequency approaches infinity. In the case of $m = \frac{1}{2}, 2/3$, the amplitude of the oscillations approaches zero.

It is convenient to write the system of the gas-dynamical equations in the Cartesian coordinates x_1, y_1 (Fig. 1).

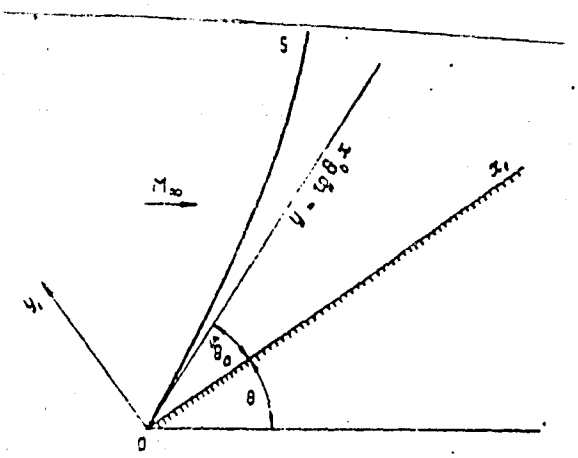

Fig. 1

Coordinate system and designations

Let the parameters with the index "0" correspond to the adiabatic (frozen) flow near the wedge. We represent the unknown functions in the form:

$$u_1(x_1, y_1) = u_0\left[1 + u(x_1, y_1)\right],$$

$$v_1(x_1, y_1) = u_0 v(x_1, y_1),$$

$$p_1(x_1, y_1) = p_0 + \rho_0 u_0^2 p(x_1, y_1),$$

$$\rho_1(x_1, y_1) = \rho_0\left[1 + \rho(x_1, y_1)\right], \tag{1}$$

$$\beta_1(x_1, y_1) = \beta_0(x_1, y_1)\left[1 + \beta(x_1, y_1)\right],$$

where the index "1" is written for the parameters of the unknown disturbed flow, and the functions of the disturbances are designated without index.

We shall model the kinetices of the chemical reactions by one reaction:

$$\frac{d\beta}{dt} = -L\beta^m \rho^{m-1} \exp\left(-\frac{E}{RT}\right),$$

where β — the relative concentration of the original reacting components of the mixture, m — the order of the reaction, P — pressure, T — temperature, E — activation energy, R — the universal gas constant, L — reaction rate constant.

Substituting (1) in the system of the gas-dynamical equations and neglecting the terms of second order of smallness with respect to the disturbances, we obtain the following system of linear equations:

$$\rho_0 \frac{\partial u}{\partial x_1} + u_0 \frac{\partial \rho}{\partial x_1} + \rho_0 \frac{\partial v}{\partial y_1} = 0 \quad ,$$

$$\frac{\partial u}{\partial x_1} + \frac{\partial \rho}{\partial x_1} = 0 \quad ,$$

$$\frac{\partial v}{\partial x_1} + \frac{\partial \rho}{\partial y_1} = 0 \quad ,$$

$$M^2 \frac{\partial \rho}{\partial x_1} + \frac{\partial v}{\partial y_1} + q_1 \frac{\partial \beta_0}{\partial x_1} = 0 \quad , \qquad (2)$$

where

$$M^2 = M_0^2 - 1 \quad , \quad q_1 = \frac{(\gamma-1)Q}{a_0^2}$$

M_0 — the Mach number, a_0 — the velocity of the sound of the undisturbed flow behind the shock wave.

Owing to the assumption of the smallness of the dimensionless parameter q_1, the system of equations (2) contains a derivative of concentration only $\beta_0(x_1, y_1)$ which is determined independently from the parameters of the disturbance, and it is a function of the undistrubed flow.

$$u_0 \frac{\partial \beta_0}{\partial x_1} = -L \beta_0^m \rho_0^{m-1} \exp\left(-\frac{E' \rho_0}{\rho_0}\right) . \qquad (3)$$

The boundary conditions in the linear theory are set at the boundary of the undisturbed flow, i.e.

at $y_1 = 0 \quad , \quad v = 0 \qquad (4)$

at $y_1 = tg\,\theta_0 x_1 \quad , \quad x > 0$

$$u = K_u f'(x_1) \quad , \quad v = K_v f'(x_1) \quad , \quad p = K_p f'(x_1) \quad ,$$

$$\rho = K_\rho f'(x_1) \quad , \quad \beta_0 = 1 \quad . \qquad (5)$$

Here $y_1 = tg\,\theta_0\, x_1 + f(x_1)$ the equation of the disturbed shock wave, K_u, K_v, K_ρ, K_p —known functions of the Mach number M_∞, wedge angle θ and the adiabatic index γ, which are determined from the linearized system of the relations in the shock wave.

For example:

$$K_p = \frac{2\gamma M_\infty^2 \cos^2\theta_0 \sin(\theta_0+\theta)}{2\gamma M_\infty^2 \sin^2(\theta_0+\theta)-(\gamma-1)} .$$

We introduce the dimensionless independent variables x, y as follows:

$$x_1 = \frac{u_0 \exp(E'\rho_0/p_0)}{L\rho_0^{m-1}} , \quad y_1 = \frac{u_0 \exp(E'\rho_0/p_0)}{L\rho_0^{m-1}} . \qquad (6)$$

Integrating equation (3) taking account of the boundary condition (5), we get:

$$\beta_0 = \left[1-(m-1)(y\,ctg\,\theta_0 - x)\right]^{\frac{1}{1-m}} \qquad (7)$$

The order m of the reaction determines the different laws of supply of heat to the gas. In the case of $m \geqslant 1$, the width of the zone of the reaction extends to infinity and, according to (7), the profile of the concentration β_0 is a continuous function. At $m < 1$ the reaction ends at a finite distance. The profile of the concentration as a function of the value of m may have a rupture in the end of the zone of the heat release. This rupture is either a discontinuity or the curvature, or of the leading derivatives (Fig. 2).

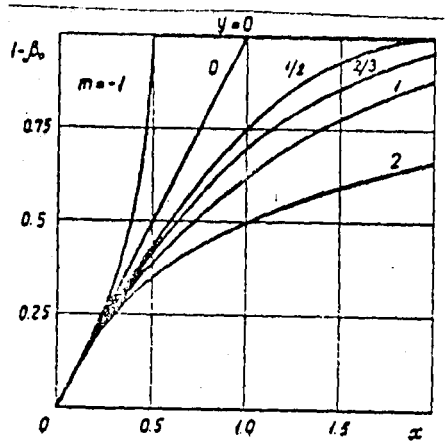

Fig. 2

Distribution of the concentration β_0 along the line of flow; m— order of the reaction.

For convenience, we determine the concentration by the function $\beta_0(x,y)$ as follows:

$$B_0(x,y)=\begin{cases}\left[1-(m-1)(y\operatorname{ctg}\theta_0-x)\right]^{\frac{1}{1-m}} & \text{at } y\operatorname{ctg}\theta_0-x\le\frac{1}{m-1}\\ 0 & \text{at } y\operatorname{ctg}\theta_0-x\ge\frac{1}{m-1}\end{cases} \qquad (8)$$

Excluding the density ρ and velocity u from the system of equations (2), we obtain nonhomogeneous wave equations for the determination of the components p and v.

$$\mu^2\frac{\partial^2 v}{\partial x^2}-\frac{\partial^2 v}{\partial y^2}=q_1\frac{\partial^2 B_0}{\partial x\,\partial y}=-q_1 m\operatorname{ctg}\theta_0 B_0^{2m-1}$$

$$\mu^2\frac{\partial^2 p}{\partial x^2}-\frac{\partial^2 p}{\partial y^2}=-q_1\frac{\partial^2 B_0}{\partial x^2}=-q_1 m B_0^{2m-1} \qquad (9)$$

Solving equations (9) and taking account of (2), the functions will be:

$$v=\frac{q_1\operatorname{ctg}\theta_0}{\operatorname{ctg}^2\theta_0-\mu^2}B_0(y\operatorname{ctg}\theta_0-x)+F(x+\mu y)-G(x-\mu y),$$

$$p=\frac{q_1}{\operatorname{ctg}^2\theta_0-\mu^2}B_0(y\operatorname{ctg}\theta_0-x)-\frac{1}{\mu}\left[F(x+\mu y)+G(x-\mu y)\right]. \qquad (10)$$

For the determination of the unknown functions F and G, we use the boundary conditions (4) and (5). From condition (5) for the shock wave it is possible to write, in particular, the following equations:

$$p=\Delta v \quad , \quad p=\delta u$$

$$\Delta=\frac{K_p}{K_v}=\frac{2\cos(\theta_0+\theta)\sin\theta_0}{\cos(\theta+2\theta_0)+\cos\theta/M_\infty^2\sin^2(\theta_0+\theta)}$$

$$\delta=\frac{K_p}{K_v}=\frac{2\cos(\theta_0+\theta)\sin\theta_0}{-\sin(\theta+2\theta_0)+\sin\theta/M_\infty^2\sin^2(\theta_0+\theta)}. \qquad (11)$$

Conditions (4) and (11) give the following system of functional equations:

$$\frac{q_1 \operatorname{ctg}\theta_0}{\operatorname{ctg}^2\theta_0 - \mu^2} B_0(y\operatorname{ctg}\theta_0 - x) + F(x) - G(x) = 0 ,$$

$$\frac{q_1 \mu(1-\Delta\operatorname{ctg}\theta_0)}{\operatorname{ctg}^2\theta_0 - \mu^2} - F[(\operatorname{ctg}\theta_0 + \mu)y](1+\Delta\mu) - G[(\operatorname{ctg}\theta_0 + \mu)y](1-\Delta\mu) = 0 . \qquad (12)$$

Excluding function G from this system, we obtain one functional equation for the determination of F:

$$F(\xi) - \lambda F(K\xi) = q_1 \left[\frac{\lambda \operatorname{ctg}\theta_0 B_0(K\xi)}{\operatorname{ctg}^2\theta_0 - \mu^2} + \frac{\mu(1-\Delta\operatorname{ctg}\theta_0)}{(1+\Delta\mu)(\operatorname{ctg}^2\theta_0 - \mu^2)} \right] , \qquad (13)$$

where

$$\lambda = -\frac{1-\Delta\mu}{1+\Delta\mu} , \quad K = \frac{\operatorname{ctg}\theta_0 - \mu}{\operatorname{ctg}\theta_0 + \mu} = \frac{\sin(\alpha - \theta_0)}{\sin(\alpha + \theta_0)}$$

$$\alpha = \arcsin 1/M_0 .$$

The functional equation of the form (13) was studied in a most detailed fashion in work [4]. The parameter λ is called the coefficient of reflection of the low disturbances from the shock wave, and it is equal to the ratio of the amplitude of the disturbance of the pressure reflected from the shock wave (along the characteristic $x + \mu y = \text{const}$) to the amplitude of the incident disturbance of the pressure (along the characteristic $x - \mu y = \text{const}$). The absolute value of the reflection coefficient λ does not exceed the unity. Its value strongly depends on the adiabatic index and at $M_\infty = \infty$, $\gamma \to 1$, $\lambda \to 1$. According to (13), the coefficient K is positive and does not exceed unity.

By solving (13) we shall have the following series ([4])

$$F(\xi) = \frac{q_1 \mu(1-\Delta\operatorname{ctg}\theta_0)}{2(\operatorname{ctg}^2\theta_0 - \mu^2)} + \frac{q_1 \operatorname{ctg}\theta_0}{\operatorname{ctg}^2\theta_0 - \mu^2} \sum_{i=1}^{\infty} \lambda^i B_0(K^i \xi) . \qquad (14)$$

Then from (12) we determine the function G (ξ)

$$G(\xi) = \frac{q_1 \mu(1-\Delta\operatorname{ctg}\theta_0)}{2(\operatorname{ctg}^2\theta_0 - \mu^2)} + \frac{q_1 \operatorname{ctg}\theta_0}{\operatorname{ctg}^2\theta_0 - \mu^2} \sum_{i=1}^{\infty} \lambda^i B_0(K^i \xi) + \frac{q_1 \operatorname{ctg}\theta_0}{\operatorname{ctg}^2\theta_0 - \mu^2} B_0(\xi) . \qquad (15)$$

Substituting the functions F and G in the formulae (9) and (10) we shall have:

$$v = A\operatorname{ctg}\theta_0 B_0(y\operatorname{ctg}\theta_0 - x) + A\mu(1 - \Delta\operatorname{ctg}\theta_0) +$$

$$+ A\operatorname{ctg}\theta_0 B_0(x - \mu y) + A\operatorname{ctg}\theta_0 \sum_{i=1}^{\infty} \lambda^i \left(B_0[K^i(x+\mu y) - \right.$$

$$\left. - B_0[K^i(x-\mu y)]\right) ; \qquad (16)$$

$$p = AB_0(y\operatorname{ctg}\theta_0 - x) - A(1 - \Delta\operatorname{ctg}\theta_0) -$$

$$- \frac{1}{\mu}\left(A\operatorname{ctg}\theta_0 B_0(x - \mu y) + \right.$$

$$\left. + A\operatorname{ctg}\theta_0 \sum_{i=1}^{\infty} \lambda^i \left\{B_0[K^i(x+\mu y)] + B_0[K^i(x-\mu y)]\right\}\right)$$

$$A = q_\infty / (\operatorname{ctg}^2\theta_0 - \mu^2) . \qquad (17)$$

It should be noted that formulae (16, 17) are equivalent to the formulae obtained in [6 , 7] in the particular case where m = 1.

From equation (2), it follows that

$$u + \rho = S(y) , \qquad (18)$$

where S (y) — a function proportional to the vortex. The function S (y) is determined from the boundary condition on the line $y\operatorname{ctg}\theta_0 = x$ and has the following form:

$$S(y) = \frac{(1+\delta)}{\delta\mu} A\operatorname{ctg}\theta_0 \left\{\mu\Delta - B_0[y(\operatorname{ctg}\theta_0 - \mu)] + \right.$$

$$\left. + \sum_{i=1}^{\infty} \lambda^i [B_0(y(\operatorname{ctg}\theta_0 + \mu) + B_0(y(\operatorname{ctg}\theta_0 - \mu))]\right\} . \qquad (19)$$

One may notice that on the surface of the wedge the function of vorticity becomes zero. Across the shock layer this function rapidly increases, so that in the neighbourhood of the surface of the wedge there is a thin vortical relaxation layer. The existence of such a vortical layer was previously pointed out in [1, 2, 6, 7]. The form of the shock wave is determined if the boundary condition (5) is used, for example

$$\rho = K_\rho f'(x)$$

setting the following equation in the argument of the functions appearing in the formula for ρ (17),

$$y = tg\,\theta_* x \ .$$

The pressure distribution on the wall of the wedge is of particular interest as its knowledge enables to calculate the aerodynamic force of the characteristics. Below we shall be limited only to the analysis of this function. The qualitative character of the behaviour of the remaining gas-dynamical functions on the wall of the wedge will be as follows:

$$p_1(x,0) = p_* + \frac{\rho_* u_*^2}{\mu} q_1 \left\{ \frac{\mu(\Delta ctg\,\theta_* - 1)}{ctg^2\theta_* - \mu^2} - \right.$$

$$\left. - \frac{B_*(x)}{ctg\,\theta_* + \mu} - \frac{2 ctg\,\theta_*}{ctg^2\theta_* - \mu^2} \sum_{i=1}^{\infty} \lambda^i B_*(\kappa^i x) \right\} , \qquad (20)$$

where

$$B_*(x) = \begin{cases} [1-(1-m)x]^{\frac{1}{1-m}} & \text{at} \quad x < \frac{1}{1-m} \\ 0 & \text{at} \quad x \geq \frac{1}{1-m} \end{cases} .$$

The equilibrium value to which the function $p_1(x,0)$ tends at $x \to \infty$ is equal to:

$$p_{1e} = p_* + \rho_* u_*^2 q_1 \frac{\Delta ctg\,\theta_* - 1}{ctg^2\theta_* - \mu^2} \ . \qquad (21)$$

Formula (20) is simplified in the case of a flow with a very high velocity around a thin wedge, i.e., when the following relations are realized:

$$M_\infty >> 1 \ , \ M_\infty \theta >> 1 \ , \ \theta << 1 \qquad (22)$$

Using condition (22), it is possible to determine the limiting values of the characteristic parameters of flow

$$S = \sqrt{\frac{\gamma-1}{2\gamma}} \ , \ \lambda = \frac{1-2S}{1+2S} \ , \ K = \frac{1-S}{1+S} \ ,$$

$$\mu \cdot \theta_* = S \ , \ \Delta\theta_* = 2S \ , \ \theta_* + \theta = \frac{\gamma+1}{2}\theta \ , \ \theta_* = \frac{\gamma-1}{2}\theta \qquad (23)$$

and formula (20) is reformed as follows:

$$p_1(x,0) = p_\infty V_\infty^2 \theta^2 \left\{ \frac{\gamma+1}{2} + \frac{(\gamma-1)\gamma}{2} q_1 \chi(x) \right\} , \qquad (24)$$

where

$$\chi(x) = 1 - \frac{1-S}{S} B_*(x) - \frac{2}{S} \sum_{i=1}^{\infty} \lambda^i B_*(K^i x) \ .$$

At the edge of the wedge at $x = 0$, the flow is approximately frozen and $\chi(0) = 0$ at $x \longrightarrow \infty$, $\chi(x) \longrightarrow 1$.

The calculation of the function $\chi(x)$ can be approximately performed; being limited to a finite number of terms in the series. The particular cases, where the sum of the series is calculated in a finite form are of specific interest. Obviously, this can be done if the order m of the reaction equals:

$$m = \frac{\ell - 1}{\ell} \qquad \ell = 1, 2, 3, \ldots n .$$

In this case, the width of the zone of combustion is finite and the distribution of the concentration in this zone is in the form of a polynomial of the power ℓ. The function $\chi(x)$ in the points $x = \frac{\ell}{\kappa i}$ $(i = 0, 1, 2, \ldots)$ as a function of ℓ has a rupture, either a discontinuity of the cervature or of the leading derivatives.

Performing expansion in the series:

$$\left(1 - \frac{x}{\ell}\right)^{\ell} = 1 - x + \frac{\ell(\ell-1)}{2!}\frac{x^2}{\ell^2} - \frac{\ell(\ell-1)(\ell-2)}{3!}\frac{x^3}{\ell^3} + \ldots$$

and performing the summation at the same powers of x, we obtain the following formula for the interval of change $0 \leq x \leq \ell$:

$$\chi(x) = \sum_{r=1}^{\ell} (-1)^r \left(\frac{1+S}{S} - \frac{2}{S}\frac{1}{1+\lambda K}\right) \frac{\ell!\, x^r}{(\ell-r)!\, r!\, \ell^r} \qquad (25)$$

or taking (23) into account, we get:

$$\chi(x) = (1-S^2)\left[\frac{2x}{1+2S^2} - \frac{3}{2}\frac{(\ell-1)}{\ell}\frac{x^2}{(1+5S^2)} + \frac{4(\ell-1)(\ell-2)\,x^3}{6\ell^2(1+9S^2)} + \ldots\right] ; \qquad (26)$$

If the order of the reaction $m = 0$, then $\chi(x)$ is a linear function increasing from zero to the maximum value at the end of the zone of combustion

$$\chi(x) = \frac{2(1-S^2)}{1+2S^2}\, x ,$$

$$\chi_{max}(1, S) = \frac{2(1-S^2)}{1+2S^2} . \qquad (27)$$

In the case of $m = \frac{1}{2}$ the curve $\chi(x)$ is a quadratic parabola with a maximum within the interval $0 < x < 2$ which exceeds the unity

$$\chi(x) = (1-S^2)\left[\frac{2x}{1+2S^2} - \frac{3}{4}\,\frac{x^2}{1+5S^2}\right],$$

$$\chi_{max} = \frac{4}{3}\left[\frac{5}{2} - \frac{3}{2(1+2S^2)}\right]. \qquad (28)$$

The abscissa of the maximum increases monotonically with the decrease of the parameter S, and the value of the maximum changes nonmonotonically with decreasing S.

In the case of $m = 2/3$, the curve $\chi(x)$ is a cubic parabola, the maximum is attained also within the interval $0 < x < 3$

$$\chi(x) = (1-S^2)\left[\frac{2x}{1+2S^2} - \frac{x^2}{1+5S^2} + \frac{4}{27}\,\frac{x^3}{1+9S^2}\right] \qquad (29)$$

It should be mentioned that in the limiting case $S = 0$, the inclination of the quadratic parabola at the end of the interval is equal to unity, and that of the cubic one is equal to zero.

On further increase of the order of the reaction, the maximum will be shifted towards equilibrium and its value will decrease. At the same time, with increasing the power ℓ of the polynomial , the number of these maxima and minima increases. The solution in the zone of combustion has an oscillatory character with rapidly decreasing amplitude and frequency of the oscillations. Thus, at $m = 1$, i.e. in the case of exponential distribution of the concentration, the first maximum is attained at $x \approx 3.2$ and it equals 1.062; the second minimum at $x \approx 12$ and equals 0.998,....

The existence of weak oscillations for this case was discovered in [3].

In the case of the determination of the function $\chi(x)$ in the interval between the discontinuities $P/K^n \le x \le P/K^{n+1}$ it is necessary to equate the first terms n of the series (24) to zero:

$$\begin{cases} m = 0 \\ \chi^{(0)}_{n,n+1}(x) = 1 - \frac{2}{S}\sum_{i=n+1}^{\infty}\lambda^i(1-K^i x) = 1 - \frac{2\lambda^{n+1}}{S}\left[\frac{1}{1-\lambda} - \frac{K^{n+1}}{1-K\lambda}\,x\right] \end{cases} \qquad (30)$$

$$\begin{cases} m = 1/2 \\ \chi^{(1/2)}_{n,n+1}(x) = 1 - \frac{2}{S}\lambda^{n+1}\left[\frac{1}{1-\lambda} - \frac{K^{n+1}}{1-K\lambda}\,x + \frac{K^{2n+2}}{1-K^2\lambda}\,\frac{x^2}{4}\right] \end{cases} \qquad (31)$$

$$\begin{cases} m = 2/3 \\ \chi^{(2/3)}_{n,n+1}(x) = 1 - \frac{2}{S}\lambda^{n+1}\left[\frac{1}{1-\lambda} - \frac{K^{n+1}}{1-K\lambda}\,x + \frac{K^{2n+2}}{1-K^2\lambda}\,\frac{x^2}{3} - \frac{K^{3n+3}}{1-K^3\lambda}\,\frac{x^3}{27}\right]. \end{cases} \qquad (32)$$

The values of the functions $\chi(x)$ in the discontinuity points are determined as follows:

$$\chi^{(0)}\left[\left(\frac{1+S}{1-S}\right)^n\right] = 1 + \frac{1-4S^2}{1+2S^2}\left(-\frac{1-2S}{1+2S}\right)^n , \tag{33}$$

$$\chi^{(1/2)}\left[2\left(\frac{1+S}{1-S}\right)^n\right] = 1 - \frac{2S}{(1+2S^2)(1+5S^2)}\left(-\frac{1-2S}{1+2S}\right)^n , \tag{34}$$

$$\chi^{(2/3)}\left[3\left(\frac{1+S}{1-S}\right)^n\right] = 1 + \frac{16S^2(1-2S)\left[1-2K(1+K)\lambda+\lambda^2K^3\right]}{(1+S)^3(1+2S)(1+\lambda)(1+K\lambda)(1+K^2\lambda)} \cdot \frac{1}{1+K^3\lambda}\left(-\frac{1-2S}{1+2S}\right)^n . \tag{35}$$

It is obvious that the values of the functions $\chi(x)$ in the discontinuity points fluctuate about unity and the decay coefficient of these oscillations is equal to the reflection coefficient of the disturbances from the shock wave; the frequency of the oscillations is determined by the parameter $K = \frac{1-S}{1+S}$.

The abscissae of the points of the extrema - function are equal to:

$$x^{(0)} = \left(\frac{1+S}{1-S}\right)^n , \tag{36}$$

$$x^{(1/2)} = 2\left(\frac{1+S}{1-S}\right)^n \frac{1+5S^2}{(1+S)(1+2S^2)} , \tag{37}$$

$$x^{(2/3)} = 3\left(\frac{1+S}{1-S}\right)^n \frac{1+\lambda K^3}{\lambda+\lambda K^3}\left[1 \pm \frac{2S}{1+S}\left(\frac{\lambda K}{(1+\lambda K)(1+\lambda K^3)}\right)^{1/2}\right] , \tag{38}$$

and the values of the extrema equal

$$\chi^{(0)}_{n,n+1} = 1 + \frac{1-4S^2}{1+2S^2}\left(-\frac{1-2S}{1+2S}\right)^n \tag{39}$$

$$\chi^{(1/2)}_{n,n+1} = 1 - \frac{S(1+S)(1-2S)^2}{(1+2S^2)^2}\left(-\frac{1-2S}{1+2S}\right)^n . \tag{40}$$

Therefore, as a function of the order of the reaction, the functions $\chi(x)$ in the intervals between the discontinuities are segments of straight lines, quadratic and cubic parabola, etc. The function $\chi(x)$ fluctuates around a unit value with an amplitude and frequency depending on the value of the parameter S (or γ).

It is important to notice the different asymptotic character of solution at m = 0 and m = $\frac{1}{2}$ and 2/3 when S $\longrightarrow$ 0. In the first case, the amplitude of the oscillations increases and approaches a finite limit; simultaneously the

frequency of the oscillations tends to infinity. In the second case, at sufficient small values of S, the amplitude decreases to zero when $S \to 0$; and the frequency of the oscillations, as previously, tends to infinity.

The mechanism of the formation of the oscillations in the two-dimensional flow behind the shock wave is illustrated in Fig. 3. Owing to the state of nonequilibrium, the disturbances of the pressure come to a point with the coordinate x along the characteristic $x - \mu y = \text{const}$. At the same time, the disturbances formed at the edge of the wedge, propagating along the characteristics of both families, repeatedly reflect from the surface of the wedge and the shock wave.

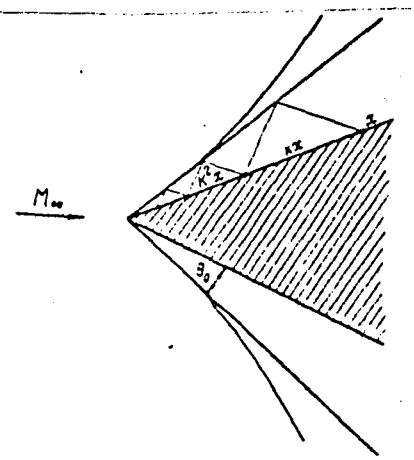

Fig. 3

Diagramatic sketch of the propagation of the disturbances in the region between the shock wave and the surface of the wedge.

As the equilibrium zone has a finite width, these disturbances accumulate. If the coefficient of reflection from the shock wave is negative, the compression wave alternates, on reflection, by a rarefaction wave, which leads to an interchange of the local compression and rarefaction on moving downstream in the near equilibrium region of the flow.

The behaviour of the function $\chi^{(m)}(x)$ is shown in Figs. 4 and 5 for certain values of the adiabatic index γ. The curves in Fig. 4 for m = 1, 2, 3 are obtained numerically. It is obvious that $m \geqslant 2$, the pressure along the wall of the wedge increases monotonically from the frozen to the equilibrium values.

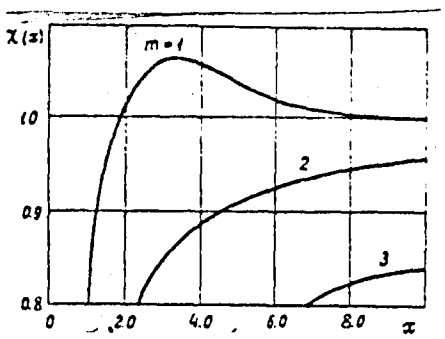

Fig. 4

Pressure distribution along the side of a thin wedge at hypersonic flow around. The case of smooth solution for m = 1; 2; 3.

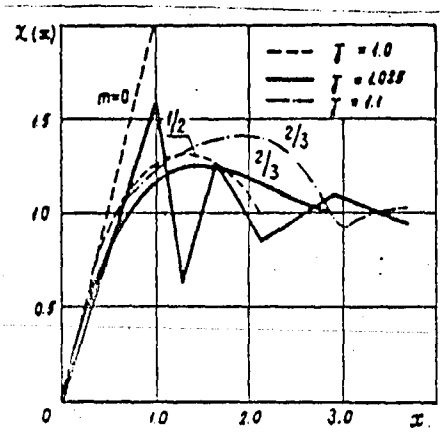

Fig. 5

Pressure distribution along the side of a thin wedge at hypersonic flow around. The case of uneven solutions for m = 0; $\frac{1}{2}$, $\frac{2}{3}$.

It is easy to see that in the general case, when the wedge is not thin, the solution of (20) can have an oscillatory character, and here the reflection coefficient λ and the parameter K will be the determining parameters. The dependence of the reflection coefficient λ on γ is very strong. For example, in the case of a sufficiently big Mach number M_∞, the change of the reflection coefficient from a positive to negative value occurs on decreasing the wedge angle θ in a very narrow interval of change of θ. On further decrease of the wedge angle within a sufficiently big interval of the change of θ at a fixed M_∞, the change of the reflection coefficient is small.

In connection with this, the formation of oscillations in the flow must be sensitive for the properties of the fuel mixture (γ , m) and the outer conditions (M_∞ , 0). The latter conclusion is confirmed in the experiments on ballistic installations [5].

References

1. Zhigulev, V.N. "Ob effekte relaksatsionnogo pogranichnogo sloya" (Upon the effect of the relaxation boundary layer).--- Dokl. AN SSSR, 144 (6), 1962.

2. Kapioks, R. and M. Vashington "Neravnovesnoe techenie okolo klina" (Nonequilibrium flow near a wedge).--- AJAAJ, No. 3, 1963.

3. Polyanskii, O.Yu. "Aerodinamicheskie kharakteristiki tonkogo kryla v giperzvukovom potoke" (Aerodynamic characteristics of a thin wing in a hypersonic flow).--- Izv. AN SSSR, MZhG, No. 6, 1967.

4. Chernyi G.G. "Techenie gaza s bol'shoi sverkhzvukovoi skorost'yu" (Gas flow with a high supersonic velocity).--- Fizmatgiz, 1959.

5. Chernyi G.G. "Sverkhzvukovoe obtekanie tel s obrazovaniem frontov detonatsii i goreniya" (Supersonic flow around a body with the formation of detonation and combustion fronts).--- Sb. "Problemy gidrodinamiki i mekhaniki sploshnoi sredy" Moskva, 1969.

6. Moore, F.E. and W.F. Gibson. Propagation of weak disturbances in a gas subject to relaxation effects, JAS, No. 2, 1960.

7. Der J.J. Linearized supersonic nonequilibrium flow past an arbitrary boundary. NASA T.R., R - 119, 1961.

8. Lighthill M.J. The flow behind a stationary shock. Phil. Mag., 40, 1949.

9. Boa-Teh Chy. On weak interaction of strong shock and Mach waves generated downstream of the shock. Journ. Aeron. Sci., 19 (7), 1952.

End of Document